

DOCTORAL THESIS

Structure Modification and Applications of Sustainable Ionic Liquids-Based Molecular Platforms

Illia Kapitanov

TALLINN UNIVERSITY OF TECHNOLOGY
DOCTORAL THESIS
66/2024

Structure Modification and Applications of Sustainable Ionic Liquids-Based Molecular Platforms

ILLIA KAPITANOV



TALLINN UNIVERSITY OF TECHNOLOGY

School of Science

Department of Chemistry and Biotechnology

This dissertation was accepted for the defence of the degree of Doctor of Philosophy in Chemistry on 14/11/2024

Supervisor:

Dr. Yevgen Karpichev
Department of Chemistry and Biotechnology
Tallinn University of Technology
Tallinn, Estonia

Opponents:

Assoc. Prof. Roman Viter
University of Latvia
Riga, Latvia

Dr. Olga Tšubrik
OÜ Alminnovo (Board member)
Tartu, Estonia

Defence of the thesis: 16/12/2024, Tallinn

Declaration:

Hereby I declare that this doctoral thesis, my original investigation and achievement, submitted for the doctoral degree at Tallinn University of Technology has not been submitted for doctoral or equivalent academic degree.

Illia Kapitanov

signature



Copyright: Illia Kapitanov, 2024

ISSN 2585-6898 (publication)

ISBN 978-9916-80-233-5 (publication)

ISSN 2585-6901 (PDF)

ISBN 978-9916-80-234-2 (PDF)

DOI <https://doi.org/10.23658/taltech.66/2024>

Printed by Koopia Niini & Rauam

Kapitanov, I. (2024). *Structure Modification and Applications of Sustainable Ionic Liquids-Based Molecular Platforms* [TalTech Press]. <https://doi.org/10.23658/taltech.66/2024>

TALLINNA TEHNIKAÜLIKOO
DOKTORITÖÖ
66/2024

**Jätkusuutlike ioonvedelikepõhiste
molekulaarsete platvormide struktuuri
muutmine ja rakendused**

ILLIA KAPITANOV

Contents

List of publications	7
Author's contribution to the publications	8
Introduction	9
Abbreviations	10
1 Literature overview	12
1.1 Green chemistry principles and design of sustainable products	12
1.2 Ionic liquids	14
1.2.1 Synthesis of ionic liquids	14
1.2.2 Physicochemical properties and application of ionic liquids	15
1.3 Surfactants, functionalized surfactants and surface-active ionic liquids	16
1.3.1 Surfactants: basic concepts and definitions	16
1.3.2 Physico-chemistry of surfactant micellization	17
1.3.3 Solubilization phenomenon in surfactant solutions	19
1.3.4 Surfactant solutions as a reaction media. Micellar catalysis	19
1.3.5 Surfactants functionalization	21
1.3.6 Surface-active ionic liquids.....	22
1.4 Evaluation of ionic liquids sustainability	22
1.4.1 Toxicity of ionic liquids	23
1.4.2 Biodegradability of ionic liquids	24
1.5 Amino-acid ionic liquids	27
1.5.1 Amino acid as sustainable building blocks in design of new chemicals	27
1.5.2 Design of amino acid ionic liquids.....	28
1.5.3 Phenylalanine-derived ionic liquids as a prospective molecular platform for future improvement and practical applications	29
1.5.4 The strategy for further study and improvement of the selected sustainable ionic liquids-based molecular platform	32
2 Aims of the present work.....	33
3 Results and discussion.....	34
3.1 Design of sustainable SAILs-based systems for solubilization of polycyclic aromatic hydrocarbons (Publication IV).....	34
3.1.1 Evaluation of pyridinium phenylalanine-derived SAILs efficacy in processes of PAHs solubilization.....	34
3.1.2 Selection of enzymatic systems and reaction condition optimization for pyridinium phenylalanine-derived SAILs decomposition	38
3.1.3 Structure improvement of PyPheOC _n SAILs: design of diamide derivatives PyPheNHC _n	41
3.1.4 Enzymatic systems screening in processes of diamide derivatives PyPheNHC _n decomposition	42
3.1.5 Sustainable pyridinium phenylalanine-derived ionic liquids in processes of polycyclic aromatic hydrocarbons extraction: application concept.....	43
3.2 Ionic liquids structure improvement: dipeptide-based ionic liquids (Publication III).....	44
3.2.1 Analysis of ILs biodegradation pathways and selection of possible transformation products and synthesis of target molecules	46

3.2.2 Microbial toxicity and biodegradation screening of amino acid ILs, dipeptide ILs and their potential transformation products	48
3.3 Functionalization of sustainable SAILs: design and new applications (Publication I and Publication II)	50
3.3.1 Objects selection, structure variation and synthesis of oxime-functionalized SAILs	51
3.3.2 Protolytic equilibria in solutions of oxime-functionalized SAILs	52
3.3.3 Aggregation properties of mixed systems oxime-functionalized SAIL / 16-s-16 surfactants	54
3.3.4 Biodegradability of oxime-functionalized SAILs	56
3.3.5 Application of oxime-functionalized SAILs: organophosphates decomposition	56
3.3.6 Application of oxime-functionalized SAILs: interaction of mixed systems 4-PyC8 / 16-10-16 with Promethazine	58
3.4 Design of acetylcholinesterase reactivators based on sustainable ionic liquids (Publication V)	59
3.4.1 Strategy of design, structure variation and synthesis of sustainable AChE reactivators	61
3.4.2 Properties evaluation of new sustainable AChE reactivators <i>in silico</i>	62
3.4.3 Toxicological properties of new sustainable AChE reactivators	66
3.4.4 Biodegradability studies of new sustainable AChE reactivators	67
3.4.5 Reactivation efficacy of oxime-functionalized ILs towards AChE inhibited by sarin, VX and paraoxon	69
3.4.6 Stability of selected oxime-functionalized ILs in human blood plasma	70
4 Conclusions	71
5 Experimental	72
List of figures	75
List of tables	77
References	78
Acknowledgements	90
Abstract	91
Lühikokkuvõte	92
Appendix 1	93
Appendix 2	107
Appendix 3	131
Appendix 4	147
Appendix 5	167
Author's publications and conference presentations	185
Curriculum vitae	189
Elulookirjeldus	190

List of publications

The list of author's publications, on the basis of which the thesis has been prepared:

- I Pandya, S.J.; Kapitanov, I.V.; Usmani, Z.; Sahu, R.; Sinha, D.; Gathergood, N.; Ghosh, K.K.; Karpichev, Y. An example of green surfactant systems based on inherently biodegradable IL-derived amphiphilic oximes. *J. Mol. Liq.* **2020**, 305, 112857
- II Pandya, S.J.; Kapitanov, I.V.; Banjare, M.K.; Behera, K.; Borovkov, V.; Ghosh, K.K.; Karpichev, Y. Mixed oxime-functionalized IL/16-s-16 Gemini surfactants system: physicochemical study and structural transitions in the presence of promethazine as a potential chiral pollutant. *Chemosensors* **2022**, 10, 46
- III Kapitanov, I.V.; Raba, G.; Špulák, M.; Vilu, R.; Karpichev, Y.; Gathergood, N. Design of sustainable ionic liquids based on L-phenylalanine and L-alanine dipeptides: Synthesis, toxicity and biodegradation studies. *J. Mol. Liq.* **2023**, 374, 121285
- IV Kapitanov, I.V.; Sudheer, S.M.; Yadav, T.; Ghosh, K.K.; Gathergood, N.; Gupta, V.K.; Karpichev, Y. Sustainable phenylalanine-derived SAILs for solubilization of polycyclic aromatic hydrocarbons. *Molecules* **2023**, 28, 4185
- V Kapitanov, I.V.; Spulak, M.; Pour, M.; Soukup O.; Marek, J.; Jun, D.; Novak, M.; Diz de Almeida, J.S.F.; Costa França, T.C.; Gathergood, N.; Kuca, K.; Karpichev, Y. Sustainable ionic liquids-based molecular platforms for designing acetylcholinesterase reactivators. *Chem.-Biol. Interact.*, **2023**, 385, 110735

Author's contribution to the publications

Contribution to the papers in this thesis are:

- I Synthesis and complete characterization of all compounds used in the publication, running and analysis of the NMR spectra and preparation of the ESI; discussion of the results obtained and contribution into the development of the idea of the manuscript; contribution manuscript preparation (Experimental part and Results and discussion) on all stages.
- II Synthesis of compounds, methodology, analysis and interpretation of obtained results, manuscript writing, reviewing and editing.
- III Methodology, data curation, original draft preparation, conceptualization, manuscript review and editing.
- IV Synthesis of compounds, experimental techniques, data curation, analysis of the results, conceptualization, methodology, analysis and interpretation, original draft preparation.
- V Conceptualization, investigation (synthesis and characterization of studied compounds), data curation, visualization, writing (original draft preparation).

Introduction

Ionic liquids (ILs) are class of organic salt-like materials which are widely used nowadays as a reaction media [1], components of different electric and electronic systems and devices (batteries, supercapacitors, displays, etc.) [2], [3], technological liquids (lubricants, thermal fluids) [4], in extraction and separation processes [5], analytical chemistry (MALDI-TOF matrices, head-space solvents in gas chromatography) [6], [7], etc. [8]. The properties of ILs satisfy many of green chemistry principles [9].

Despite significant advantages over conventional solvents and materials [8], [9], very often ionic liquids cannot be considered as really sustainable due to problems with toxicity to many living organisms [10], [11], [12] and persistence in environment (ecological systems) [13], [14].

The efforts of the last years were focused on systematic analysis of ecological and toxicological properties of ILs, and design of sustainable low-toxic ecologically friendly molecules [13], [15], [16], [17], [18], [19].

The main tasks of current study were, taken previously selected sustainable L-phenylalanine derived ILs, to test them in scope of practical application (**Publication IV**), evaluate possible ways and approaches of their structure improvement (**Publications I–V**), and perform a testing of improved structures for some new practical applications (**Publications I, II, V**). The chosen strategy can also help to demonstrate a high flexibility of selected sustainable ionic liquid-based molecular platform in solving different practical tasks and their significant potential for future improvement.

The obtained results have been presented to scientific community in **Publications I–V** (articles in international peer-reviewed journals) and as the reports at different conferences in Estonia, Hungary, Czech Republic, Ukraine and Slovenia.

Abbreviations

AAIL	Amino acid ionic liquid
AChE	Acetylcholinesterase
Ala	Alanine
Ant	Anthracene
BBB	Blood-brain barrier
Boc	tert-Butyloxycarbonyl
CAC	Critical aggregation concentration
[cat]	Cationic form of the molecule
CBT	Closed Bottle Test
CMC	Critical micelle concentration
CNS	Central nervous system
CTABr	Cetyltrimethylammonium bromid
CWA	Chemical warfare agents
DLS	Dynamic light scattering
DMF	<i>N,N</i> -dimethylformamide
DMSO	Dimethyl sulfoxide
Et	Ethyl
FTIR	Fourier-transform infrared spectroscopy
GB	Isopropyl methylphosphonofluoridate (Sarin)
HRMS	High resolution mass spectrometry
IL	Ionic liquid
Me	Methyl
MIC	Minimum inhibitory concentration
Nap	Naphthalene
NMR	Nuclear magnetic resonance
OP	Organophosphorus compounds (Organophosphates)
PAH	polycyclic aromatic hydrocarbon
2-PAM	2-Pyridine aldoxime methyl chloride (Pralidoxime)
Ph	Phenyl
Phe	Phenylalanine
PMZ	Promethazine
PNPDP	4-Nitrophenyl diphenyl phosphate
PON	4-Nitrophenyl diethyl phosphate (Paraoxon)
ppm	Parts per million
PTP	Potential transformation product
PTSA	p-Toluenesulfonic acid
Py	Pyridine
Pyr	Pyrene
SAIL	Surface active ionic liquid

SDS	Sodium dodecyl sulfate
TLC	Thin-layer chromatography
TMS	Tetramethylsilane
TP	Transformation product
UV	Ultraviolet
Vis	Visible
VX	O-ethyl-S-diisopropylaminomethyl methylphosphonothiolate
[zw]	zwitter-ionic form of the molecule

1 Literature overview

1.1 Green chemistry principles and design of sustainable products

Green chemistry is focused on the design of chemical products and processes that reduce or eliminate the generation of hazardous substances [20].

The most important points of green chemistry concept were formulated by P. Anastas and J. Warner in 1998 and now they are well-known as 12 principles of green chemistry [21]:

1. Prevention: it is much easier to prevent waste than find the ways of its proper utilization / disposal; chemical processes should be designed with focus on minimization of wastes formation.

2. Atom economy: target product should include a maximal number of atoms which were present in the starting reagents.

3. Less hazardous chemical syntheses: reagents and transformation products should be low of non-toxic for humans and the environment.

4. Design safer chemicals: the functionality of the target product should remain unchanged compared to analogs, but their toxicity should decrease (or to be non-toxic for humans and the environment).

5. Safer solvents and auxiliaries: solvents and other auxiliary chemicals should not be used in the processes or selected safest ones.

6. Design for energy efficiency: chemical processes designed should not require special conditions and, in the ideal case, can be performed at the room temperature and normal pressure.

7. Use of renewable feedstocks: renewable starting materials / feedstocks should be used when it is possible.

8. Reduce derivatives: minimization or excluding compounds derivatization steps (protection/deprotection, temporary structure modification, etc.) from designed process for reducing of possible waste formation.

9. Catalysis: catalytic reaction should be used to provide optimal reaction condition (proper selectivity, low energetic barrier, etc.).

10. Design for degradation: at the end of the product's life cycle, it may easily degrade and not form products that are persistent in the environment.

11. Real-time analysis for pollution prevention: the proper analytical approach should be developed to make possible detect deviation in the process before it starts generating hazardous substances or byproducts.

12. Inherently safer chemistry for accident prevention: the choice of chemical reagents and reaction conditions should minimize risks of possible accidents (explosions, fires, etc.).

Several quantitative parameters and approaches have been developed to evaluate and compare different processes and their improvements in scope of compliance with the green chemistry principles [22], [23], [24]. The one of the most convenient instruments for this is CHEM21 metrics toolkit, which was proposed by James H. Clark and co-authors [25]. It has included an evaluation of chemical processes on four levels:

- zero pass (for reaction screening; parameters: yield, conversion and selectivity, atom economy, reaction mass efficiency, solvents, reagents and safety);

- first pass (for promising reactions; parameters: mass intensity / process mass intensity, detailed solvents, catalyst, critical elements, energy work up, health and safety, chemicals of concern, availability, applicability);
- second pass (for kilo/pilot plant reactions; parameters: mass intensity / process mass intensity, catalyst, renewables intensity, reagent preparation, appropriate safety study, life cycle assessment, costs);
- third pass (detailed energy investigation, recovery/recycling, waste).

For early-stage process optimization (on laboratory scale level) only zero and first pass are used [24]. They included evaluation of classical parameters, which are widely used for reaction characterization – reaction yield, conversion and selectivity. They could be calculated using equations (1) – (3) [24], [25]:

$$\text{Percentage yield} = \frac{\text{moles of product}}{\text{moles of limiting reactant}} \cdot 100 \quad (1)$$

$$\text{Percentage conversion} = 100 - \frac{\text{final mass of limiting reactant}}{\text{moles of limiting reactant}} \cdot 100 \quad (2)$$

$$\text{Percentage selectivity} = \frac{\% \text{ yield}}{\% \text{ conversion}} \cdot 100 \quad (3)$$

In addition to reaction yield, conversion and selectivity for more deep process evaluation are used atom economy (AE), reaction mass efficiency (RME) and optimum efficiency (OE) parameters (equations (4) – (6); [24], [25]):

$$\text{AE} = \frac{\text{molecular weight of product}}{\text{total molecular weight of reactants}} \cdot 100 \quad (4)$$

$$\text{RME} = \frac{\text{mass of isolated product}}{\text{total mass of reactants}} \cdot 100 \quad (5)$$

$$\text{OE} = \frac{\text{RME}}{\text{AE}} \cdot 100 \quad (6)$$

On the first pass the processes are also evaluated using mass intensity (MI; for a single step) or process mass intensity (PMI; for an entire process) parameters, which take into account all mass-based inputs (solvents, catalysts, reagents, work up etc.) [25]:

$$\text{Mass intensity} = \frac{\text{total mass in a process or process step}}{\text{mass of product}} \cdot 100 \quad (7)$$

As a very important part of process evaluation on zero and first passes are health and safety aspects check [25].

The process evaluation using CHEM21 metrics toolkit can provide not only quantitative information for comparison, but it also could help to indicate critical aspects for future improvement and more detailed evaluation (especially, related to health and safety, availability, applicability, etc.) [25].

1.2 Ionic liquids

1.2.1 Synthesis of ionic liquids

One of the first ionic liquids, ethyl ammonium nitrate, was described in 1914 [26]. Since then, numerous examples of ionic liquids have been obtained and studied in detail [27], [28], [29]. A typical ionic liquid consists of an organic cation and an inorganic or organic anion (Figure 1) [26], [27]. A theoretically possible number of cations and anions combinations for ILs reach ca. 10^{18} [30], which is significantly higher than the number of available organic solvents [31].

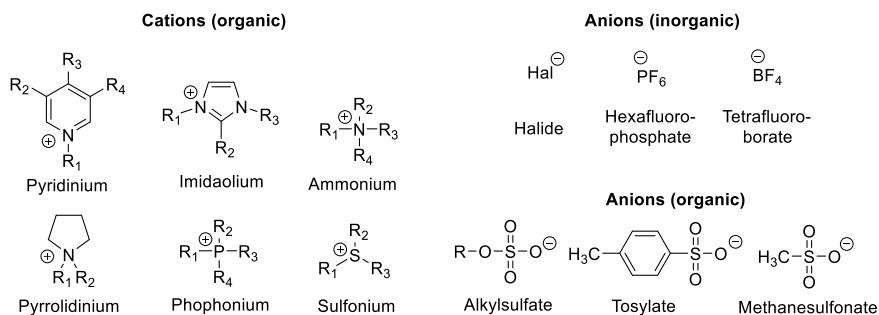
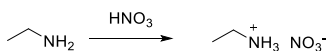


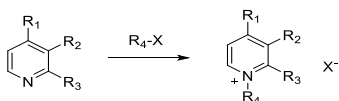
Figure 1. Structure of ionic liquids.

The following chemical reactions are mainly used for the synthesis of ionic liquids [27], [28], [29]:

1) neutralization of a base with an acid, which leads to formation of the corresponding salt



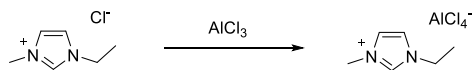
2) alkylation (quaternization)



3) ion exchange



4) chemical transformation of the anion in quaternary salts



1.2.2 Physicochemical properties and application of ionic liquids

Ionic liquids are organic salts that melt below a specific temperature, which is usually limited to 100°C [27], [28], [29]. In liquid state they are very viscous and colourless (or slightly yellowish) [27], [28], [29]. ILs often demonstrate outstanding thermal stability (do not show any degradation products at temperatures below 300 °C) [32], low vapour pressure (less than 1 Pa at room temperature) [33] and non-flammability [34].

Due to these properties, ILs are often considered as a good alternative to conventional organic solvents in various technological processes and devices [35], [36], [37], since their use significantly reduces the fire incident risks [35], and the other unique properties open new horizons for their industrial and laboratory applications (Figure 2) [[1], [7], [8].

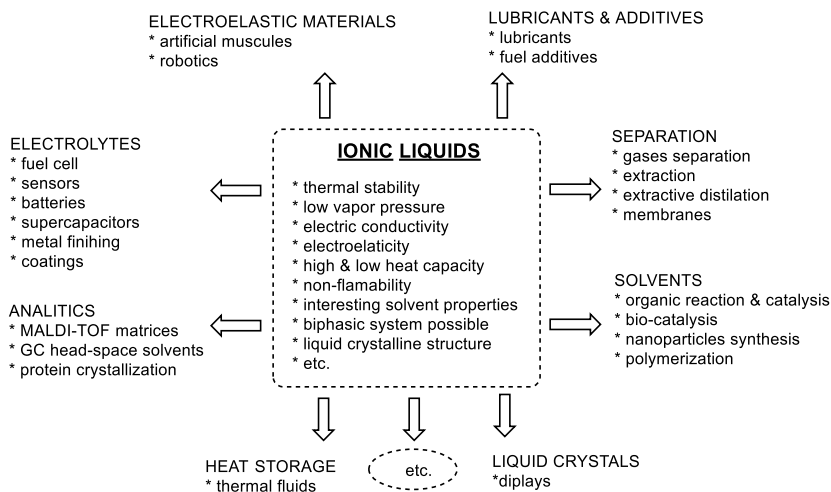


Figure 2. Application of ionic liquids.

For example, a broad variation of ILs heat capacity (from ca. 120 J·mol⁻¹·K⁻¹ to ca. 1500 J·mol⁻¹·K⁻¹) can help to design not only the systems for heat storage, but also a energy efficient reaction media with low heat capacity for heating processes in chemical synthesis [38], [39]. The high ionic conductivity and wide electrochemical potential window make possible to use them in batteries, supercapacitors, and other electrical devices [2], [3]. ILs are used as special lubricants with electrical conductivity in electric engines [40].

ILs found an application in analytical chemistry [6]. They are widely used as solvents in samples preparation in gas chromatography, capillary electrophoresis, as MALDI-TOF matrices, modifiers for chromatography columns and components of sensors for detection of volatile organic compounds [6], [7], [40].

ILs are a new media for chemical synthesis and advanced catalytic transformations [29]. They have been used for performance of many standard chemical reactions (substitution, elimination, polymerization, etc.) [8], [41], ionic-liquid-supported asymmetric organic synthesis [1] and metals catalysis [42], [43].

For reactions performance ILs supported standard synthetic techniques (heating, stirring, etc.) [26], [27], as well as new synthetic approaches (photochemical reactions [44], microwave-assisted synthesis [45], and other [46]).

Since first examples of ILs introduction in commercial large-scale industrial processes (tetrahydrofuran production by Eastman Chemical Company, 1996 [47], and invention of BASIL™ process, established by BASF in 2002 [48]), the industrial use of ILs were significantly expanded [8], [49]. Now, ILs are successfully used in oil recovery [50], lignocellulosic biomass pre-treatment [51], extraction and separation processes [5], gases purification and storage [8], [52], polymers recycling [53], etc. [8].

The one of the most remarkable achievements of the last years is development of ILs-based technology of PET-plastic recycling with possibility to produce “virgin quality” products [54]. Taking into account significant amount of not recycled PET wastes [55] and a request for such technologies from the leading PET-packaging consumers (e.g., the Coca-Cola Company declare in the ‘World Without Waste’ Program, that it will use 50% recycled material in packaging by 2030 [56]), the outcome from cooperation of these companies could help to improve a situation with plastic pollution.

1.3 Surfactants, functionalized surfactants and surface-active ionic liquids

1.3.1 Surfactants: basic concepts and definitions

Surfactants (**surface-active agents**) are chemical compounds that decrease the surface tension or interfacial tension between two liquids, a liquid and a gas, or a liquid and a solid [57], [58]. The molecules of surfactants are amphiphilic and consist of covalently connected hydrophobic and hydrophilic parts. Depend on hydrophilic part nature they can be classified on cationic, anionic, zwitter-ionic (amphoteric) or non-ionic surfactants (Figure 3) [57], [58].


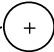

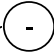

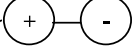

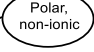
Hydrophobic group	Polar group	Class of surfactants	Typical example
		<i>Cationic surfactants</i>	$C_{16}H_{33}-N^+ \text{ (benzene ring)} Br^-$
		<i>Anionic surfactants</i>	$C_{12}H_{25}O-SO_3^- Na^+$
		<i>Zwitter-ionic (amphoteric) surfactants</i>	$C_{12}H_{25}-N^+(CH_3)_2-CH_2-C(=O)O^-$
		<i>Non-ionic surfactants</i>	$C_{12}H_{25}-(OCH_2CH_2)_nOH$

Figure 3. Structure and classification of surfactants.

Surfactants have a tendency to adsorb preferentially on surfaces / interfaces, but after reaching specific concentration (critical aggregation concentration, CAC) they also can form supramolecular aggregates in solution (micelles, vesicles, etc.; Figure 4) [57], [58]. These aggregates are dynamic – surfactant molecules enter and leave them with mean exchange time 10^{-5} to 10^{-6} s [59]. Formation of aggregates dramatically changes the solution properties (surface tension, conductivity, viscosity, etc.) [57], [58] and usually performs with decreasing of free Gibbs energy of the system [58], [60], [61]. It means that this process is spontaneous, and aggregates formed are thermodynamically stable [58], [60]. The driving force of aggregates formation in water is hydrophobic interactions [58], [60].

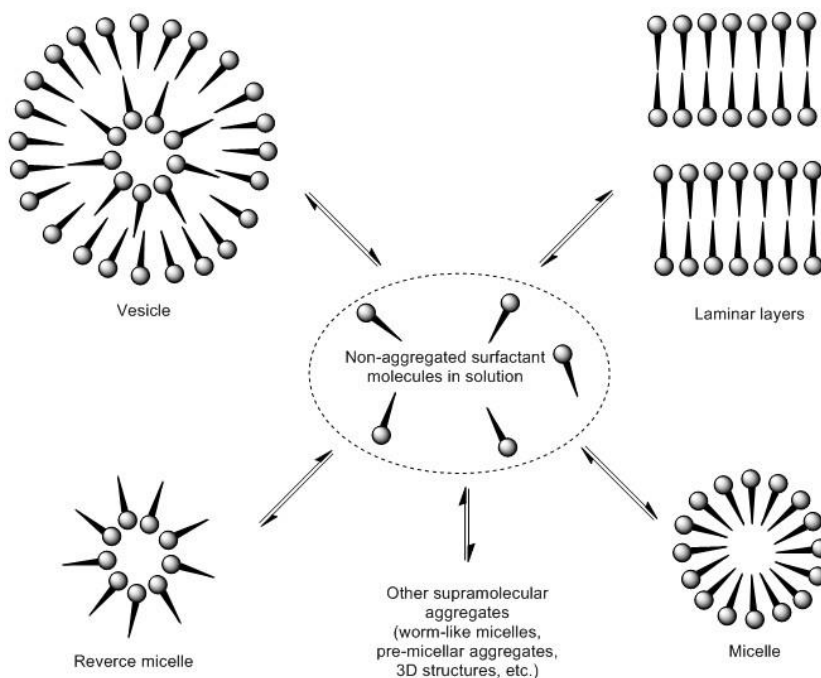


Figure 4. *Surfactant aggregates in solution.*

Surfactants and surfactant solutions are widely used in different technological processes (oil recovery [62], polymerization [63], chemical synthesis [64], [65]), analytical chemistry [66], [67], food industry [68], [69], health care / pharmacy [70], [71] and many others [57]. Due to structural similarity to biological amphiphiles (phospholipids – the main component of biological membranes – are, in fact, anionic surfactants [72]), they have found an application in design of biomimetic systems [73], composition for drugs [70], [71] and genes [74] delivery, creation of enzyme-like esterolytic systems [75], etc. Of course, surfactants are also critically important component of every-day use household chemicals (e.g., laundry liquids, soaps, etc.) [76].

1.3.2 Physico-chemistry of surfactant micellization

The fundamental theory of such aggregates formation (specially, micelles) are well-developed and can adequately describe observed phenomenon and regularities [57], [58]. The following energetic parameters are mainly used: Gibbs free energy of micellization (ΔG°_m), Gibbs free energy of micellization per alkyl tail ($\Delta G^\circ_{m,tail}$), Gibbs energy of transfer (ΔG°_{trans}), standard free energy of adsorption (ΔG_{ads}) and Gibbs free energy of the given air/water interface ($\Delta G^{(s)}_{min}$) [58], [60], [61]. All these parameters are calculated based on analysis of dependencies of surface tension of surfactant solution from surfactant concentration. From these dependencies are determined also surface tension at CMC (γ_{cmc}), surface pressure at the CMC (π_{cmc}), value of the maximum surface excess (Γ_{max}) and value of the minimum area per molecule (A_{min}), which are used for energetic parameters calculation.

The next equations are essential for characterisation of micelles formation [58], [60], [61]:

- the surface pressure at the CMC (π_{cmc})

$$\pi_{\text{cmc}} = \gamma_0 - \gamma_{\text{cmc}}, \quad (8)$$

where

γ_0 – surface tension of the pure water;

γ_{cmc} – surface tension at CMC.

- value of the maximum surface excess (Γ_{max})

$$\Gamma_{\text{max}} = -\frac{1}{2.303nRT} \cdot \left[\frac{d\gamma}{d \log C} \right]_{T,P}, \quad (9)$$

where

$(d\gamma / d \log C)$ – surface activity at specified temperature and concentration (C);

R – universal gas constant ($8.314 \text{ J} \cdot \text{K}^{-1} \cdot \text{mol}^{-1}$);

T – absolute Temperatur (in Kelvin);

n – constant (pre-factor), which value corresponds to number of species, which are forms after molecule dissolution.

- value of the minimum area per molecule (A_{min})

$$A_{\text{min}} = 1 / (\Gamma_{\text{max}} \cdot N_A), \quad (10)$$

where

Γ_{max} – maximum surface excess;

N_A – Avogadro's number ($6.022 \cdot 10^{23} \text{ mol}^{-1}$).

- Gibbs free energy of micellization (ΔG°_m) [general equation for ionic micelles]:

$$\Delta G^\circ_m \approx (1 + \beta) RT \ln \text{CMC}, \quad (11)$$

where

R – universal gas constant ($8.314 \text{ J} \cdot \text{K}^{-1} \cdot \text{mol}^{-1}$);

T – absolute temperature (in Kelvin);

CMC – critical micelle concentration;

β – constant (pre-factor).

- Gibbs free energy of micellization per alkyl tail ($\Delta G^\circ_{m,\text{tail}}$)

$$\Delta G^\circ_{m,\text{tail}} = \Delta G^\circ_m / N_{\text{tail}}, \quad (12)$$

where

ΔG°_m – Gibbs free energy of micellization;

N_{tail} – number of alkyl tail (chains) in surfactant.

- Gibbs energy of transfer ($\Delta G^{\circ}_{\text{trans}}$)

$$\Delta G^{\circ}_{\text{trans}} = \Delta G^{\circ}_{\text{m (mixed system)}} - \Delta G^{\circ}_{\text{m (standard system)}} , \quad (13)$$

where

$\Delta G^{\circ}_{\text{m (mixed system)}}$ – Gibbs free energy of micellization for mixed system or media;

$\Delta G^{\circ}_{\text{m (standard system)}}$ – Gibbs free energy of micellization for standard system or media.

- standard free energy of adsorption ($\Delta G^{\circ}_{\text{ads}}$)

$$\Delta G^{\circ}_{\text{ads}} = (\Delta G^{\circ}_{\text{m}} - \pi_{\text{cmc}}) / \Gamma_{\text{max}} , \quad (14)$$

where

$\Delta G^{\circ}_{\text{m}}$ – Gibbs free energy of micellization;

π_{cmc} – surface pressure at the CMC;

Γ_{max} – maximum surface excess.

- Gibbs free energy of the given air/water interface ($\Delta G^{(s)}_{\text{min}}$)

$$\Delta G^{(s)}_{\text{min}} = A_{\text{min}} \cdot \gamma_{\text{cmc}} \cdot N_{\text{A}} , \quad (15)$$

where

A_{min} – minimum area per molecule;

γ_{cmc} – surface tension at CMC;

N_{A} – Avogadro's number ($6.022 \cdot 10^{23} \text{ mol}^{-1}$).

1.3.3 Solubilization phenomenon in surfactant solutions

Solubilization is increasing of solubility of the low-polar compounds in water in the presence of surfactant micelles [57], [77], [78]. Solubilization, as well as micellization, is connected with hydrophobic interactions. According to actual theory [57], solubilization is the dissolution of organic substances in surfactant micelles. The substance, which dissolved in micelles, called a solubilize or substrate. After solubilization of substrate with surfactant micelles thermodynamically stable isotropic solutions are formed. The solubilization process is dynamic – the substrate is distributed between the aqueous phase and micelles according to corresponding partition coefficient, which depends on the nature and hydrophilic-lipophilic balance of both substances – surfactant and substrate [57].

Typically, the amount of solubilized substance increases proportionally to the surfactant concentration in solution in the region of spherical micelles formation and additionally increases sharply with the formation of lamellar micelles [57], [78].

1.3.4 Surfactant solutions as a reaction media. Micellar catalysis

In case of use the surfactant solutions as a reaction media the reaction rates could be significantly changed due to realization of “micellar catalysis” effects [64], [65], [75], [78], [79], [80], [81]. The main mechanisms of this phenomenon connected with changes in the local concentrations and reactivity of substrates and reagents when the reaction is transferred from the water to surfactant micelles (to micellar pseudophase).

Also, significant influence could have changes in the position of protolytic equilibria in such systems [75].

There are two main approaches which are used for description and evaluation of micellar effects: pseudophase partitioning (PPM) [78], [80] and ion-exchange (IEM) [78], [81] models. Pseudophase model is applicable for the overwhelming majority of micellar catalysis cases except of specific situations, when high concentrations of ionic reagents are used and ion exchange processes in Stern layer become rate-limiting (this situation is covered by ion-exchange model) [81].

The main postulates of pseudophase model are next [78], [80]:

- 1) there are two phases (aqueous phase and micellar pseudophase) in surfactant solutions above the CMC;
- 2) there is an equilibrium in distribution of reagents which stay unchanged (the equilibrium is not dependent on reactions in the system);
- 3) reagents and reaction in the micellar system do not change micelles structure and CMC.

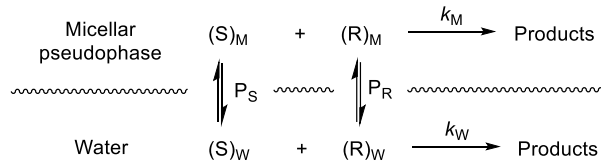


Figure 5. General scheme of bimolecular reaction in micellar system.

The general kinetic scheme of bimolecular reaction in micellar system according to pseudophase model is presented on the Figure 5 and can be described with equation (16) [78], [80]:

$$k_{\text{obs}} = \frac{k_M P_R P_S (C_{\text{surf}}^0 - \text{CMC}) V_M + k_W (1 - (C_{\text{surf}}^0 - \text{CMC}) V_M)}{(1 + (P_R - 1)(C_{\text{surf}}^0 - \text{CMC}) V_M) \cdot (1 + (P_S - 1)(C_{\text{surf}}^0 - \text{CMC}) V_M)} , \quad (16)$$

where

k_{obs} – observed rate constant;

k_M and k_W – rate constants in micellar pseudophase and water, correspondently;

P_R and P_S – partition coefficients of the reagent and substrate, correspondently;

C_{surf}^0 – analytical concentration of surfactant;

CMC – critical micelle concentration;

V_M – partial molar volume of surfactant.

Taking into account, that $CV_M \ll 1$ (the part of micellar pseudophase in solution is not significant) and $P_R \gg 1$, $P_S \gg 1$ (the reagent and substrate effectively bind with micelles), equation (16) can be transform to equation (17):

$$k_{\text{obs}} = \frac{(k_M/V_M) K_R K_S (C_{\text{surf}}^0 - \text{CMC}) + k_W}{(1 + K_R (C_{\text{surf}}^0 - \text{CMC})) \cdot (1 + K_S (C_{\text{surf}}^0 - \text{CMC}))} , \quad (17)$$

where

$K_R = (P_R - 1) V_M \approx P_R V_M$ – binding constant of reagent with micellar pseudophase;

$K_S = (P_S - 1) V_M \approx P_S V_M$ – binding constant of substrate with micellar pseudophase.

1.3.5 Surfactants functionalization

The equation (16) shows that efficiency of reagent and substrate binding with micellar pseudophase are critically important to have high reaction rates. This fact gives a theoretical background for conception of design of functionalized surfactants: introduction of reactive fragment into surfactant molecule structure via covalent bonds can help to provide maximal concentration of reactive species in micelles and high reaction rates even in cases diluted surfactant solutions [78], [80].

In case of surfactant functionalization with group, which is active in studied reactions in deprotonated form (e.g., oxime-functionalized surfactants in acyl substrates decomposition processes [75]), the observed rate constant can be described with equation (18):

$$k_{\text{obs}} = \frac{(k_2^M/V_M)K_S(C_{\text{surf}}^0 - \text{CMC}) + k_{\text{OH}}^W[\text{OH}^-]}{(1 + K_S(C_{\text{surf}}^0 - \text{CMC}))} \cdot \frac{K_{a(\text{app})}}{K_{a(\text{app})} + a_{\text{H}^+}}, \quad (18)$$

where

- k_{obs} – observed rate constant;
- k_2^M – second order rate constant for substrate decomposition in micelles by surfactant functional group;
- k_{OH}^W – second order rate constant for substrate decomposition with OH^- ions in water;
- $K_S = (P_S - 1) V_M \approx P_S V_M$ – binding constant of substrate with micellar pseudophase;
- C_{surf}^0 – analytical concentration of surfactant;
- CMC – critical micelle concentration;
- $[\text{OH}^-]$ – concentration of OH^- ions in water;
- V_M – partial molar volume of surfactant;
- $K_{a(\text{app})}$ – apparent acid ionization constant of surfactant functional fragment;
- a_{H^+} – hydrogen ion activity.

In cases where the substrate effectively binds with surfactant micelles ($K_S > 1000$), the contribution of hydrolysis of the substrate in the aqueous phase to the observed reaction rate becomes insignificant and the denominator $[1 + K_S(C_{\text{surf}}^0 - \text{CMC})] \approx [K_S(C_{\text{surf}}^0 - \text{CMC})]$, which allows to transform equation (18) to (19):

$$k_{\text{obs}} \approx (k_2^M/V_M) \cdot \alpha, \quad (19)$$

where

$$\alpha = K_{a(\text{app})} / (K_{a(\text{app})} + a_{\text{H}^+}) - \text{degree of deprotonation of the functional group.}$$

Functionalization of surfactant molecules with different reactive fragments (oximate [75], hydroxamate [82], amidoximate [83], o-iodosylcarboxylate [84], hydroxyl [85] and imidazolyl [85], [86] groups, Figure 6, and other [87]) have brought outstanding results – the systems for efficient decomposition of toxic organophosphorous neurotoxins (pesticides and chemical warfare agents) were successfully developed [75], [82]. Some of these systems (e.g., oximate [75] and hydroxamate [82] functionalized surfactants) demonstrate also interesting aggregation properties, which could be used in design of pH-sensitive supramolecular aggregates [88], surfactant-polymer composites [89] and metallomicelles [90].

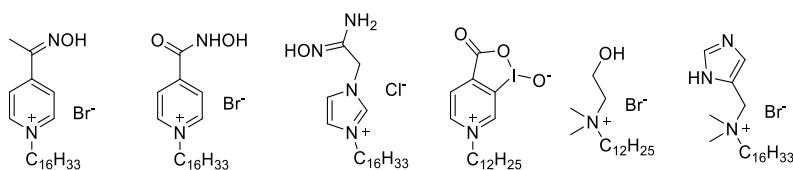


Figure 6. Structures of surfactants, functionalized with oximate, hydroxamate, amidoximate, o-iodosylcarboxylate, hydroxyl and imidazolyl groups (representative examples).

It should be specially noticed that head group of oximate and hydroxamate functionalized surfactants is structurally similar to acetylcholinesterase reactivators, which is used in treatment of organophosphate poisoning [91], [92], [93], and analogs of these functionalized surfactants with short alkyl chain are of undoubted interest for testing as potential reactivators.

1.3.6 Surface-active ionic liquids

Surface-active ionic liquids (SAILs) represent a unique class of ionic liquids engineered with amphiphilic properties, making them proficient in interfacial interactions. These compounds consist of an ionic head and a hydrophobic tail (usually longer than eight carbon atoms), allowing them to self-assemble at interfaces, such as liquid-liquid or liquid-air interfaces (Figure 7) [94]. This amphiphilic nature endows SAILs with exceptional surface activity, and they exhibit surfactant-like behavior while retaining the distinctive characteristics of ionic liquids.

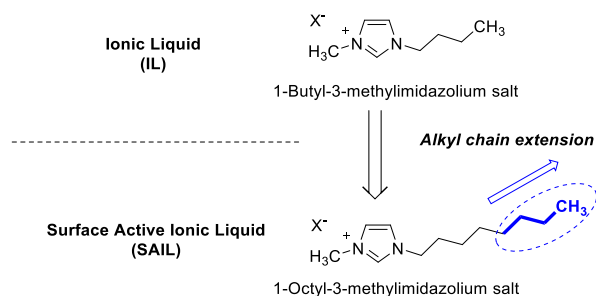


Figure 7. Structural changes in ILs, which lead to the formation of SAILs.

The dual functionality of these compounds imparts versatility, finding applications in various domains, from enhancing solubilization in biphasic systems to stabilizing emulsions and facilitating the extraction of target compounds [50], [95]. Additionally, the tunable nature of both the ionic head and hydrophobic tail in SAILs offers a platform for tailoring their physicochemical properties, thus broadening their utility in areas such as from chemical technology [50], [94], [95] to biomedical applications [94], [96], [97].

1.4 Evaluation of ionic liquids sustainability

Despite the promising applications of ionic liquids, they face challenges that prevent their smooth integration as environmentally friendly materials – for example, some ionic liquids have demonstrated toxicity to aquatic organisms, highlighting the critical need for judicious selection of IL structural components [10], [11], [12], [13], [14], [98]. The challenge lies in understanding the structure-toxicity relationships within ILs, underscoring the

importance of selecting cations and anions that minimize adverse effects [13], [14], [19]. This meticulous approach during the design phase ensures that resulting ILs are not only effective for intended applications but also environmentally benign [13], [19]. Rigorous toxicity assessments and comprehensive studies on IL behavior in different environmental compartments are essential to establish safe usage guidelines [19]. Advancements in designing inherently safer ILs become paramount for realizing their full potential while mitigating adverse effects on aquatic ecosystems and human well-being [14].

Moreover, the extended persistence of specific ILs in the environment raises concerns about their biodegradability and potential long-term effects on ecosystems [13]. ILs' resistance to degradation can lead to accumulation, posing challenges for environmental remediation and sustainability [12], [13]. Understanding the mechanisms governing IL fate in different environmental matrices is crucial for assessing overall impact. Studies focused on biodegradation pathways and the formation of degradation products are imperative to evaluate ecological consequences [15], [19]. Addressing these questions is fundamental for developing environmentally responsible ILs, ensuring their use aligns with broader sustainability goals without compromising delicate ecosystem balances.

1.4.1 Toxicity of ionic liquids

Understanding and comprehensive systematic analysis of the toxicological properties of ionic liquids is challenging due to the diversity of biological entities used for toxicity screening (from enzymes and mammalian cells to bacteria, microalgae, vertebrates and invertebrates) and the significant variability of the ionic liquids structure. It requires a careful approach to analysis and synthesis using the concept of structure-activity relationships [10], [11], [12], [13], [14], [98], [99].

The several IL toxicity mechanisms were identified [10] as follows:

- interruption of the cell membrane caused by high affinity of amphiphilic ILs to membrane lipids (typical for the long chains IL's cations) [100], [101];
- hyperpolarization of the mitochondrial membrane which leads to the production of reactive oxygen and, finally, to cell apoptosis (mechanism is observed for imidazolium-based ILs) [102];
- the lipid membrane lysis [103];
- inducing reactive oxygen stress by increasing of MDA and/or H₂O₂ contents, and enhanced the activity of catalase [104], [105];
- morphological changes in the cell wall and some organs by damaging numerous cell structures [106];
- induced genetic toxicity [107];
- formation of micro-structured domain in water solutions and cytoplasm [108].

In these studies, IL structures were subject to systematic changes, including variations in cation and anion alkyl chain lengths, cation headgroups, anion types, and substituent placement to clarify a role of each component on ILs in toxicity.

It is especially noteworthy that studies conducted using bacteria have shown a clear relationship between the toxicity of ionic liquids and the nature of their cationic part, and especially with the length of the alkyl chain of the cations and the nature of the positively charged center [10], [11], [12], [109]. Such significant influence of cations can be explained by their relatively high lipophilicity and affinity for the phospholipid membrane of microorganisms due to electrostatic interactions between the positive cationic center and the negatively charged phosphocholine or phosphoserine in the cell membrane layer [109].

Although anions with smaller molecular structure and negative charges have lower lipophilicity and lower adsorption affinity for membranes, their effect on toxicity, although less pronounced than cations, remains noteworthy. Judicious selection of anions has proven crucial in reducing overall toxicity [10].

The some general structure-toxicity relationships for ionic liquids are presented on the Figure 8 [10], [98].

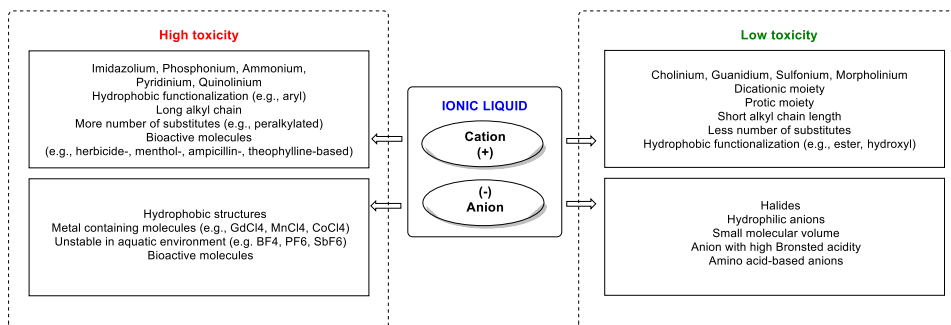


Figure 8. Structure-toxicity relationships for ionic liquids.

1.4.2 Biodegradability of ionic liquids

Information about ILs biodegradability is one more essential parameter, which should be taken into account when ILs sustainability is evaluated. According to OECD 301 Guideline [110] achieving a biodegradation level of 60% within 28 days is typically required to consider chemicals as biodegradable compound. Despite the fact that ionic liquids consist of two structural elements – cation and anion – when assessing their biodegradation, ionic liquids are considered as a single molecule. Nevertheless, the structure of both the cation and the anion can have a significant impact on the result obtained [13].

Influence of cation structure on ILs biodegradability. The structure of the cation is undoubtedly one of the key factors influencing the biodegradation of ionic liquids [13], [14], [19]. The cation, in turn, consists of a charged center of different nature (ammonium, pyridinium, imidazolium, phosphonium, etc.) and substituents at the charged center (protons in case of protic ILs or alkyl / aryl in case of aprotic ILs) [26], [27], [28], [29], [30]. Examples of IL's cations and their abbreviations are presented on a Figure 9.

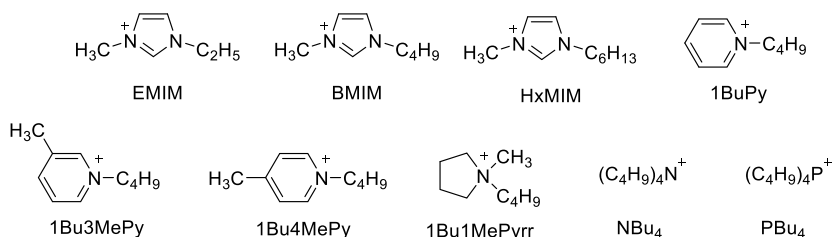


Figure 9. Examples of ILs' cations and their abbreviations.

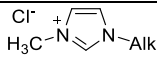
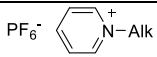
The evaluation of ILs biodegradability data for compounds with variety of charged center nature does not shown any clear trend (see Table 1): the tendency in series of ionic liquids with variety of charged center is not reproducible for similar series, but with other anion. This fact indicates complexity and cross-interaction between ILs structural components.

Table 1. Biodegradation results for ionic liquids with different cations and Tf_2N^- , PF_6^- , BF_4^- anions [13].

Cation (Cat ⁺)	Anion (X ⁻)		
	Tf_2N^-	PF_6^-	BF_4^-
	IL biodegradability, %		
BMIM	90	65	80
1BuPy	86	80	–
1Bu3MePy	17	–	35
1Bu4MePy	30	78	–
1Bu1MePyrr	> 95	–	49
NBu ₄	64	–	–
PBu ₄	–	66	41

In contrast to the nature of the charged cationic center, the influence of the length of alkyl substituent on the biodegradation of ionic liquids is clearer: increasing of the alkyl substituent length leads to decreasing of the ILs biodegradation ability (Table 2). This trend is observed both – imidazolium and pyridinium – ionic liquids.

Table 2. Influence of alkyl chain on biodegradation results for imidazolium and pyridinium ionic liquids [13].

Alkyl chain (Alk)	IL structure	
	Cl^- 	PF_6^- 
	IL biodegradability, %	
C ₂ H ₅	53	> 95
C ₄ H ₉	39	80
C ₆ H ₁₃	37	62
C ₈ H ₁₇	32	–
C ₁₀ H ₂₁	12	–

Influence of anion structure on ILs biodegradability. In ILs, the anions could have organic or inorganic nature [26], [27], [28], [29]. Organic anions, unlike most inorganic ones, can also biodegrade, affecting the observed result (e.g., in case of carbon reach biodegradable C₈H₁₇OSO₃⁻ anion, their presence in the IL molecule should improve observed IL biodegradability [13], [14]). Due to coulombic interaction between cation and anion in ILs [26], [27], [28], [29], it is not expected, that nature of anion can have any influence on cation biodegradability, nevertheless available biodegradation data [13] demonstrate not only influence of anion nature on IL biodegradation (Table 3), but also change of this influence depends on cation structure (Table 4).

For example, 1-butyl-3-methylimidazolium bromide is in ca. 2 times more biodegradable, than 1-butyl-3-methylimidazolium chloride (compare corresponding values in the Table 3).

Table 3. Biodegradation results for 1-butyl-3-methylimidazolium ionic liquids [13].

Anion (X ⁻)	IL biodegradability, %
C ₈ H ₁₇ OSO ₃ ⁻	> 95
Tf ₂ N ⁻	90
[BF ₄] ⁻	80
(CN) ₂ N ⁻	77
Br ⁻	75
CH ₃ SO ₃ ⁻	75
[PF ₆] ⁻	65
CH ₃ COO ⁻	51
Cl ⁻	39
CF ₃ SO ₃ ⁻	34
CF ₃ COO ⁻	20

Analysis of biodegradability data for groups of ILs with different anions (Table 4) demonstrates absence of common group-to-group regularities:

for EMIM biodegradability decreases [PF₆]⁻ > Tf₂N⁻;

for BMIM – Tf₂N⁻ > [BF₄]⁻ > [PF₆]⁻;

for HxMIM – Tf₂N⁻ ≈ [PF₆]⁻ > [BF₄]⁻;

for 1BuPy – Tf₂N⁻ ≈ [PF₆]⁻;

for 1Bu4MePy – [PF₆]⁻ > Tf₂N⁻;

for 1Bu3MePy – [BF₄]⁻ > Tf₂N⁻;

for 1Bu1MePyrr – Tf₂N⁻ > [BF₄]⁻.

Table 4. Biodegradation results for ILs with Tf₂N⁻, [BF₄]⁻ and [PF₆]⁻ anions [13].

	Cation						
	EMIM	BMIM	HxMIM	1BuPy	1Bu4MePy	1Bu3MePy	1Bu1MePyrr
Anion	IL biodegradability, %						
Tf ₂ N ⁻	67	90	73	86	30	17	> 95
[BF ₄] ⁻	–	80	40	–	–	35	49
[PF ₆] ⁻	87	65	70	80	78	–	–

This complex relationship between the structural components of ILs and their biodegradability highlights the need to continue to study their properties in detail to understand role of all factors in observed phenomenon.

1.5 Amino-acid ionic liquids

1.5.1 Amino acid as sustainable building blocks in design of new chemicals

Amino acids – fundamental biomolecules and the building blocks of proteins [111] – stand as promising and sustainable elements for the design of chemicals, embodying unique features that propel them into the forefront of green and sustainable chemistry [13], [19], [112], [113]. These offer distinct advantages that make them a compelling choice in the creation of environmentally friendly and sustainable chemical compounds [13], [19], [114], [115], [116], [117].

One of the primary advantages of amino acids lies in their abundance and renewability [118]. Derived from natural sources, amino acids are readily available from agricultural products or even through biofermentation processes [119], [120]. This contrasts sharply with traditional chemical building blocks, many of which are derived from petrochemical sources, contributing to environmental degradation and resource depletion [114]. The renewable nature of amino acids aligns with the principles of sustainability, offering a pathway to reduce the dependence on finite fossil resources [21], [112].

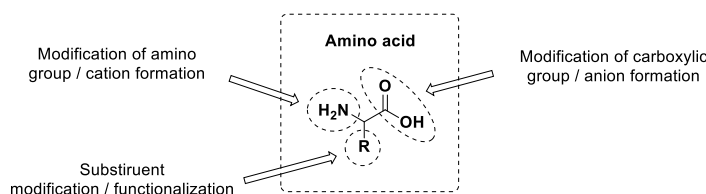


Figure 10. Possible ways of amino acid modification.

The bifunctional structure of amino acids is another key advantage. Combining both amine and carboxylic acid groups, amino acids provide a versatile platform for chemical design (Figure 10). This dual functionality allows for the facile construction of diverse chemical structures [121]. The presence of amino and carboxyl groups enables the creation of amino acid-based salts, esters, and amides, and, in combination with possibility to modify substituent (R) in some structures, offering a rich diversity in the types of sustainable chemicals that can be synthesized (Figure 10). This flexibility in chemical design contributes to the adaptability of amino acids in various applications [115], [116], [121], [122], [123].

Moreover, the potential biocompatibility of amino acids adds another layer of appeal to their use in sustainable chemical design [13], [15], [19]. Amino acids are intrinsic to biological systems, and their compatibility with living organisms positions them as ideal candidates for applications where toxicity and environmental impact are critical considerations [115]. This biocompatibility not only enhances the safety profile of amino acid-based chemicals, but also opens avenues for applications in fields such as pharmaceuticals, cosmetics, and food industries, aligning with the growing demand for eco-friendly and health-conscious products [13], [115], [116], [121], [122], [123].

1.5.2 Design of amino acid ionic liquids

Due to attractive properties of amino acid as sustainable building blocks [21], [112], they were used in design of sustainable ionic liquids [13], [15], [19], [115], [116], [117].

Amino acids were introduced into ionic liquids structure as a counter ion without modification (Figure 11) [115], [117] as well as structurally modified fragment (Figure 12) [115], [117].

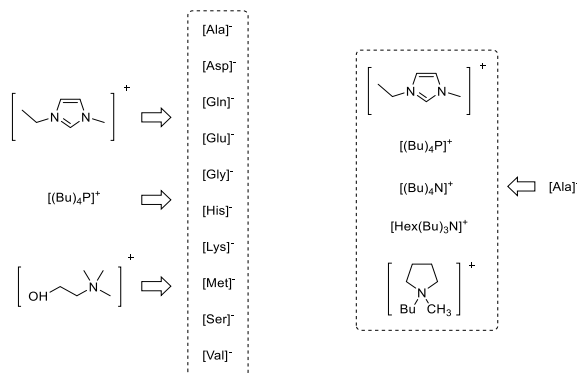


Figure 11. Examples of ionic liquids with non-modified amino acids as counter ion.

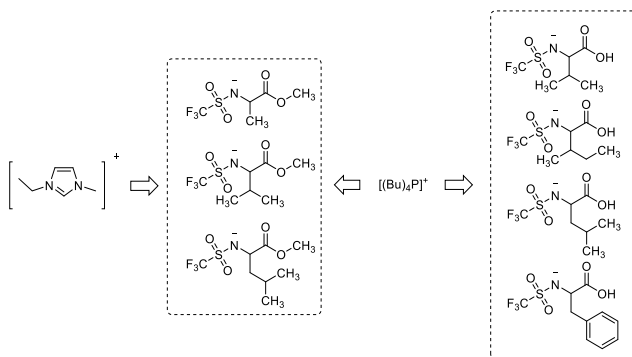


Figure 12. Examples of ionic liquids with modified amino acids as counter ion.

Also, they were introduced into ionic liquids structure as a covalently bonded fragment (Figure 13) [124]

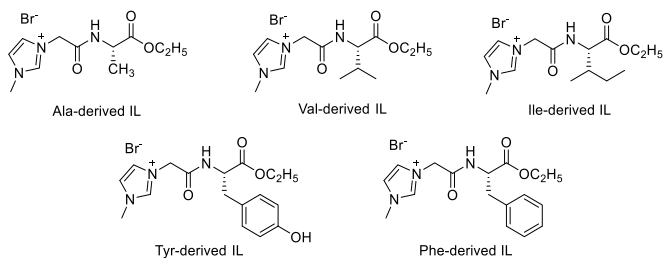


Figure 13. Examples of imidazolium ionic liquids with amino acids in their structure.

Analysis of available literature data [13], [14], [15], [16], [17], [18], [19] can help to highlight *phenylalanine* as one of most prospective amino acid for design of low toxic and biodegradable ionic liquids.

1.5.3 Phenylalanine-derived ionic liquids as a prospective molecular platform for future improvement and practical applications

For phenylalanine-derived ionic liquids a broad variation of positively charged center nature was performed (see Figure 14) [16], [17].

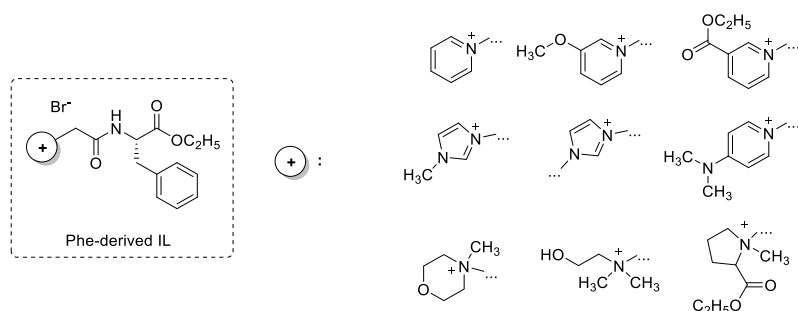
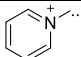
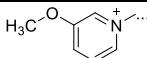
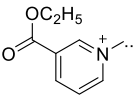
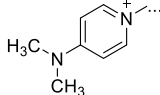
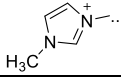
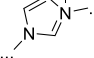
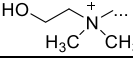
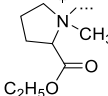
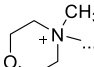


Figure 14. Variation of the positively charged center structure for phenylalanine-derived ionic liquids.

Biodegradability data for these compounds (see Table 5; [16]) shows that among studied structures a most prospective for future application is phenylalanine-derived ionic liquid with pyridinium cation, because it demonstrates 63 % biodegradability and according to OECD 301 Guideline [110] can be classified as biodegradable. All other cations demonstrate lower biodegradability. It is worth noting that derivatization of pyridinium fragment leads to decreasing of biodegradability, but nature of substituent is important – carboxylic group in position 3 of pyridinium ring decrease biodegradability to 32%, while the methoxy group in the same position reduces biodegradation only to 52%. The less attractive are cations which alkylammonium charged center – biodegradability of these compounds does not exceed 24%.

Table 5. Biodegradation results for phenylalanine-derived ionic liquids [16].

Positively charged center (\oplus) structure	IL biodegradability
	63 %
	52 %
	32 %
	33 %
	47 %
	40 %
	24 %
	21–24 %
	17 %

The comprehensive study of the influence of the alkyl chain length on different properties (aggregation behavior, bacterial / fungal toxicity, ecotoxicity, biodegradability, biotransformation pathways study, etc.) of pyridinium, imidazolium and cholinium phenylalanine-derived ionic liquids (Figure 15) was performed in works [17], [18], [19].

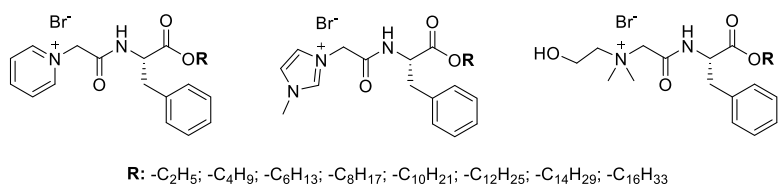


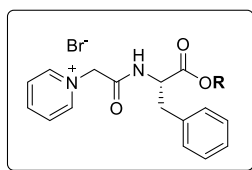
Figure 15. Alkyl chain length variation for pyridinium, imidazolium and cholinium phenylalanine-derived ionic liquids.

The key conclusions of this multiparameter evaluation were:

- the nature of the cationic head group and the chain length impacted on the mineralization, biodegradability of the studied ILs [17], [19];
- the toxicity of studied ILs was largely driven by the length of the alkyl chain (hydrophobicity) and not the type of cationic part of the ILs [17], [18];
- the biodegradability of ILs decreased in the order $PyPheC_n > ImPheC_n > CholPheC_n$ [19];

- completely biodegradable ILs were only identified in the PyPheC_n series [19];
- the ecotoxicity of the studied ILs was increasing in parallel to their hydrophobicity up to log $K_{ow} = 1$ (C₈–C₁₀) and then leveling up, being consistent with the previously obtained analogous data sets (the “cut-off” effect) [18];
- bacterial and fungal toxicities were strictly dependent on the side chain length and aggregation properties, and changed from low to high for compounds C₂–C₁₀/C₁₂, then “cut-off” effect also observed [17];
- the phenyl group of the L-phenylalanine moiety essentially contributing to the self-assembling properties in addition to the lipophilic side chain [17];
- the medium chain length (C₆ to C₈) pyridinium SAILs have been recommended as the most prospective green alternatives for conventional cationic surfactants [19].

Thus, among studied compounds, pyridinium phenylalanine-derived ionic liquids (Figure 16) represent a most compelling class of molecules with significant potential for future advancements and practical applications.



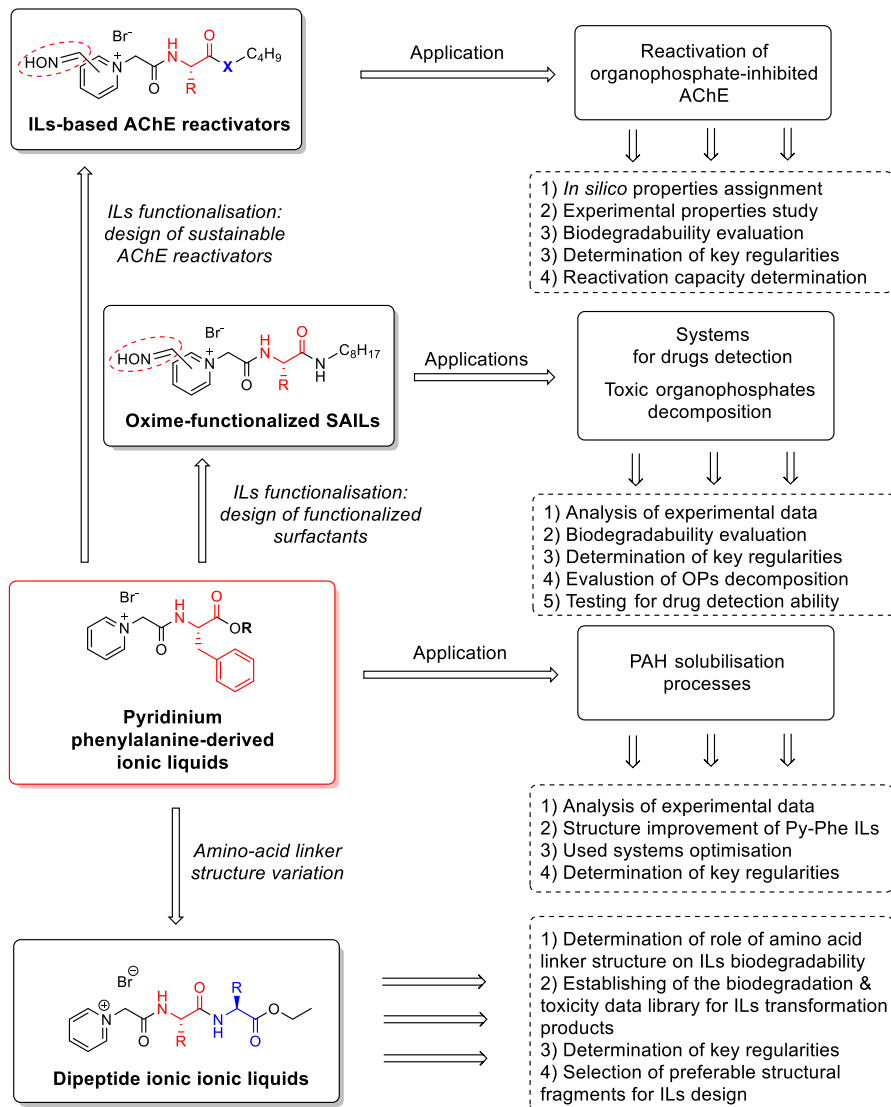
R: -C₂H₅; -C₄H₉; -C₆H₁₃; -C₈H₁₇; -C₁₀H₂₁; -C₁₂H₂₅; -C₁₄H₂₉; -C₁₆H₃₃

Figure 16. Pyridinium phenylalanine-derived ionic liquids – prospective object for future studies and improvements.

Derived from the amino acid phenylalanine, these ionic liquids exhibit unique properties that make them versatile candidates for various applications in chemistry and materials science. The inherent structural features of phenylalanine contribute to the design of tailored ionic liquids, allowing for precise control over their physicochemical properties. This tunability is pivotal for creating molecular platforms with desirable characteristics, such as solubility [17], biodegradability [17], [19], toxicological [17], [18] and aggregation properties [17], making them promise for applications ranging from green solvents to advanced materials.

1.5.4 The strategy for further study and improvement of the selected sustainable ionic liquids-based molecular platform

Taking into account discussed features of the structure of selected pyridinium phenylalanine-derived ionic liquids, the strategy of their possible practical application and further structure improvement could be presented using the scheme below:



This strategy will define the main aims of the present work.

2 Aims of the present work

The pyridinium phenylalanine-derived ionic liquids represent a group of sustainable products, developed in accordance with green chemistry principles. These compounds are intriguing not only as materials for direct application, but also as a promising molecular platform that can be easily modified and adapted to address a new range of problems.

Therefore, the main aims of the present work are:

- to determine efficiency of pyridinium phenylalanine-derived ionic liquids in solubilization of polycyclic aromatic hydrocarbons;
- to develop and propose a concept of sustainable process for polycyclic aromatic hydrocarbons extraction using pyridinium phenylalanine-derived ionic liquids;
- to evaluate possible ways of structure improvement for pyridinium phenylalanine-derived ionic liquids;
- to determinate structure-properties relationship for structural fragments of amino acid derived ionic liquids and create a fragments library for future use in design of sustainable ionic liquids;
- to design and investigate functionalized surfactants based on pyridinium-derived ionic liquids with focus on application of these compounds in processes of toxic organophosphates decompositions and compounds detection;
- to synthesize and study new sustainable acetylcholinesterase reactivators based on pyridinium-derived ionic liquids.

3 Results and discussion

3.1 Design of sustainable SAILs-based systems for solubilization of polycyclic aromatic hydrocarbons (Publication IV)

Polycyclic aromatic hydrocarbons (PAHs) are important industrial products [125] and, in the same time, they can be dangerous environmental pollutants [126]. In different technological processes for extraction of PAHs are usually used organic solvents [127], but this approach cannot be considered as acceptable from green chemistry point of view [21], [112], [113] and has serious safety issues (many of organic solvents used are volatile, flammable and toxic) [127]. The prospective alternatives for organic solvent in such processes are solutions of surfactants (Figure 17), which, from one side, use green and safe solvent – water – as a main component of the system [21], [112], [113], and, from other side, can effectively dissolve (solubilize) PAHs in surfactant micelles [128].

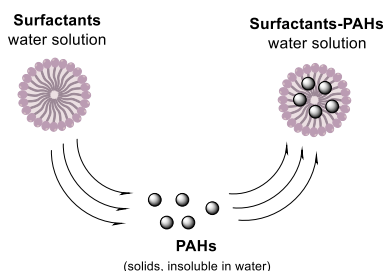


Figure 17. PAHs solubilization in water solutions of surfactants.

The problems of surfactant systems, which limit their use, connected with difficulties of PAHs separation from surfactant micelles [128] and surfactants persistence in the environment and/or their toxicity to aquatic organisms [129], [130]. Surface active pyridinium phenylalanine-derived ionic liquids (Figure 17; were discussed in the section 1.5.3), look very attractive for this application due to low toxicity and biodegradability [17], [18], [19].

3.1.1 Evaluation of pyridinium phenylalanine-derived SAILs efficacy in processes of PAHs solubilization

Efficacy of pyridinium phenylalanine-derived SAILs (PyPheOC_n; structure see on Figure 16) in processes of PAHs solubilization was evaluated related to typical polycyclic aromatic hydrocarbons – naphthalene, anthracene and pyrene – and compared with efficacy of classical cationic surfactant – cetyltrimethylammonium bromide [CTABr] (Figure 18). Evaluation of efficacy was performed based on comparison of solubilization capacity of studied systems.

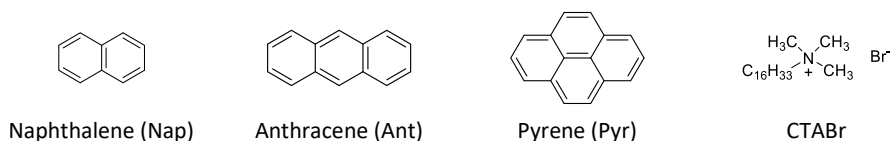


Figure 18. Structures of PAHs and cetyltrimethylammonium bromide [CTABr].

Solubilization capacity of the surfactant (S) [57], [131], related to corresponding PAH, was determined from dependency of absorbance A of studied solution (surfactant/water system saturated with PAH) from surfactant concentration C_{surf} (Figure 19) using the ratio $S = \beta/\epsilon$ (β – the slope of the linear part of the dependence; ϵ , $\text{M}^{-1} \cdot \text{cm}^{-1}$ – molar extinction coefficient of PAH on chosen wavelength; the brake-point on a graph corresponds to cmc of surfactant).

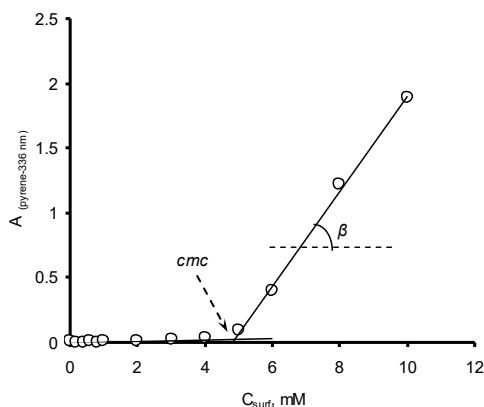


Figure 19. Dependency of the absorbance of solution A on the wavelength 336 nm from surfactant concentration C_{surf} for the system PyPheOC_8 / pyrene [the figure was taken from Publication IV].

Obtained results are summarized on the Figure 20 and in the Table 6. In all studied cases solubilization capacity increases with increasing of number of carbon atoms (n) in ester side chain of pyridinium phenylalanine-derived SAILs PyPheOC_n . This regularity is typical for surfactants and connected with increasing of their hydrophobicity [57], [131]. The solubilization capacity of conventional cationic surfactant CTABr is comparable to solubilization capacity of PyPheOC_n with $n \approx 10$ –12 (for Pyr), $n \approx 10$ –12 (for Nap) and $n \approx 12$ –14 (for Ant), and follows cmc of these surfactants (Table 6). It demonstrates that efficacy of pyridinium phenylalanine-derived SAILs PyPheOC_n in processes of PAHs solubilization is similar to conventional cationic surfactants, and they could be used as an alternative for conventional cationic surfactants.

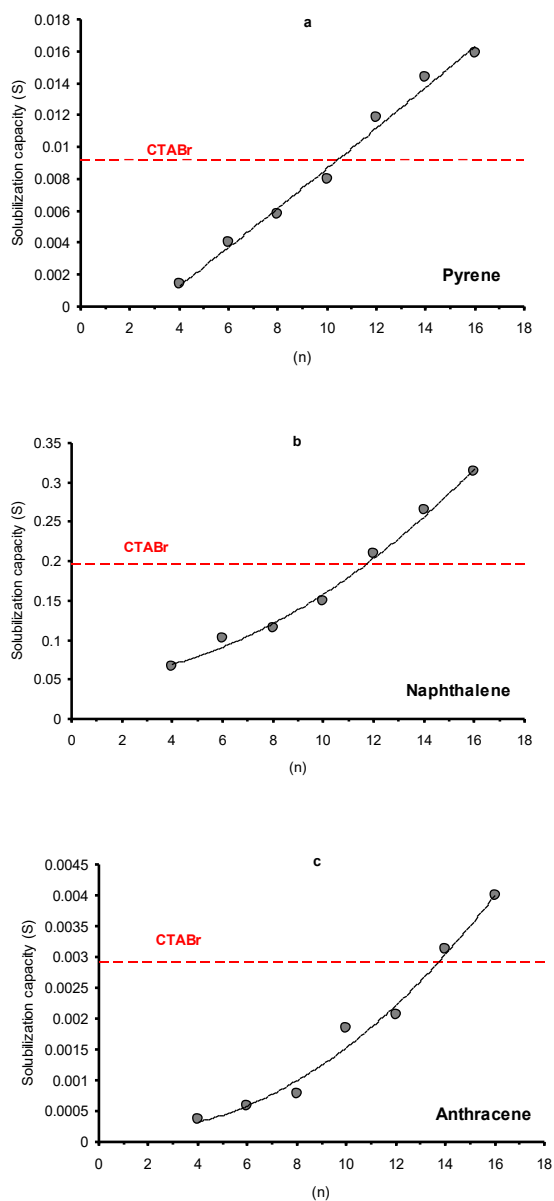


Figure 20. Dependencies of solubilization capacity (S) on alkyl chain length (n) of PyPheOC _{n} SAILs towards pyrene (a), naphthalene (b), and anthracene (c) compared to solubilization capacity of CTABr [the figure was taken from Publication IV].

Table 6. Physico-chemical parameters for PyPheOC_n and CTABr surfactant systems in processes of PAHs solubilization [taken from Publication IV].

PyPheOC _n chain length (n)	cmc, mM					β			Solubilization capacity (S)		
	Surface tension*	Conductivity*	Solubilization								
			Nap	Ant	Pyr	Nap	Ant	Pyr	Nap	Ant	Pyr
4	57	89	80	90	80	21.4	5.6	90.4	0.067	0.00037	0.0014
6	11	19.9	25	23	26	32.7	9	251.9	0.102	0.00060	0.0040
8	2.25	4.9	5.2	3.7	4.9	36.9	11.7	366.6	0.115	0.00077	0.0058
10	0.65	1.6	1.6	1	1.4	48.1	27.9	503	0.150	0.00185	0.0080
12	0.19	0.5	0.2	0.1	0.3	67.1	31.3	745.7	0.210	0.00207	0.0119
14	0.056	0.18	0.1	0.07	0.08	84.9	47.4	905.2	0.265	0.00314	0.0144
16	0.0125	0.037	0.05	0.04	0.05	100.5	60.3	996	0.314	0.00399	0.0159
CTABr **	0.9	1	1	1	0.8	62.5	43.9	573.6	0.195	0.00291	0.0091

Notes:

* Values of critical micelle concentration (cmc) for PyPheOC_n surfactants, found by means of surface tension and conductivity methods, were taken from [17];

** values of critical micelle concentration (cmc) for CTABr, found by means of surface tension and conductivity methods, were taken from [131]

3.1.2 Selection of enzymatic systems and reaction condition optimization for pyridinium phenylalanine-derived SAILs decomposition

Pyridinium phenylalanine-derived SAILs PyPheOC_n have in their structure two bonds – amide and ester bonds in phenylalanine fragment – which could be cleaved with formation of products, suitable for future resynthesis of initial SAIL structure (Figure 21).

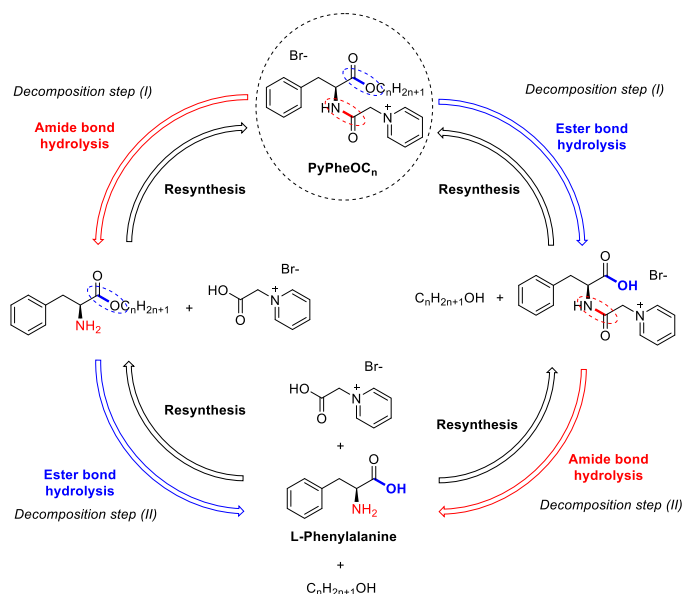


Figure 21. Possible decomposition / resynthesis pathways for PyPheOC_n SAILs.

Decomposition of PyPheOC_n component of surfactant-PAH aggregates will be led to loss of solution ability to keep PAH dissolved (solubilized), and PAH will precipitate from solution (Figure 22).

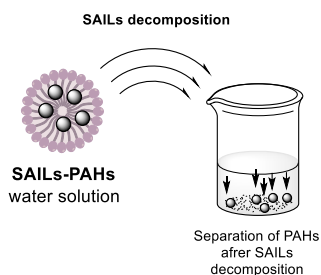


Figure 22. Separation of PAHs after PyPheOC_n SAILs decomposition.

Due to the presence of amino acid fragment (phenylalanine) in the structure of PyPheOC_n SAILs, these compounds could be tested as a substrate for esterase, amidase and protease enzymes.

Enzymes are unique biological catalysts which combine high selectivity with outstanding efficiency in mild reaction conditions [111], [132]. Using enzymatic systems for performance of chemical transformations is highly recommended from green chemistry perspective, because it helps to decrease energy costs, avoid side reactions and toxic waste accumulation, and perform processes fast and selectively [21], [112], [113].

To proof of the concept of enzymatic systems application for PyPheOC_n SAILS decomposition 24 different commercially available immobilized enzymes (2 amidases, 2 esterases and 20 proteases) from different sources were tested (Table 7). As a substrate, represents PyPheOC_n SAILS, compound PyPheOC₄ with n = 4 was used.

Table 7. Immobilized enzymes tested in PyPheOC_n SAILS decomposition processes.

Enzyme	Source	Activity
A1	<i>Escherichia coli</i>	NLT 850 U/g
A2	<i>Achromobacter</i>	NLT 250 U/g
E1	<i>Pichia sp.</i>	NLT 10000 PLU/g
E2	<i>Pichia sp.</i>	NLT 10000 PLU/g
P1	<i>Bacillus Sp.</i>	400 ELU/g
P2	<i>Bacillus Sp.</i>	750 ELU/g
P3	<i>Bacillus Sp.</i>	100 ELU/g
P4	<i>Bacillus Sp.</i>	275 ELU/g
P5	<i>Mucor miehei</i>	8 ELU/g
P6	<i>Bacillus licheniformis</i>	400 ELU/g
P7	<i>Bacillus amyloliquefaciens</i>	15 ELU/g
P8	<i>Geobacillus sp.</i>	5 ELU/g
P9	<i>Trichoderma reesei</i>	5 ELU/g
P10	<i>Bacillus subtilis</i>	225 ELU/g
P11	<i>Bacillus subtilis</i>	400 ELU/g
P12	<i>Aspergillus oryzae</i> var.	5 ELU/g
P13	<i>Aspergillus oryzae</i>	65 ELU/g
P14	<i>Bacillus subtilis</i>	150 ELU/g
P15	<i>Aspergillus niger</i>	5 ELU/g
P16	<i>Bacillus subtilis</i>	10 ELU/g
P17	<i>Bacillus subtilis</i>	175 ELU/g
P18	<i>Carica papaya</i>	5 ELU/g
P19	<i>Pineapple stem</i>	5 ELU/g
P20	<i>Fig tree latex</i>	5 ELU/g

In parallel to immobilized enzymes activities screening, the optimization of the reaction conditions (substrate concentration, quantities of enzymes, pH, temperature, shaking speed and incubation period) was performed (Table 8). Monitoring of PyPheOC₄ decomposition processes was performed using the ¹H NMR technique. Activity of enzymes was evaluated on each step of process optimization, but for final step of testing only amidases 1 & 2 and proteases P1-P4, P6, P10, P11, P13, P14, P17 were selected as most active enzymes (Figure 23). All selected enzymes in the final test demonstrated 100% ester bond hydrolysis in substrate. Amide bond hydrolysis in any significant quantities was observed only in case of P13 enzyme (about 10–20%).

Table 8. Optimization of the reaction conditions for PyPheOC₄ enzymatic decomposition.

#	PyPheOC ₄ conc. (% w/v)	pH	Enzymes tested	Enzyme test conc. (g)	Incubating temperature (°C)	Shaking speed (rpm)	Incubation time (days)
1	2	5.5	Amidase 1&2	0.2	40	170	3
2	1	5.5	Amidase 1&2 Esterase 1&2	0.2	40	170	3
3	1	5.5	Amidase 1&2 Protease 1-20	0.1	50	100	7
4	0.5	6.5	Amidase 1&2 Protease (P1-P4, P6, P10, P11, P13, P14, P17)	0.1	50	100	7

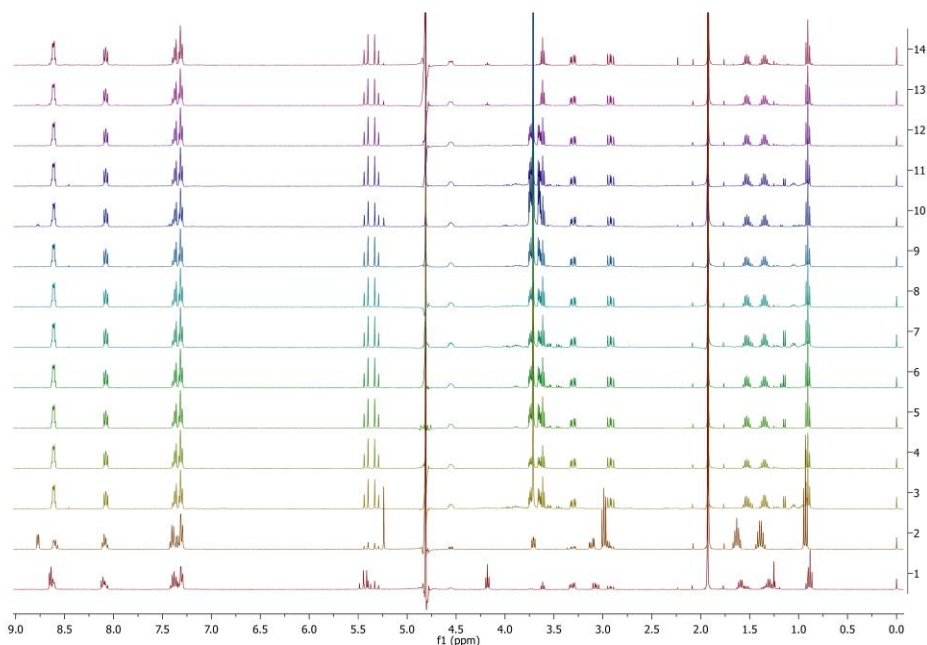


Figure 23. ¹H NMR spectra of PyPheOC₄ solutions after incubations with selected amidase and protease enzymes at pH 6.5 (concentration of PyPheOC₄ 0.5%). Spectrum 1 (bottom) correspond to PyPheOC₄ after incubation in buffer without enzymes; spectrum 2 recorded for model mixture of expected hydrolytic products; spectra 3–12 represent incubation with proteases P1, P2, P3, P4, P6, P10, P11, P13, P14, P17; spectra 13 and 14 represent incubation with amidase 1 and amidase 2, correspondingly [the figure was taken from Publication IV].

3.1.3 Structure improvement of PyPheOC_n SAILs: design of diamide derivatives PyPheNHC_n

The analysis of reaction products in processes of PyPheOC_n SAILs enzymatic decomposition clearly shows that ester bond hydrolysis is a fast preferable process. Further decomposition of Py⁽⁺⁾-CH₂-CO-NH-Phe-COOH (see Figure 21) with studied enzymes is problematic. Only in case of P13 enzyme, amide bond degradation products was observed in relatively big amounts. This fact indicates that esterolysis product is problematic substrate for enzymes (most probably due to its poor affinity to active site caused by formation of negative charge on carboxylic group in solution [132]).

The prospective way to improve PyPheOC_n SAILs properties is exchange of ester bond in their structure on amide bond with formation of diamide derivatives PyPheNHC_n (see Figure 24). These molecules compared with initial structures will be more resistant to chemical non-enzymatic hydrolysis (because the amide bond is less reactive [133]). This change can help to additionally expand application possibilities for PyPheNHC_n and cover alkali solutions as possible media for extraction or reaction processes. Also changes in the structure can have an influence on enzymatic degradation and can change preferable degradation pathway.

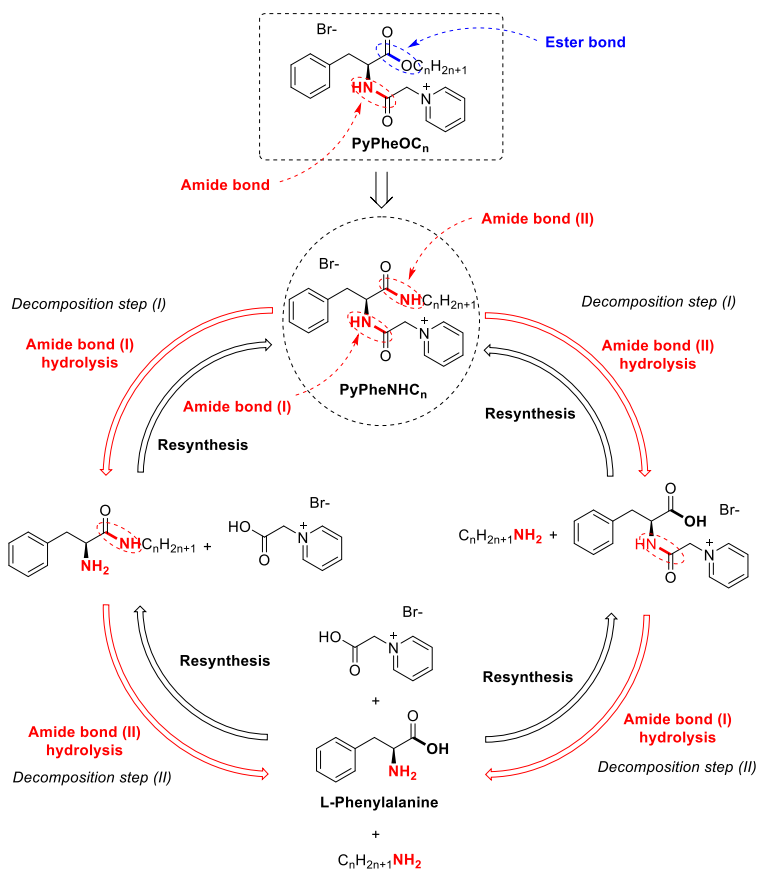


Figure 24. Structure modification for PyPheOC_n SAILs and possible decomposition / resynthesis pathways for PyPheNHC_n SAILs.

3.1.4 Enzymatic systems screening in processes of diamide derivatives PyPheNHC_n decomposition

In the screening of enzymatic systems for diamide derivatives PyPheNHC_n decomposition the compound PyPheNHC₄ with $n = 4$ was used as their representative example. The enzymatic systems selection approach remains the same as in case of PyPheOC_n SAILs: the initial activities screening and process optimization were performed for all amidases 1 & 2 and proteases P1–20 enzymes, but for future conditions improvement were selected only most active ones (P1, P2, P3, P4, P6, P10, P11, P13, P14, P17 proteases and amidase 1 & 2). It should be noted, that protease P13 (source – *Aspergillus oryzae*; enzyme activity 65 ELU/g) on a step of preliminary optimization have already demonstrate 87% amide bond hydrolysis in PyPheNHC₄ substrate. The repetition of PyPheNHC₄ hydrolysis in the optimized conditions (substrate concentration 0.5% w/v; 50 °C, 100 rpm and 7 days incubation time) with selected enzymes shows, that protease P13 gives 100% amide bond hydrolysis (Figure 25).

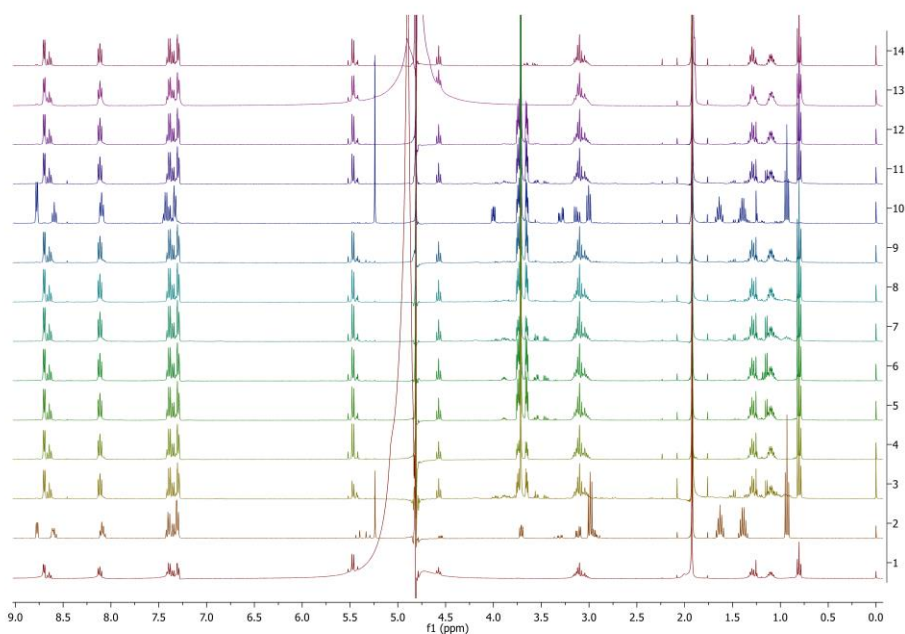


Figure 25. ¹H NMR spectra of PyPheNHC₄ solutions after incubations with selected amidase and protease enzymes at pH 6.5 (concentration of PyPheNHC₄ 0.5%). Spectrum 1 (bottom) corresponds to PyPheNHC₄ after incubation in buffer without enzymes; spectrum 2 recorded the model mixture of expected hydrolytic products; spectra 3–12 represent incubation with proteases P1, P2, P3, P4, P6, P10, P11, P13, P14, P17; spectra 13 and 14 represent incubation with amidase 1 and amidase 2, correspondingly [the figure was taken from Publication IV].

Aspergillus oryzae (*A. oryzae*) is a filamentous micro-fungus that is used for centuries in fermentation of different foods in many countries all over the world [134]. The prevalence and extensive experience with this enzyme source make P13 protease attractive for further use in processes of PyPheNHC_n hydrolytic decomposition.

3.1.5 Sustainable pyridinium phenylalanine-derived ionic liquids in processes of polycyclic aromatic hydrocarbons extraction: application concept

The results obtained allow us to propose an application concept of pyridinium phenylalanine-derived ionic liquids in processes of polycyclic aromatic hydrocarbons extraction (Figure 26): the low toxic biodegradable phenylalanine-derived SAILs will be used for preparation of the water solutions for extraction / solubilization of PAHs, which is in compliance with green chemistry principles. After PAHs extraction / solubilization with water solution of phenylalanine-derived SAILs obtained PAHs/SAILs solution could be segregated and treated with immobilized enzymes to decompose SAILs, which will lead to precipitation of PAHs. PAHs could be separated from the water solution of SAILs decomposition products by filtration. The composition of SAILs hydrolysis product mixture can be adjusted depends on SAILs type (PyPheOC_n or PyPheNHC_n) and enzymatic system used. Water solutions of SAILs hydrolysis products could be used for resynthesis of initial SAILs structure, and then used in the next cycle of PAHs extraction / solubilization. Aqueous solutions of SAILs hydrolysis products could be excluded from the process and biodegraded. Thus, proposed process concept follows green chemistry principles [21], [112], [113] not only in process design itself, but also covers a problem of the fate of reagents after process completion.

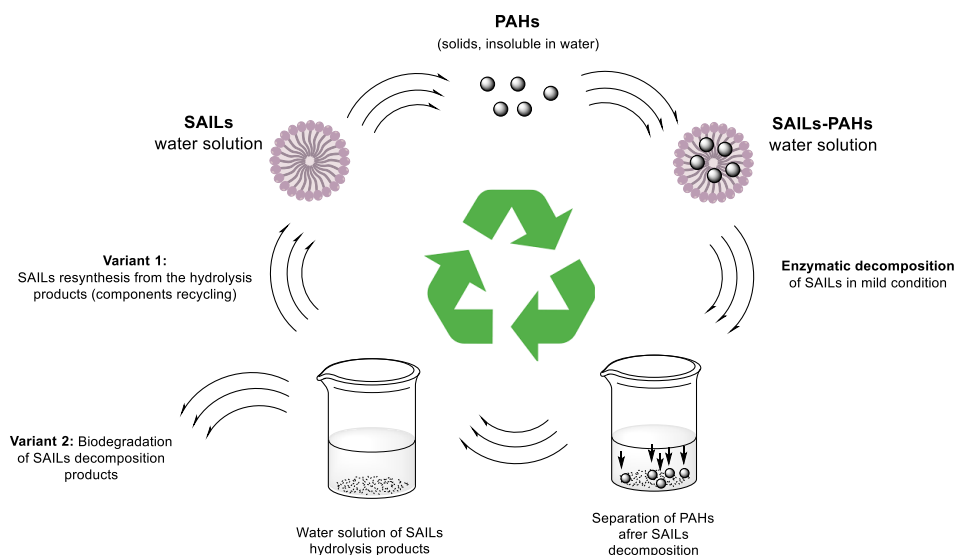


Figure 26. Application concept of pyridinium phenylalanine-derived ionic liquids in processes of polycyclic aromatic hydrocarbons extraction.

3.2 Ionic liquids structure improvement: dipeptide-based ionic liquids (Publication III)

Amino acids are prospective sustainable building blocks for designing new materials [117], [121], [122], [123]. To bring a new properties and functionality to existing molecules designed based on amino acids, the strategy inspired by nature could be used – extension of amino acid scaffold in the molecule. Expanding of the pyridinium phenylalanine-derived ionic liquids application can be performed through introduction of new amino acid fragments into basic IL structure. These changes should be supported by understanding of relationship between compound structure and their properties.

To make the design of new amino acid-derived ionic liquids more predictable and to collect data about molecular fragments suitable for design of sustainable molecules, the several structures were considered for future study and evaluation (Figure 27).

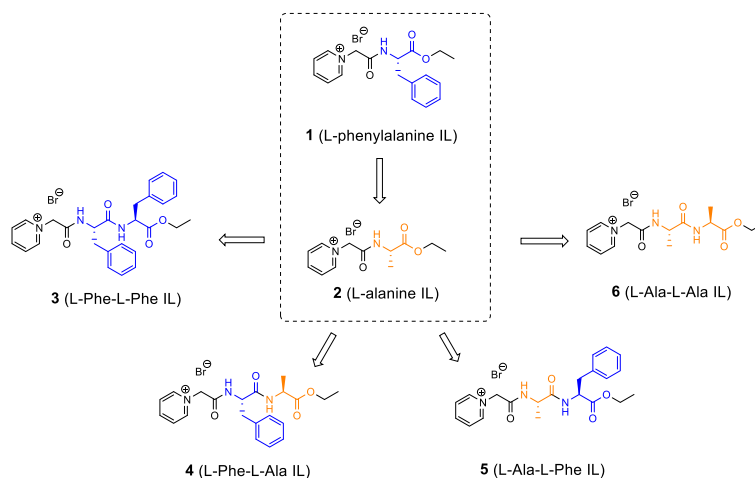


Figure 27. Amino acid ILs (1, 2) and dipeptide ILs (3–6) with L-phenylalanine and L-alanine moiety in structure.

In current study compound **1** represents pyridinium phenylalanine-derived ionic liquids (PyPheOC_n with n = 2), compound **2** is alanine analog of compound **1**, which can help to clarify a role of hydrophobic substituent on toxicological properties and biodegradation, dipeptide ILs **3–6** will be used for determination of role of dipeptide fragment in IL structure.

The first step of amino acid derived ILs biodegradation connected with hydrolysis of amide and ester bonds in ILs structure [19]. The hydrolysis products can then undergo further transformation and, in the case of biodegradable intermediates, give as final products CO₂, H₂O and N₂. If persistent products are formed, their further biodegradation will stop and they will accumulate in the system [13], [14].

To avoid the formation of persistent transformation products the structure of ILs should be designed without problematic fragments, which after ILs hydrolysis can give these persistent metabolites. For the realization of this strategy the information about biodegradability and toxicological properties of different possible transformation products is critically important. The creation of such a library is one more task of this work.

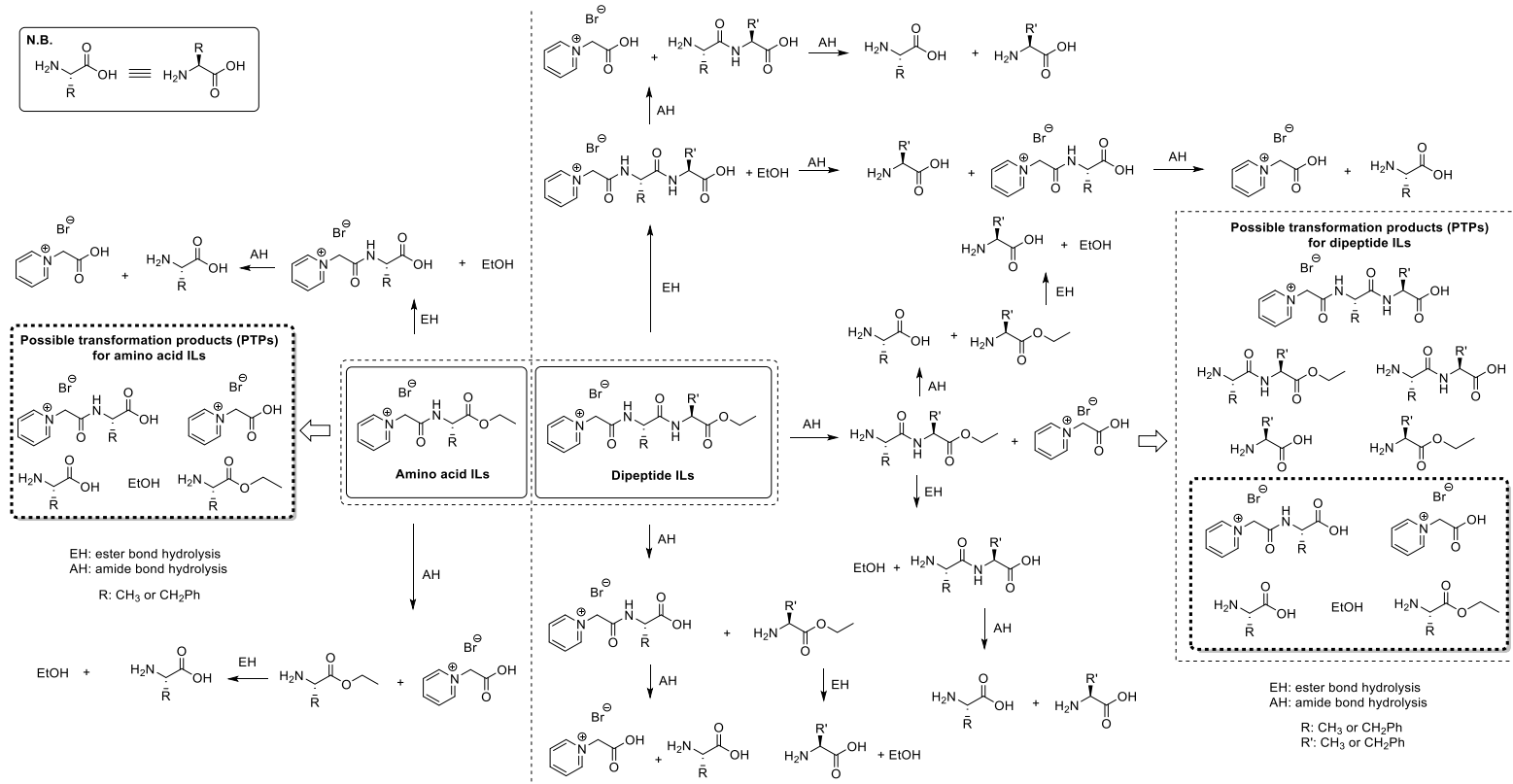


Figure 28. Biodegradation pathway analysis and selection of possible transformation products [the figure was taken from Publication III].

3.2.1 Analysis of ILs biodegradation pathways and selection of possible transformation products and synthesis of target molecules

The possible biodegradation pathways for ILs **1–6** are presented in Figure 29. Despite the variety of possible hydrolysis directions, the careful analysis of all these transformations demonstrated significant overlap in expected structure of transformation products (TPs). For example, all TPs, expected for ILs **1** and **2**, could be observed also in case of decomposition of ILs **3–6** (see Figure 28).

The structure of all possible transformation products for ILs **1–6** are collected in Figure 29.

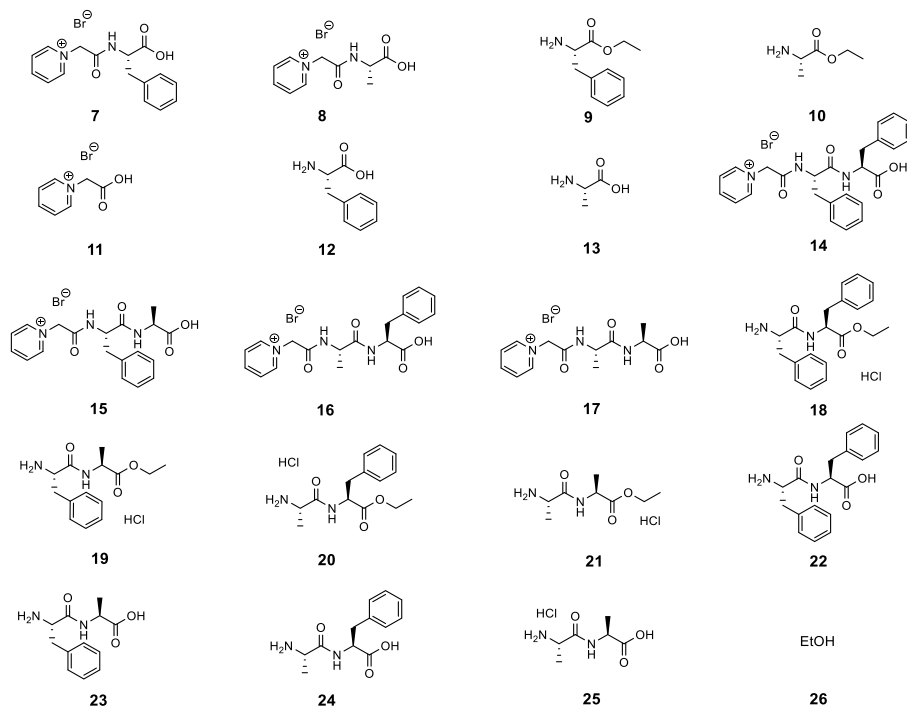


Figure 29. Structures of possible transformation products in processes of amino acid ILs (**1**, **2**) and dipeptide ILs (**3–6**) biodegradation.

The synthesis of these TPs for investigation, as well as ILs **1–6**, was performed according to the scheme, presented on the Figure 30. The TPs **22–25** are commercially available and purchased from Fluorochem Ltd. Ethanol (**26**) was not tested and considered as biodegradable and not toxic, because it is normal metabolite of all living organisms and in conditions of modified closed bottle test (aerobic biodegradation testing according to OECD 301D guidelines [110]) its concentration ($< 5 \text{ mg L}^{-1}$) is not enough to demonstrate antiseptic properties [135].

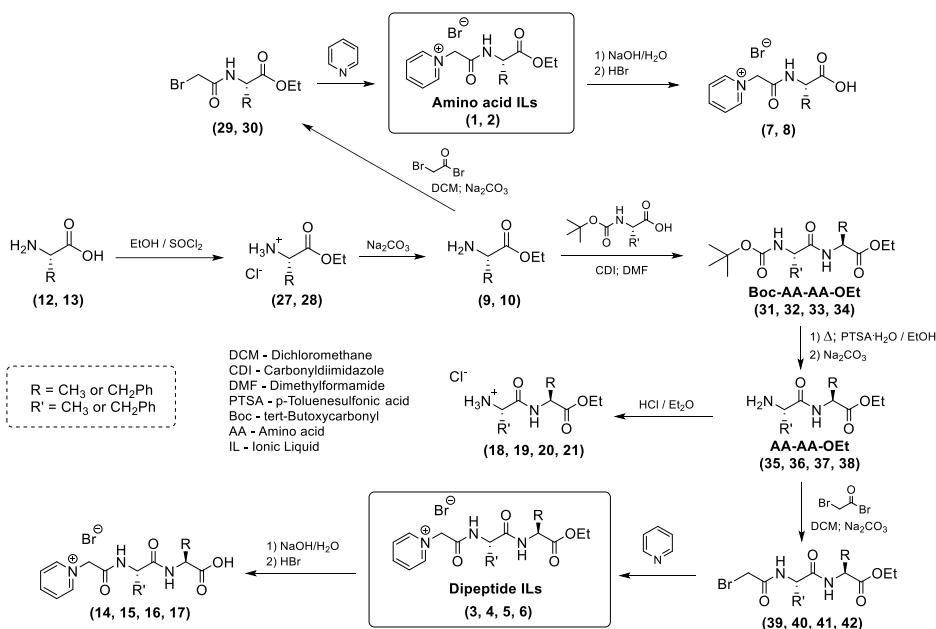


Figure 30. Synthesis of ILs 1–6 and their possible transformation products.

The procedures of compounds 1–21 synthesis was evaluated according to Green Chemistry principles using J. Clark's Green Chemistry metrics toolkit [25] on zero and first pass level. The majority of reactions give the yield, conversion, and selectivity above 90% (only in one case the yield and selectivity were slightly lower – 87%). Atom economy (AE) and reaction mass efficiency (RME) were in range 70–100% and 40–99%, correspondently. The optimum efficiency (OE) for most reactions was above 80%. According to classification [25], most of obtained values can be rated with green flag, except of several of them which can be rated with amber flag. Evaluation of process mass intensity (PMI) parameters indicates that further improvement of reactions / processes used should be oriented on reducing of the solvents volume in the workup steps.

For synthesis of compounds 1–21 green (water, ethanol, ethyl acetate, acetone; [25]) as well as problematic solvents (e.g. DMF, DCM, diethyl ether and petroleum ether; [25]) were used. The usage of problematic solvents is considered as acceptable due to possibility of implementation of solvent recovery process with solvent recovery yield > 80%.

In synthesis of target products were used only elements from supply remaining list marked with green or amber flags.

By energy parameters, any from synthesis or workup steps can't be marked with red flag, nevertheless for some of synthesis steps (e.g. synthesis of compounds 7, 8, 14, 15, 16, 17) further improvements are possible – the process could be realized in flow regime using immobilized enzymes, which is preferable form Green Chemistry position.

Thus, evaluation of the processes for the synthesis of compounds 1–21 using J. Clark's Green Chemistry metrics toolkit [25] allows us to determine those process parameters that can be further improved to make the used processes greener.

More details about application of J. Clark's Green Chemistry metrics toolkit [25] for evaluation of compounds 1–21 synthesis processes are given in Publication III.

3.2.2 Microbial toxicity and biodegradation screening of amino acid ILs, dipeptide ILs and their potential transformation products

Toxicity screening of amino acid ILs **1** & **2**, dipeptide ILs **3–6** and their potential transformation products **7–25** against Gram-positive and Gram-negative bacteria (*Staphylococcus aureus* spp. *aureus* (ATCC 29213); *Staphylococcus aureus* spp. *aureus* (ATCC 43300); *Staphylococcus epidermis* (clinical isolate); *Enterococcus faecalis* (ATCC 29212); *Escherichia coli* (ATCC 25922); *Klebsiella pneumoniae* (clinical isolate); *Serratia marcescens* (clinical isolate); *Pseudomonas aeruginosa* (ATCC 27853)) as well as yeast and fungi (*Candida albicans* (ATCC 24433); *Candida albicans* (ATCC 90028); *Candida krusei* (ATCC 6258); *Candida glabrata* (ATCC 90030); *Candida parapsilosis* (ATCC 22019); *Candida tropicalis* (ATCC 750); *Pichia quilliermondii* (ATCC 90877); *Saccharomyces cerevisiae* (ATCC 9763); *Aspergillus fumigatus* (ATCC 204305); *Aspergillus flavus* (CCM 8363); *Absidia corymbifera* (CCM 8077); *Microsporium canis* (CCM8353); *Trichophyton interdigitale* (ATCC 9533)) does not indicate any toxic compound (with MIC < 10 µM in 24 h). Usually, for tested compounds MIC is > 2000 µM (or more than maximal concentration tested) in 24 h and 48 h. Some compounds (dipeptide ILs **6** and TPs **9**, **10** and **18**) have demonstrated antimicrobial activity against selected strains of microorganisms, but, nevertheless, they can't be classified as toxic [136], [137], [138]. E.g., MIC for dipeptide ILs **6** against *Staphylococcus aureus* spp. *aureus* (ATCC 29213) was 125 / 500 µM (24 h/48 h), against *Staphylococcus aureus* spp. *aureus* (ATCC 43300) – 500 / 500 µM (24 h/48 h), against *Staphylococcus epidermis* (clinical isolate) – 1000 / 2000 µM (24 h/48 h), *Enterococcus faecalis* (ATCC 29212) – 2000 / > 2000 µM (24 h/48 h), *Escherichia coli* (ATCC 25922) – 1000 / 1000 µM (24 h/48 h), *Klebsiella pneumoniae* (clinical isolate) – 2000 / 2000 µM (24 h/48 h); for other Gram-positive / Gram-negative bacteria, and all yeast and fungi tested dipeptide ILs **6** did not show any toxicity effects at maximal concentration used for testing.

TPs **9**, **10** and **18** sometimes demonstrate activity against selected yeast and fungi strains (but not against Gram-positive / Gram-negative bacteria) with MIC 1000 – 2000 µM.

Based on the toxicological data obtained, it is expected that the toxicological properties of compounds **1–25** will not influence the results of the biodegradability tests of these compounds in the Closed bottle test (CBT) performed in compliance with recommendations of the OECD 301 D protocol [110].

Absence of influence of tested compounds on microorganisms in inoculum, used for CBT, was verified and confirmed for each tested compounds within special “toxicity series”, which was always carried out in parallel with the main experiment (Figure 31).

In the current study the standard Closed bottle test (OECD 301 D protocol) was extended up to 42 days (instead of standard 28 days) following recommendations from [19].

Results of biodegradability testing of compounds **1–25** in modified CBT (OECD 301 D protocol) are collected in the Table 9.

Table 9. Results of biodegradability testing of compounds **1–25** in modified CBT (OECD 301 D protocol).

Comp. number	Conc. in CBT, μM	10-day-window analysis				D% 14 days	D% 28 days	D% 42 days
		Start day	Start D%	End D%	$\Delta\text{D}\%$			
1	7.8	6	11 \pm 2	45 \pm 4	34	43 \pm 6	64 \pm 3	66 ^a \pm 3
2	12.0	2	13 \pm 1	20 \pm 1	7	22 \pm 1	25 \pm 2	30 \pm 1
3	5.2	5	11 \pm 2	55 \pm 6	44	52 \pm 4	76 \pm 1	84 \pm 1
4	6.8	2	16 \pm 1	59 \pm 14	38	61 \pm 14	83 \pm 8	91 \pm 5
5	6.8	4	12 \pm 4	26 \pm 16	14	26 \pm 16	52 \pm 4	73 \pm 4
6	9.8	13	10 \pm 5	36 \pm 11	26	13 \pm 6	46 \pm 7	61 \pm 5
7	9.2	5	31 \pm 1	46 \pm 2	15	46 \pm 2	65 \pm 6	66 ^a \pm 6
8	15.6	19	16 \pm 7	41 \pm 5	25	7 \pm 3	40 \pm 6	43 ^a \pm 4
9	12.0	2	26 \pm 2	48 \pm 3	22	51 \pm 3	60 \pm 5	61 \pm 3
10	26.0	4	42 \pm 1	66 \pm 1	24	66 \pm 1	73 \pm 1	74 \pm 1
11	22.3	2	11 \pm 1	16 \pm 2	5	17 \pm 2	61 \pm 16	93 \pm 3
12	15.6	5	50 \pm 4	58 \pm 1	8	54 \pm 1	65 \pm 2	74 ^b \pm 4
13	52.1	2	26 \pm 9	36 \pm 1	10	34 \pm 1	48 \pm 1	62 ^b \pm 3
14	5.8	4	22 \pm 2	34 \pm 1	12	34 \pm 1	46 \pm 2	49 \pm 2
15	7.8	4	20 \pm 1	39 \pm 11	19	39 \pm 11	56 \pm 2	62 \pm 3
16	7.8	4	17 \pm 10	27 \pm 11	10	27 \pm 11	41 \pm 9	45 \pm 10
17	12.0	6	11 \pm 1	19 \pm 4	8	18 \pm 4	40 \pm 1	48 \pm 1
18	6.8	3	11 \pm 1	43 \pm 1	32	45 \pm 1	59 \pm 4	60 \pm 3
19	9.8	2	12 \pm 4	49 \pm 1	37	51 \pm 1	66 \pm 4	67 \pm 7
20	9.8	4	17 \pm 1	53 \pm 1	36	53 \pm 2	71 \pm 2	75 \pm 1
21	17.4	4	16 \pm 1	52 \pm 1	36	52 \pm 1	73 \pm 2	80 \pm 1
22	7.8	2	12 \pm 1	50 \pm 1	38	52 \pm 1	68 \pm 1	68 \pm 1
23	12.0	4	35 \pm 1	62 \pm 1	27	62 \pm 1	71 \pm 1	73 \pm 1
24	12.0	4	35 \pm 1	51 \pm 2	16	51 \pm 2	57 \pm 2	59 \pm 2
25	26.0	4	26 \pm 1	35 \pm 1	9	35 \pm 1	57 \pm 1	64 \pm 1

^a 33 days, ^b 37 days

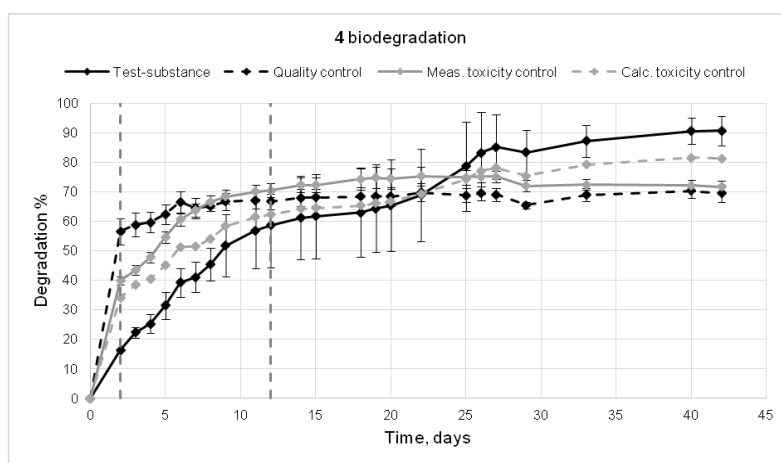


Figure 31. Biodegradation curve for compound **4** (L-Phe-L-Ala IL) with quality control, measured and calculated toxicity control curves (representative example; 10-day-window is indicated by two vertical dashed lines).

IL **1**, synthesized based on amino acid L-phenylalanine, demonstrated ca. 2 times higher biodegradability compared with L-alanine-based IL **2** (64% vs 25% after 28 days incubation time; Table 9) and according to OECD 301 D requirements [110] can be considered as biodegradable. Obtained results confirm that presence of hydrophobic phenyl fragment makes IL **1** more preferable substrate for biodegradation, than much less hydrophobic IL **2**. Introduction of second amino acid residue into initial IL structure helps significantly improve biodegradability: after 28 days incubation time dipeptide ILs **3**, **4**, **5**, **6** demonstrate biodegradability 76 %, 83 %, 52 % and 46%, correspondently. In extended CBT test (42 days incubation time) all studied dipeptide ILs pass 60% threshold for biodegradable compounds, prescribed by OECD 301 D [110]. Important to note, that position of L-phenylalanine fragment in dipeptide IL has a big influence on IL's biodegradability. IL **4** (Py⁺-Phe-Ala IL) with phenylalanine fragment connected to charged pyridinium ring compared with its isomer IL **5** (Py⁺-Ala-Phe IL), which has alanine fragment connected to charged pyridinium ring, shows after 28 days on ca. 30 % higher biodegradability and pass 60% threshold. Compound **4** according to 10-day-window criteria is very close to requirements for readily biodegradable molecules (a molecule could be classified as ready biodegradable if it shows at least 60% biodegradability in 10 day window after reaching of 10 % degradation [19], [110]) while IL **5** is quite far from this limit.

Analysis of Figure 28 is shown that IL **1** could give TPs **7**, **9**, **11**, **12**, **26**; IL **2** – TPs **8**, **10**, **11**, **13**, **26**; IL **3** – TPs **7**, **9**, **11**, **12**, **14**, **18**, **22**, **26**; IL **4** – TPs **7**, **10**, **11**, **12**, **13**, **15**, **19**, **23**, **26**; IL **5** – TPs **8**, **9**, **11**, **12**, **13**, **16**, **20**, **24**, **26**; IL **6** – TPs **8**, **10**, **11**, **13**, **17**, **21**, **25**, **26**.

In extended CBT test the overwhelming majority of these TPs demonstrate biodegradability more or close to 60 %. Only for selected TPs biodegradability was in range 40-60% (Table 9).

The analysis of biodegradability data for TPs **7–25** confirms, that introduction of L-alanine fragment can bring more problematic products compared with compounds, designed based on L-phenylalanine residues.

3.3 Functionalization of sustainable SAILs: design and new applications (Publication I and Publication II)

Introduction of new functional groups into the compounds structure is a prospective way to bring a new functionality to the molecule. This strategy was widely used last years for design of advanced materials [139]. Functionalization of surfactant molecules with functional groups, which can participate in protolytic equilibria in solution, helps to create pH-responsible supramolecular systems with tunable properties [88], mixed polyelectrolyte / surfactant composites [89] and enzyme-like micellar hydrolytic systems [75], [88]. In all these cases the surfactant molecules were functionalized with oxime moiety, which, from one side, can initiate the changes in aggregates structure due to ability to dissociate depends on pH [88], from other side, it can be transformed to very reactive nucleophilic species (oximate ions are high reactive α -nucleophiles, which demonstrate outstanding reactivity in acyl group transfer processes [75], [88]). Combination of these properties makes oxime group very attractive as a candidate for introduction to SAILs structure and future testing of obtained functionalized SAILs for different applications.

3.3.1 Objects selection, structure variation and synthesis of oxime-functionalized SAILs

The most convenient place for introduction of oxime moiety into L-phenylalanine-derived SAILs structure is a pyridinium ring, because corresponding pyridine derivatives (pyridinium aldoximes), which is necessary for synthesis of target compounds, are not expensive and commercially available products. The variation of oxime group position in pyridinium ring can help to evaluate the influence of this factor on the compounds properties and functionality. To increase the stability of oxime derivatives in alkali solutions it makes sense to substitute the ester bond, presented in initial SAILs structure, on amide bond. To evaluate the role of amino acid fragment structure, L-phenylalanine residue in the L-phenylalanine-derived functionalized SAILs (4-PyPheC8) was substituted on L-alanine fragment (4-PyAlaC8) and compared with compound (4-PyC8), which does not contain amino acid fragment in the structure. All target products were synthesized with C₈H₁₇ alkyl substituent, which based on available literature data [17], [18], [19] could be considered as an optimal for such type of surfactants (Figure 32).

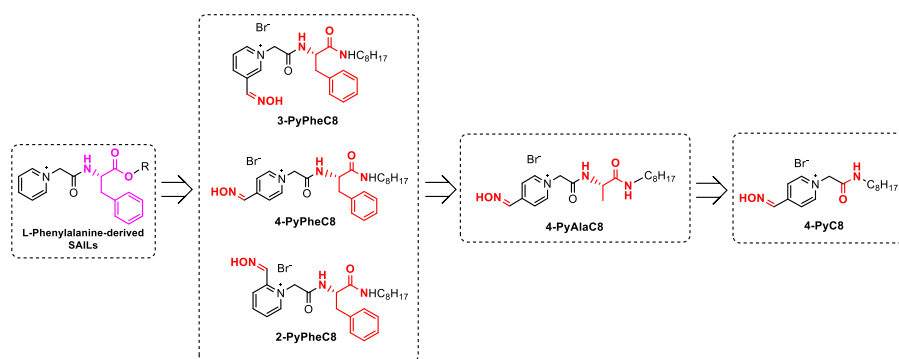


Figure 32. Objects selection and structure variation for oxime-functionalized SAILs.

The target oxime-functionalized SAILs were synthesized according to common synthetic scheme, presented on the Figure 33.

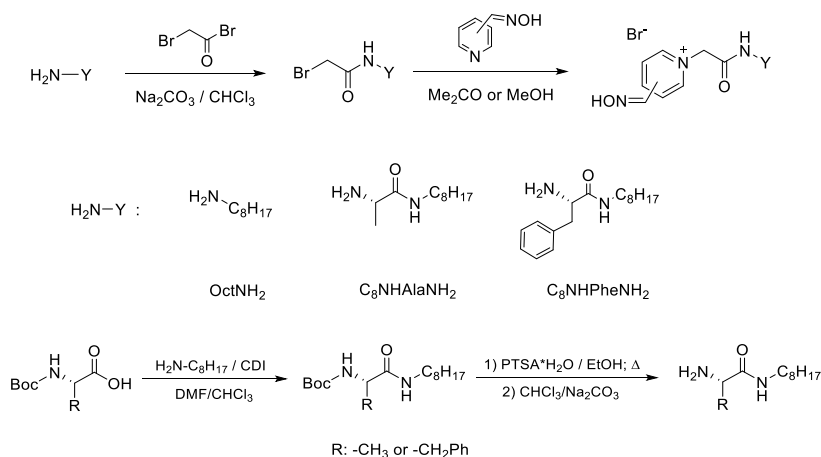


Figure 33. Synthesis of the target oxime-functionalized SAILs.

3.3.2 Protolytic equilibria in solutions of oxime-functionalized SAILs

Determination of pK_a values for oxime-functionalized SAILs in different conditions (including presence of different types of co-surfactants) is an important step in rational design of supramolecular systems on their basis.

The protolytic equilibria in solutions of oxime-functionalized SAILs could be described with scheme, presented on the Figure 34. Oxime moiety can dissociate in solution and transforms to oximate anion, which is α -nucleophile [75], [88]. Also, deprotonation of oxime group changes a molecule total charge, which could have an influence on aggregates formation in SAILs solution.

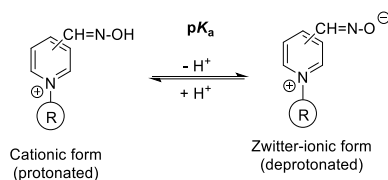


Figure 34. The protolytic equilibria in solutions of oxime-functionalized SAILs.

In current study pK_a values of oxime-functionalized SAILs were determined for individual compounds and for their comicelles with cationic gemini surfactants (12-4-12 and 16-10-16) and anionic surfactant SDS (Figure 35) by spectrophotometric technique (Figure 36).

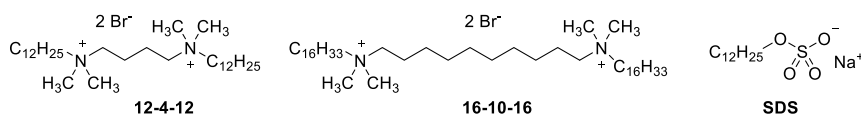


Figure 35. The structures of surfactants 12-4-12, 16-10-16 and SDS.

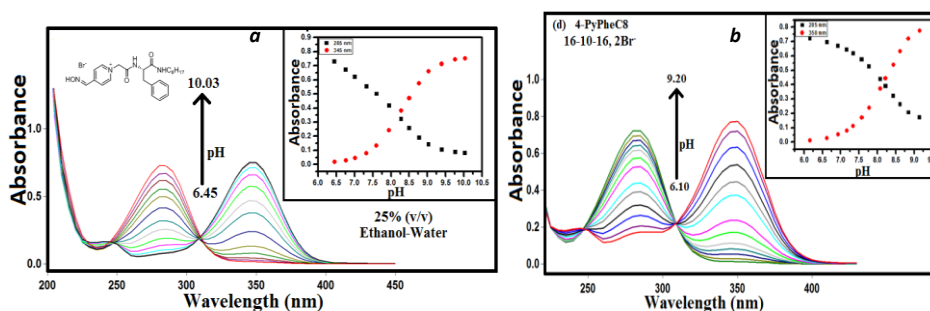


Figure 36. Representative absorption spectra and plots at two selected wavelength for individual SAIL **4-PyPheC8** (a) and for system **4-PyPheC8 / 16-10-16** (b) at different pH values; 27 °C.

The obtained pK_a values are collected in the Table 10. For individual oxime-functionalized SAILs pK_a values increase slightly in the series **4-PyC8** \approx **4-PyAlaC8** > **4-PyPheC8**, which could be connected with realization of π - π stacking between phenyl ring in phenylalanine and pyridinium core for **4-PyPheC8**. Impotent to notice, that studied oxime-functionalized SAILs in comicelles with cationic surfactants 12-4-12 and 16-10-16 do not

demonstrate difference in pK_a values (most probably due to interaction of phenyl ring of **4-PyPheC8** with positively charged ammonium fragments of co-surfactants used). This assumption is also confirmed an observation of regularity **4-PyC8** \approx **4-PyAlaC8** > **4-PyPheC8** in pK_a values for comicelles with SDS, which is similar to regularity for individual oxime-functionalized SAILs. SDS due to negative charge cannot interact with phenyl ring of **4-PyPheC8**. SDS as co-surfactant, in general, makes dissociation of oxime group of oxime-functionalized SAILs less preferable, which affects on pK_a values.

Table 10. pK_a values of oxime-functionalized SAILs in the absence and in the presence of co-surfactants; 27 °C, $[D]_0 = 10$ mM.

Compound	Medium	pK_a	$pK_{a,app}$ (in presence of co-surfactants) ^b		
			12-4-12	16-10-16	SDS
4-PyC8	Water	8.08	8.21	8.22	8.93
4-PyAlaC8	25% (v/v) Ethanol-Water	8.12	8.27	8.24	8.82
4-PyPheC8	25% (v/v) Ethanol- water	8.48	8.21	8.25	9.25
3-PyPheC8	25% (v/v) Ethanol- water	9.00	–	9.21	–
2-PyPheC8	25% (v/v) Ethanol- water	7.89	8.01	7.98	9.40
4-PAM	Water (1M KCl)	8.61 ± 0.04^a	–	–	–
3-PAM	Water (1M KCl)	9.51 ± 0.06^a	–	–	–
2-PAM	Water (1M KCl)	8.04 ± 0.05^a	–	–	–

Notes: *a* – literature data [140], [141]; *b* – water; CMC of 12-4-12 is 1.17 mM [142], 16-10-16 is 0.051 mM [143] and SDS is 8.2 mM [144].

The regularities in changes of pK_a values for oxime-functionalized SAILs with different positions of oxime group in pyridinium ring (**2-PyPheC8** > **4-PyPheC8** > **3-PyPheC8**) remains unchanged both for solutions of individual SAILs and for their co-micelles with cationic surfactant 16-10-16. This regularity represents the classical influence of electronic effects of substituents on the functional group [133] and follows the trend for methylpyridinium aldoximes (**2-PAM** > **4-PAM** > **3-PAM**) know from the literature [140], [141] (structures of methylpyridinium aldoximes are presented on the Figure 37).

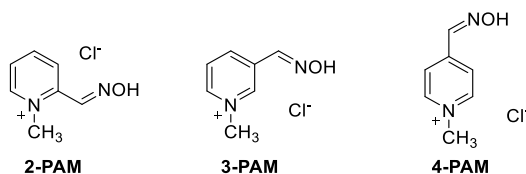


Figure 37. Structure of methylpyridinium aldoximes.

3.3.3 Aggregation properties of mixed systems oxime-functionalized SAIL / 16-s-16 surfactants

For detailed investigation of aggregation properties of mixed systems oxime-functionalized SAIL / co-surfactant were selected **4-PyC8** (Figure 32) as representative examples of oxime-functionalized SAILs and two cationic gemini surfactants 16-s-16 with $s = 10$ and 12 (Figure 38).

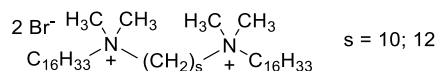


Figure 38. Structure of cationic gemini surfactants 16-s-16.

The aggregation properties of **4-PyC8** / 16-s-16 systems were characterized using standard approaches – tensiometry, conductivity and fluorescence techniques – and obtained results are summarized in the Table 11.

The critical micelle concentration for mixed **4-PyC8** / 16-s-16 systems significantly decreases compared with CMC of individual 16-s-16 surfactants. The effect of **4-PyC8** introduction on CMC values is mostly connected with decreasing of the electrostatic repulsion of positively charged head groups of 16-s-16 surfactants due to incorporation of **4-PyC8** molecules between 16-s-16 molecules in comicelles. Counter ion dissociation (α), surface pressure at CMC (π_{CMC}), surface excess parameters (Γ_{max}), aggregation numbers (N_{agg}) and Stern–Volmer constants (K_{SV}) are decreasing, minimum surface area per molecule (A_{min}) and surface tension at CMC (γ_{CMC}) with increasing of contents (wt%) of the functionalized IL **4-PyC8** in **4-PyC8** / 16-s-16 comicelles.

The Gibbs energy parameters ($\Delta G_{\text{min}}^{(s)}$, $\Delta G_{\text{m}}^{\circ}$, $\Delta G_{\text{m,tail}}^{\circ}$, $\Delta G_{\text{ads}}^{\circ}$, $\Delta G_{\text{trans}}^{\circ}$) indicate, that formation of aggregates in solutions for studied systems is energetically favorable process and they are thermodynamically stable.

Investigation of **4-PyC8** / 16-s-16 systems using NMR and IR methods does not indicate any specific interaction in comicelles. It means that for these systems the main driving force of aggregates formation is non-specific hydrophobic interactions (like in case of “classical” micelles [57], [58]).

Table 11. Physico-chemical properties of the systems gemini surfactants 16-s-16 / 4-PyC8 with different contents (wt%) of the functionalized IL 4-PyC8 at 300 K.

IL 4-PyC8 (wt%)	CMC (mM)			α	γ_{CMC} (mN·m ⁻¹)	π_{CMC} (mN·m ⁻¹)	Γ_{max} (10 ⁶ mol·m ⁻²)	A_{min} 10 ²⁰ (m ² mol ⁻¹)	$\Delta G_{\text{min}}^{(\text{s})}$ (kJ/mol)	$\Delta G_{\text{m}}^{\circ}$ (kJ/mol)	$\Delta G_{\text{m,tail}}^{\circ}$ (kJ/mol)	$\Delta G_{\text{ads}}^{\circ}$ (kJ/mol)	$\Delta G_{\text{trans}}^{\circ}$ (kJ/mol)	N_{agg}	K_{SV}
	Conductivity	Surface tension	Fluorescence												
16-10-16															
Water	0.028 ^a	0.029	0.030 ^b	0.60	38	34.1	2.10	79.18	18.12	-14.69	-7.34	-30.95	—	57	6.99
0.2	0.023	0.024	0.025	0.51	41	31.4	1.30	128.36	31.48	-16.55	-8.27	-40.82	-1.86	53	6.50
0.5	0.023	0.021	0.021	0.31	45	27.1	1.22	135.75	36.79	-20.23	-10.11	-42.40	-5.54	51	6.17
0.7	0.016	0.016	0.017	0.23	46	25.6	1.19	139.04	38.93	-22.10	-11.05	-43.55	-7.41	49	5.88
1.0	0.013	0.013	0.013	0.23	49	22.9	0.99	167.09	49.51	-22.68	-11.34	-45.74	-7.99	45	5.45
16-12-16															
Water	0.021 ^a	0.022	0.023 ^b	0.67	40	31.0	1.99	83.88	20.46	-14.11	-7.57	-29.69	—	51	6.25
0.2	0.017	0.016	0.016	0.44	45	26.5	1.27	131.45	35.62	-18.49	-9.24	-39.4	-4.38	50	6.12
0.5	0.011	0.011	0.011	0.39	50	21.5	1.26	132.04	39.76	-20.39	-10.10	-37.49	-6.28	48	5.85
0.7	0.009	0.009	0.009	0.29	53	18.5	1.20	138.21	44.12	-22.75	-11.30	-38.15	-8.64	46	5.55
1.0	0.005	0.006	0.006	0.25	55	16.5	0.93	178.72	59.19	-25.08	-12.50	-42.83	-10.97	43	5.18

Notes:

^a Literature data, ref. [145]; ^b literature data, refs. [146, 147]; the calculations of aggregation numbers (N_{agg}) and Stern–Volmer constants (K_{SV}) are described in details in *Publication II*.

CMC – critical micelle concentration;

α – counter ion dissociation;

γ_{CMC} – surface tension at CMC;

π_{CMC} – surface pressure at CMC;

Γ_{max} – surface excess parameter;

A_{min} – minimum surface area per molecule;

$\Delta G_{\text{min}}^{(s)}$ – Gibbs free energy of the given air/water interface;

$\Delta G_{\text{m}}^{\circ}$ – Gibbs free energy of micellization;

$\Delta G_{\text{m,tail}}^{\circ}$ – Gibbs free energy of micellization per alkyl tail;

$\Delta G_{\text{ads}}^{\circ}$ – standard free energy of adsorption;

$\Delta G_{\text{trans}}^{\circ}$ – Gibbs energy of transfer;

N_{agg} – aggregation number;

K_{SV} – Stern-Volmer constant.

References: [145], [146], [147]

3.3.4 Biodegradability of oxime-functionalized SAILs

The biodegradability of oxime-functionalized SAILs was evaluated using Closed bottle test (OECD 301 D protocol [17], [110]). Compounds **2-PyPheC8** / **3-PyPheC8** / **4-PyPheC8** does not demonstrate significant difference in biodegradability depends on position of oxime group in pyridinium ring and moderately biodegradable (Table 12). Compared with biodegradability of ester non-functionalized compound PyPheOC₁₀, biodegradability of oxime-functionalized L-phenylalanine-derived SAILs is lower, but extended CBT demonstrated that these compounds could be considered as inherently biodegradable amphiphiles.

Table 12. Results of biodegradability testing of oxime-functionalized SAILs in CBT (OECD 301 D protocol).

Structures	Standard CBT: D% 28 days	Extended CBT: D% 42 days
4-PyC8	4	11
4-PyAlaC8	9	19
2-PyPheC8	24	37
3-PyPheC8	20	34
4-PyPheC8	25	39
PyPheOC₁₀	36 [17]	–

The biodegradability of oxime-functionalized SAILs decreases in direction Phe > Ala > > non-amino acid derivative. This tendency is similar to tendency, observed for dipeptide ILs (see Chapter 3.2): introduction of amino acid fragments improves biodegradability of compounds; introduction of L-phenylalanine fragment is more preferable compared with L-alanine fragment, because L-phenylalanine derivatives are more biodegradable.

3.3.5 Application of oxime-functionalized SAILs: organophosphates decomposition

Oxime-functionalized surfactants demonstrate outstanding efficiency in reactions of toxic organophosphates cleavage [75], [88]. Oxime-functionalized SAILs, which have similar structure and properties, should also demonstrate high nucleophilic reactivity and could be tested in scope of application in organophosphates decomposition processes.

These tests were performed for representative example of studied SAILs – **4-PyC8** – in reaction of 4-nitrophenyl diphenyl phosphate (PNPDPP) nucleophilic decomposition (Figure 39).

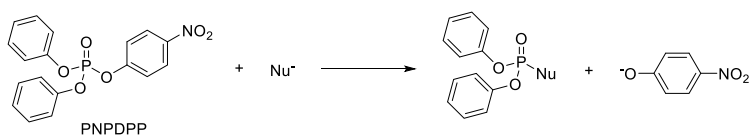


Figure 39. PNPDPP decomposition with nucleophilic reagents.

The reaction was performed at two different pH – 8.4 and 9.0. Taking into account the value of ionization constant for **4-PyC8** ($pK_a = 8.08$), the deprotonation degree of the oxime group in these conditions is 0.66 and 0.89, correspondently. The elevated reaction

rates with increasing deprotonation degree of the oxime group (Figure 40 and Table 13) clearly indicates that reactive species in studied reaction is oximate ion. Important to notice that observed rate constant for **4-PyC8** at pH 9.0 (0.0177 s^{-1}) is higher than observed rate constants for oxime functionalized surfactants with similar head group structure (but with alkyl chain $\text{C}_{10}\text{--}\text{C}_{16}$) in the same reaction condition (the maximal reported value is 0.0162 s^{-1} [148]).

Table 13. Decomposition of *p*-nitrophenyl diphenyl phosphate (PNPDPP) in the presence of **4-PyC8** ([PNPDPP] = 0.5 mM; 27 °C).

[4-PyC8], mM	$k_{\text{obs}} \cdot 10^3, (\text{s}^{-1})$	
	pH = 8.4	pH = 9.0
0	0.76	5.72
0.5	2.57	9.27
1.0	5.44	13.30
3.0	11.10	17.70
5.0	9.67	15.90

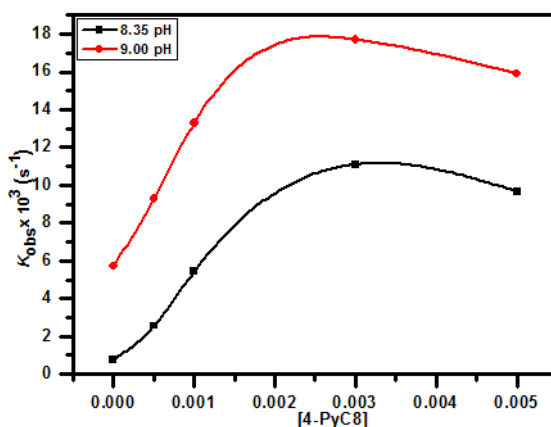


Figure 40. Dependencies of observed pseudo-first order rate constants ($k_{\text{obs}}, \text{s}^{-1}$) from $[\text{4-PyC8}]_0$ for reaction of PNPDP decomposition; water, 27 °C; [PNPDPP] = 0.5 mM [the figure was taken from Publication I]

The second order rate constant k_2^{m} for decomposition of PNPDP in micellar pseudophase with oximate ion can be calculated from kinetic data using equation (19) for hydrophobic substrates from Chapter 1.3.5 (binding constant K_{s} of PNPDP is $\geq 10^4 \text{ M}^{-1}$ [148]):

$$k_{\text{obs,max}} \cong (k_2'/V_{\text{M}}) \approx (k_2^{\text{M}}/V_{\text{M}}) \cdot \alpha$$

Obtained k_2^{m} values are $6.7 \text{ M}^{-1} \text{ s}^{-1}$ for pH 8.4 and $7.9 \text{ M}^{-1} \text{ s}^{-1}$ for pH 9.0.

In optimal concentration condition the half-life times of PNPDP in presence of **4-PyC8** are 62 s (pH 8.4) and 40 s (pH 9.0), which corresponds to best examples of such reagents known from literature [75], [148].

3.3.6 Application of oxime-functionalized SAILs: interaction of mixed systems 4-PyC8 / 16-10-16 with Promethazine

Oxime-functionalized surfactants can form not only pH-responsive mixed self-assembly aggregates with other amphiphilic molecules [75], [88], but also supramolecular complexes with polymers [89] and pharmaceuticals [149]. The possibility to interact with pharmaceuticals is very important because it could be used for analytical purposes (detection / identification of target molecules) [7], [66], [67], [71] or for design of drug specific delivery systems [70], [74].

In current study we investigate interaction of mixed systems **4-PyC8** / 16-10-16 with phenothiazine drug Promethazine (PMZ; Figure 41) using dynamic light scattering and zeta potential measurements.

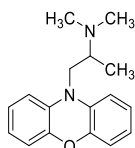


Figure 41. Structure of phenothiazine drug Promethazine (PMZ).

The gemini surfactant 16-10-16 in solution without additives in concentration 1 mM, which is significantly higher than CMC (in ca. 35 times, see Table 11), forms aggregates with mean hydrodynamic diameter 124 nm (Table 14). This size based on literature data [150] most probably reflected the intermicellar aggregates. Introduction of Promethazine in concentration 0.01 mM to studied system increase aggregate size to approximately 270 nm. The additives of 4-PyC8 to the system (16-10-16 : PMZ) initiate aggregates reorganisation (Table 14; Figure 42): in presence of 0.1 wt% 4-PyC8 two type of aggregates (210 nm and 825 nm) formed; the future increasing of 4-PyC8 content to 0.5 wt% and then to 1.0 wt% gives aggregates with diameter 182 nm and then with 1.4 nm. All of these dramatic structural changes are accompanied by only relatively small changes in zeta potential (Table 14).

Table 14. Aggregate size d (nm) as a size distribution by number and zeta potential in the presence of various concentrations of the IL 4-PyC8 in the drug PMZ and the gemini 16-10-16 surfactant solution.

System Composition	Aggregate Parameters	
	d (nm)	Zeta Potential, ξ (mV)
16-10-16 (1 mM)	124 (105–164)	22.6
16-10-16 + PMZ (0.01 mM)	270 (220–395)	24.8
16-10-16 + PMZ + 0.1 wt% 4-PyC8	210 (165–255) 825 (615–1105)	24.1
16-10-16 + PMZ + 0.5 wt% 4-PyC8	182 (142–220)	20.6
16-10-16 + PMZ + 1.0 wt% 4-PyC8	1.4 (1.1–1.8)	23.7

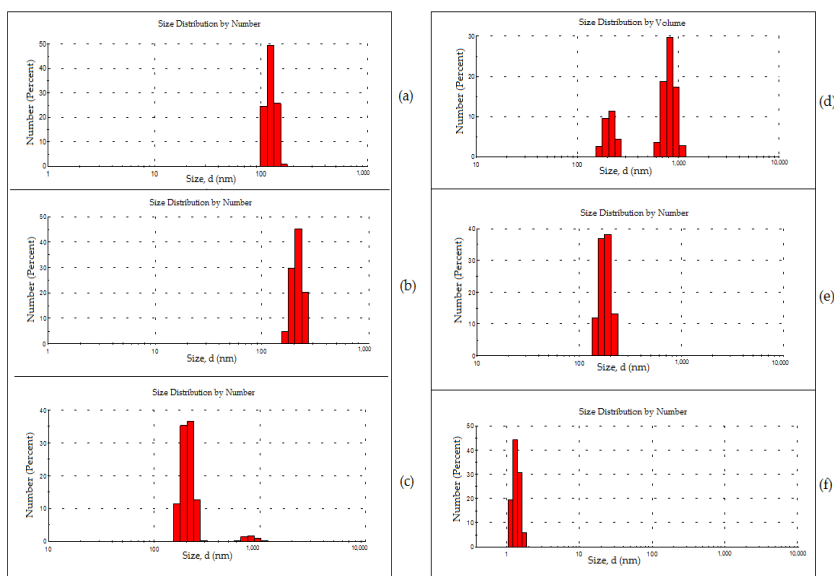


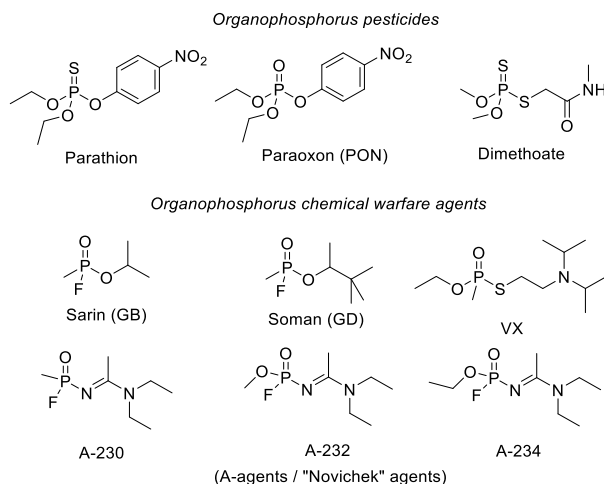
Figure 42. Aggregates size distribution (by numbers) obtained from DLS for various concentrations of the IL 4-PyC8 in drug PMZ and gemini surfactant 16-10-16 [the figure was taken from Publication I]: (a) 16-10-16 (without additives), (b) 16-10-16:PMZ, (c) 16-10-16:PMZ:0.1 wt% IL 4-PyC8, (d) 16-10-16:PMZ:0.1 wt% IL 4-PyC8 [distribution by volume, for information], (e) 16-10-16:PMZ:0.5 wt% IL 4-PyC8 and (f) 16-10-16:PMZ:1.0 wt% IL 4-PyC8.

A significant diversity in aggregates size depends on 16-10-16 : PMZ : 4-PyC8 system composition indicate presence of strong specific interaction between system components. Due to absence of specific interaction in system 16-10-16 : 4-PyC8, which was confirmed by NMR and IR studies (see Chapter 3.3.3; NMR and IR spectra and their detailed discussion are presented in the Publication II), the most probable participants of specific interactions are PMZ and 4-PyC8. Also, specific interactions in similar system were reported in [149].

The structural transitions in 16-10-16 : PMZ : 4-PyC8 system could be used as analytical response in design of selective systems for detection of phenothiazine drugs (and, potentially, other biologically important molecules) in different objects (final dosage forms, biological liquids, pharmaceutical wastes, etc.).

3.4 Design of acetylcholinesterase reactivators based on sustainable ionic liquids (Publication V)

The one of important and widely used group of pesticides is organophosphates (parathion, dimethoate, paraoxon, etc.; Figure 43) [151]. Their use in modern agriculture helps to protect plants and save significant amounts of harvest [152]. Unfortunately, organophosphates usage is always connected with risks of agricultural workers poisoning. According to recently published review the number of unintentional pesticide poisoning is approximately 740000 cases per year [153]. Also, some most toxic organophosphates (sarin, soman, VX, Novichok agents, etc.; Figure 43) are used as chemical warfare agents [154], [155] and number of incidents with these compounds increases last years [155], [156], [157], [158], [159].



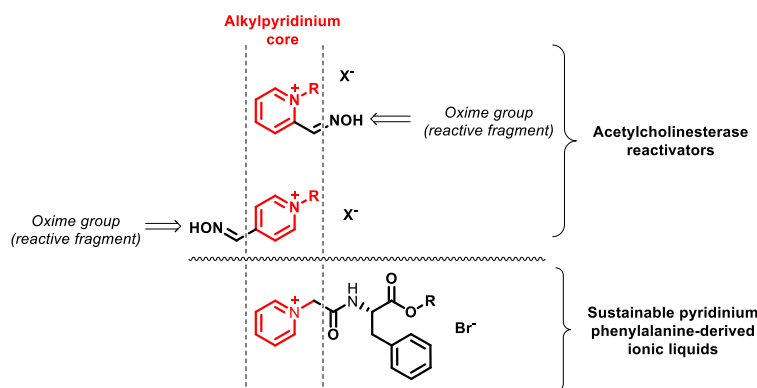


Figure 45. Structure comparison of typical AChE reactivators and sustainable pyridinium phenylalanine-derived ionic liquids (PyPheOC_n).

3.4.1 Strategy of design, structure variation and synthesis of sustainable AChE reactivators

The structure comparison of typical AChE reactivators and sustainable pyridinium phenylalanine-derived ionic liquids, presented on Figure 45, demonstrates, that the most simple way to use the phenylalanine-derived ionic liquid based molecular platform for design of new sustainable antidotes is the introduction of oxime group in pyridinium ring of PyPheOC_n compounds (Figure 46).

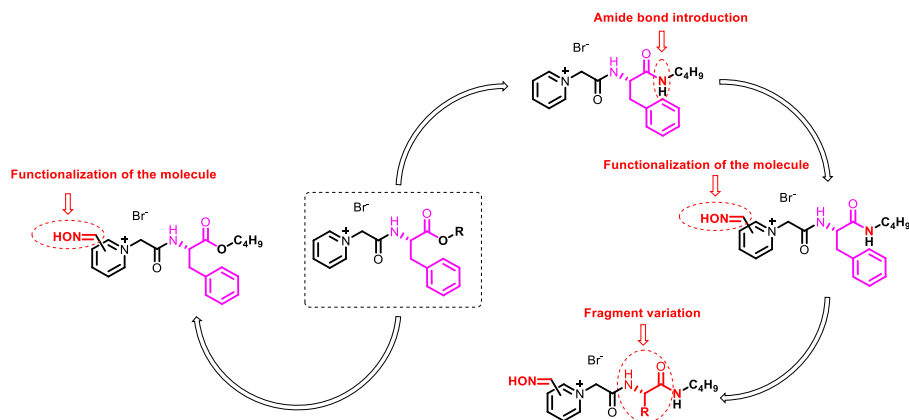


Figure 46. Strategy of design of cholinesterase reactivators using sustainable ionic liquid-based molecular platform.

The alternative way of phenylalanine-derived ionic liquid based molecular platform modification oriented on increasing of molecular platform stability to hydrolysis (Figure 46): amide bond is introduced instead of ester bond between phenylalanine residue and alkyl chain, and only after that functionalization of pyridinium ring is performed. The further development of this direction of structural modification is variation of fragment between alkyl chain and acetylpyridinium fragment in the molecule to clarify the role of this component on compounds properties.

Following the strategy, presented on the Figure 46, the four types of compounds (Figure 47) were selected for synthesis and future investigation.

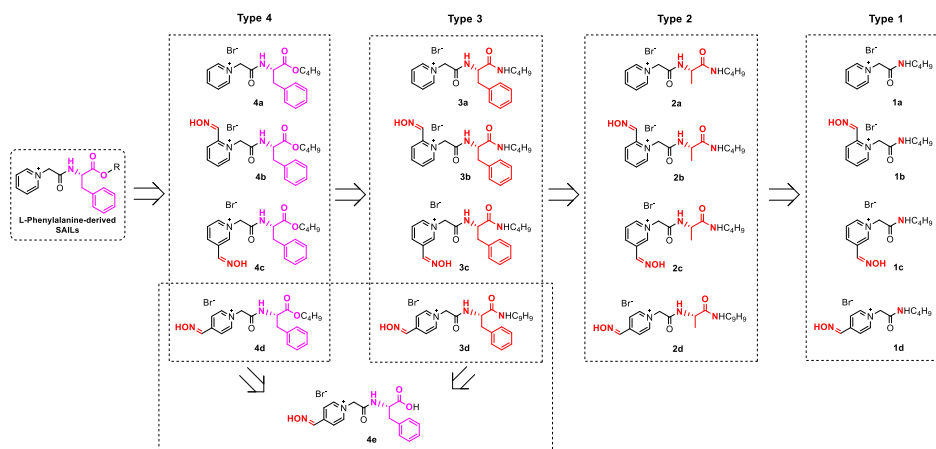


Figure 47. Cholinesterase reactivators based on sustainable ionic liquid molecular platforms: target structure for synthesis.

Selected compounds (Figure 47) were synthesized according to general synthetic scheme, presented on the Figure 48.

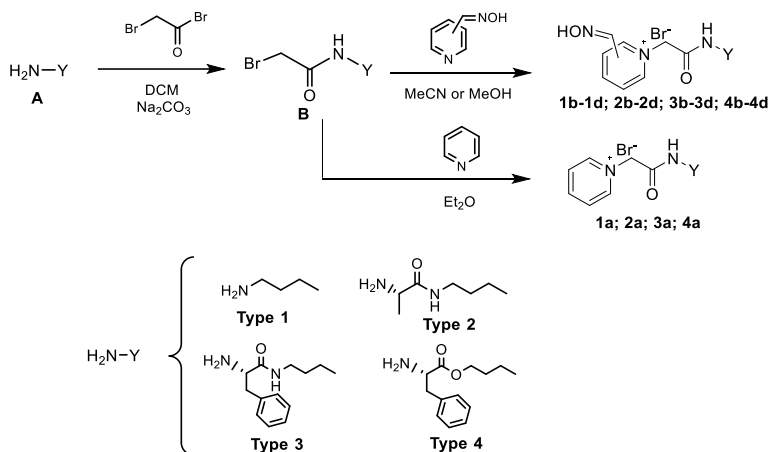


Figure 48. Synthesis of the target cholinesterase reactivators based on sustainable ionic liquids molecular platforms.

3.4.2 Properties evaluation of new sustainable AChE reactivators *in silico*

Before start of experimental studies of new sustainable AChE reactivators, presented on the Figure 46, their properties were evaluated *in silico* to identify possible problematic objects on early stage of project realization.

For all target molecules (Figure 47) pK_a values, $\log P_{o/w}$ and BBB scope (blood-brain barrier permeability parameters) were evaluated for two possible compounds forms (cationic [cat] and zwitter-ionic [zw]; see also Figure 34) using on-line predictors Molinspiration (www.molinspiration.com), VCCLAB (www.vcclab.org) [161], www.cbligand.org and Chemicalize (www.chemicalize.com).

The best correlation for dependencies “ $\log P_{o/w}$ – BBB score” were obtained for combination of VCCLAB predictor (for $\log P_{o/w}$) with predictor www.cbligand.org / fingerprint PubChem (for BBB score) (Figure 49 a) and only these results (Table 15) were used for further analysis and evaluation. All other combinations of online predictors and / or fingerprints do not give any satisfactory results (Figure 49 b).

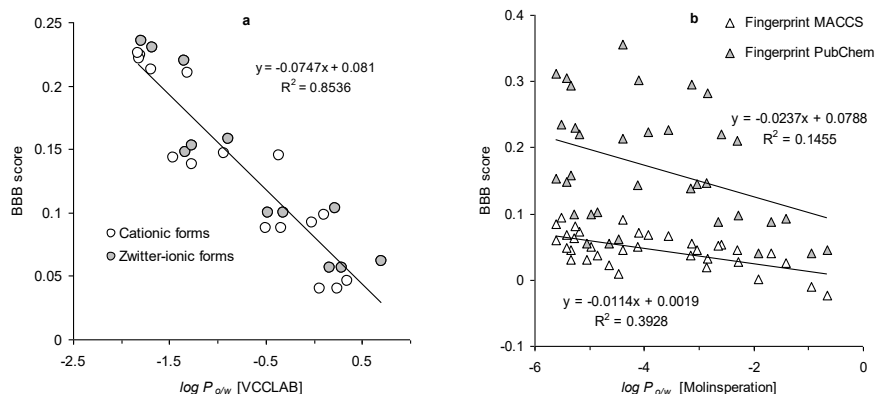


Figure 49. Dependencies of BBB score values on $\log P_{o/w}$ obtained with different on-line predictors and fingerprints used: a – predictor www.vcclab.org (for $\log P_{o/w}$) and www.cbligand.org (for BBB score; fingerprint PubChem); b – predictor www.molinspiration.com (for $\log P_{o/w}$) and www.cbligand.org (for BBB score; fingerprints PubChem & MACCS).

In general, cationic and zwitter ionic forms of the same compound demonstrate similar $\log P_{o/w}$ (Table 15). Compounds **b** (2-substetuted derivatives) have highest changes in $\log P_{o/w}$ compared with non-functionalized analogs (compounds **a**). The changes in hydrophobicity of compounds **c** & **d** (3- & 4-substetuted derivatives) compared with compounds **a** are less significant.

BBB score values (Table 15) do not demonstrate sensitivity to either the introduction of the oxime group into the IL structure or its position on the pyridine core. Also, cationic and zwitter ionic forms of the same compound have comparable BBB score.

For all calculated cases BBB score is classified as (BBB+). It means that compounds Type 1 – Type 4 in both forms (cationic and zwitter-ionic) expected to cross blood – brain barrier, which is very important for compounds therapeutic effects [155].

Table 15. Parameters pK_a , $\log P_{o/w}$ and BBB score for ILs Types 1 – Type 4, obtained using Chemicalize, VCCLAB and www.cbligand.org (fingerprint PubChem) on-line tools.

Compound	pKa (Chemicalize)	log $P_{o/w}$ (VCCLAB)		BBB score (www.cbligand.org)	
		Cationic form	Zwitter-ionic form	Cationic form	Zwitter-ionic form
1a	–	-1.8	–	0.224	–
1b	6.72	-1.31	-1.34	0.21	0.22
1c	7	-1.81	-1.68	0.221	0.23
1d	7.87	-1.82	-1.79	0.226	0.235
2a	–	-1.69	–	0.213	–
2b	6.69	-0.93	-0.89	0.147	0.158
2c	6.98	-1.26	-1.33	0.138	0.148
2d	7.87	-1.46	-1.27	0.143	0.153
3a	–	-0.36	–	0.145	–
3b	6.66	-0.02	0.22	0.092	0.103
3c	6.98	-0.34	-0.32	0.088	0.1
3d	7.87	-0.5	-0.47	0.088	0.1
4a	–	0.11	–	0.098	–
4b	6.61	0.35	0.7	0.046	0.062
4c	6.98	0.25	0.29	0.04	0.056
4d	7.87	0.06	0.17	0.04	0.056
4e	7.87 *	-1.09	-0.92	0.03	0.049

Notes. * Value corresponds to pK_a of oxime fragment; calculated pK_a of carboxylic group in **4e** is 3.16.

Possibility to be AChE reactivators were accessed for representative examples of studied compounds – functionalized ionic liquids **3d**, **4d**, and their potential transformation product **4e** – using molecular docking studies. The docking was performed inside active site of AChE blocked with different types of organophosphates (*HssAChE-GB*, *HssAChE-VX* and *HssAChE-PON*). The model of active site was constructed based on corresponding crystallographic data, available in RSCB PDB Protein Data Bank (<http://www.rcsb.org/pdb/home/home.do>) under codes 2Y2V (for *HssAChE-GB*), 6CQZ (for *HssAChE-VX*) and 5HF9 (for *HssAChE-PON*). The docking protocol was validated using re-docking result obtained for HI-6 inside *HssAChE-PON*.

The docking calculations for **3d**, **4d**, and **4e** were performed for all species, which could be present at physiological pH. The conclusion about possibility of corresponding species formation was done based on corresponding pK_a values, calculated with Chemicalize (<https://chemicalize.com/>; see Table 15).

The docking results for each compound (**3d**, **4d**, and **4e**) inside *HssAChE-GB*, *HssAChE-VX* and *HssAChE-PON* are presented in the Table 16 and Figure 50. Obtained data confirm that compounds **3d**, **4d**, and **4e** are effectively interact [162], [163] with *HssAChE-GB*, *HssAChE-VX* and *HssAChE-PON* active sites and potentially can be AChE reactivators.

Performed *in silico* studies do not indicate any potential problems and allows to precede further steps of new sustainable oxime-functionalized ionic liquids testing as AChE reactivators.

Table 16. Best docking results for compounds 3d, 4d and 3e on HssAChE-GB, HssAChE-VX and HssAChE-PON.

IL	HssAChE-GB				HssAChE-VX				HssAChE-PON			
	E _{inter} kcal.mol ⁻¹	E _{Hbond} kcal.mol ⁻¹	H-bond	Distance O-P (Å)	E _{inter} kcal.mol ⁻¹	E _{Hbond} kcal.mol ⁻¹	H-bond	Distance O-P (Å)	E _{inter} kcal.mol ⁻¹	E _{Hbond} kcal.mol ⁻¹	H-bond	Distance O-P (Å)
3d (cat)	-162.37	-1.64	Asp74 Tyr124 Tyr133 Tyr337	5.53	-89.98	-3.12	Tyr124 Tyr341	5.05	-147.55	-1.99	Tyr124 OP	3.82
3d (zw)	-148.87	-0.03	Tyr124	7.08	No pose meeting the selection criteria was obtained				-143.63	-0.70	Tyr124	3.92
4d (cat)	-155.39	-1.93	Gly120 Tyr133	6.22	-73.35	-2.22	Tyr72 Tyr124	5.59	-140.06	-0.58	Tyr124 OP	3.57
4d (zw)	-145.13	-1.66	Asp74 Tyr133	6.00	-87.83	-1.97	Tyr124 Tyr341	5.30	-139.57	-4.06	Tyr124 Tyr337	5.81
4e (cat ⁻)	-144.19	-2.01	Ser125 Glu202 Tyr341* Tyr124	4.65	No pose meeting the selection criteria was obtained				-130.97	-1.50	Tyr124 Trp286 Trp286*	5.82
4e (zw ⁻)	-124.49	-2.12	Ser125 Arg296	7.25	-99.19	-1.87	Tyr124 Ser293	5.33	-145.95	-0.56	Tyr124	6.34
IL	HssAChE-GB			HssAChE-VX			HssAChE-PON					
	Lowest E _{inter} kcal.mol ⁻¹	% Poses OP/active site	% Poses PAS	Lowest E _{inter} kcal.mol ⁻¹	% Poses OP/active site	% Poses PAS	Lowest E _{inter} kcal.mol ⁻¹	% Poses OP/active site	% Poses PAS			
3d (cat)	-184.65 (active site)	37	63	-94.34 (PAS)	10	90	-164.28 (PAS)	13	87			
3d (zw)	-163.17 (PAS)	17	83	-101.42	0	100	-155.55 (PAS)	17	83			
4d (cat)	-168.77 (PAS)	34	66	-97.65 (PAS)	3	97	-165.44 (PAS)	20	80			
4d (zw)	-172.56 (PAS)	47	53	-98.47	17	83	-149.18 (PAS)	20	80			
4e (cat ⁻)	-165.11 (PAS)	20	80	-101.19 (PAS)	0	100	-141.62 (PAS)	20	80			
4e (zw ⁻)	-155.05 (PAS)	10	90	-103.20 (PAS)	3	97	-162.63 (PAS)	53	47			

Notes. * Hydrophobic interactions.

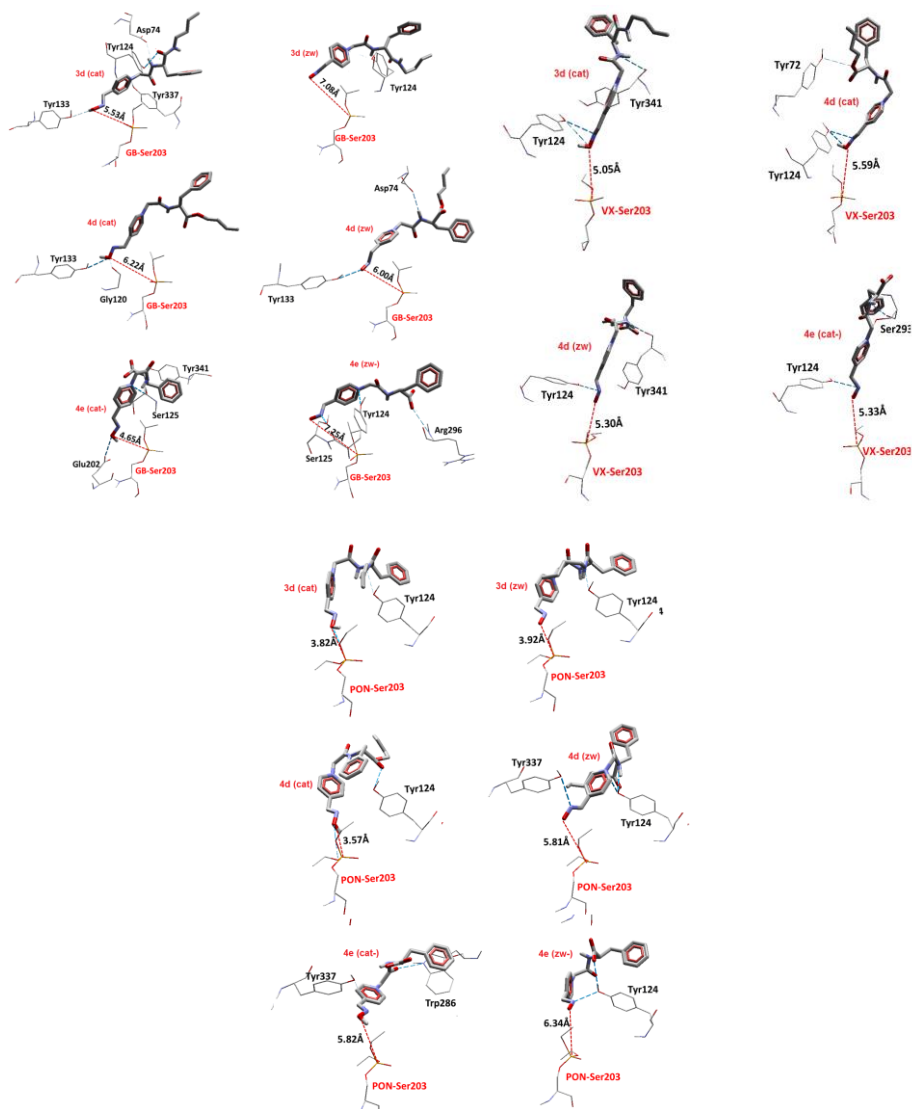


Figure 50. Best docking poses of the compounds **3d**, **4d** and **3e** on HssAChE-GB, HssAChE-VX and HssAChE-PON [the figure was taken from Publication V].

3.4.3 Toxicological properties of new sustainable AChE reactivators

In vitro toxicity screening for all studied compounds was performed using several different organisms / cell lines:

- Gram-positive bacteria (*Staphylococcus aureus* subsp. *Aureus* [ATCC 29213]; *Staphylococcus aureus* subsp. *aureus* methicillin resistant [ATCC 43300]; *Staphylococcus epidermidis* [HK6966, 112-2016, dialysis tube, University Hospital Hradec Králové, Institute of Clinical Microbiology]; *Enterococcus faecalis* [ATCC 29212]);

- Gram-negative bacteria (*Escherichia coli* [ATCC 25922]; *Klebsiella pneumoniae* [HK 11750, 64-2016, urine catheter tube, University Hospital Hradec Králové, Institute of Clinical Microbiology]; *Serratia marcescens* [clinical isolate, 163-2016, University Hospital Hradec Králové, Institute of Clinical Microbiology], *Pseudomonas aeruginosa* [ATCC 27853]);

- fungi (*Candida albicans* [ATCC 24433]; *Candida albicans* [ATCC 90028]; *Candida krusei* [ATCC 6258]; *Candida glabrata* [ATCC 90030]; *Candida parapsilosis* [ATCC 22019]; *Candida tropicalis* [ATCC 750]; *Pichia quilliermondii* [ATCC 90877]; *Saccharomyces cerevisiae* [ATCC 9763]; *Aspergillus fumigatus* [ATCC 204305]; *Aspergillus flavus* [CCM 8363]; *Absidia corymbifera* [CCM 8077]; *Microsporium canis* [CCM 8353]; *Trichophyton interdigitale* [ATCC 9533]);

- mammalian cells (Chinese hamster ovary cell line CHO-K1).

Among all tested compounds only certain examples demonstrate moderate toxicity against bacteria and fungi, but the main part of them do not show any toxicity effects up to 2 mM (maximal concentration of tested compounds, used in the study).

Influence of compounds Type 1 – Type 4 on the mammalian cells viability was evaluated using CHO-K1 cell line. The toxicity effects were observed only for concentrations more than 3 mM (Table 17), which is significantly higher, then expected concentration of these compounds in blood in case of treatment [164].

Table 17. The effect of compounds Type 1 – Type 4 on the mammalian cell viability (CHO-K1 cell line).

Compound	IC ₅₀ ^a (mM ± SEM)	Compound	IC ₅₀ ^a (mM ± SEM)
1a	19.2 ± 0.4 ^b	3a	4.9 ± 0.9 ^b
1b	10.8 ± 0.3 ^b	3b	>10 ^c
1c	7.1 ± 0.7 ^b	3c	7.5 ± 0.7 ^c
1d	9.9 ± 0.5 ^c	3d	3.2 ± 0.6 ^c
2a	63.9 ± 12.3 ^b	4a	4.0 ± 0.2 ^b
2b	5.9 ± 1.3 ^b	4b	3.8 ± 0.2 ^c
2c	24.7 ± 7.8 ^b	4c	3.7 ± 0.6 ^c
2d	>10 ^c	4d	6.2 ± 0.7 ^c
–	–	4e	>10 ^c
Notes. ^a Mean ± SEM (mM); ^b n=2; ^c n=3.			

3.4.4 Biodegradability studies of new sustainable AChE reactivators

In Closed bottle test (OECD 301 D protocol [110]) after 28 days among all ILs tested only non-functionalized compound **4a** demonstrate significant biodegradability (Table 18). Exchange of ester bond in **4a** on amide fragment (compound **3a**) as well as introduction of oxime group in any position of pyridinium ring (compounds **4b**, **4c**, **4d**) dramatically decreases biodegradability.

Table 18. Biodegradability of compounds Type 1 – Type 4 and their potential transformation products in Closed bottle test (OECD 301 D protocol).

Compound	Biodegradability (D%), 28 days	Compound	Biodegradability (D%), 28 days
1a	4	4a	49*
1b	4	4b	11
1c	0	4c	13
1d	0	4d	18
2a	3	4e	13
2b	9	BuNH ₂ ·HCl	66
2c	7	Butylamide of L-Ala·HCl	20
2d	0		
3a	0	Butylamide of L-Phe·HCl	62
3b	8		
3c	8	Butyl ester of L-Phe·HCl	99
3d	9		

Notes. * Literature data [17]; biodegradability reaches 72 % after extension of CBT to 42 days [19].

Despite low biodegradation values compounds Type 1 – Type 4 could be effectively biodegraded if a combination of approaches is applied: according to results, presented in Chapter 3.1, ionic liquid PyPhenHC₄ (which is compound **3a**) could be completely hydrolyzed using commercially available immobilized enzyme P13 with formation of pyridinium acetic acid, L-phenylalanine and butylamine (see Figure 24 from Chapter 3.1). Pyridinium acetic acid (corresponds to TP # 11 from the Chapter 3.2, Figure 29), L-phenylalanine (corresponds to TP # 12 from the Chapter 3.2, Figure 29) and possible hydrolysis semi-products (corresponds to TPs # 7 from the Chapter 3.2, Figure 29 and butylamide of L-phenylalanine hydrochloride from the Table 18) are biodegradable (biodegradability after 28 days is 61 %, 65 %, 65% and 62%, correspondently; see Table 9 in Chapter 3.2.2 and Table 18). Butylamine is also biodegradable (66% after 28 days; see Table 18). It means that after enzymatic pre-treatment of **3a** solutions obtained hydrolysis mixture contains only products, which could be completely biodegraded (Figure 51). This approach combination could be also extended on other studied ILs.

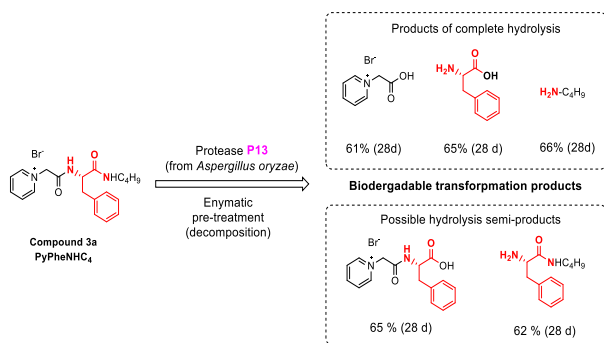


Figure 51. Combination of enzymatic pre-treatment with further hydrolysis products biodegradation.

3.4.5 Reactivation efficacy of oxime-functionalized ILs towards AChE inhibited by sarin, VX and paraoxon

Reactivation capacity of studied oxime-functionalized ILs was evaluated *in vitro* towards human recombinant AChE inhibited by sarin (GB), VX and paraoxon (PON). As reference compounds two conventional antidotes (2-PAM and obidoxime) were used. Obtained results are summarized in the Table 19. Compounds, functionalized with oxime group in position 4 of pyridinium ring, in most cases demonstrate higher reactivation capacity compared with 2 and 3-substituted derivatives. Introduction of L-alanine residue (compounds Type 2) does not bring any significant advantages compared with compounds Type 1 (which do not contain an amino acid residue in the structure), however introduction of L-phenylalanine fragment (ILs Type 3 and Type 4) helps to significantly improve reactivation capacity, especially for sarin- and VX-inhibited AChE.

Table 19. Reactivation capacity of oxime-functionalized ILs and conventional antidotes towards OP-inhibited AChE.

#	Sarin (10 μ M)		VX (10 μ M)		Paraoxon (10 μ M)	
	Compound (100 μ M)	Compound (10 μ M)	Compound (100 μ M)	Compound (10 μ M)	Compound (100 μ M)	Compound (10 μ M)
1b	0.22	0.23	1.09	2.26	1.8	1.1
1c	0.94	0.25	0.62	0.22	1.54	1.46
1d	2.99	0	7.58	2.12	4.15	2.02
2b	1.61	1.27	0.33	0.17	0.21	0.48
2c	3.15	0	2.32	1.65	1.63	1.28
2d	2.11	0	5.26	1.52	2.65	0
3b	0	0	1.16	0	0	0
3c	0	0	0	0	0	0
3d	8.66	0	18.5	3.17	2.91	0
4b	n.d.	n.d.	n.d.	n.d.	n.d.	n.d.
4c	n.d.	n.d.	n.d.	n.d.	n.d.	n.d.
4d	9.91	1.32	10.9	0	1.48	0
4e	1.22	1.02	1.45	0	0	0
2-PAM	32.9	10.0	11.4	2.81	19.3	2.53
Obidoxime	33.73	11.57	17.05	5.54	70.26	34.66

Notes. n.d. – reactivation cannot be measured due to full inhibition of the enzyme by given compound.

Among tested compounds oxime-functionalized ionic liquids **3d** and **4d** demonstrate activity in reaction with sarin- and VX-inhibited AChE, which is comparable to activity of conventional antidotes 2-PAM and obidoxime (in case of VX-inhibited AChE compound **3d** gives even the best result). It allows you to select **3d** and **4d**, and their potential transformation product **4e**, for further, more detailed studies and confirms that sustainable ionic liquids-based molecular platform could be successfully used for design of new acetylcholinesterase reactivators.

3.4.6 Stability of selected oxime-functionalized ILs in human blood plasma

Investigation of compounds stability in human blood plasma is an important step in their assessment as potential pharmaceuticals. This property is directly connected with lifetime of molecules in blood and possible duration of therapeutic effects [165].

In human blood plasma compounds **3d** and **4d** could be decomposed (hydrolyzed) with formation of products, presented on the Figure 52.

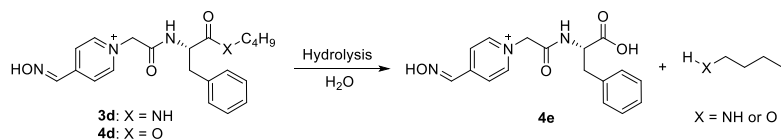


Figure 52. Hydrolysis of compounds **3d** and **4d**.

Important to notice that activity in processes of OP-inhibited AChE reactivation for hydrolysis product **4e**, which can form from **3d** and **4d**, is much lower than activity of non-hydrolysed molecules (see Table 19). It indicates that **3d** and **4d** decomposition in human blood plasma could affect the observed effects.

The stability of **3d** and **4d** in human blood plasma was evaluated within 2 h incubation time with control by LCMS. Compound **3d** does not show significant degradation, whereas compound **4d** demonstrated low plasma stability and was almost fully decomposed within 60 min (Figure 53). This property of **4d** is in contrast to compound **3d** and can be explained by the presence of an ester bond in the molecule **3d** (which is much more reactive [133]).

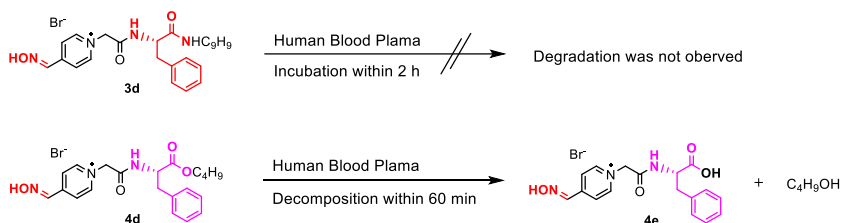


Figure 53. Stability study in human blood plasma for compounds **3d** and **4d**.

4 Conclusions

Based on pyridinium phenylalanine-derived ionic liquids were developed sustainable systems for different practical applications. Initial structures were successfully modified and adopted for solving different specific practical tasks.

The main results of the present work are:

- efficiency of pyridinium phenylalanine-derived ionic liquids in solubilization of polycyclic aromatic hydrocarbons was demonstrated;
- concept of sustainable process for polycyclic aromatic hydrocarbons extraction using pyridinium phenylalanine-derived ionic liquids was proposed;
- possible ways of structure improvement for pyridinium phenylalanine-derived ionic liquids were evaluated and justified;
- structure-properties relationship for structural fragments of amino acid derived ionic liquids was determined and the fragments library for future use in design of sustainable ionic liquids was created;
- functionalized surfactants based on pyridinium-derived ionic liquids were designed and investigated with focus on application of these compounds in processes of toxic organophosphates decompositions and compounds detection;
- new sustainable acetylcholinesterase reactivators based on pyridinium-derived ionic liquids were designed, synthesized and studied.

The high flexibility and big potential for further improvement of used ionic liquid-based molecular platforms are demonstrated.

5 Experimental

Reagents and materials. The commercially available chemicals were purchased from Merck, Sigma Aldrich, Alfa Aesar, or TCI Europe and used without further purification. The synthesis of other required chemicals were performed using standard synthetic approaches. The structures of synthesized compounds were characterized using different NMR techniques (^1H , ^{13}C , ^1H - ^1H , ^1H - ^{13}C and other), mass-spectroscopy, IR and elemental analysis. Results of compounds characterization are presented in corresponding publications. Reagents and materials (e.g., 16-s-16 gemini surfactants, organophosphorous compounds, microorganisms strains, cell lines, etc.), provided / used by partner's laboratories, were properly identified and characterized.

NMR spectroscopy. For NMR studies Bruker Avance III 400 MHz spectrometer operating at 400 MHz for ^1H NMR and 101 MHz for ^{13}C NMR was used. The tested samples were prepared in deuterated water (D_2O), chloroform (CDCl_3), methanol (CD_3OD) or dimethyl sulfoxide ($\text{DMSO}-d_6$). The deuterated solvents were purchased from Deutero GmbH (Germany). In publications the chemical shifts δ were reported in ppm (parts per million), coupling constants (J) were measured in Hertz (Hz). As an internal standard TMS or residual signal of solvents were used. For NMR studies of enzymatic hydrolysis products water suppression method was applied.

Mass spectroscopy. The identification of compounds with HRMS method was performed using Agilent 6540 UHD Accurate-Mass Q-TOF LC/MS G6540A Mass Spectrometer.

Melting points determination. For melting points determination, the Stuart SMP40 apparatus was used. The melting point analysis performed with $2\text{ }^\circ\text{C}$ per minute ramp, results reported in $^\circ\text{C}$.

Conductivity. Conductivity measurements were performed with Systronics (Type 304) digital conductivity meter. Used conductivity cell had the cell constant 1.01 cm^{-1} . For calibration of conductivity cell standard solutions of potassium chloride (KCl) across a 0.01 M to 0.1 M concentration range was used.

Surface Tension Measurements. Determination of surface tension was performed by Du Noüy ring detachment method using a KYOWA automatic surface tensiometer (DY-300). For tensiometer calibration Millipore water ($72\text{ mN}\cdot\text{m}^{-1}$ at 300 K) was used. The platinum ring was decontaminated with flame after each measurement.

Fluorescence Measurements. The fluorescence spectra were recorded using spectrophotometer Cary Eclipse Fluorescence (Agilent Technology).

FTIR Spectroscopy. The FTIR spectra were measured on a Bruker-ECO-ATR Model-i55 FTIR Spectrophotometer in the spectral range of $4000\text{--}400\text{ cm}^{-1}$ at 298 K.

Dynamic Light Scattering. Dynamic Light Scattering studies were used to get information about the hydrodynamic diameter, size distribution and zeta potential of the aggregates in solutions. All measurements were performed using Zetasizer Nano instrument (Malvern) with a He-Ne laser (633 nm , 10 mW ; $\theta = 173^\circ$). For data acquisition and processing Malvern DTS Software ver. 7.11 was used.

Antibacterial and antifungal activity screening. The antibacterial and antifungal activity were performed according to EUCAST (The European Committee on Antimicrobial Susceptibility Testing) recommendations [136], [137], [138].

Inoculum for aerobic biodegradation testing. The inoculum for aerobic biodegradation testing was taken from Paljassaare municipal wastewater treatment plant (Tallinn, Estonia; 59°27'55.5"N 24°42'08.8"E). Before using in aerobic biodegradation tests inoculum was filtered through a cellulose filter (Grade 1, pore size 11 µm).

Aerobic biodegradation testing. Aerobic biodegradation testing was performed according to OECD 301D guidelines using modified closed bottle test (CBT) [110]. Biological oxygen consumption was controlled by optode oxygen sensor system with PTFE-lined PSt3 oxygen sensor spots (Fibox 3 PreSens, Regensburg, Germany).

UV-Visible spectroscopy. UV-Vis spectroscopy was used for studies of solubilization capacity, determination of acid dissociation constant (pK_a) and reaction kinetics monitoring. The measurements were carried out on Cary 60 UV-Vis (Agilent Technologies) and JASCO V-730 spectrophotometers. Methodology of solubilization capacity determination is described in [131]. Determination of acid dissociation constants (pK_a) performed using spectrophotometric method described by Albert and Sergeant [166]. Kinetic studies methodology is described in [75], [83], [88].

pH measurements. The pH values were controlled using pH meter Eutech pH 700 with Inlab® Expert Pro glass electrode (accuracy of ± 0.01 units). Calibration of pH meter was performed by two-point calibration method with standard buffer solutions.

Compounds hydrophobicity and BBB penetration ability calculations. The hydrophobicity ($\log P_{o/w}$) of studied compounds was calculated using on-line cheminformatics tools: Molinspiration Cheminformatics free web services, Slovensky Grob, Slovakia (www.molinspiration.com), and VCCLAB (www.vcclab.org; [161]). Blood-Brain Barrier Predictor (www.cbiligand.org; version 0.9) was used for BBB score calculations.

Molecular docking studies. Information about the spatial structure of AChE and AChE-inhibitor complexes, required for docking studies, was taken from RSCB PDB Protein Data Bank (<http://www.rcsb.org/pdb/home/home.do>) and UniProt Data Bank (<https://www.uniprot.org/>). The model validation of was performed using the server PDBSum (www.ebi.ac.uk/pdbsum/). The three-dimensional structures of studied oxime were built with PC Spartan Pro® software [167]. Protonation equilibria for studied molecules at physiologic pH (7.4) were accessed using Chemicalize (<https://chemicalize.com/>) software. Docking energies were calculated using the Molegro Virtual Docker (MVD)® software [168].

In vitro cell viability assessment. In vitro cell viability assessment was performed in ECACC recommended conditions. Procedure is described in details in [169]. As a model mammalian cells the CHO-K1 cell line (Chinese hamster ovary, ECACC, Salisbury, UK) was used.

In vitro stability testing in human blood plasma. The stability testing protocol is described in [170]. For *in vitro* tests human plasma Human Pooled Plasma (Batch S00G71, Biowest, France) was used. The monitoring of tested compods stability was performed

using LC-MS system consisting of UHPLC Dionex Ultimate 3000 RS coupled with a Q Exactive Plus orbitrap mass spectrometer (Thermo Fisher Scientific, Bremen, Germany).

AChE reactivation assay. In all tests human recombinant AChE was used. Evaluation of AChE reactivation assay was performed according to protocol from [171], [172].

Additional experimental details are provided in Publications I–V.

Compounds numbers in the PhD Thesis correspond to compounds numbers in Publications I–V.

List of figures

- Figure 1. Structure of ionic liquids.
- Figure 2. Application of ionic liquids.
- Figure 3. Structure and classification of surfactants.
- Figure 4. Surfactant aggregates in solution.
- Figure 5. General scheme of bimolecular reaction in micellar system.
- Figure 6. Structures of surfactants, functionalized with oximate, hydroxamate, amidoximate, o-iodosylcarboxylate, hydroxyl and imidazolyl groups (representative examples).
- Figure 7. Structural changes in ILs, which lead to formation of SAILs.
- Figure 8. Structure-toxicity relationships for ionic liquids.
- Figure 9. Examples of IL's cations and their abbreviations.
- Figure 10. Possible ways of amino acid modification.
- Figure 11. Examples of ionic liquids with non-modified amino acids as counter ion.
- Figure 12. Examples of ionic liquids with modified amino acids as counter ion.
- Figure 13. Examples of imidazolium ionic liquids with amino acids in their structure.
- Figure 14. Variation of the positively charged center structure for phenylalanine-derived ionic liquids.
- Figure 15. Alkyl chain length variation for pyridinium, imidazolium and cholinium phenylalanine-derived ionic liquids.
- Figure 16. Pyridinium phenylalanine-derived ionic liquids – prospective object for future studies and improvements.
- Figure 17. PAHs solubilization in water solutions of surfactants.
- Figure 18. Structures of PAHs and cetyltrimethylammonium bromide [CTABr].
- Figure 19. Dependency of the absorbance of solution A on the wavelength 336 nm from surfactant concentration C_{surf} for the system PyPheOC₈ / pyrene.
- Figure 20. Dependencies of solubilization capacity (S) on alkyl chain length (n) of PyPheOC_n SAILs towards pyrene (a), naphthalene (b), and anthracene (c) compared to solubilization capacity of CTABr.
- Figure 21. Possible decomposition / resynthesis pathways for PyPheOC_n SAILs.
- Figure 22. Separation of PAHs after PyPheOC_n SAILs decomposition.
- Figure 23. ¹H NMR spectra of PyPheOC₄ solutions after incubations with selected amidase and protease enzymes at pH 6.5 (concentration of PyPheOC₄ 0.5%).
- Figure 24. Structure modification for PyPheOC_n SAILs and possible decomposition / resynthesis pathways for PyPheNHC_n SAILs.
- Figure 25. ¹H NMR spectra of PyPheNHC₄ solutions after incubations with selected amidase and protease enzymes at pH 6.5 (concentration of PyPheNHC₄ 0.5%).
- Figure 26. Application concept of pyridinium phenylalanine-derived ionic liquids in processes of polycyclic aromatic hydrocarbons extraction.
- Figure 27. Amino acid ILs (1, 2) and dipeptide ILs (3–6) with L-phenylalanine and L-alanine moiety in structure.
- Figure 28. Biodegradation pathway analysis and selection of possible transformation products.
- Figure 29. Structures of possible transformation products in processes of amino acid ILs (1, 2) and dipeptide ILs (3–6) biodegradation.

Figure 30. Synthesis of ILs 1–6 and their possible transformation products.

Figure 31. Biodegradation curve for compound 4 (L-Phe-L-Ala IL) with quality control, measured and calculated toxicity control curves (representative example; 10-day-window is indicated by two vertical dashed lines).

Figure 32. Objects selection and structure variation for oxime-functionalized SAILs.

Figure 33. Synthesis of the target oxime-functionalized SAILs.

Figure 34. The protolytic equilibria in solutions of oxime-functionalized SAILs.

Figure 35. The structures of surfactants 12-4-12, 16-10-16 and SDS.

Figure 36. Representative absorption spectra and plots at two selected wavelength for individual SAIL 4-PyPheC8 (a) and for system 4-PyPheC8 / 16-10-16 (b) at different pH values; 27 °C.

Figure 37. Structure of methylpyridinium aldoximes.

Figure 38. Structure of cationic gemini surfactants 16-s-16.

Figure 39. PNPDP decomposition with nucleophilic reagents.

Figure 40. Dependencies of observed pseudo-first order rate constants (k_{obs} , s^{-1}) from $[4\text{-PyC8}]_0$ for reaction of PNPDP decomposition; water, 27 °C; $[\text{PNPDPP}] = 0.5 \text{ mM}$

Figure 41. Structure of phenothiazine drug Promethazine (PMZ).

Figure 42. Aggregates size distribution (by numbers) obtained from DLS for various concentrations of the IL 4-PyC8 in drug PMZ and gemini surfactant 16-10-16

Figure 43. Structure of typical toxic organophosphates.

Figure 44. Structure of typical AChE reactivators, used in clinical practice.

Figure 45. Structure comparison of typical AChE reactivators and sustainable pyridinium phenylalanine-derived ionic liquids (PyPheOC_n).

Figure 46. Strategy of design of cholinesterase reactivators using sustainable ionic liquid-based molecular platform.

Figure 47. Cholinesterase reactivators based on sustainable ionic liquid molecular platforms: target structure for synthesis.

Figure 48. Synthesis of the target cholinesterase reactivators based on sustainable ionic liquids molecular platforms.

Figure 49. Dependencies of BBB score values on $\log P_{\text{o/w}}$ obtained with different on-line predictors and fingerprints used.

Figure 50. Best docking poses of the compounds 3d, 4 d and 3e on HssAChE-GB, HssAChE-VX and HssAChE-PON.

Figure 51. Combination of enzymatic pre-treatment with further hydrolysis products biodegradation.

Figure 52. Hydrolysis of compounds 3d and 4d.

Figure 53. Stability study in human blood plasma for compounds 3d and 4d.

List of tables

Table 1. Biodegradation results for ionic liquids with different cations and Tf_2N^- , PF_6^- , BF_4^- anions.

Table 2. Influence of alkyl chain on biodegradation results for imidazolium and pyridinium ionic liquids.

Table 3. Biodegradation results for 1-butyl-3-methylimidazolium ionic liquids.

Table 4. Biodegradation results for ILs with Tf_2N^- , $[\text{BF}_4]^-$ and $[\text{PF}_6]^-$ anions.

Table 5. Biodegradation results for phenylalanine-derived ionic liquids.

Table 6. Physico-chemical parameters for PyPheOC_n and CTABr surfactant systems in processes of PAHs solubilization.

Table 7. Immobilized enzymes tested in PyPheOC_n SAILs decomposition processes.

Table 8. Optimization of the reaction conditions for PyPheOC_4 enzymatic decomposition.

Table 9. Results of biodegradability testing of compounds 1–25 in modified CBT (OECD 301 D protocol).

Table 10. pK_a values of oxime-functionalized SAILs in the absence and in the presence of co-surfactants; 27 °C, $[\text{D}]_0 = 10 \text{ mM}$.

Table 11. Physico-chemical properties of the systems gemini surfactants 16-s-16 / 4-PyC8 with different contents (wt%) of the functionalized IL 4-PyC8 at 300 K.

Table 12. Results of biodegradability testing of oxime-functionalized SAILs in CBT (OECD 301 D protocol).

Table 13. Decomposition of p-nitrophenyl diphenyl phosphate (PNPDPP) in the presence of 4-PyC8 ($[\text{PNPDPP}] = 0.5 \text{ mM}$; 27 °C).

Table 14. Aggregate size d (nm) as a size distribution by number and zeta potential in the presence of various concentrations of the IL 4-PyC8 in the drug PMZ and the gemini 16-10-16 surfactant solution.

Table 15. Parameters pK_a , $\log P_{o/w}$ and BBB scope for ILs Types 1 – Type 4, obtained using Chemicalize, VCLLAB and www.cbiligand.org (fingerprint PubChem) on-line tools.

Table 16. Best docking results for compounds 3d, 4 d and 3e on HssAChE-GB, HssAChE-VX and HssAChE-PON.

Table 17. The effect of compounds Type 1 – Type 4 on the mammalian cell viability (CHO-K1 cell line).

Table 18. Biodegradability of compounds Type 1 – Type 4 and their potential transformation products in Closed bottle test (OECD 301 D protocol).

Table 19. Reactivation capacity of oxime-functionalized ILs and conventional antidotes towards OP-inhibited AChE.

References

- [1] B. Karimi, M. Tavakolian, M. Akbari, and F. Mansouri, "Ionic Liquids in Asymmetric Synthesis: An Overall View from Reaction Media to Supported Ionic Liquid Catalysis," *ChemCatChem*, vol. 10, no. 15, pp. 3173–3205, Aug. 2018, doi: 10.1002/cctc.201701919.
- [2] S. Pan, M. Yao, J. Zhang, B. Li, C. Xing, X. Song, P. Su, H. Zhang "Recognition of Ionic Liquids as High-Voltage Electrolytes for Supercapacitors," *Front Chem*, vol. 8, May 2020, doi: 10.3389/fchem.2020.00261.
- [3] A. Ray and B. Saruhan, "Application of Ionic Liquids for Batteries and Supercapacitors," *Materials*, vol. 14, no. 11, p. 2942, May 2021, doi: 10.3390/ma14112942.
- [4] Y. Zhou and J. Qu, "Ionic Liquids as Lubricant Additives: A Review," *ACS Appl Mater Interfaces*, vol. 9, no. 4, pp. 3209–3222, Feb. 2017, doi: 10.1021/acsami.6b12489.
- [5] S. P. M. Ventura, F. A. e Silva, M. V. Quental, D. Mondal, M. G. Freire, and J. A. P. Coutinho, "Ionic-Liquid-Mediated Extraction and Separation Processes for Bioactive Compounds: Past, Present, and Future Trends," *Chem Rev*, vol. 117, no. 10, pp. 6984–7052, May 2017, doi: 10.1021/acs.chemrev.6b00550.
- [6] M. Koel, "Ionic Liquids in Chemical Analysis," *Crit Rev Anal Chem*, vol. 35, no. 3, pp. 177–192, Jul. 2005, doi: 10.1080/10408340500304016.
- [7] M. J. Trujillo-Rodríguez, H. Nan, M. Varona, M. N. Emaus, I. D. Souza, and J. L. Anderson, "Advances of Ionic Liquids in Analytical Chemistry," *Anal Chem*, vol. 91, no. 1, pp. 505–531, Jan. 2019, doi: 10.1021/acs.analchem.8b04710.
- [8] A. J. Greer, J. Jacquemin, and C. Hardacre, "Industrial Applications of Ionic Liquids," *Molecules*, vol. 25, no. 21, p. 5207, Nov. 2020, doi: 10.3390/molecules25215207.
- [9] *Ionic Liquids and Their Application in Green Chemistry*. Elsevier, 2023. doi: 10.1016/C2021-0-01782-X.
- [10] C.-W. Cho, T. P. T. Pham, Y. Zhao, S. Stolte, and Y.-S. Yun, "Review of the toxic effects of ionic liquids," *Science of The Total Environment*, vol. 786, p. 147309, Sep. 2021, doi: 10.1016/j.scitotenv.2021.147309.
- [11] D. Kowalska, J. Maculewicz, P. Stepnowski, and J. Dołzonek, "Ionic liquids as environmental hazards – Crucial data in view of future PBT and PMT assessment," *J Hazard Mater*, vol. 403, p. 123896, Feb. 2021, doi: 10.1016/j.jhazmat.2020.123896.
- [12] A. R. P. Gonçalves, X. Paredes, A. F. Cristino, F. J. V. Santos, and C. S. G. P. Queirós, "Ionic Liquids—A Review of Their Toxicity to Living Organisms," *Int J Mol Sci*, vol. 22, no. 11, p. 5612, May 2021, doi: 10.3390/ijms22115612.
- [13] A. Jordan and N. Gathergood, "Biodegradation of ionic liquids – a critical review," *Chem Soc Rev*, vol. 44, no. 22, pp. 8200–8237, 2015, doi: 10.1039/C5CS00444F.
- [14] A.-K. Amsel, O. Olsson, and K. Kümmerer, "Inventory of biodegradation data of ionic liquids," *Chemosphere*, vol. 299, p. 134385, Jul. 2022, doi: 10.1016/j.chemosphere.2022.134385.

- [15] A. Haiß, A. Jordan, J. Westphal, E. Logunova, N. Gathergood, and K. Kümmerer, "On the way to greener ionic liquids: identification of a fully mineralizable phenylalanine-based ionic liquid," *Green Chemistry*, vol. 18, no. 16, pp. 4361–4373, 2016, doi: 10.1039/C6GC00417B.
- [16] A. Jordan, A. Haiß, M. Spulak, Y. Karpichev, K. Kümmerer, and N. Gathergood, "Synthesis of a series of amino acid derived ionic liquids and tertiary amines: green chemistry metrics including microbial toxicity and preliminary biodegradation data analysis," *Green Chemistry*, vol. 18, no. 16, pp. 4374–4392, 2016, doi: 10.1039/C6GC00415F.
- [17] I. V. Kapitanov *et al.*, "Synthesis, self-assembly, bacterial and fungal toxicity, and preliminary biodegradation studies of a series of *L*-phenylalanine-derived surface-active ionic liquids," *Green Chemistry*, vol. 21, no. 7, pp. 1777–1794, 2019, doi: 10.1039/C9GC00030E.
- [18] D. K. A. Kusumahastuti, M. Sihtmäe, I. V. Kapitanov, Y. Karpichev, N. Gathergood, and A. Kahru, "Toxicity profiling of 24 *L*-phenylalanine derived ionic liquids based on pyridinium, imidazolium and cholinium cations and varying alkyl chains using rapid screening *Vibrio fischeri* bioassay," *Ecotoxicol Environ Saf*, vol. 172, pp. 556–565, May 2019, doi: 10.1016/j.ecoenv.2018.12.076.
- [19] M. Suk *et al.*, "Design rules for environmental biodegradability of phenylalanine alkyl ester linked ionic liquids," *Green Chemistry*, vol. 22, no. 14, pp. 4498–4508, 2020, doi: 10.1039/D0GC00918K.
- [20] U.S. Environmental Protection Agency. Basics of Green Chemistry. <https://www.epa.gov/greenchemistry/basics-green-chemistry> (accessed 2024-10-22).
- [21] J. C. Warner and P.T. Anastas, *Green Chemistry: Theory and Practice*. New York: Oxford University Press, 1998.
- [22] F. Roschangar, R. A. Sheldon, and C. H. Senanayake, "Overcoming barriers to green chemistry in the pharmaceutical industry – the Green Aspiration Level™ concept," *Green Chemistry*, vol. 17, no. 2, pp. 752–768, 2015, doi: 10.1039/C4GC01563K.
- [23] K. Van Aken, L. Strekowski, and L. Patiny, "EcoScale, a semi-quantitative tool to select an organic preparation based on economical and ecological parameters," *Beilstein Journal of Organic Chemistry*, vol. 2, Mar. 2006, doi: 10.1186/1860-5397-2-3.
- [24] A. Lapkin and D. J. C. Constable, Eds., *Green Chemistry Metrics*. Wiley, 2008. doi: 10.1002/9781444305432.
- [25] C. R. McElroy, A. Constantinou, L. C. Jones, L. Summerton, and J. H. Clark, "Towards a holistic approach to metrics for the 21st century pharmaceutical industry," *Green Chemistry*, vol. 17, no. 5, pp. 3111–3121, 2015, doi: 10.1039/C5GC00340G.
- [26] Z. Lei, B. Chen, Y.-M. Koo, and D. R. MacFarlane, "Introduction: Ionic Liquids," *Chem Rev*, vol. 117, no. 10, pp. 6633–6635, May 2017, doi: 10.1021/acs.chemrev.7b00246.
- [27] T. Welton, "Room-Temperature Ionic Liquids. Solvents for Synthesis and Catalysis," *Chem Rev*, vol. 99, no. 8, pp. 2071–2084, Aug. 1999, doi: 10.1021/cr980032t.

- [28] J. P. Hallett and T. Welton, "Room-Temperature Ionic Liquids: Solvents for Synthesis and Catalysis. 2," *Chem Rev*, vol. 111, no. 5, pp. 3508–3576, May 2011, doi: 10.1021/cr1003248.
- [29] S. K. Singh and A. W. Savoy, "Ionic liquids synthesis and applications: An overview," *J Mol Liq*, vol. 297, p. 112038, Jan. 2020, doi: 10.1016/j.molliq.2019.112038.
- [30] J. D. Holbrey and K. R. Seddon, "Ionic Liquids," *Clean Technol Environ Policy*, vol. 1, no. 4, pp. 223–236, Dec. 1999, doi: 10.1007/s100980050036.
- [31] R. A. Sheldon, "The greening of solvents: Towards sustainable organic synthesis," *Curr Opin Green Sustain Chem*, vol. 18, pp. 13–19, Aug. 2019, doi: 10.1016/j.cogsc.2018.11.006.
- [32] C. Xu and Z. Cheng, "Thermal Stability of Ionic Liquids: Current Status and Prospects for Future Development," *Processes*, vol. 9, no. 2, p. 337, Feb. 2021, doi: 10.3390/pr9020337.
- [33] S. Ravula, N. E. Larm, M. A. Mottaleb, M. P. Heitz, and G. A. Baker, "Vapor Pressure Mapping of Ionic Liquids and Low-Volatility Fluids Using Graded Isothermal Thermogravimetric Analysis," *ChemEngineering*, vol. 3, no. 2, p. 42, Apr. 2019, doi: 10.3390/chemengineering3020042.
- [34] Y. Li, Y. Pan, G. Huang, Q. Wang, Q. Wei, and J. Jiang, "Flammability hazard analysis of imidazolium-based ionic liquid binary mixtures under high temperatures," *J Loss Prev Process Ind*, vol. 64, p. 104081, Mar. 2020, doi: 10.1016/j.jlp.2020.104081.
- [35] K. Pan *et al.*, "Insights into Ionic Liquids for Flame Retardant: A Study Based on Bibliometric Mapping," *Safety*, vol. 9, no. 3, p. 49, Jul. 2023, doi: 10.3390/safety9030049.
- [36] G. Kaur, H. Kumar, and M. Singla, "Diverse applications of ionic liquids: A comprehensive review," *J Mol Liq*, vol. 351, p. 118556, Apr. 2022, doi: 10.1016/j.molliq.2022.118556.
- [37] K. S. Egorova, E. G. Gordeev, and V. P. Ananikov, "Biological Activity of Ionic Liquids and Their Application in Pharmaceuticals and Medicine," *Chem Rev*, vol. 117, no. 10, pp. 7132–7189, May 2017, doi: 10.1021/acs.chemrev.6b00562.
- [38] Y. U. Paulechka, A. G. Kabo, A. V. Blokhin, G. J. Kabo, and M. P. Shevelyova, "Heat Capacity of Ionic Liquids: Experimental Determination and Correlations with Molar Volume," *J Chem Eng Data*, vol. 55, no. 8, pp. 2719–2724, Aug. 2010, doi: 10.1021/je900974u.
- [39] Z. Dai, Y. Chen, C. Liu, X. Lu, Y. Liu, and X. Ji, "Prediction and verification of heat capacities for pure ionic liquids," *Chin J Chem Eng*, vol. 31, pp. 169–176, Mar. 2021, doi: 10.1016/j.cjche.2020.10.040.
- [40] *Ionic Liquids in Analytical Chemistry*. Elsevier, 2021. doi: 10.1016/C2019-0-04941-2.
- [41] N. K. Singha, K. Hong, and J. W. Mays, "Polymerization in Ionic Liquids," in *Polymerized Ionic Liquids*, The Royal Society of Chemistry, 2017, pp. 1–22. doi: 10.1039/9781788010535-00001.
- [42] K. Sood, Y. Saini, and K. K. Thakur, "Ionic liquids in catalysis: A review," *Mater Today Proc*, vol. 81, pp. 739–744, 2023, doi: 10.1016/j.matpr.2021.04.225.

- [43] M. M. Seitkalieva, D. E. Samoylenko, K. A. Lotsman, K. S. Rodygin, and V. P. Ananikov, "Metal nanoparticles in ionic liquids: Synthesis and catalytic applications," *Coord Chem Rev*, vol. 445, p. 213982, Oct. 2021, doi: 10.1016/j.ccr.2021.213982.
- [44] H. Garcia and S. Navalon, "CHAPTER 9. Photochemistry in Ionic Liquids," pp. 474–507. doi: 10.1039/9781849737210-00474.
- [45] M. Guimarães, N. Mateus, V. de Freitas, L. C. Branco, and L. Cruz, "Microwave-Assisted Synthesis and Ionic Liquids: Green and Sustainable Alternatives toward Enzymatic Lipophilization of Anthocyanin Monoglucosides," *J Agric Food Chem*, vol. 68, no. 28, pp. 7387–7392, Jul. 2020, doi: 10.1021/acs.jafc.0c02599.
- [46] M. Kathiresan and D. Velayutham, "Ionic liquids as an electrolyte for the electro synthesis of organic compounds," *Chemical Communications*, vol. 51, no. 99, pp. 17499–17516, 2015, doi: 10.1039/C5CC06961K.
- [47] "Recalling COIL," *Green Chemistry*, vol. 8, no. 5, p. 411, 2006, doi: 10.1039/b605378p.
- [48] "CHEMISTRY BASF'S SMART IONIC LIQUID," *Chemical & Engineering News Archive*, vol. 81, no. 13, p. 9, Mar. 2003, doi: 10.1021/cen-v081n013.p009.
- [49] N. V. Plechkova and K. R. Seddon, "Applications of ionic liquids in the chemical industry," *Chem. Soc. Rev.*, vol. 37, no. 1, pp. 123–150, 2008, doi: 10.1039/B006677J.
- [50] P. Pillai, M. Maiti, and A. Mandal, "Mini-review on Recent Advances in the Application of Surface-Active Ionic Liquids: Petroleum Industry Perspective," *Energy & Fuels*, vol. 36, no. 15, pp. 7925–7939, Aug. 2022, doi: 10.1021/acs.energyfuels.2c00964.
- [51] Z. Usmani *et al.*, "Ionic liquid based pretreatment of lignocellulosic biomass for enhanced bioconversion," *Bioresour Technol*, vol. 304, p. 123003, May 2020, doi: 10.1016/j.biortech.2020.123003.
- [52] T. U. Rashid, "Ionic liquids: Innovative fluids for sustainable gas separation from industrial waste stream," *J Mol Liq*, vol. 321, p. 114916, Jan. 2021, doi: 10.1016/j.molliq.2020.114916.
- [53] M. Zunita, H. P. Winoto, M. F. K. Fauzan, and R. Haikal, "Recent advances in plastics waste degradation using ionic liquid-based process," *Polym Degrad Stab*, vol. 211, p. 110320, May 2023, doi: 10.1016/j.polymdegradstab.2023.110320.
- [54] F. Liu, X. Cui, S. Yu, Z. Li, and X. Ge, "Hydrolysis reaction of poly(ethylene terephthalate) using ionic liquids as solvent and catalyst," *J Appl Polym Sci*, vol. 114, no. 6, pp. 3561–3565, Dec. 2009, doi: 10.1002/app.30981.
- [55] T. Muringayil Joseph *et al.*, "Polyethylene terephthalate (PET) recycling: A review," *Case Studies in Chemical and Environmental Engineering*, vol. 9, p. 100673, Jun. 2024, doi: 10.1016/j.cscee.2024.100673.
- [56] "The Coca-Cola Company. Press release: What is a World Without Waste?" Accessed: Oct. 22, 2024. [Online]. Available: <https://www.coca-colacompany.com/about-us/faq/what-is-world-without-waste#:~:text=Make%20100%25%20of%20our%20packaging,refillable%2Freturnable%20packaging%20by%202030>
- [57] K. Holmberg, Ed., *Handbook of Applied Surface and Colloid Chemistry*. Weinheim: Wiley-VCH Verlag GmbH & Co, KGaA, 2001.
- [58] J. T. K. M.J. Rosen, *Surfactants and Interfacial Phenomena*. Hoboken, New Jersey: John Wiley & Sons, 2012.

- [59] Y. Kondo, H. Miyazawa, H. Sakai, M. Abe, and N. Yoshino, "First Anionic Micelle with Unusually Long Lifetime: Self-Assembly of Fluorocarbon–Hydrocarbon Hybrid Surfactant," *J Am Chem Soc*, vol. 124, no. 23, pp. 6516–6517, Jun. 2002, doi: 10.1021/ja0178564.
- [60] J. B. Rosenholm, T. E. Burchfield, and L. G. Hepler, "Thermodynamics of micelle formation: Standard states, temperature dependence of the critical micelle concentration, and thermal expansion of the solvent," *J Colloid Interface Sci*, vol. 78, no. 1, pp. 191–194, Nov. 1980, doi: 10.1016/0021-9797(80)90506-8.
- [61] K. Motomura, "Thermodynamic studies on adsorption at interfaces. I. General formulation," *J Colloid Interface Sci*, vol. 64, no. 2, pp. 348–355, Apr. 1978, doi: 10.1016/0021-9797(78)90371-5.
- [62] O. Massarweh and A. S. Abushaikh, "The use of surfactants in enhanced oil recovery: A review of recent advances," *Energy Reports*, vol. 6, pp. 3150–3178, Nov. 2020, doi: 10.1016/j.egy.2020.11.009.
- [63] H.-P. Hentze and E. W. Kaler, "Polymerization of and within self-organized media," *Curr Opin Colloid Interface Sci*, vol. 8, no. 2, pp. 164–178, Jun. 2003, doi: 10.1016/S1359-0294(03)00018-9.
- [64] T. Shen *et al.*, "Recent advances on micellar catalysis in water," *Adv Colloid Interface Sci*, vol. 287, p. 102299, Jan. 2021, doi: 10.1016/j.cis.2020.102299.
- [65] C. Tang and B. T. McInnes, "Cascade Processes with Micellar Reaction Media: Recent Advances and Future Directions," *Molecules*, vol. 27, no. 17, p. 5611, Aug. 2022, doi: 10.3390/molecules27175611.
- [66] G. L. McIntire and J. G. Dorsey, "Micelles in Analytical Chemistry," *Crit Rev Anal Chem*, vol. 21, no. 4, pp. 257–278, Jan. 1990, doi: 10.1080/10408349008051631.
- [67] D. N. Unal, S. Yildirim, S. Kurbanoglu, and B. Uslu, "Current trends and roles of surfactants for chromatographic and electrochemical sensing," *TrAC Trends in Analytical Chemistry*, vol. 144, p. 116418, Nov. 2021, doi: 10.1016/j.trac.2021.116418.
- [68] I. Kralova and J. Sjöblom, "Surfactants Used in Food Industry: A Review," *J Dispers Sci Technol*, vol. 30, no. 9, pp. 1363–1383, Sep. 2009, doi: 10.1080/01932690902735561.
- [69] B. G. Ribeiro, J. M. C. Guerra, and L. A. Sarubbo, "Biosurfactants: Production and application prospects in the food industry," *Biotechnol Prog*, vol. 36, no. 5, Sep. 2020, doi: 10.1002/btpr.3030.
- [70] M. Y. de Freitas Araújo Reis *et al.*, "A General Approach on Surfactants Use and Properties in Drug Delivery Systems," *Curr Pharm Des*, vol. 27, no. 42, pp. 4300–4314, Nov. 2021, doi: 10.2174/1381612827666210526091825.
- [71] D. R. Pokhrel, M. K. Sah, B. Gautam, H. K. Basak, A. Bhattarai, and A. Chatterjee, "A recent overview of surfactant–drug interactions and their importance," *RSC Adv*, vol. 13, no. 26, pp. 17685–17704, 2023, doi: 10.1039/D3RA02883F.
- [72] H. Watson, "Biological membranes," *Essays Biochem*, vol. 59, pp. 43–69, Nov. 2015, doi: 10.1042/bse0590043.
- [73] S. K. Mehta, S. Sharma, N. Mehta, and S. S. Cameotra, "Biomimetic Amphiphiles: Properties and Potential Use," 2010, pp. 102–120. doi: 10.1007/978-1-4419-5979-9_8.
- [74] C. Bombelli, L. Giansanti, P. Luciani, and G. Mancini, "Gemini Surfactant Based Carriers in Gene and Drug Delivery," *Curr Med Chem*, vol. 16, no. 2, pp. 171–183, Jan. 2009, doi: 10.2174/092986709787002808.

- [75] N. Singh, Y. Karpichev, A. K. Tiwari, K. Kuca, and K. K. Ghosh, "Oxime functionality in surfactant self-assembly: An overview on combating toxicity of organophosphates," *J Mol Liq*, vol. 208, pp. 237–252, Aug. 2015, doi: 10.1016/j.molliq.2015.04.010.
- [76] L.T.T. Ho, Ed., *Formulating Detergents and Personal Care Products: A Complete Guide to Product Development*. New York: AOCS Press, 2000.
- [77] H. B. Klevens, "Solubilization.," *Chem Rev*, vol. 47, no. 1, pp. 1–74, Aug. 1950, doi: 10.1021/cr60146a001.
- [78] K. L. Mittal, Ed., *Micellization, Solubilization, and Microemulsions*. Boston, MA: Springer US, 1977. doi: 10.1007/978-1-4613-4157-4.
- [79] F. Fabris, M. Illner, J.-U. Repke, A. Scarso, and M. Schwarze, "Is Micellar Catalysis Green Chemistry?," *Molecules*, vol. 28, no. 12, p. 4809, Jun. 2023, doi: 10.3390/molecules28124809.
- [80] K. Martinek, A. K. Yatsimirski, A. P. Osipov, and I. V. Berezin, "Micellar effects on kinetics and equilibrium of synthesis and hydrolysis of benzylidenedianiline," *Tetrahedron*, vol. 29, no. 7, pp. 963–969, Jan. 1973, doi: 10.1016/0040-4020(73)80046-8.
- [81] A. A. and M. N. K. M.-Y. Cheong, "A Comparative Analysis of Pseudophase Ion-Exchange (PIE) Model and Berezin Pseudophase (BPP) Model: Analysis of Kinetic Data for Ionic Micellar-mediated Semi-ionic Bimolecular Reaction," *Bull Korean Chem Soc*, vol. 28, no. 7, pp. 1135–1140, Jul. 2007, doi: 10.5012/bkcs.2007.28.7.1135.
- [82] N. Singh *et al.*, "From α -nucleophiles to functionalized aggregates: exploring the reactivity of hydroxamate ion towards esterolytic reactions in micelles," *Org Biomol Chem*, vol. 13, no. 10, pp. 2827–2848, 2015, doi: 10.1039/C4OB02067G.
- [83] Yu. S. Simanenko *et al.*, "Functional Detergents Containing an Imidazole Ring and Typical Fragments of α -Nucleophiles Underlying Micellar Systems for Cleavage of Esters of Proosphorus Acids," *Russian Journal of Organic Chemistry*, vol. 40, no. 2, pp. 206–218, Feb. 2004, doi: 10.1023/B:RUJO.0000034943.58369.eb.
- [84] R. A. Moss and H. Zhang, "Toward a broad-spectrum decontaminant for reactive toxic phosphates/phosphonates: N-alkyl-3-iodosopyridinium-4-carboxylates," *Tetrahedron Lett*, vol. 34, no. 39, pp. 6225–6228, Sep. 1993, doi: 10.1016/S0040-4039(00)73716-6.
- [85] R. A. Moss, R. C. Nahas, and S. Ramaswami, "Sequential bifunctional micellar catalysis," *J Am Chem Soc*, vol. 99, no. 2, pp. 627–629, Jan. 1977, doi: 10.1021/ja00444a062.
- [86] J. M. Brown, C. A. Bunton, S. Diaz, and Y. Ihara, "Dephosphorylation in functional micelles. The role of the imidazole group," *J Org Chem*, vol. 45, no. 21, pp. 4169–4174, Oct. 1980, doi: 10.1021/jo01309a021.
- [87] R. A. Moss, T. F. Hendrickson, and G. O. Bizzigotti, "Esterolytic chemistry of vesicular thiocholine surfactant," *J Am Chem Soc*, vol. 108, no. 18, pp. 5520–5527, Sep. 1986, doi: 10.1021/ja00278a025.
- [88] I. V. Kapitanov *et al.*, "Physicochemical properties and esterolytic reactivity of oxime functionalized surfactants in pH-responsive mixed micellar system," *Colloids Surf A Physicochem Eng Asp*, vol. 524, pp. 143–159, Jul. 2017, doi: 10.1016/j.colsurfa.2017.04.039.

- [89] D. R. Gabdrakhmanov *et al.*, "Supramolecular Systems Based on Novel Amphiphiles and a Polymer: Aggregation and Selective Solubilization," *J Surfactants Deterg*, vol. 22, no. 4, pp. 865–874, Jul. 2019, doi: 10.1002/jsde.12257.
- [90] F. Hampl, F. Liska, F. Mancin, P. Tecilla, and U. Tonellato, "Metallomicelles Made of Ni(II) Complexes of Lipophilic 2-Pyridineketoximes as Powerful Catalysts of the Cleavage of Carboxylic Acid Esters," *Langmuir*, vol. 15, no. 2, pp. 405–412, Jan. 1999, doi: 10.1021/la980861+.
- [91] G. Mercey *et al.*, "Reactivators of Acetylcholinesterase Inhibited by Organophosphorus Nerve Agents," *Acc Chem Res*, vol. 45, no. 5, pp. 756–766, May 2012, doi: 10.1021/ar2002864.
- [92] L. Gorecki *et al.*, "Progress in acetylcholinesterase reactivators and in the treatment of organophosphorus intoxication: a patent review (2006–2016)," *Expert Opin Ther Pat*, vol. 27, no. 9, pp. 971–985, Sep. 2017, doi: 10.1080/13543776.2017.1338275.
- [93] J. D. Figueroa-Villar, E. C. Petronilho, K. Kuca, and T. C. C. Franca, "Review about Structure and Evaluation of Reactivators of Acetylcholinesterase Inhibited with Neurotoxic Organophosphorus Compounds," *Curr Med Chem*, vol. 28, no. 7, pp. 1422–1442, Feb. 2021, doi: 10.2174/0929867327666200425213215.
- [94] C. S. Buettner, A. Cognigni, C. Schröder, and K. Bica-Schröder, "Surface-active ionic liquids: A review," *J Mol Liq*, vol. 347, p. 118160, Feb. 2022, doi: 10.1016/j.molliq.2021.118160.
- [95] N. Tafur, A. Mamonov, M. A. Islam Khan, A. Soto, T. Puntervold, and S. Strand, "Evaluation of Surface-Active Ionic Liquids in Smart Water for Enhanced Oil Recovery in Carbonate Rocks," *Energy & Fuels*, vol. 37, no. 16, pp. 11730–11742, Aug. 2023, doi: 10.1021/acs.energyfuels.3c01488.
- [96] A. T. Silva, C. Teixeira, E. F. Marques, C. Prudêncio, P. Gomes, and R. Ferraz, "Surfing the Third Wave of Ionic Liquids: A Brief Review on the Role of Surface-Active Ionic Liquids in Drug Development and Delivery," *ChemMedChem*, vol. 16, no. 17, pp. 2604–2611, Sep. 2021, doi: 10.1002/cmdc.202100215.
- [97] M. Wojcieszak *et al.*, "Surface-Active Ionic Liquids and Surface-Active Quaternary Ammonium Salts from Synthesis, Characterization to Antimicrobial Properties," *Molecules*, vol. 29, no. 2, p. 443, Jan. 2024, doi: 10.3390/molecules29020443.
- [98] T. P. Thuy Pham, C.-W. Cho, and Y.-S. Yun, "Environmental fate and toxicity of ionic liquids: A review," *Water Res*, vol. 44, no. 2, pp. 352–372, Jan. 2010, doi: 10.1016/j.watres.2009.09.030.
- [99] J. E. S. J. Reid, H. Prydderch, M. Spulak, S. Shimizu, A. J. Walker, and N. Gathergood, "Green profiling of aprotic versus protic ionic liquids: Synthesis and microbial toxicity of analogous structures," *Sustain Chem Pharm*, vol. 7, pp. 17–26, Mar. 2018, doi: 10.1016/j.scp.2017.11.001.
- [100] S. Kumar *et al.*, "Effect of the Alkyl Chain Length of Amphiphilic Ionic Liquids on the Structure and Dynamics of Model Lipid Membranes," *Langmuir*, vol. 35, no. 37, pp. 12215–12223, Sep. 2019, doi: 10.1021/acs.langmuir.9b02128.
- [101] J. Dołzonek, C.-W. Cho, P. Stepnowski, M. Markiewicz, J. Thöming, and S. Stolte, "Membrane partitioning of ionic liquid cations, anions and ion pairs – Estimating the bioconcentration potential of organic ions," *Environmental Pollution*, vol. 228, pp. 378–389, Sep. 2017, doi: 10.1016/j.envpol.2017.04.079.

- [102] C. Pereira, R. D. Silva, L. Saraiva, B. Johansson, M. J. Sousa, and M. Côrte-Real, "Mitochondria-dependent apoptosis in yeast," *Biochimica et Biophysica Acta (BBA) - Molecular Cell Research*, vol. 1783, no. 7, pp. 1286–1302, Jul. 2008, doi: 10.1016/j.bbamcr.2008.03.010.
- [103] G. Bhattacharya *et al.*, "Structural changes in cellular membranes induced by ionic liquids: From model to bacterial membranes," *Chem Phys Lipids*, vol. 215, pp. 1–10, Sep. 2018, doi: 10.1016/j.chemphyslip.2018.06.001.
- [104] X. Xia, R. Wan, P. Wang, W. Huo, H. Dong, and Q. Du, "Toxicity of imidazoles ionic liquid [C16mim]Cl to Hela cells," *Ecotoxicol Environ Saf*, vol. 162, pp. 408–414, Oct. 2018, doi: 10.1016/j.ecoenv.2018.07.022.
- [105] R. Biczak, "Quaternary ammonium salts with tetrafluoroborate anion: Phytotoxicity and oxidative stress in terrestrial plants," *J Hazard Mater*, vol. 304, pp. 173–185, Mar. 2016, doi: 10.1016/j.jhazmat.2015.10.055.
- [106] Y. Xia, D. Liu, Y. Dong, J. Chen, and H. Liu, "Effect of ionic liquids with different cations and anions on photosystem and cell structure of *Scenedesmus obliquus*," *Chemosphere*, vol. 195, pp. 437–447, Mar. 2018, doi: 10.1016/j.chemosphere.2017.12.054.
- [107] R. Wan, X. Xia, P. Wang, W. Huo, H. Dong, and Z. Chang, "Toxicity of imidazoles ionic liquid [C16mim]Cl to HepG2 cells," *Toxicology in Vitro*, vol. 52, pp. 1–7, Oct. 2018, doi: 10.1016/j.tiv.2018.05.013.
- [108] K. S. Egorova, A. V. Posvyatenko, A. N. Fakhruddinov, A. S. Kashin, and V. P. Ananikov, "Assessing possible influence of structuring effects in solution on cytotoxicity of ionic liquid systems," *J Mol Liq*, vol. 297, p. 111751, Jan. 2020, doi: 10.1016/j.molliq.2019.111751.
- [109] D. O. Hartmann *et al.*, "Plasma membrane permeabilisation by ionic liquids: a matter of charge," *Green Chemistry*, vol. 17, no. 9, pp. 4587–4598, 2015, doi: 10.1039/C5GC01472G.
- [110] "OECD. OECD Guideline for Testing of Chemicals - Ready Biodegradability." 1992.
- [111] M. C. D.L. Nelson, *Lehninger Principles of Biochemistry*, 8th ed. W.H.Freeman & Co Ltd., 2021.
- [112] I. T. Horváth, "Introduction: Sustainable Chemistry," *Chem Rev*, vol. 118, no. 2, pp. 369–371, Jan. 2018, doi: 10.1021/acs.chemrev.7b00721.
- [113] "Importance of Green and Sustainable Chemistry in the Chemical Industry," *ACS Sustain Chem Eng*, vol. 10, no. 26, pp. 8239–8241, Jul. 2022, doi: 10.1021/acssuschemeng.2c03306.
- [114] R. Mori, "Replacing all petroleum-based chemical products with natural biomass-based chemical products: a tutorial review," *RSC Sustainability*, vol. 1, no. 2, pp. 179–212, 2023, doi: 10.1039/D2SU00014H.
- [115] H. Ohno and K. Fukumoto, "Amino Acid Ionic Liquids," *Acc Chem Res*, vol. 40, no. 11, pp. 1122–1129, Nov. 2007, doi: 10.1021/ar700053z.
- [116] X.-D. Hou, Q.-P. Liu, T. J. Smith, N. Li, and M.-H. Zong, "Evaluation of Toxicity and Biodegradability of Cholinium Amino Acids Ionic Liquids," *PLoS One*, vol. 8, no. 3, p. e59145, Mar. 2013, doi: 10.1371/journal.pone.0059145.
- [117] S. Kirchhecker and D. Esposito, "Amino acid based ionic liquids: A green and sustainable perspective," *Curr Opin Green Sustain Chem*, vol. 2, pp. 28–33, Oct. 2016, doi: 10.1016/j.cogsc.2016.09.001.

- [118] Y. Usuda, Y. Hara, and H. Kojima, "Toward Sustainable Amino Acid Production," 2016, pp. 289–304. doi: 10.1007/10_2016_36.
- [119] M. Ding, S. Song, and X. Li, "A perspective on renewable production of amino acids from biomass through the chemocatalytic method," *Green Chemistry*, 2024, doi: 10.1039/D4GC00846D.
- [120] M. D'Este, M. Alvarado-Morales, and I. Angelidaki, "Amino acids production focusing on fermentation technologies – A review," *Biotechnol Adv*, vol. 36, no. 1, pp. 14–25, Jan. 2018, doi: 10.1016/j.biotechadv.2017.09.001.
- [121] Q. Xu, H. Deng, X. Li, and Z.-S. Quan, "Application of Amino Acids in the Structural Modification of Natural Products: A Review," *Front Chem*, vol. 9, Apr. 2021, doi: 10.3389/fchem.2021.650569.
- [122] A. Bongioanni, M. S. Bueno, B. A. Mezzano, M. R. Longhi, and C. Garnerio, "Amino acids and its pharmaceutical applications: A mini review," *Int J Pharm*, vol. 613, p. 121375, Feb. 2022, doi: 10.1016/j.ijpharm.2021.121375.
- [123] J. Guo, L. Sun, F. Zhang, B. Sun, B. Xu, and Y. Zhou, "Review: Progress in synthesis, properties and application of amino acid surfactants," *Chem Phys Lett*, vol. 794, p. 139499, May 2022, doi: 10.1016/j.cplett.2022.139499.
- [124] D. Coleman, M. Špulák, M. T. Garcia, and N. Gathergood, "Antimicrobial toxicity studies of ionic liquids leading to a 'hit' MRSA selective antibacterial imidazolium salt," *Green Chemistry*, vol. 14, no. 5, p. 1350, 2012, doi: 10.1039/c2gc16090k.
- [125] J. G. Speight, *The Chemistry and Technology of Petroleum*. CRC Press, 2006. doi: 10.1201/9781420008388.
- [126] A. B. Patel, S. Shaikh, K. R. Jain, C. Desai, and D. Madamwar, "Polycyclic Aromatic Hydrocarbons: Sources, Toxicity, and Remediation Approaches," *Front Microbiol*, vol. 11, Nov. 2020, doi: 10.3389/fmicb.2020.562813.
- [127] M. R. Pérez-Gregorio, M. S. García-Falcón, E. Martínez-Carballo, and J. Simal-Gándara, "Removal of polycyclic aromatic hydrocarbons from organic solvents by ashes wastes," *J Hazard Mater*, vol. 178, no. 1–3, pp. 273–281, Jun. 2010, doi: 10.1016/j.jhazmat.2010.01.073.
- [128] S. Lamichhane, K. C. Bal Krishna, and R. Sarukkalige, "Surfactant-enhanced remediation of polycyclic aromatic hydrocarbons: A review," *J Environ Manage*, vol. 199, pp. 46–61, Sep. 2017, doi: 10.1016/j.jenvman.2017.05.037.
- [129] S. O. Badmus, H. K. Amusa, T. A. Oyehan, and T. A. Saleh, "Environmental risks and toxicity of surfactants: overview of analysis, assessment, and remediation techniques," *Environmental Science and Pollution Research*, vol. 28, no. 44, pp. 62085–62104, Nov. 2021, doi: 10.1007/s11356-021-16483-w.
- [130] S. Rebello, A. K. Asok, S. Mundayoor, and M. S. Jisha, "Surfactants: toxicity, remediation and green surfactants," *Environ Chem Lett*, vol. 12, no. 2, pp. 275–287, Jun. 2014, doi: 10.1007/s10311-014-0466-2.
- [131] A. A. Serdyuk *et al.*, "Effect of structure of polycyclic aromatic substrates on solubilization capacity and size of cationic monomeric and gemini 14-s-14 surfactant aggregates," *Colloids Surf A Physicochem Eng Asp*, vol. 509, pp. 613–622, Nov. 2016, doi: 10.1016/j.colsurfa.2016.09.068.
- [132] T. Bugg, *Introduction to Enzyme and Coenzyme Chemistry*. Wiley, 2004. doi: 10.1002/9781444305364.
- [133] M.B. Smith, *March's Advanced Organic Chemistry: Reactions, Mechanisms, and Structure*, 8th ed. John Wiley & Sons, 2020.

- [134] G. M. Daba, F. A. Mostafa, and W. A. Elkhateeb, "The ancient koji mold (*Aspergillus oryzae*) as a modern biotechnological tool," *Bioresour Bioprocess*, vol. 8, no. 1, p. 52, Jun. 2021, doi: 10.1186/s40643-021-00408-z.
- [135] A. Sauerbrei, "Bactericidal and virucidal activity of ethanol and povidone-iodine," *Microbiologyopen*, vol. 9, no. 9, Sep. 2020, doi: 10.1002/mbo3.1097.
- [136] "EUCAST. Method for the Determination of Broth Dilution Minimum Inhibitory Concentrations of Antifungal Agents for Yeasts - EUCAST Definitive Document EDEF 7.3.1." 2017.
- [137] "EUCAST. Method for the Determination of Broth Dilution Minimum Inhibitory Concentrations of Antifungal Agents for Conidia Forming Moulds – EUCAST Definitive Document EDEF 9.3.1." 2015.
- [138] "ESCMID. (ESCMID) European Committee for Antimicrobial Susceptibility Testing (EUCAST) of the European Society of Clinical Microbiology and Infectious Diseases. Eucast Discussion Document E. Dis 5.1. Determination of Minimum Inhibitory Concentrations (MICs) of An. Clinical Microbiology and Infection." 2003.
- [139] R. Afshari and A. Shaabani, "Materials Functionalization with Multicomponent Reactions: State of the Art," *ACS Comb Sci*, vol. 20, no. 9, pp. 499–528, Sep. 2018, doi: 10.1021/acscombsci.8b00072.
- [140] T. M. Prokop'eva, Yu. S. Simanenko, I. P. Suprun, V. A. Savelova, T. M. Zubareva, and E. A. Karpichev, "Nucleophilic Substitution at a Four-Coordinate Sulfur Atom: VI. Reactivity of Oximate Ions," *Russian Journal of Organic Chemistry*, vol. 37, no. 5, pp. 655–666, 2001, doi: 10.1023/A:1012487415041.
- [141] A. Kovalevsky, D. K. Blumenthal, X. Cheng, P. Taylor, and Z. Radić, "Limitations in current acetylcholinesterase structure-based design of oxime antidotes for organophosphate poisoning," *Ann N Y Acad Sci*, vol. 1378, no. 1, pp. 41–49, Aug. 2016, doi: 10.1111/nyas.13128.
- [142] L. Grosmaire, M. Chorro, C. Chorro, S. Partyka, and R. Zana, "Alkanediyl- α,ω -Bis(dimethylalkylammonium Bromide) Surfactants," *J Colloid Interface Sci*, vol. 246, no. 1, pp. 175–181, Feb. 2002, doi: 10.1006/jcis.2001.8001.
- [143] H. Akbaş, A. Elemenli, and M. Boz, "Aggregation and Thermodynamic Properties of Some Cationic Gemini Surfactants," *J Surfactants Deterg*, vol. 15, no. 1, pp. 33–40, Jan. 2012, doi: 10.1007/s11743-011-1270-7.
- [144] J. Lakra *et al.*, "Mixed micellization of gemini and cationic surfactants: Physicochemical properties and solubilization of polycyclic aromatic hydrocarbons," *Colloids Surf A Physicochem Eng Asp*, vol. 451, pp. 56–65, Jun. 2014, doi: 10.1016/j.colsurfa.2014.03.037.
- [145] I. A. Khan, R. Mohammad, Md. S. Alam, and Kabir-ud-Din, "Effect of Alkylamine Chain Length on the Critical Micelle Concentration of Cationic Gemini Butanediyl- α,ω -bis(dimethylcetylammmonium bromide) Surfactant," *J Dispers Sci Technol*, vol. 30, no. 10, pp. 1486–1493, Nov. 2009, doi: 10.1080/01932690903123361.
- [146] D. S. Karpovich and G. J. Blanchard, "Relating the polarity-dependent fluorescence response of pyrene to vibronic coupling. Achieving a fundamental understanding of the py polarity scale," *J Phys Chem*, vol. 99, no. 12, pp. 3951–3958, Mar. 1995, doi: 10.1021/j100012a014.

- [147] D. C. Dong and M. A. Winnik, "The Py scale of solvent polarities," *Can J Chem*, vol. 62, no. 11, pp. 2560–2565, Nov. 1984, doi: 10.1139/v84-437.
- [148] N. Singh *et al.*, "Physicochemical Properties and Supernucleophilicity of Oxime-Functionalized Surfactants: Hydrolytic Catalysts toward Dephosphorylation of Di- and Triphosphate Esters," *J Phys Chem B*, vol. 117, no. 14, pp. 3806–3817, Apr. 2013, doi: 10.1021/jp310010q.
- [149] M. K. Banjare, K. Behera, R. K. Banjare, S. Pandey, K. K. Ghosh, and Y. Karpichev, "Molecular interactions between novel synthesized biodegradable ionic liquids with antidepressant drug," *Chemical Thermodynamics and Thermal Analysis*, vol. 3–4, p. 100012, Sep. 2021, doi: 10.1016/j.ctta.2021.100012.
- [150] Pisárčik, Polakovičová, Markuliak, Lukáč, and Devínsky, "Self-Assembly Properties of Cationic Gemini Surfactants with Biodegradable Groups in the Spacer," *Molecules*, vol. 24, no. 8, p. 1481, Apr. 2019, doi: 10.3390/molecules24081481.
- [151] *Sittig's Handbook of Pesticides and Agricultural Chemicals*. Elsevier, 2015. doi: 10.1016/C2012-0-02568-9.
- [152] J. Popp, K. Pető, and J. Nagy, "Pesticide productivity and food security. A review," *Agron Sustain Dev*, vol. 33, no. 1, pp. 243–255, Jan. 2013, doi: 10.1007/s13593-012-0105-x.
- [153] W. Boedeker, M. Watts, P. Clausing, and E. Marquez, "The global distribution of acute unintentional pesticide poisoning: estimations based on a systematic review," *BMC Public Health*, vol. 20, no. 1, p. 1875, Dec. 2020, doi: 10.1186/s12889-020-09939-0.
- [154] *Handbook of Toxicology of Chemical Warfare Agents*. Elsevier, 2020. doi: 10.1016/C2018-0-04837-9.
- [155] C. Voros, J. Dias, C. M. Timperley, F. Nachon, R. C. D. Brown, and R. Baati, "The risk associated with organophosphorus nerve agents: from their discovery to their unavoidable threat, current medical countermeasures and perspectives," *Chem Biol Interact*, p. 110973, Apr. 2024, doi: 10.1016/j.cbi.2024.110973.
- [156] J. Opravil *et al.*, "A-agents, misleadingly known as 'Novichoks': a narrative review," *Arch Toxicol*, vol. 97, no. 10, pp. 2587–2607, Oct. 2023, doi: 10.1007/s00204-023-03571-8.
- [157] L. Carlsen, "After Salisbury Nerve Agents Revisited," *Mol Inform*, vol. 38, no. 8–9, Aug. 2019, doi: 10.1002/minf.201800106.
- [158] D. Steindl *et al.*, "Novichok nerve agent poisoning," *The Lancet*, vol. 397, no. 10270, pp. 249–252, Jan. 2021, doi: 10.1016/S0140-6736(20)32644-1.
- [159] J. Brooks, T. B. Erickson, S. Kayden, R. Ruiz, S. Wilkinson, and F. M. Burkle, "Responding to chemical weapons violations in Syria: legal, health, and humanitarian recommendations," *Confl Health*, vol. 12, no. 1, p. 12, Dec. 2018, doi: 10.1186/s13031-018-0143-3.
- [160] D. M. Quinn, "Acetylcholinesterase: enzyme structure, reaction dynamics, and virtual transition states," *Chem Rev*, vol. 87, no. 5, pp. 955–979, Oct. 1987, doi: 10.1021/cr00081a005.
- [161] I. V. Tetko *et al.*, "Virtual Computational Chemistry Laboratory – Design and Description," *J Comput Aided Mol Des*, vol. 19, no. 6, pp. 453–463, Jun. 2005, doi: 10.1007/s10822-005-8694-y.

- [162] J. A. V. da Silva, E. Nepovimova, T. C. Ramalho, K. Kuca, and T. Celmar Costa França, "Molecular modelling studies on the interactions of 7-methoxytacrine-4-pyridinealdoxime, 4-PA, 2-PAM, and obidoxime with VX-inhibited human acetylcholinesterase: a near attack conformation approach," *J Enzyme Inhib Med Chem*, vol. 34, no. 1, pp. 1018–1029, Jan. 2019, doi: 10.1080/14756366.2019.1609953.
- [163] D. Bondar *et al.*, "N-substituted arylhydroxamic acids as acetylcholinesterase reactivators," *Chem Biol Interact*, vol. 365, p. 110078, Sep. 2022, doi: 10.1016/j.cbi.2022.110078.
- [164] M. Eddleston and F. R. Chowdhury, "Pharmacological treatment of organophosphorus insecticide poisoning: the old and the (possible) new," *Br J Clin Pharmacol*, vol. 81, no. 3, pp. 462–470, Mar. 2016, doi: 10.1111/bcp.12784.
- [165] L. Di, E. H. Kerns, Y. Hong, and H. Chen, "Development and application of high throughput plasma stability assay for drug discovery," *Int J Pharm*, vol. 297, no. 1–2, pp. 110–119, Jun. 2005, doi: 10.1016/j.ijpharm.2005.03.022.
- [166] E. P. S. A. Albert, *The Determination of Ionization Constants: A Laboratory Manual*, 3rd ed. London / New York: Chapman and Hall, 1984.
- [167] "PC SPARTAN pro Molecular Modeling for the Desktop," *Chemical & Engineering News Archive*, vol. 77, no. 17, p. 2, Apr. 1999, doi: 10.1021/cen-v077n017.p002.
- [168] G. B. Rocha, R. O. Freire, A. M. Simas, and J. J. P. Stewart, "RM1: A reparameterization of AM1 for H, C, N, O, P, S, F, Cl, Br, and I," *J Comput Chem*, vol. 27, no. 10, pp. 1101–1111, Jul. 2006, doi: 10.1002/jcc.20425.
- [169] O. Soukup *et al.*, "In vitro and in silico Evaluation of Non-Quaternary Reactivators of AChE as Antidotes of Organophosphorus Poisoning - a New Hope or a Blind Alley?," *Med Chem (Los Angeles)*, vol. 14, no. 3, pp. 281–292, Apr. 2018, doi: 10.2174/1573406414666180112105657.
- [170] V. Finger *et al.*, "2,6-Disubstituted 7-(naphthalen-2-ylmethyl)-7H-purines as a new class of potent antitubercular agents inhibiting DprE1," *Eur J Med Chem*, vol. 258, p. 115611, Oct. 2023, doi: 10.1016/j.ejmech.2023.115611.
- [171] G. L. Ellman, K. D. Courtney, V. Andres, and R. M. Featherstone, "A new and rapid colorimetric determination of acetylcholinesterase activity," *Biochem Pharmacol*, vol. 7, no. 2, pp. 88–95, Jul. 1961, doi: 10.1016/0006-2952(61)90145-9.
- [172] D. Jun, L. Musilova, K. Musilek, and K. Kuca, "In Vitro Ability of Currently Available Oximes to Reactivate Organophosphate Pesticide-Inhibited Human Acetylcholinesterase and Butyrylcholinesterase," *Int J Mol Sci*, vol. 12, no. 3, pp. 2077–2087, Mar. 2011, doi: 10.3390/ijms12032077.

Acknowledgements

The author wants to acknowledge the supervisor Dr. Yevgen Karpichev, all publications co-authors, colleagues, friends and family for support.

Also, author acknowledges fundings from Estonian Research Council (grants PUT1656, ETAG20049 [COVSG5]), NATO (SPS MYP No. G5565 DEFIR) and EU FP7 (grant No. 621364 [TUTIC-Green]).

The special acknowledge to Tallinn University of Tectnology (TalTech) and TalTech administration (on all levels) for understanding and providing a chance to perform and submit for defense this PhD thesis.

Abstract

Structure Modification and Applications of Sustainable Ionic Liquids-Based Molecular Platforms

The development of sustainable chemicals is crucial for mitigating environmental impact while meeting industrial and societal needs. In this context, amino acids have emerged as prospective building blocks for designing sustainable chemicals due to their inherent biocompatibility and versatility. Pyridinium phenylalanine-derived ionic liquids (ILs) exemplify a group of sustainable products developed in accordance with green chemistry principles. These ILs serve as promising molecular platforms that can be modified to address various practical challenges.

The present work focuses on the development and adaptation of sustainable ionic liquids-based molecular platforms for diverse practical applications.

Performed studies confirm efficiency of tested pyridinium phenylalanine-derived ILs in polycyclic aromatic hydrocarbons (PAHs) solubilisation processes and make possible to propose a concept of a sustainable process for PAH extraction using these ILs. Additionally, potential ways for structure improving were evaluated.

A series of dipeptide ILs with L-phenylalanine and L-alanine fragments were synthesized and analyzed for their biodegradability, providing insights into the design of sustainable chemicals using amino acid moieties as a next step of ionic liquids-based molecular platforms improvement. The library of structural fragments for future design of sustainable chemicals was established.

Furthermore, oxime-functionalized surface active ILs were designed and investigated for applications in processes of toxic organophosphates decomposition and pharmaceuticals detection.

Sustainable acetylcholinesterase reactivators based on ionic liquids-based molecular platforms were designed, synthesized, and studied. The one of obtained compounds – (S)-1-(2-(((1-(butylamino)-1-oxo-3-phenylpropan-2-yl)amino)-2-oxoethyl)-4-((hydroxyimino)methyl) pyridin-1-ium bromide – was shown to reveal remarkable activity against the AChE inhibited by VX, exceeding conventional reactivators 2-PAM and obidoxime.

Overall, this research demonstrates the great potential of amino acid-derived ILs as sustainable molecular platform for designing environmentally friendly chemicals, with applications ranging from pollutant remediation to pharmaceuticals. The findings contribute to the growing body of knowledge on green chemistry approaches and offer insights into the development of sustainable solutions for various industrial and environmental challenges.

Lühikokkuvõte

Jätkusuutlike ionovedelikpõhiste molekulaarsete platvormide struktuuri muutmine ja rakendused

Jätkusuutlike keemiliste ainete arendamine on kriitilise tähtsusega keskkonnamõjude leevendamiseks ning tööstuse ja ühiskonna vajaduste rahuldamiseks. Sellest vaatenurgast on aminohapped osutunud paljutöötavateks ehitusplokkideks jätkusuutlike kemikaalide kavandamisel nende loomuliku bioühilduvuse ja mitmekülsuse tõttu. Püridiiniumfenüülalaniinist saadud ionovedelikud (IL-id) on näide jätkusuutlikest toodetest, mis on välja töötatud rohelise keemia põhimõtete kohaselt. Need IL-id toimivad paindliku molekulaarse platvormina, mida saab kohandada erinevate praktiliste probleemide lahendamiseks.

Käesolev töö keskendub jätkusuutlike ionovedelikpõhiste molekulaarsete platvormide arendamisele ja kohandamisele mitmesuguste praktiliste rakenduste jaoks. Teostatud uuringud kinnitavad püridiiniumfenüülalaniinist saadud IL-ide efektiivsust polütsükliiliste aromaatsete süsivesinike (PAH-ide) lahustumisprotsessides ja võimaldavad pakkuda lähenemist jätkusuutlikuks PAH-ide ekstraksiooniks nende IL-ide abil. Lisaks hinnati potentsiaalseid viise struktuuri parandamiseks.

Sünteesiti ja analüüsiti L-fenüülalaniini ja L-alaniini fragmentidega dipeptiidi IL-e nende biolagundatavuse hindamiseks, andes ülevaate jätkusuutlike kemikaalide kavandamisest aminohappemoodulite abil, mis on järgmine samm ionovedelikpõhiste molekulaarsete platvormide täiustamisel. Koostati struktuurifragmentide raamatukogu tulevaste jätkusuutlike kemikaalide disainiks.

Lisaks kavandati ja uuriti oksiim-funktsionaliseeritud pindaktiivseid IL-e, et rakendada neid toksiliste organofosfaatide lagundamise ja ravimite tuvastamise protsessides.

Töö käigus kavandati, sünteesiti ja uuriti jätkusuutlikke atsetüülkoliinesteraasi reaktivaatoreid, mis põhinevad ionovedelikpõhistel molekulaarsetel platvormidel. Üks saadud ühenditest – (S)-1-(2-((1-(butüülamino)-1-okso-3-fenüülpropaan-2-üül)amino)-2-oksoetüül)-4-((hüdrosü-imino)) metüül)püridiin-1-ium bromiid – näitas märkimisväärset aktiivsust VX-ga inhibeeritud AChE suhtes, ületades tavalisi reaktivaatoreid 2-PAM ja obidoksiimi.

Kokkuvõtteks demonstreerib see teadustöö aminohappest saadud IL-ide suurt potentsiaali jätkusuutlike molekulaarsete platvormidena keskkonnasõbralike kemikaalide kavandamisel, mille rakendused ulatuvad reostuse likvideerimisest ravimiteni. Leiud aitavad kaasa rohelise keemia lähenemisviiside laiemale arengule ja pakuvad ülevaadet jätkusuutlike lahenduste arendamisest erinevates tööstuslikes ja keskkonnaprobleemides.

Appendix 1

Publication I

Pandya, S.J.; Kapitanov, I.V.; Usmani, Z.; Sahu, R.; Sinha, D.; Gathergood, N.; Ghosh, K.K.; Karpichev, Y. An example of green surfactant systems based on inherently biodegradable IL-derived amphiphilic oximes. *J. Mol. Liq.* **2020**, 305, 112857

Reproducing is permitted by Elsevier Copyright policy / Authors' rights in the article.



An example of green surfactant systems based on inherently biodegradable IL-derived amphiphilic oximes

Subhashree Jayesh Pandya^{a,1}, Illia V. Kapitanov^{b,1,2}, Zeba Usmani^b, Reshma Sahu^a, Deepak Sinha^c, Nicholas Gathergood^{b,d}, Kallol K. Ghosh^{a,*}, Yevgen Karpichev^{b,*}

^a School of Studies in Chemistry, Pt. Ravishankar Shukla University, Raipur, (C.G.) 492010, India

^b Department of Chemistry and Biotechnology, Tallinn University of Technology (TalTech), Tallinn 12618, Estonia

^c Government Nagarjuna Post Graduate College of Science, Raipur, (C.G.) 492010, India

^d School of Chemistry, University of Lincoln, Lincoln, Lincolnshire LN6 7DL, United Kingdom

ARTICLE INFO

Article history:

Received 9 November 2019

Received in revised form 5 March 2020

Accepted 6 March 2020

Available online 10 March 2020

Keywords:

Ionic liquids

Oximes

Biodegradability

Closed bottle test

Acid dissociation constant

Chemical decontamination

ABSTRACT

Progress in the development of biodegradable ionic liquids (ILs) leads to designing green surfactant formulations for miscellaneous applications. In this work, we present synthesis of a series of novel IL-derived amphiphilic pyridinium oximes composed by octylamide tail linked to the headgroup by means of amide, 4-((hydroxyimino)methyl)-1-(2-(octylamino)-2-oxoethyl)pyridin-1-iumbromide, **4-PyC8**, alanyl ((S)-4-((hydroxyimino)methyl)-1-(2-((1-(octylamino)-1-oxopropan-2-yl)amino)-2-oxoethyl)pyridin-1-ium bromide, **4-PyAlaC8**), or phenylalanyl ((S)-2-((hydroxyimino)methyl)-1-(2-((1-(octylamino)-1-oxo-3-phenylpropan-2-yl)amino)-2-oxoethyl)pyridin-1-ium bromide, **2-PyPheC8**), S)-3-((hydroxyimino)methyl)-1-(2-((1-(octylamino)-1-oxo-3-phenylpropan-2-yl)amino)-2-oxoethyl)pyridin-1-iumbromide, **3-PyPheC8**), and (S)-4-((hydroxyimino)methyl)-1-(2-((1-(octylamino)-1-oxo-3-phenylpropan-2-yl)amino)-2-oxoethyl)pyridin-1-ium bromide, **4-PyPheC8**) moiety. Their biodegradability examined in the closed bottle test shown the dependence on the amino acid structure and follows the tendency Phe > Ala > amide. Phenylalanine-based oximes demonstrate >30% of degradation in the CBT after 42 days and can be considered as inherently degradable. The acid ionization constant (pK_a) of studied oximes determined by means of UV–vis spectroscopy at 27 °C were found to be in the range from 8.00 to 9.00. The pK_{a,app} values of oximes in the presence of cationic gemini surfactants, 12-4-12- and 16-10-16, change insignificantly whereas they shifted upwards in the presence of anionic surfactant SDS. The nucleophilic cleavage of organophosphorus triester PNPDP under optimal concentration conditions of **4-PyC8** come about with half-life times 40 s under mild condition (pH 9.00). These results provide new information on control the green microorganized nucleophilic systems for chemical decontamination.

© 2020 Elsevier B.V. All rights reserved.

1. Introduction

Ionic liquids (ILs) are increasingly seen nowadays as an integral part of green chemistry applications [1–3] with a particular attention to their biocompatibility and biodegradability [4–7]. An attractive feature of ILs is the ability to refine the structure, to tailor the properties for a desired application. The ILs with long chains are capable to form aggregates in aqueous solutions similar to that of conventional surfactants and are called the surface-active ionic liquids (SAILs) [8,9]. This overlapping

between surfactant and IL chemistry causes the increased interest to the synthesis, self-organization, and applications of SAILs, including developing micellar catalytic systems [10,11]. Progress in the development of biodegradable ionic liquids ILs allowed finding sustainable fragments to assist the synthesis of sustainable molecules by means of “benign by design” approach [12,13]. The novel SAILs are expected to combine advanced colloid properties with lowered risk for the environment [14]. We have reported recently a versatile approach towards the synthesis of biodegradable amino acid derived ILs [12,13] to open the opportunities for developing SAILs with optimized environmental toxicity [15] and tunable properties [16] in their self-assembly, antimicrobial activity, and biodegradability. Among the L-phenylalanine (Phe) derived SAILs reported in our recent report [16], the medium chain length (namely, *n*-hexyl and *n*-octyl esters) derivatives bearing pyridinium headgroup were pointed out to be the prospective green alternatives for conventional surfactants and to be considered as the base for miscellaneous applications.

* Corresponding authors.

E-mail addresses: kallolkghosh@yahoo.com (K.K. Ghosh), yevgen.karpichev@ttu.ee (Y. Karpichev).

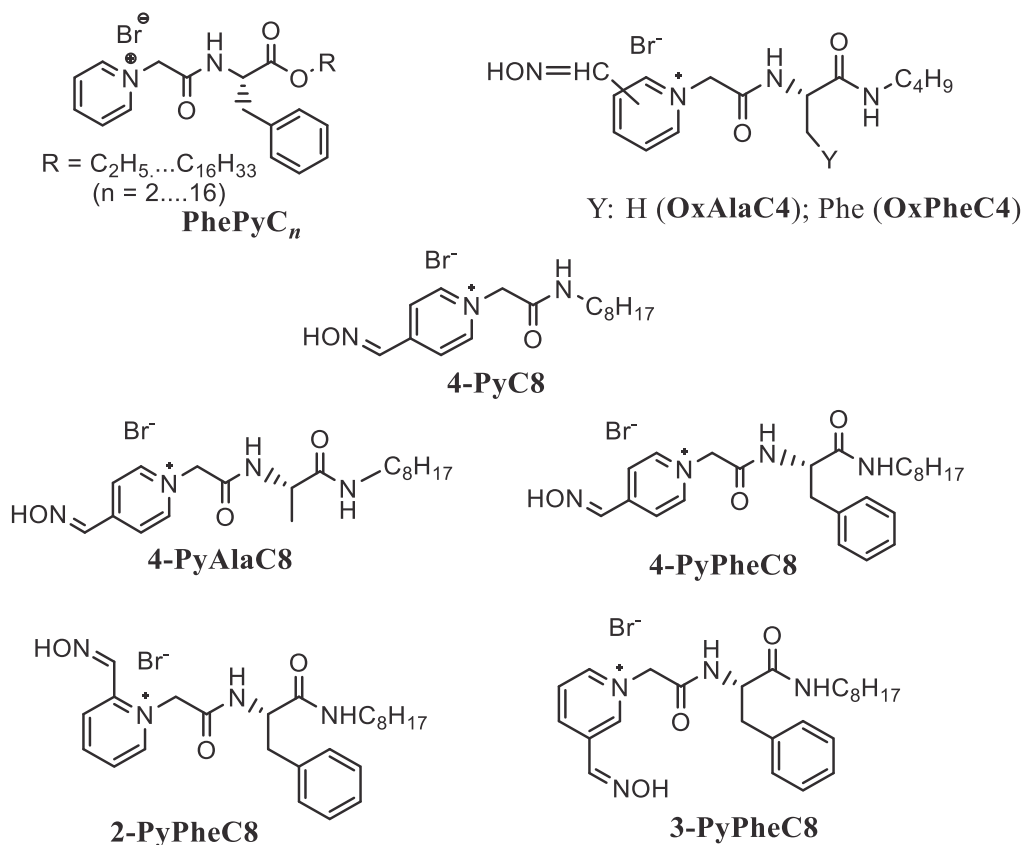
¹ Contributed equally to the publication.

² Current address: Gemini Pharm Chem Mannheim GmbH, 68305 Mannheim, Germany.

A problem of both theoretical and practical importance is the fast and irreversible detoxification of organophosphorus compounds (OP), either used as pesticides or chemical warfare agents (CWA) [17–21]. The comprehensive approach of solving problems related to the crisis management, e.g. remedial measures to mitigate manmade disasters or a terrorist attack towards civilians [22,23] is also far from complying with the principles of green chemistry. During an incident involving exposure of civilians, there usually exists a delay between initial exposure of poisonous agents and on-scene arrival of the effective countermeasures and trained personnel to apply best military practices [17]. Formulations, which are environmentally friendly and easy-to-use by both first responders and volunteers are on demand, and they are far from being fully fitted to the green chemistry criteria. The significance of the international efforts towards environmentally benign methods of chemical decontamination was sharply highlighted by the OPCW's Initiative on Green and Sustainable Chemistry [24] aimed at enhancing implementation of the Chemical Weapons Convention.

The non-functionalized SAILs aggregates have been reported to solubilize OP pesticides [25] or act as micellar hydrolytic system bringing together OP pesticide and a weak nucleophile in the micellar pseudophase [26]. Oximes are among the most effective nucleophiles providing high rate of the detoxification of OPs under mild pH [27–29]. One of the promising ways to advance micellar catalytic system is attaching specific functional moiety to the surfactant headgroup. It allows one to produce high "local" concentration of the reactive species in the region close to the micellar interface [30]. The commonly used

antidotes [31,32] and functionalized surfactants [33] for effective cleavage and degradation of toxic organophosphorus compounds (OP) are zwitterionic salts (in their reactive form oxime group is deprotonated) containing quaternary ammonium (pyridinium, in essence) group. The results on studies of oxime supernucleophilic systems in the reactions towards toxic organophosphorus esters have been rationalized in a terms of micellar kinetic in relation to the oxime structure and basicity [31,34–39]. The CMC values for the Phe-derived SAILs reported in [16], see Scheme 1, are significantly (up to 10 times) lower than those for conventional surfactants with the same length of the side chain. This phenomenon was supposed to be related with the role the aromatic ring of Phe moiety plays in the aggregation. The pyridinium headgroup non-functionalized Phe-derived ester IL with *n*-butyl chain ($R = C_4H_9$) has considerably high, as for practical use, CMC value of ≥ 60 mM, but *n*-octyl derivative ($R = C_8H_{17}$) was reported to demonstrate CMC ca. 2 mM that is comparable with much less (bio)degradable conventional cationic surfactants with tetradecyl or hexadecyl chains. Combined with data on toxicity and biodegradability [15,16], it makes octyl derivatives among the most suitable SAILs for practical applications. The short-chain Phe-derived oxime (*n*-butyl esters and amides, see Scheme 1) have been recently reported as the potential antidotes-reactivators of human acetyl cholinesterase inhibited by OP insecticide paraoxon and nerve agents sarin and VX [40]. Our approach presented in this work includes extension of the side chain of the hydroximinopyridinium IL-based short-chain salts [40] in order to obtain amphiphilic oximes/functional surfactants [41], which may lead



Scheme 1. Phe-derived non-functionalized SAILs [15] (top left), their short chain oxime-functionalized antidotes [34] (top right), and oxime-functionalized IL-derived surfactants with *n*-octyl chain reported in this work.

to the environmentally benign micellar systems for chemical decontamination [31]. Since oxime possess alpha effect properties in its deprotonated form, the acid dissociation constant (pK_a) [29] is an important physicochemical parameter to analyze the “effective pH” allowing oximate ion (zwitterionic species of the structures represented on Scheme 1) attack the unsaturated center of a substrate [42,43]. The apparent pK_a of oxime values may vary in the presence of an added surfactant of different structure in the mixed micellar systems [38,39].

Analysis of acid-base equilibria of the environmentally benign amphiphilic oximes and observed effects towards OP, either real agents or their low toxic simulants, may give a guidance to the designing biodegradable constituents for chemical decontamination systems.

We report here the synthesis and characterization of a series of novel IL-derived amphiphilic oximes **4-PyC8**, **4-PyAlaC8**, **2-PyPheC8**, **3-PyPheC8**, and **4-PyPheC8** (Scheme 1) followed by the studies of their biodegradability under aerobic aquatic condition using Closed Bottle Test (OECD 301D). We present determination of pK_a values of oximes studied in the bulk and in the presence of gemini (16-4-16 and 12-10-12) and anionic (SDS) surfactants (see Scheme 2), along with kinetics of the oximolysis of model OP, 4-nitrophenyl diphenyl phosphate (PNPDPP) in the presence of one of the above surfactants at “mild” pH values of 8.35 and 9.00.

2. Experimental section

2.1. Materials

All commercial chemicals and solvents were purchased from Sigma Aldrich, Alfa Aesar, or TCI Europe and used without further purification. Silica gel 60 F254 plates were used for TLC. Gemini surfactants were synthesized in the laboratory of Dr. P. Quagliotto, Department of Chemistry,

University of Torino, Italy. PNPDP was prepared at Defence Research Development Establishment, Gwalior (India), sodium dodecylsulfate (SDS), potassium dihydrogen phosphate and dipotassium - hydrogen phosphate were purchased from Sigma - Aldrich and used without further purification. All the reagents used were of analytical grade. Double distilled or demineralized water was used throughout the experiments.

2.1.1. Characterization of products

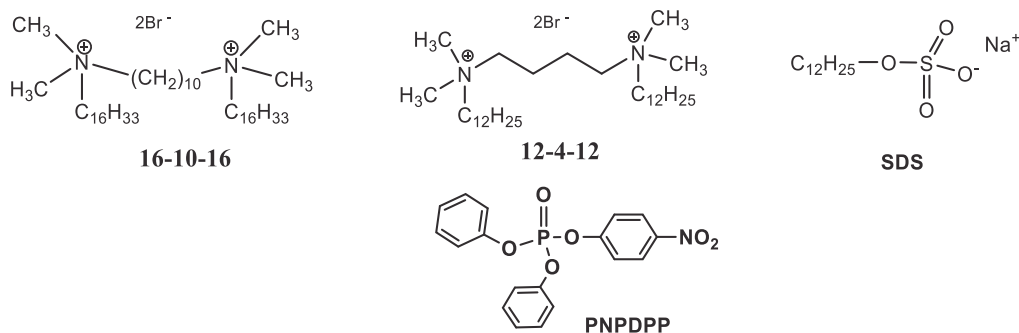
Melting points were determined with Stuart SMP40 apparatus with parameters for the melting point analysis set at 2 °C per minute ramp; values are expressed in °C. The HRMS identification of compounds was performed on Agilent 6540 UHD Accurate-Mass Q-TOF LC/MS G6540A Mass Spectrometer. Bruker Avance III 400 MHz spectrometer operating at 400 MHz for ^1H NMR and 101 MHz for ^{13}C NMR. Samples were recorded in deuterated chloroform (CDCl_3) or dimethyl sulfoxide ($\text{DMSO}-d_6$) where appropriate. All chemical shifts δ are reported in parts per million (ppm) are relative to the internal standard TMS and coupling constants (J) are measured in Hertz (Hz).

2.1.2. Synthesis of the IL-derived amphiphilic oximes

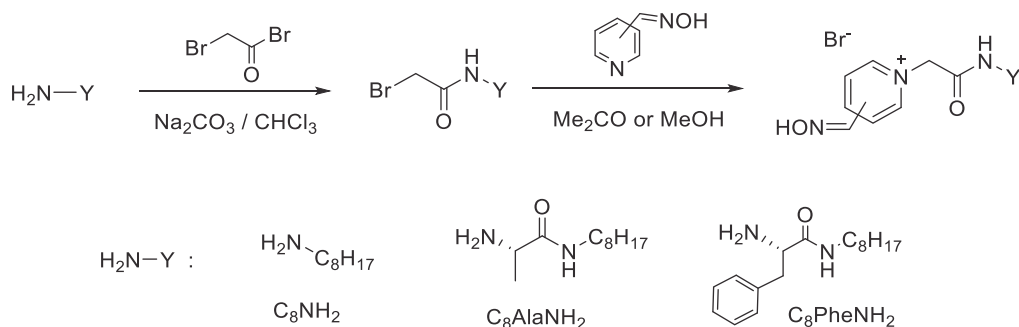
We report synthesis of the series of novel SAILs-derived oximes obtained from corresponding amines similar to a general Scheme 3 similarly to the method published for amide ILs [44,45] and a series of L-phenylalanine (Phe) ILs we have published previously [13,16].

Precursors C_8AlaNH_2 and C_8PheNH_2 were synthesized from corresponding commercially available Boc-protected amino acids (see Scheme 4).

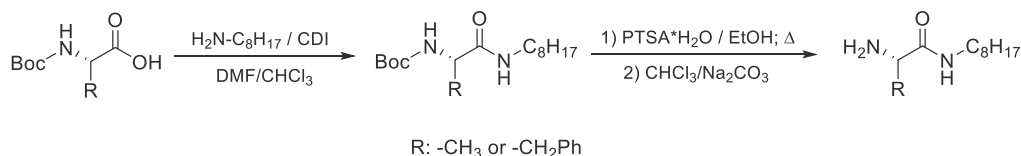
2.1.2.1. Boc-protected octylamides. The corresponding N-(Boc)-L-amino acid (0.05 mol; Boc-N-Phe or Boc-N-Ala) was dissolved in dry DMF (25 mL) under argon atmosphere and the reaction mixture was cooled



Scheme 2. Structure of surfactants and OP substrate used in the present work.



Scheme 3. General method of synthesis of oximes studied in this work.



Scheme 4. Synthesis of key precursors for studied oximes.

to 0 °C. Then to stirred solution was added portionwise carbonyldiimidazole (8.11 g; 0.05 mol). The reaction mixture was stirred 15 min more after stopped of gas formation. Subsequently a solution of 1-octylamine (8.26 mL; 0.05 mol) in alcohol-free amylene-stabilized chloroform (25 mL) was added dropwise to reaction mixture. The reaction mixture was stirred 24 h at room temperature under argon atmosphere. Next, solvents from reaction mixture was evaporated in vacuo, residue dissolved in chloroform (100 mL) and washed with 0.1 N HCl (2 × 50 mL), 0.1 N Na₂CO₃ (2 × 50 mL) and water (2 × 50 mL). The organic layer was dried over anhydrous sodium sulfate and concentrated in vacuo to afford the title compounds. The yields were 95–97%.

2.1.2.2. Boc-deprotection of C₈AlaNH₂ and C₈PheNH₂. To a solution of corresponding N-(Boc)-L-amino acid octyl amide (0.05 mol) in ethanol (150 mL) was added PTSA·H₂O (12.36 g; 0.065 mol) and refluxed with stirring for 12 h. Then solvent was removed in vacuo. Residue was dissolved in chloroform (150 mL) and washed with solution of Na₂CO₃ (0.1 mol; 10.6 g) in water (150 mL), and then with water (2 × 100 mL). The organic layer was dried over anhydrous sodium sulfate and concentrated in vacuo to afford the title compounds (yield 96–98%).

2.1.2.3. Synthesis of N-bromoacetyl derivatives. To a stirred solution of the corresponding substituted amine (0.05 mol) in alcohol-free chloroform (50 mL) was added solid Na₂CO₃ (7.95 g, 0.075 mol). To this mixture was added dropwise bromoacetyl bromide (5.65 mL, 0.065 mol) and stirred for 12 h. Then 50 mL of water added carefully to reaction mixture and then transferred to a separating funnel. The organic layer was separated, washed with 0.1 N Na₂CO₃ (2 × 50 mL) and water (3 × 50 mL). The organic phase was dried over sodium sulfate, filtered, and volatiles were removed in vacuo to afford the title compounds. The yields were 94–98%.

2.1.2.4. Synthesis of pyridinium aldioximes. The stirring solution of corresponding N-bromoacetyl derivative (0.01 mol) and corresponding pyridinealdoxime (1.22 g; 0.01 mol) in 25 mL of acetone (for 2- and 3-pyridine aldoxime) or 25 mL of methanol (for 4-pyridinealdoxime) was refluxed for 12 h. After cooling to room temperature the solid product was filtered, washed with cold acetone (3 × 10 mL), then with diethyl ether (2 × 20 mL), and dried in vacuo. The titled compounds was isolated with yields 38–70%. ¹H and ¹³C NMR spectra, HRMS and mp of the obtained compounds are collected in the **Appendix A**.

2.2. Methods

2.2.1. Aerobic biodegradation test

Biodegradation was studied using the Closed Bottle Test (CBT) method OECD 301D described in the previous papers [12,13]. Effluent from wastewater treatment plant was collected from a municipal wastewater treatment plant in Tallinn, Estonia (Paljassaare wastewater treatment plant, 59°27'55.5"N 24°42'08.8"E). WWTP effluent was filtered through a Whatman cellulose filter paper (90 mm diameter, Grade 1, pore size 11 μm) before being used as inoculum. Aerobic biodegradation testing was done using modified CBT (OECD 301D). CBT setup with modification where biological oxygen consumption is measured with an optode oxygen sensor system using PTFE-lined PST3

oxygen sensor spots (Fibox 3 PreSens, Regensburg, Germany) allows measuring BOD without opening the flasks and thereby reducing the number of parallels needed for each compound and increasing test throughput. It has also shown to improve reproducibility compared to the original OECD 301D guideline [46]. Each CBT run consisted of four different series, each have been repeated in duplicates. First was „reference series“ in which readily biodegradable sodium acetate in known concentration (6.41 mg/L) was added to a flask of mineral medium inoculated with effluent from wastewater treatment plant. In „test series“ „test compound, as a source of carbon was added to the inoculated mineral medium. The test compound was added in concentration corresponding to theoretical oxygen demand (ThOD) of approximately 5 mg/L. ThOD was calculated assuming nitrification would take place as each of the 25 studied compounds included nitrogen atom(s) in their structure. „Toxicity series“ containing both sodium acetate and test compound in their respective concentrations were used to evaluate test compounds' toxicity against inoculum – if biodegradation values in these bottles were significantly lower compared to reference series it was concluded that test compound could be inhibiting or even toxic to microbes in WWTP effluent. Each run was extended from 28 days (suggested by OECD 301D protocol) to 42 days.

Results from each run were accepted if following criteria were met:

i) difference of extremes of replicate values at the plateau is <20%, ii) oxygen concentration in test series bottles must not fall below 0.5 mg/L at any time, iii) sodium acetate in reference series must be degraded ≥60% by day 14. Blank bottles oxygen consumption was also monitored to avoid possibility of system turning from aerobic to anaerobic.

2.2.2. pH measurements

The pH of the buffer solutions was determined using a pH meter Eutech pH 700, equipped with an Inlab® Expert Pro glass electrode with an accuracy of ±0.01 units. The pH meter was calibrated using the two-point calibration method with commercially available standard buffer solutions at pH 4.00 and 9.00.

2.2.3. UV-visible spectroscopy

The spectrophotometric measurements were recorded by Cary 60 UV-Vis spectrophotometer (Agilent Technologies) in the range of 200–400 nm. All the spectra were recorded at 27 °C. The solutions of different pH (6.20–10.50) were used in spectrometric analysis. The quartz cells were attached to Peltier element for maintaining the constant temperature (27 ± 0.5 °C). The stock solution of the oxime-functionalized salt **4-PyC8** was prepared solution in water, and the stock solutions of other oximes **4-PyAlaC8**, **2-PyPheC8**, **4-PyPheC8**, and **3-PyPheC8** were prepared in 25% (v/v) ethanol-water, as they were sparingly soluble in water. An aliquot of 3 mL from stock solution of 0.5 mM of oxime in double distilled water was diluted with 25 mL phosphate buffer solution of pH 6.2 and the spectrum was recorded using buffer solution as a blank. The pH was calibrated to the desired value by using sodium hydroxide (NaOH) solution. After balancing each pH, the absorption spectra were recorded at selected wavelengths 200 to 400 nm (Fig. 1). Similarly, the effect of surfactants (gemini and anionic) with functionalized oximes based ionic liquids were done. The concentration of surfactants was 10 mM.

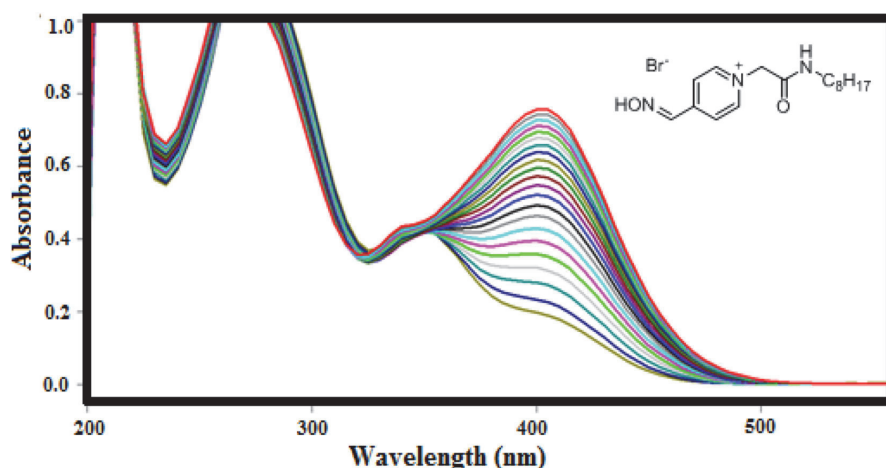


Fig. 1. UV-vis spectra collected at different reaction times showing the increase in absorbance of *p*-nitrophenoxide anion for the cleavage of PNPDP with **4-PyC8**.

2.2.4. Determination of acid dissociation constant (pK_a)

The pK_a values of all oximes studied in this work have been determined by spectrophotometric method described by Albert and Sergeant [47]. All the spectrophotometric measurements were made at 27 °C and the spectra were recorded within the range of 200–400 nm. The absorbance spectra of all the compounds where noted in aqueous solution **4-PyC8** and in 25% (v/v) ethanol-water **4-PyAlaC8**, **2-PyPheC8**, **4-PyPheC8**, **3-PyPheC8** of different pH, see Fig. 1. The shorter wavelength absorption maximum, appearing at lower pH values, reflects the absorption of the non-ionized oxime group(s) in all investigated compounds, whereas the longer wavelength maximum, observed at higher pH values, is due to the absorption of the reactivator with an ionized oxime group(s). The pH-dependent absorption spectra show the presence of isobestic point. The pK_a values have been evaluated from the absorbance vs. pH data by the general method of Albert and Sergeant using Eq. (4).

The ionization behavior of oxime may be represented as,



Then the apparent acidity constant K_a of the acid HA is defined as the equilibrium constant

$$K_a = \frac{[H^+][A^-]}{[HA]} \quad (2)$$

By taking the logarithms and reconstructing the Eq. (2) we get the Henderson- Hasselbalch equation

$$pH = pK_a + \log \frac{[A^-]}{[HA]} \quad (3)$$

This equation can be written as shown in Eq. (4)

$$pK_a = pH_{exp} - \log \frac{Abs_{\varphi} - Abs_{Hox}}{Abs_{Ox} - Abs_{\varphi}} \quad (4)$$

where, Abs_{Hox} is the absorbance of unionized form of an oxime, Abs_{φ} is the absorbance of partially ionized form of oxime, and Abs_{Ox} is the absorbance of completely deprotonated form of oxime at particular pH.

2.2.5. Reaction kinetics

The pseudo-first order rate constants for the hydrolysis of PNPDP phosphate esters in the presence of different composition of concentration of the oxime **4-PyC8** were determined at 8.35 and 9.00 pH at 27 °C. The reaction were monitoring as the appearing of the leaving *p*-nitrophenoxide anion at wavelength 400 nm shown in Fig. 1 recorded by Cary 60 UV-Vis spectrophotometer (Agilent Technologies) with a temperature controller (Peltier element). Phosphate buffer (0.1 M) was employed to control the pH for all the reaction process. All the pH measurements were obtained using a pH meter Eutech pH 700, equipped with an Inlab® Expert Pro glass electrode with an accuracy of ± 0.01 units. All kinetic reactions were conducted under pseudo-first order conditions, i.e. with large excess of oximate anions over the PNPDP.

Each experiment was repeated until observed rate constants were reproducible within an accuracy of $\pm 5\%$ or better. For all the kinetic reaction run, the plots of absorbance verses rate results fits very well for the first-order rate Eq. (5).

$$\ln(A_{\infty} - A_t) = \ln(A_{\infty} - A_0) - kt \quad (5)$$

The progressive reaction of pseudo-first-order rate constants (k_{obs}) were determined from the plots of absorbance verses time with A_0 , A_t , and A_{∞} being the absorbance significance at zero, time and infinite time, respectively. The substrate (PNPDP) concentration was being kept constant for all the kinetic runs (0.05 mM). The reaction were performed at various concentration of functionalized oxime-based **4-PyC8** to explore the effect of an amphiphilic oxime on the cleaving potency of PNPDP.

3. Results and discussion

3.1. Biodegradability of IL-derived oximes

Studies into the ultimate biodegradability of studied amphiphilic oximes have been set a requirement for implementation of the EU regulation on detergents [48]. Ultimate biodegradation, or mineralisation, is achieved when the test compound is totally utilized by microorganisms (inoculum) resulting in the production of primarily carbon dioxide, water, mineral and salts. In the stringent tests, such as CBT, it is used to operate the term “readily biodegradable” for those chemicals which have passed CBT showing 60% of biodegradability or more. It is assumed that such compounds will rapidly and completely biodegrade in aquatic

environments under aerobic conditions. Compounds for which there is unequivocal evidence of biodegradation in the extent from 20% to 60% are called inherently biodegradable. An extension of the time of the experiment (e.g. from the standard 28 days to 33 or 42 days) may provide an additional insight into the inherent biodegradability of the sample. The “traffic light” classification [49] is used to facilitate recognition of the certain biodegradability, to place the green light for readily biodegradable chemicals, amber light for inherently biodegradable, and red light – for those that have not reached 20% threshold of the biodegradability during the test.

The studied oximes have different solubilities in water so only in the case of **4-PyC8** water was used to prepare its stock solution. For the oximes **4-PyAlaC8**, **2-PyPheC8**, **3-PyPheC8**, and **4-PyPheC8** the DMSO was added along with MilliQ water to overcome this solubility issue and prepare their stock solutions. To negate the effect of inoculum, blank bottles containing only inoculum and mineral medium were added to the CBT run and the values of these bottles were subtracted from other bottles of IL-derived oximes (“blank DMSO”). Another set of DMSO constituting blank was also added to negate the effect of inoculum and DMSO. The data on CBT within 28 days and 42 days are collected in the Table 1. It is worth noting that none of the samples passed CBT within 28 days whereas extension to 42 days demonstrate tendency of the studied salts to biodegrade, see Table 1, Fig. 2, and Figs. S1–S2. The amide salt **4-PyC8** demonstrate low biodegradability (11%) even after 42 days, even since the biodegradation slightly accelerates (ascending curve to develop) after the induction period about 20 days of the no plateau reached yet upon the 42 days, see Fig. 2a. Alanine derivative **4-PyAlaC8** shows better results (19% after 42 days) but not overcoming 20% threshold, Fig. 2b. All three phenylalanine derivatives demonstrate comparable tendency to biodegradability: 20% (**3-PyPheC8**), 24% (**2-PyAlaC8**), 25% (**4-PyAlaC8**) after 28 days, and 34% (**3-PyPheC8**), 37% (**2-PyAlaC8**), and 39% (**4-PyPheC8**) after 42 days, Fig. 2c, Figs. S1–S2. The biodegradability for all oximes are inferior to that of the parent phenylalanine SAIL, see Table 1. Thus, short-chain ethyl Phe IL is a readily biodegradable (mineralisable) compound within standard 28-days CBT [12,13], and the decanoyl (C10) derivative SAIL can be characterized as inherently biodegradable based on 28-day run [16]. The data presented in Table 1 confirms that the Phe ILs-derived oximes can be considered as inherently biodegradable amphiphiles.

There are several possible reasons causing lower biodegradability for the IL-derived oximes, compared to parent ILs. The PhePyCn salts reported in our recent paper [16] have been prepared based on the Phe esters (from C2 to C16), and are not tolerant to the nucleophilic attack of OH[−] under alkaline conditions or to the esterolysis by oximate ion. To

expand the window of pH for potential application (chemical decontamination, in essence), the C8 oximes have been prepared as amides, tolerant to hydrolysis in the wide interval of pH. Enzymatic cleavage of the amide bond of the shorter chain salts (C4) by the inoculum microorganisms occurs slower than esterolysis [50].

An additional factor one should take into account is the order of cleaving the two amide bonds present in the IL-derived oxime structure. It was previously reported [13] that it is amide bond from the N-side of Phe to be cleaved first to provide readily biodegradation of the **PhePyC2** salt. Cleavage of the C-side bond resulted in accumulation of the corresponding pyridinium linked phenylalanine carboxylic acid that is more persistent than pair of the transformation product Phe-ester (Phe-amide) + *N*-carboxymethylpyridinium salt. Another reason of the retardation of biodegradation as compared to the parent ILs could be introducing oxime moiety into the pyridinium ring that makes the biotransformation process more complex, as compared to unsubstituted pyridinium salts. The abilities of most fungi and bacteria to metabolize Z-oximes to use them as a source of reduced nitrogen is described elsewhere [51], the most usual mechanism to be conversion into the corresponding nitrile, amide, and carboxylic acid with a concomitant release of ammonia. Therefore, this process is expected to occur in the presence of oximinomethyl pyridinium salts irrespectively of the side chain structure. Indeed, the position of the oximino moiety does not affect the CBT results. At the same time, the biodegradability is dependent on the amino acid structure and follows the tendency Phe > Ala > amide. This tendency supports that the introducing amino acid fragment into the surfactant structures increases its biodegradability, compared to the amide salts. We suggest that better biodegradability of the Phe-containing salts as compared to Ala analogs may be related to facilitated enzymatic aminolysis of the Phe salts as the first transformation stage. Therefore, the Phe-containing oximes are the most promising functional compounds in the series. Due to their inherent biodegradability, they can be among prospective candidates for environmental application, in particular, to use as a basis for chemical decontamination formulations. Even if they did not fulfil the criterion of ultimate biodegradation within the stipulated period, these amphiphilic oximes can be considered, according to current detergent regulation [48] for special applications (i.e. those promoted for the chemical decontamination).

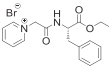
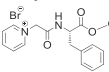
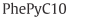
3.2. Acid dissociation constant (pK_a)

The acid base equilibrium of oxime can be represented as below (Scheme 5).

A number of approaches have been used to determine the pK_a value including potentiometry, conductometry, spectrophotometry, solubility, and liquid–liquid partitioning. Out of all the techniques UV–Vis absorption spectrophotometry is used due to being more reproducible and requiring lower amount of analyte. This technique requires very low analyte concentrations and can measure absorbance in aqueous solution even for products with low solubility in water [52–57]. There are number of the studies on oximes with reported pK_a values determined by means of spectrophotometry in water [28,58] as well as in aqueous mixture with organic solvent [29] (e.g. 50% (v/v) water-acetonitrile [58]). Mixture of water with water-miscible organic solvent is used to apply to determine the pK_a values for compounds imperfectly soluble in water [59–62]. We considered the average values of ten measurements as the pK_a of the compound with respect to oxime group, following the recommendations by Ghosh and co-workers [63].

The absorption spectra of different oximes at various pH values 6.20–10.50 are shown in Fig. 3. The change in the absorption spectra with the change in the pH indicates that the dissociation of the oxime group into the oximate occurs in the studied pH range. The absorption spectra of all studied salts show mainly two pH dependent absorption maxima: (i) the shorter wavelength absorption maximum, appearing at lower pH values in the range from 280 to 300 nm, reflects the

Table 1
CBT results on biodegradability of studied oximes and their non-functionalized Phe-derived IL precursors; color coded according to the traffic light classification [49].

Structures	D% 28 days	D% 42 days
4-PyC8	4	11
4-PyAlaC8	9	19
2-PyPheC8	24	37
3-PyPheC8	20	34
4-PyPheC8	25	39
	63 [13]	–
PhePyC2		
	36 [16]	–
PhePyC10		
		

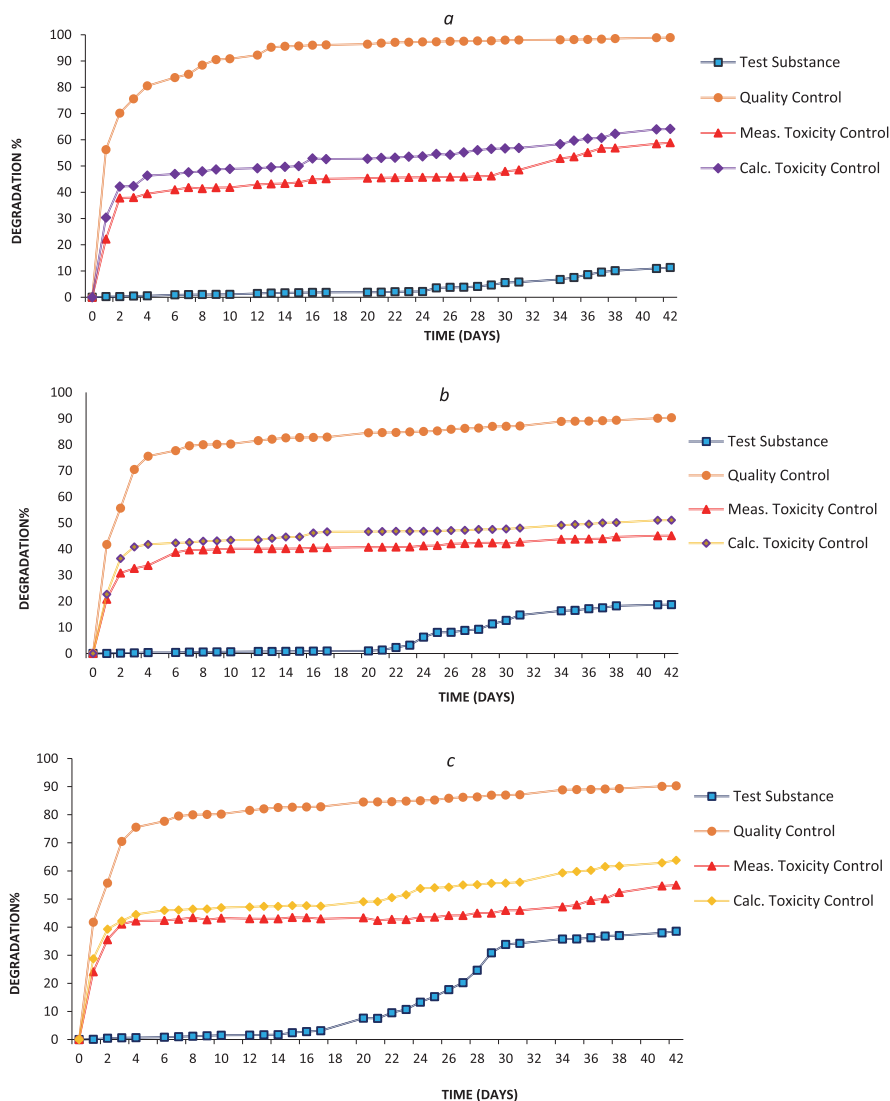
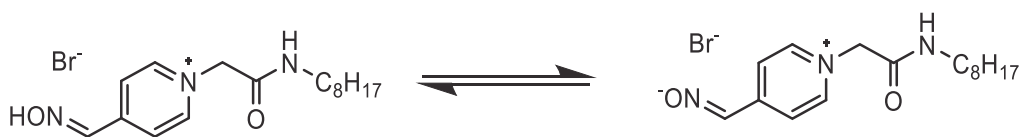


Fig. 2. Biodegradability data for 42 days CBT experiment; a - 4-PyC8; b - 4-PyAlaC8; c - 4-PyPheC8.

absorption of the non-ionized oxime group in all the analyzed compounds, (ii) the longer wavelength maximum, observed at higher pH values in the range from 345 to 350 nm, is due to the absorption of the ionized oxime group [64]. Both maxima are in accordance with the change of $\pi \rightarrow \pi^*$ transitions within the aromatic ring of pyridinium ring. Upon increasing the pH, the absorbance of the shorter band

decreases, while that of the longer band increases. A typical effect of pH on the absorption spectra of all functionalized oxime based ionic liquids were reflected by the dissociation of either oxime groups exhibits a well organized by overlapping ionization equilibria i.e., isosbestic point at 310 nm denoting the existence of an equilibrium essentially an acid base between the NO^- , which has an absorption maximum at 345 to



Scheme 5. Schematic representation of the acid-base equilibrium of the amphiphilic oxime 4-PyC8.

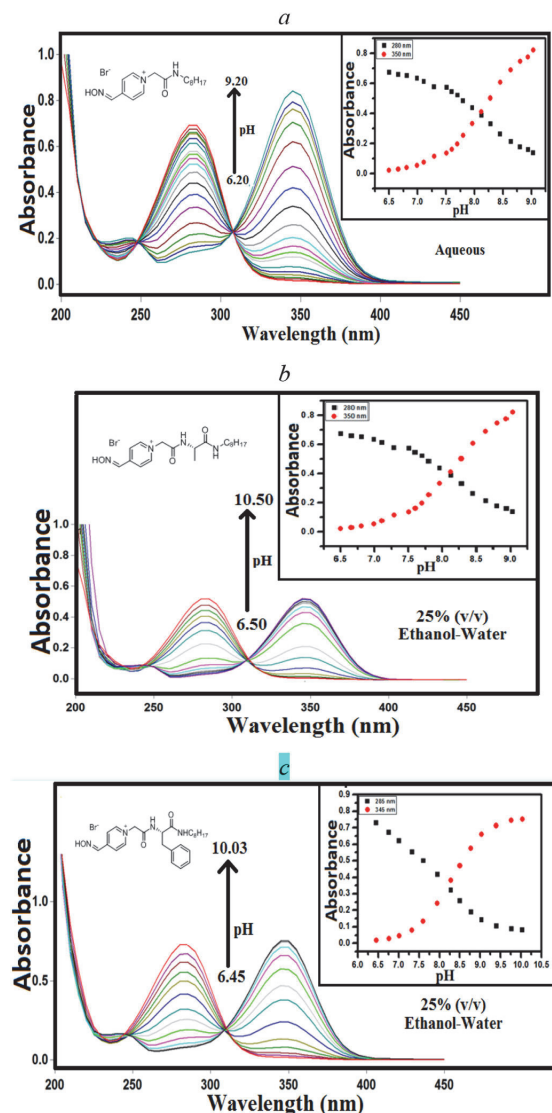


Fig. 3. Representative absorption spectra of oximes (a – 4-PyC8; b – 4-PyAlaC8; c – 4-PyPheC8; at different pH values; water, 27 °C. Inset: plots against pH and absorbance for oximes in aqueous solution of $[Ox]_0 = 50$ mM; pH = 6.20–10.50.

350 nm and the other form NOH, which has an absorption maximum at 280 to 300 nm [64]. It was observed that the resulting pK_a values revealed that pH of the oximes were between the pH range of 7.89–8.48 which had the oxime group at *ortho* and *para* position whereas when the oxime was present at meta position its pH was found to be have pK_a values 9.00. The pK_a values are collected in Table 2.

The absorbances of 4-PyC8 at 280 and 350 nm, for 4-PyAlaC8 at 285 and 350 nm, for 2-PyPheC8 at 300 and 350 nm, for 4-PyPheC8 at 285 and 345 nm and for 3-PyPheC8 at 245 and 290 nm were plotted against pH values of the buffer solution shows the solid curves represent the nonlinear regression square fit curves (inset of Fig. 2) is obtained. It was seen that the pK_a of 3-PyPheC8 (9.05) was moderately higher as compared to the pK_a of 4-PyC8, 4-PyAlaC8, 2-PyPheC8, and 4-PyPheC8 (8.08–8.48) were found to be in lower range. These differences in the

Table 2

Acid dissociation constants of studied oximes in the absence and in the presence of surfactants; 27 °C, $[D]_0 = 10$ mM.

Sr. no.	Oxime	Medium	pK_a	$pK_{a,app}$ (in presence of surfactants) ^b		
				12-4-12	16-10-16	SDS
1.	4-PyC8	Water	8.08	8.21	8.22	8.93
2.	4-PyAlaC8	25% (v/v) Ethanol-water	8.12	8.27	8.24	8.82
3.	4-PyPheC8	25% (v/v) Ethanol-water	8.48	8.21	8.25	9.25
4.	3-PyPheC8	25% (v/v) Ethanol-water	9.00	–	9.21	–
5.	2-PyPheC8	25% (v/v) Ethanol-water	7.89	8.01	7.98	9.40
6.	2-PAM	Water (1 M KCl)	8.04 ± 0.05^a	–	–	–
7.	3-PAM	Water (1 M KCl)	8.61 ± 0.04^a	–	–	–
8.	4-PAM	Water (1 M KCl)	9.51 ± 0.06^a	–	–	–

^a Ref. [28, 75].

^b Water; CMC of 12-4-12, 16-10-16 and SDS reported in literature are 1.17 mM [76], 0.051 mM [77] and 8.2 mM [78], correspondingly.

pK_a values can be explained with the help of resonating concepts in which the meta position of oxime group of 3-PyPheC8 having comparatively lesser resonating structure than that of 4-PyC8, 4-PyAlaC8 and 4-PyPheC8 in which oxime having oximino group at *ortho* position respectively. As they proceed through a resonating structure where the positive charge of pyridinium ring have established oneself on the carbon atom at second and forth (*ortho* and *para* position) isomers. These circumstances allow oxime to demonstrate more remarkable electron withdrawing effect as compared to 3-PyPheC8, i.e., third isomer (meta position) which lead to the lower pK_a values of second and forth (*ortho* and *para* position) isomers [63]. Apparently, the pK_a value was ruled by the position of oximino function in pyridinium ring and the position of linker had a little effect in corresponding pK_a value. In structure of functionalized oxime based ionic liquid, presence of oxime along with their position (*ortho* and *para*) play an important role on the reactivation and detoxification of OP compounds [33].

3.3. Effects of added surfactants on the $pK_{a,app}$ of oxime

The micellar systems can be regarded to be a system consisting of an aqueous phase and a micellar pseudophase [65,66]. Micelles can influence the pK_a values of protogenic groups due to the combination of electrostatic and minute environmental effects of the micellar system [67–70]. The effect of micellar systems on acid-base equilibria has been suggested to arise from an intrinsic factor (due to the energy difference between the aqueous and the nonpolar media) and a potential effect that is due to the electrically charged micellar surface [68].

The incorporation of the studied oximes into the mixed surfactant aggregate can affect the acid-base equilibrium. The appeared effects will depend on hydrophilic-lipophilic balance of oxime amphiphile and nature of micellar surface [67]. For analysis of this influence we have chosen two gemini surfactants with different properties of the aggregate surface (12-4-12, 16-10-16) and one anionic surfactant (Scheme 2) and have studied an ionization process in pH range 6.20–10.50. The absorption spectra are shown in Fig. 4. The pK_a for each wavelength was calculated using Eq. 4. The pK_a values of studied salts, which were determined without any added surfactant, are used as a reference in presented analysis, see Table 2.

The data indicate that the interchange of the neutral form of functionalized oxime based ionic liquids (HA) is stronger than that of the anionic species (deprotonated oximes A^-) [71]. The effect of SDS on the observed dissociation constant of oxime based ionic liquids, having higher pK_a . It is of interest to explain the increase in the pK_a values in the micellar phase, because SDS as an anionic surfactant and form the

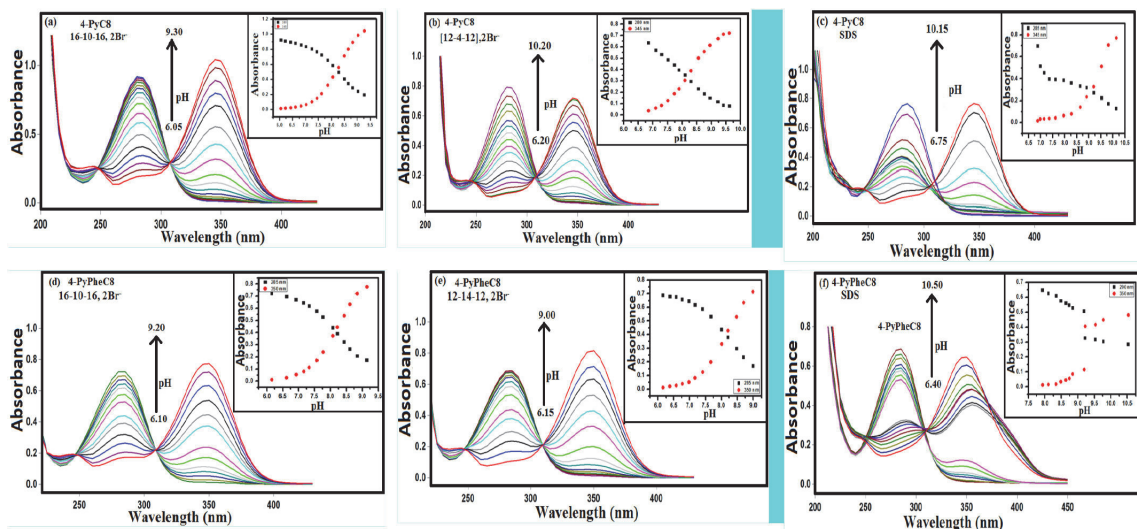


Fig. 4. Absorbance spectra of mixtures of IL-derived oximes (a–c, **4-PyC8**; d–f, **4-PyAlaC8**) with gemini surfactants 16-10-16 and 12-4-12, and anionic surfactant SDS. [Oxime]₀ = 50 mM; [D]₀ = 10 mM; 27 °C. Inset: Plots of absorbance vs pH for studied oximes in micellar solution.

anionic micelles so as to concentrate the protons in the aggregate's interface and slightly suppressed the protonation of the aromatic oxime group [72–74].

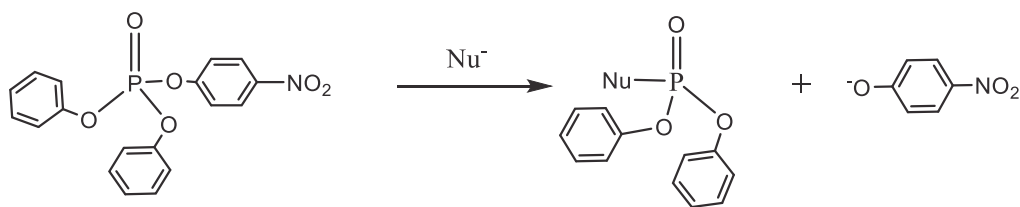
The presence of cationic surfactants in mixed micellar system with oxime-functionalized surfactants was reported previously elsewhere [37,39] to cause decreasing of apparent pK_a value ($pK_{a,app}$) of the oxime moiety. In this study, we did not report a significant effect of the surfactant on the deprotonation constant, they remain within the standard experimental errors, see Table 2. We also report here that the role of the gemini head group structure on the pK_a of oximes is negligible, in spite of the fact that 12-4-12 with relatively rigid spacer tend to form different aggregates as compared to 16-10-16, gemini surfactant with a long flexible spacer. We may suggest that levelling this difference off is a result of interaction of amide bond with micellar surface repulsing oxime moieties outside the micellar surface. The moderate hydrophobic properties of *n*-octyl chain and introduction of the amino acid fragments (in essence, hydrophobic phenyl ring of Phe promoting micellization of the Phe SAILs [16], see Scheme 1), the factors promoting micelle formation, seems not to be factors sufficient to outweigh this interaction and move oxime moiety closer to the micellar surface. SDS increased basicity of the hydroximino groups could be explained in terms of electrostatic interactions at the negatively charged SDS aggregate interface (anion repulsion and cation attraction). This surfactant affected the oxime group of all examined functionalized oxime based ionic liquids in the same manner; that is, an increase of basicity due to its negatively charged interface acted to stabilize the protonated hydroximino group. Decreasing apparent oxime basicity in

the presence of anionic SDS suggested hydrophobic interactions under the experimental analysis and lipophilic hydrocarbon chain that takes oxime group apart [74]. In other words, these two effects are against each other and showed higher variation in the pK_a values. The positively charged pyridinium headgroup undergo repulsion in the interaction to the cationic gemini headgroups so hydrophobic interaction remain the only driving force to form the mixed aggregates in such a system. This may not cause sufficient shift of the $pK_{a,app}$ value of the oxime group.

4. Effect on cleavage of PNPDP

The main expected advantages of low toxicity/biodegradable functional surfactant systems are an opportunity to ensure environmentally benign decontamination. PNPDP is a phosphotriester which has been widely recruited as a stimulant (surrogate) and its hydrolytic reactions have been investigated [30,38,79,80], see Scheme 6. Since PNPDP is water insoluble, microheterogeneous (micellar, in essence) systems have been generally enroll as a reaction mechanism for the cleavage of PNPDP. In such a medium, the organic reactants are partitioned into the surfactant aggregates by electrostatic and hydrophobic interactions. The observed rate assistance occurs mainly due to the increased localization of the reactants as well as the typical physical chemical properties of the micellar environment, which is remarkably different from those of the bulk solvents.

The **4-PyC8** was taken to estimate the reactivity in process of OP cleavage. In order to determine the efficiency of IL-derived oxime **4-PyC8** in decomposition of PNPDP, kinetic studies have been performed



Scheme 6. Nucleophilic attack at phosphorus atom of PNPDP

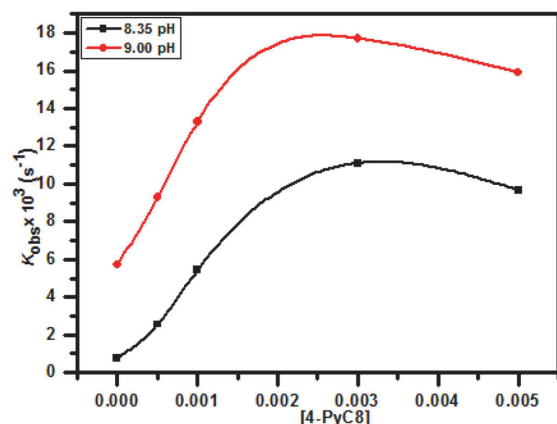


Fig. 5. Observed pseudo-first order rate constants ($k_{\text{obs}} \text{ s}^{-1}$) vs. $[\text{4-PyC8}]_0$ for reaction of PNPDPDP cleavage; water, 27 °C; $[\text{PNPDPDP}] = 0.5 \text{ mM}$.

at two different pH. The first-order rate constants been determined at pH 8.35 and 9.00, see Fig. 5. The nucleophilic concentration dependent first-order rate constants were determined spectrophotometrically for the reaction of PNPDPDP with oxime in excess (Table 3; Scheme 6). The rate constant increases in both the concentration of nucleophile and pH of the system. The obtained kinetic data entirely supports the hypothesis that oximate ion acting as a reactive species and possesses its α -effect properties. The observed reaction rates at pH 9.0 are substantially higher than reported in our previous study [38] for all oxime-functionalized surfactants (N-alkylated oximino pyridinium salts with C10 to C14 side chain), and comparable (but still higher, 0.0177 s^{-1} vs 0.0162 s^{-1}) to cetyl derivative.

Taking into account binding constant K_S of PNPDPDP, a very hydrophobic OP substrate to be $\geq 10^4 \text{ M}^{-1}$ [37], the second-order rate constant can be estimated from k_{obs} according to Eq. (6)

$$k_{\text{obs, max}} \equiv (k_2' / V_m) = (k_2^m / V_m) \cdot \alpha \quad (6)$$

where k_2^m , $\text{M}^{-1} \text{ s}^{-1}$ is the second-order rate constant characterizing the nucleophilicity of the oximate fragment, V_m , M^{-1} is the partial molar volume of surfactant, which for this type of surfactants usually 0.4 M^{-1} , α – degree of deprotonation of the nucleophilic moiety. With the parameter α equal to 0.66 and 0.89 at pH 8.4 and 9.0, correspondingly, the k_2^m values can be calculated from kinetic data, which gives the values of $6.7 \text{ M}^{-1} \text{ s}^{-1}$ (pH 8.4) and $7.9 \text{ M}^{-1} \text{ s}^{-1}$ (pH 9.0) $\text{M}^{-1} \text{ s}^{-1}$.

The practical procedure of chemical decontamination requires the smallest time possible for detoxification of an agent. The half-life times for oxymolysis of PNPDPDP in optimal concentration conditions of [4-PyC8] calculated from the kinetic data (Table 3) are found to be ca. 62 s (pH 8.37) and ca. 40 s (pH 9.00), respectively. The values testify

this system is capable to cleave by half the model OP within 1 min of less under mild experimental conditions.

5. Conclusion

In this work, we presented synthesis of a series of novel IL-derived amphiphilic pyridinium oximes composed by octylamide tail linked to the headgroup by means of amide (4-PyC8), alanyl (4-PyAlaC8), or phenylalanyl (2-PyPheC8, 3-PyPheC8, and 4-PyPheC8) moiety. The biodegradability has been examined in the closed bottle test (CBT) to demonstrate that it is dependent on the amino acid structure and follows the tendency Phe > Ala > amide. The oximes demonstrate 34–39% of degradation in the CBT after 42 days and can be considered as inherently degradable. The acid ionization constant (pK_a) of studied oximes determined by means of UV–vis spectroscopy at 27 °C were found to be in the range from 8.00 to 9.00. The $\text{pK}_{a,\text{app}}$ of studied oximes changes insignificantly in the presence of cationic gemini surfactants, 12-4-12- and 16-10-16, and shifted upwards in the presence of anionic surfactant SDS. The oxymolysis of OP triester PNPDPDP under optimal concentration conditions of 4-PyC8 occurs with half-life times ca. 62 s and ca. 40 s at pH 8.37 and 9.00, respectively. Therefore, by means of nucleophilic attack of the α effect nucleophile, this IL-derives oxime system can provide cleavage one half of the model OP within 1 min of less under mild experimental conditions. Results of this study can be useful in developing green and biodegradable compounds for chemical decontamination systems.

Authors' statement

SJP - primary contribution into physico-chemical studies of the novel functionalized ILs: acid-base equilibria (including recording, interpretation, and discussion of the UV spectra), mixed systems, chemical kinetics; result interpretation and discussion, preparation of the preliminary report and the draft of the manuscript.

IVK: overall contributed equally to the SJP; synthesis and complete characterization of the all compounds used in the current study, running and analysis of the NMR spectra and preparation of the ESI; discussion of the results obtained and contribution into the development of the idea of the manuscript; contribution manuscript preparation (Experimental part and Results and discussion) on the all stages.

ZU: performing biodegradability studies via CBT – planning, sample preparation, running the experiment, data treatment and discussion; participation in the preparation of ESI and the final manuscript version.

RS and DS: participation in the physico-chemical studies of the novel compounds, including sample preparation containing mixed micelle system with gemini surfactants and an anionic surfactant determination of the pK_a values in the mixed micellar systems, oxymolysis of the CWA simulant (PNPDPDP) in the presents of the oxime IL.

NG: development of the idea, contribution into the planning of the biodegradability experiment and the projects topic related to the green chemistry issues, analysis and discussion of the data and contribution into the writing the manuscript; extended decisive work on the improvement of the language of the final version of the manuscript on the stage of its resubmission.

KKG: development of the idea, supervision over the physico-chemical experiments running, results discussion, contribution into the writing the manuscript on the all stages; one of the persons for correspondence.

YK: conceived of the presented idea, development and coordination of the synthesis and planning and coordination of the studies of the novel compounds, overall results discussion, manuscript preparation with the primary help of SP and IK, and under support of NG, manuscript submission.

Table 3

Hydrolysis of *p*-nitrophenyl diphenyl phosphate (PNPDPDP) in the presence of 4-PyC8. Reaction condition: $[\text{PNPDPDP}] = 0.5 \text{ mM}$; 27 °C.

Sr. no.	[D] mM	103 kobs, (s-1)	
		pH	
		8.37	9.00
1.	0	0.76	5.72
2.	0.5	2.57	9.27
3.	1.0	5.44	13.30
4.	3.0	11.10	17.70
5.	5.0	9.67	15.90

Declaration of competing interest

The authors Subhashree Jayesh Pandya, Illia V. Kapitanov, Zeba Usmani, Reshma, Deepak Sinha, Nicholas Gathergood, Kallol K. Ghosh, and Yevgen Karpichev declare that they have no known competing financial interests or personal relationships that could have appeared to

Acknowledgment

Financial support of this work by the DST-FIST [No. SR/ST/CSI-259/2014(C)] and UGC-SAP [No. F-540/7/DRS-II/2016 (SAP-I)] is gratefully acknowledged. IK, NG, and YK acknowledge funding from EU FP7 under grant agreement No. 621364 (TUTIC-Green). YK acknowledges NATO SPS MYP No. G5565 (DEFIR). The authors are grateful to Prof. Shamsh Pervez, Head, School of Studies in Chemistry, Pt. Ravishankar Shukla University, Raipur (C.G.), India, for providing laboratory facility.

Appendix A. Supplementary data

Supplementary data to this article can be found online at <https://doi.org/10.1016/j.molliq.2020.112857>.

References

- [1] P. Anastas, N. Eghbali, Green chemistry: principles and practice, *Chem. Soc. Rev.* 39 (2010) 301–312.
- [2] M. Petkovic, K.R. Seddon, L.P.N. Rebelo, C.S. Pereira, Ionic liquids: a pathway to environmental acceptability, *Chem. Soc. Rev.* 40 (2011) 1383–1403.
- [3] C.W. Cho, U. Preiss, C. Jungnickel, S. Stolte, J. Arning, J. Ranke, A. Klamt, I. Krossing, J. Thoming, Ionic liquids: predictions of physicochemical properties with experimental and/or DFT-calculated LFER parameters to understand molecular interactions in solution, *J. Phys. Chem. B* 115 (2011) 6040–6050.
- [4] D. Coleman, N. Gathergood, Biodegradation studies of ionic liquids, *Chem. Soc. Rev.* 39 (2010) 600–637.
- [5] A. Jordan, N. Gathergood, Biodegradation of ionic liquids – a critical review, *Chem. Soc. Rev.* 44 (2015) 8200–8237.
- [6] K.S. Egorova, V.P. Ananikov, Toxicity of ionic liquids: eco(cyto)activity as complicated, but unavoidable parameter for task-specific optimization, *ChemSusChem* 7 (2014) 336–360.
- [7] Y. Deng, I. Beadham, M. Ghavre, M.F.C. Gomes, N. Gathergood, P. Husson, B. Legeret, B. Quilty, M. Sancelme, P. Besse-Hoggan, When can ionic liquids be considered readily biodegradable? Biodegradation pathways of pyridinium, pyrrolidinium and ammonium-based ionic liquids, *Green Chem.* 17 (2015) 1479–1491.
- [8] Ionic Liquid-Based Surfactant Science: Formulation, Characterization, and Applications., John Wiley & Sons, Inc, Hoboken, NJ, 2015 ISBN: 978-1-118-85435-8, 576 p.
- [9] A. Cornellas, L. Perez, F. Comelles, I. Ribosa, A. Manresa, M. Teresa Garcia, Self-aggregation and antimicrobial activity of imidazolium and pyridinium based ionic liquids in aqueous solution, *J. Colloid Interface Sci.* 355 (2011) 164–171.
- [10] A. Cognigni, P. Gaertner, R. Zirbs, H. Peterlik, K. Prochazka, C. Schroder, K. Bica, Surface-active ionic liquids in micellar catalysis: impact of anion selection on reaction rates in nucleophilic substitutions, *Phys. Chem. Chem. Phys.* 18 (2016) 13375–13384.
- [11] M. Taskin, A. Cognigni, R. Zirbs, E. Reimhult, K. Bica, Surface-active ionic liquids for palladium-catalysed cross coupling in water: effect of ionic liquid concentration on the catalytically active species, *RSC Adv.* 7 (2017) 41144–41151.
- [12] A. Haiss, A. Jordan, J. Westphal, E. Logunova, N. Gathergood, K. Kuemmerer, On the way to greener ionic liquids: identification of a fully mineralizable phenylalanine-based ionic liquid, *Green Chem.* 18 (2016) 4361–4373.
- [13] A. Jordan, A. Hail, M. Spulak, Y. Karpichev, K. Kuemmerer, N. Gathergood, Synthesis of a series of amino acid derived ionic liquids and tertiary amines: green chemistry metrics including microbial toxicity and preliminary biodegradation data analysis, *Green Chem.* (2016) 4374–4392.
- [14] M.C. Bubalo, K. Radosevic, I.R. Redovnikovic, J. Halambek, V.G. Sreck, A brief overview of the potential environmental hazards of ionic liquids, *Ecotoxicol. Environ. Saf.* 99 (2014) 1–12.
- [15] D.K.A. Kusumahastuti, M. Sihtmae, I.V. Kapitanov, Y. Karpichev, N. Gathergood, A. Kahr, Toxicity profiling of 24 L-phenylalanine derived ionic liquids based on pyridinium, imidazolium and cholinium cations and varying alkyl chains using rapid screening *Vibrio fischeri* bioassay, *Ecotoxicol. Environ. Saf.* 172 (2019) 556–565.
- [16] I. Kapitanov, A. Jordan, Y. Karpichev, M. Spulak, L. Perez, A. Kellett, K. Kuemmerer, N. Gathergood, Synthesis, self-assembly, antimicrobial activity, and preliminary biodegradation studies of a series of L-phenylalanine-derived surface active ionic liquids, *Green Chem.* 21 (2019) 1777–1794.
- [17] R.P. Chilcott, Managing mass casualties and decontamination, *Environ. Int.* 72 (2014) 37–45.
- [18] Brian J. Lukey, James A. Romano Jr., Harry Salem (Eds.), Chemical Warfare Agents: Biomedical and Psychological Effects, Medical Countermeasures, and Emergency Response, 3rd edition CRC Press, Boca Raton, USA, 2019, ISBN 9781498769211.
- [19] A. Devereaux, D.E. Amundson, J.S. Parrish, A.A. Lazarus, Vesicants and nerve agents in chemical warfare – decontamination and treatment strategies for a changed world, *Postgrad. Med.* 112 (2002) 90–96.
- [20] Y. Kim, Y.J. Jang, S.V. Mulya, T.T.T. Nguyen, D.G. Churchill, Fluorescent sensing of a nerve agent simulant with dual emission over wide pH range in aqueous solution, *Chem Eur J* 23 (2017) 7785–7790.
- [21] Y.J. Jang, O.G. Tsay, D.P. Murale, J.A. Jeong, A. Segev, D.G. Churchill, Novel and selective detection of Tabun mimics, *Chem. Commun.* 50 (2014) 7531–7534.
- [22] B. Durodie, S. Wesely, Resilience or panic? The public and terrorist attack, *Lancet* 360 (2002) 1901–1902.
- [23] M. Eddleston, N.A. Buckley, P. Eyer, A.H. Dawson, Management of acute organophosphorus pesticide poisoning, *Lancet* 371 (2008) 597–607.
- [24] M.C. Cesa, V.F. Ferreira, J.E. Forman, C. Tang, C.M. Timperley, C. Tran, B. West, OPCW-IUPAC workshop on innovative technologies for chemical security, *Pure Appl. Chem.* 90 (2018) 1501–1506.
- [25] T.F. Fan, C. Chen, T.T. Fan, F.M. Liu, Q.R. Peng, Novel surface-active ionic liquids used as solubilizers for water-insoluble pesticides, *J. Hazard. Mater.* 297 (2015) 340–346.
- [26] P. Pavez, G. Oliva, D. Millán, Green solvents as a promising approach to degradation of organophosphate pesticides, *ACS Sustain. Chem. Eng.* 4 (2016) 7023–7031.
- [27] G. Becker, A. Kawan, L. Szinicz, Direct reaction of oximes with sarin, soman, or tabun in vitro, *Arch. Toxicol.* 71 (1997) 714–718.
- [28] T.M. Prokop'eva, Y.S. Simanenko, I.P. Suprun, V.A. Savelova, T.M. Zubareva, E.A. Karpichev, Nucleophilic substitution at a four-coordinate sulfur atom: VI. Reactivity of oximate ions, *Russ. J. Org. Chem.* 37 (2001) 655–666.
- [29] Z. Rappoport, J.F. Liebman, The Chemistry of Hydroxylamines, Oximes and Hydroxamic Acids, 2009 ISBN: 978-0-470-51261-6, 1076 p.
- [30] C.A. Bunton, F.H. Hamed, L.S. Romsted, Quantitative treatment of reaction-rates in functional micelles and comicelles, *J. Phys. Chem.* 86 (1982) 2103–2108.
- [31] R. Sharma, B. Gupta, T. Yadav, S. Sinha, A.K. Sahu, Y. Karpichev, N. Gathergood, J. Marek, K. Kuca, K.K. Ghosh, Degradation of organophosphate pesticides using pyridinium based functional surfactants, *ACS Sustain. Chem. Eng.* 4 (2016) 6962–6973.
- [32] G. Saint-Andre, M. Kliachyna, S. Kodepelly, L. Louise-Leriche, E. Gillon, P.Y. Renard, F. Nachon, R. Baati, A. Wagner, Design, synthesis and evaluation of new alpha-nucleophiles for the hydrolysis of organophosphorus nerve agents: application to the reactivation of phosphorylated acetylcholinesterase, *Tetrahedron* 67 (2011) 6352–6361.
- [33] N. Singh, Y. Karpichev, A.K. Tiwari, K. Kuca, K.K. Ghosh, Oxime functionality in surfactant self-assembly: an overview on combating toxicity of organophosphates, *J. Mol. Liq.* 208 (2015) 237–252.
- [34] Y.S. Simanenko, E.A. Karpichev, T.M. Prokop'eva, B.V. Panchenko, Micelles of an oxime-functionalized imidazolium surfactant. Reactivities at phosphoryl and sulfonyl groups, *Langmuir* 17 (2001) 581–582.
- [35] Y.S. Simanenko, A.F. Popov, E.A. Karpichev, T.M. Prokop'eva, V.A. Savelova, C.A. Bunton, Micelle effects of functionalized surfactants, 1-cetyl-3-(2-hydroxyiminopropyl)imidazolium halides, in reactions with p-nitrophenyl p-toluenesulfonate, diethyl p-nitrophenyl phosphate, and ethyl p-nitrophenyl ethylphosphonate, *Russ. J. Org. Chem.* 38 (2002) 1314–1325.
- [36] Y.S. Simanenko, E.A. Karpichev, T.M. Prokop'eva, A. Lattes, A.F. Popov, V.A. Savelova, I.A. Belousova, Functional detergents containing an imidazole ring and typical fragments of alpha-nucleophiles underlying micellar systems for cleavage of esters of phosphorus acids, *Russ. J. Org. Chem.* 40 (2004) 206–218.
- [37] I.V. Kapitanov, I.A. Belousova, M.K. Turovskaya, E.A. Karpichev, T.M. Prokop'eva, A.F. Popov, Reactivity of micellar systems based on supernucleophilic functional surfactants in processes of acyl group transfer, *Russ. J. Org. Chem.* 48 (2012) 651–662.
- [38] N. Singh, Y. Karpichev, B. Gupta, M.L. Satnami, J. Marek, K. Kuca, K.K. Ghosh, Physicochemical properties and supernucleophilicity of oxime-functionalized surfactants: hydrolytic catalysts toward dephosphorylation of di- and triphosphate esters, *J. Phys. Chem. B* 117 (2013) 3806–3817.
- [39] I.V. Kapitanov, A.B. Mirgorodskaya, F.G. Valeeva, N. Gathergood, K. Kuca, L.Y. Zakharova, Y. Karpichev, Physicochemical properties and esterolytic reactivity of oxime functionalized surfactants in pH-responsive mixed micellar system, *Colloids and Surfaces A-Physicochemical and Engineering Aspects* 524 (2017) 143–159, <https://doi.org/10.1016/j.colsurfa.2017.04.039>.
- [40] Y. Karpichev, I. Kapitanov, N. Gathergood, O. Soukup, V. Hepnarova, D. Jun, K. Kuca, Acetylcholinesterase reactivators based on oxime-functionalized biodegradable ionic liquids, *Military Medicine Science Letters* 87 (2018) 87. <https://www.mmsl.cz/pdfs/mms/2018/88/87.pdf>.
- [41] R. Cibulka, F. Hampel, H. Kotoucová, J. Mazac, F. Liska, Quaternary pyridinium ketoximes – new efficient micellar hydrolytic catalysts, *Collect. Czechoslov. Chem. Commun.* 65 (2000) 227–242.
- [42] F. Terrier, P. Rodriguez-Dafonte, E. Le Guevel, G. Moutiers, Revisiting the reactivity of oximate alpha-nucleophiles with electrophilic phosphorus centers. Relevance to detoxification of sarin, soman and DFP under mild conditions, *Organic & Biomolecular Chemistry* 4 (2006) 4352–4363.
- [43] B. Gupta, R. Sharma, N. Singh, Y. Karpichev, M.L. Satnami, K.K. Ghosh, Reactivity studies of carbon, phosphorus and sulfur-based acyl sites with tertiary oximes in gemini surfactants, *J. Phys. Org. Chem.* 26 (2013) 632–642.
- [44] A.K. Valiveti, U.M. Bhalariao, J. Acharya, H.N. Karade, R. Gundapu, A.K. Halve, M.P. Kaushik, Synthesis and in vitro kinetic study of novel mono-pyridinium oximes as reactivators of organophosphorus (OP) inhibited human acetylcholinesterase (hAChE), *Chem. Biol. Interact.* 237 (2015) 125–132.
- [45] M. Teresa Garcia, I. Ribosa, L. Perez, A. Manresa, F. Comelles, Self-assembly and antimicrobial activity of long-chain amide-functionalized ionic liquids in aqueous solution, *Colloids and Surfaces B-Biointerfaces* 123 (2014) 318–325.

- [46] J. Friedrich, A. Langin, K. Kummerer, Comparison of an electrochemical and luminescence-based oxygen measuring system for use in the biodegradability testing according to closed bottle test (OECD 301D), *Clean-Soil Air Water* 41 (2013) 251–257.
- [47] A. Albert, E.P. Sergeant, *The Determination of Ionization Constants: A Laboratory Manual*, 3rd ed. Chapman and Hall, London; New York, 1984 218 p. ISBN 0412242907.
- [48] Regulation EC no 648/2004 of the European Parliament and the Council of 31 March 2004 on detergents, *EC Official Journal L* 104 (2004) 1–35.
- [49] R.G. Gore, L. Myles, M. Spulak, I. Beadham, M.T. Garcia, S.J. Connon, N. Gathergood, A new generation of aprotic yet Bronsted acidic imidazolium salts: effect of ester/amide groups in the C-2, C-4 and C-5 on antimicrobial toxicity and biodegradation, *Green Chem.* 15 (2013) 2747–2760.
- [50] S. Sudheer, G. Raba, I. Kapitanov, Y. Karpichev, R. Vilu, V.K. Gupta, N. Gathergood, A greener approach to hydrolyse ionic liquids, *Basic & Clinical Pharmacology & Toxicology* 124 (2018) 21.
- [51] M. Sorensen, E.H.J. Neilson, B.L. Moller, Oximes: unrecognized chameleons in general and specialized plant metabolism, *Mol. Plant* 11 (2018) 95–117.
- [52] Z.M. Qiang, C. Adams, Potentiometric determination of acid dissociation constants ($pK(a)$) for human and veterinary antibiotics, *Water Res.* 38 (2004) 2874–2890.
- [53] J.L. Beltrán, N. Sanli, G. Fonrodona, D. Barrón, G. Özkan, J. Barbosa, Spectrophotometric, potentiometric and chromatographic pK_a values of polyphenolic acids in water and acetonitrile–water media, *Anal. Chim. Acta* 484 (2003) 253–264.
- [54] V. Evagelou, A. Tsantili-Kakoulidou, M. Koupparis, Determination of the dissociation constants of the cephalosporins cefepime and cefpirome using UV spectrometry and pH potentiometry, *J. Pharm. Biomed. Anal.* 31 (2003) 1119–1128.
- [55] R. Wróbel, L. Chmurzyński, Potentiometric pK_a determination of standard substances in binary solvent systems, *Anal. Chim. Acta* 405 (2000) 303–308.
- [56] Y.-J. Seok, K.-S. Yang, S.-O. Kang, A simple spectrophotometric determination of dissociation constants of organic compounds, *Anal. Chim. Acta* 306 (1995) 351–356.
- [57] R.I. Allen, K.J. Box, J.E.A. Comer, C. Peake, K.Y. Tam, Multiwavelength spectrophotometric determination of acid dissociation constants of ionizable drugs, *J. Pharm. Biomed. Anal.* 17 (1998) 699–712.
- [58] S. Tiwari, K.K. Ghosh, J. Marek, K. Kuca, Spectrophotometric determination of the acidity constants of some oxime-based alpha-nucleophiles, *Journal of Chemical and Engineering Data* 55 (2010) 1153–1157.
- [59] J. Acharya, D.K. Dubey, A.K. Srivastava, S.K. Raza, In vitro reactivation of sarin-inhibited human acetylcholinesterase (AChE) by bis-pyridinium oximes connected by xylene linkers, *Toxicol. in Vitro* 25 (2011) 251–256.
- [60] G. Volgyi, R. Ruiz, K. Box, J. Comer, E. Bosch, K. Takacs-Novak, Potentiometric and spectrophotometric $pK(a)$ determination of water-insoluble compounds: validation study in a new cosolvent system, *Anal. Chim. Acta* 583 (2007) 418–428.
- [61] S. Babic, A.J.M. Horvat, D.M. Pavlovic, M. Kastelan-Macan, Determination of $pK(a)$ values of active pharmaceutical ingredients, *TRAC-Trends in Analytical Chemistry* 26 (2007) 1043–1061.
- [62] C. Ráfols, M. Rosés, E. Bosch, A comparison between different approaches to estimate the aqueous pK_a values of several non-steroidal anti-inflammatory drugs, *Anal. Chim. Acta* 338 (1997) 127–134.
- [63] B. Gupta, N. Singh, R. Sharm, B. Foretic, K. Musilek, K. Kuca, J. Acharya, M.L. Satnami, K.K. Ghosh, Assessment of antidotal efficacy of cholinesterase reactivators against paraoxon: in vitro reactivation kinetics and physicochemical properties, *Bioorg. Med. Chem. Lett.* 24 (2014) 4743–4748.
- [64] F. Ahmadi, M.A. Daneshmehr, M. Rahimi, The effect of anionic and cationic surfactants on indicators and measurement of dissociation constants with two different methods, *Spectrochimica Acta Part A-Molecular and Biomolecular Spectroscopy* 67 (2007) 412–419, <https://doi.org/10.1016/j.saa.2006.07.033>.
- [65] I.V. Berezin, K. Martinek, A.K. Yatsimirskii, Physicochemical foundations of micellar catalysis, *Russ. Chem. Rev.* 42 (1973) 787.
- [66] L.S. Romsted, C.A. Bunton, J.H. Yao, Micellar catalysis, a useful misnomer, *Curr. Opin. Colloid Interface Sci.* 2 (1997) 622–628.
- [67] C.A. Bunton, F. Nome, F.H. Quina, L.S. Romsted, Ion binding and reactivity at charged aqueous interfaces, *Acc. Chem. Res.* 24 (1991) 357–364.
- [68] C.A. Bunton, L.B. Robinson, Micellar effects on acidity functions, *J. Phys. Chem.* 73 (1969) 4237–4241.
- [69] D.G. Hall, Micellar effects on reaction rates and acid-base equilibria, *J. Phys. Chem.* 91 (1987) 4287–4297.
- [70] G.S. Hartley, J.W. Roe, Ionic concentrations at interfaces, *Trans. Faraday Soc.* 35 (1940) 101–109.
- [71] N. Pourreza, S. Rastegarzadeh, Spectrophotometric determination of the dissociation constant of 5-(p-dimethylaminobenzylidene)rhodanine in micellar media, *Journal of Chemical and Engineering Data* 50 (2005) 206–210.
- [72] O.A. El Seoud, Effects of organized surfactant assemblies on acid-base equilibria, *Adv. Colloid Interf. Sci.* 30 (1989) 1–30.
- [73] F.M.A. Altalbawy, E.-S.A.M. Al-Sherbini, Spectrophotometric determination of acidity constant of 1-methyl-4-4'-aminostyryl quinolinium iodide in aqueous buffer and micellar solutions in the ground and excited states, *Asian J. Chem.* 25 (2013) 6181–6185.
- [74] M.R. Popovic, G.V. Popovic, D.D. Agbaba, The effects of anionic, cationic, and non-ionic surfactants on acid-base equilibria of ACE inhibitors, *Journal of Chemical and Engineering Data* 58 (2013) 2567–2573, <https://doi.org/10.1021/jc400397p>.
- [75] A. Kovalevsky, D.K. Blumenthal, X.L. Cheng, P. Taylor, Z. Radic, Limitations in current acetylcholinesterase structure-based design of oxime antidotes for organophosphate poisoning, in: J.D. Laskin, D. Braaten (Eds.), *Countermeasures against Chemical Threats II*, Blackwell Science Publ, Oxford 2016, pp. 41–49, <https://doi.org/10.1111/nyas.13128>.
- [76] I. Grosmaire, M. Chorro, C. Chorro, S. Partyka, R. Zana, Alkanediyl-alpha, omega-bis (dimethylalkylammonium bromide) surfactants –9. Effect of the spacer carbon number and temperature on the enthalpy of micellization, *J. Colloid Interface Sci.* 246 (2002) 175–181.
- [77] H. Akbas, A. Elemenli, M. Boz, Aggregation and thermodynamic properties of some cationic gemini surfactants, *J. Surfactant Deterg.* 15 (2012) 33–40.
- [78] J. Lakra, D. Tikariha, T. Yadav, S. Das, S. Ghosh, M.L. Satnami, K.K. Ghosh, Mixed micellization of gemini and cationic surfactants: physicochemical properties and solubilization of polycyclic aromatic hydrocarbons, *Colloids and Surfaces A-Physicochemical and Engineering Aspects* 451 (2014) 56–65, <https://doi.org/10.1016/j.colsurfa.2014.03.037>.
- [79] L.M. Goncalves, T.G. Kobayakawa, D. Zanette, H. Chaimovich, I.M. Cuccovia, Effects of micelles and vesicles on the oximolysis of p-nitrophenyl diphenyl phosphate: a model system for surfactant-based skin-defensive formulations against organophosphates, *J. Pharm. Sci.* 98 (2009) 1040–1052.
- [80] S. Tiwari, K.K. Ghosh, J. Marek, K. Kuca, Functionalized surfactant mediated reactions of carboxylate, phosphate and sulphonate esters, *J. Phys. Org. Chem.* 23 (2010) 519–525.

Appendix 2

Publication II

Pandya, S.J.; Kapitanov, I.V.; Banjare, M.K.; Behera, K.; Borovkov, V.; Ghosh, K.K.; Karpichev, Y. Mixed oxime-functionalized IL/16-s-16 Gemini surfactants system: physicochemical study and structural transitions in the presence of promethazine as a potential chiral pollutant. *Chemosensors* **2022**, 10, 46

Reproducing is permitted by MDPI Open Access Information and Policy / open access Creative Common CC BY license.

Article

Mixed Oxime-Functionalized IL/16-s-16 Gemini Surfactants System: Physicochemical Study and Structural Transitions in the Presence of Promethazine as a Potential Chiral Pollutant

Subhashree Jayesh Pandya ¹, Illia V. Kapitanov ^{2,†} , Manoj Kumar Banjare ^{1,3} , Kamalakanta Behera ⁴ , Victor Borovkov ^{2,*} , Kallol K. Ghosh ^{1,*} and Yevgen Karpichev ^{2,*}

¹ School of Studies in Chemistry, Pt. Ravishankar Shukla University, Raipur 492010, India; subhashree210490@gmail.com (S.J.P.); manojbanjare7@gmail.com (M.K.B.)

² Department of Chemistry and Biotechnology, Tallinn University of Technology (TalTech), 12618 Tallinn, Estonia; illia.kapitanov@taltech.ee

³ MATS School of Sciences, MATS University, Pagariya Complex, Pandri, Raipur 492001, India

⁴ Department of Applied Chemistry (ASAS), Amity University, Gurgaon 122413, India; kamala.iitd@gmail.com

* Correspondence: victor.borovkov@taltech.ee (V.B.); kallolkghosh@gmail.com (K.K.G.); yevgen.karpichev@taltech.ee (Y.K.); Tel.: +91-771-2263146 (K.K.G.); +372-620-4381 (Y.K.)

† Current Address: Gemini Pharm Chem Mannheim GmbH, 68305 Mannheim, Germany.



Citation: Pandya, S.J.; Kapitanov, I.V.; Banjare, M.K.; Behera, K.; Borovkov, V.; Ghosh, K.K.; Karpichev, Y. Mixed Oxime-Functionalized IL/16-s-16 Gemini Surfactants System: Physicochemical Study and Structural Transitions in the Presence of Promethazine as a Potential Chiral Pollutant. *Chemosensors* **2022**, *10*, 46. <https://doi.org/10.3390/chemosensors10020046>

Academic Editor: Núria Serrano

Received: 30 November 2021

Accepted: 17 January 2022

Published: 25 January 2022

Publisher's Note: MDPI stays neutral with regard to jurisdictional claims in published maps and institutional affiliations.



Copyright: © 2022 by the authors. Licensee MDPI, Basel, Switzerland. This article is an open access article distributed under the terms and conditions of the Creative Commons Attribution (CC BY) license (<https://creativecommons.org/licenses/by/4.0/>).

Abstract: The increasing concern about chiral pharmaceutical pollutants is connected to environmental contamination causing both chronic and acute harmful effects on living organisms. The design and application of sustainable surfactants in the remediation of polluted sites require knowledge of partitioning between surfactants and potential pollutants. The interfacial and thermodynamic properties of two gemini surfactants, namely, alkanediyi- α,ω -bis(dimethylhexadecyl ammonium bromide) (16-s-16, where $s = 10, 12$), were studied in the presence of the inherently biodegradable oxime-functionalized ionic liquid (IL) 4-((hydroxyimino)methyl)-1-(2-(octylamino)-2-oxoethyl)pyridin-1-ium bromide (4-PyC8) in an aqueous solution using surface tension, conductivity, fluorescence, FTIR and ^1H NMR spectroscopic techniques. The conductivity, surface tension and fluorescence measurements indicated that the presence of the IL 4-PyC8 resulted in decreasing CMC and facilitated the aggregation process. The various thermodynamic parameters, interfacial properties, aggregation number and Stern–Volmer constant were also evaluated. The IL 4-PyC8-gemini interactions were studied using DLS, FTIR and NMR spectroscopic techniques. The hydrodynamic diameter of the gemini aggregates in the presence of promethazine (PMZ) as a potential chiral pollutant and the IL 4-PyC8 underwent a transition when the drug was added, from large aggregates (270 nm) to small micelles, which supported the gemini:IL 4-PyC8:promethazine interaction. The structural transitions in the presence of promethazine may be used for designing systems that are responsive to changes in size and shape of the aggregates as an analytical signal for selective detection and binding pollutants.

Keywords: mixed surfactant system; ionic liquid; gemini surfactants; chiral pollutants; promethazine; dynamic light scattering

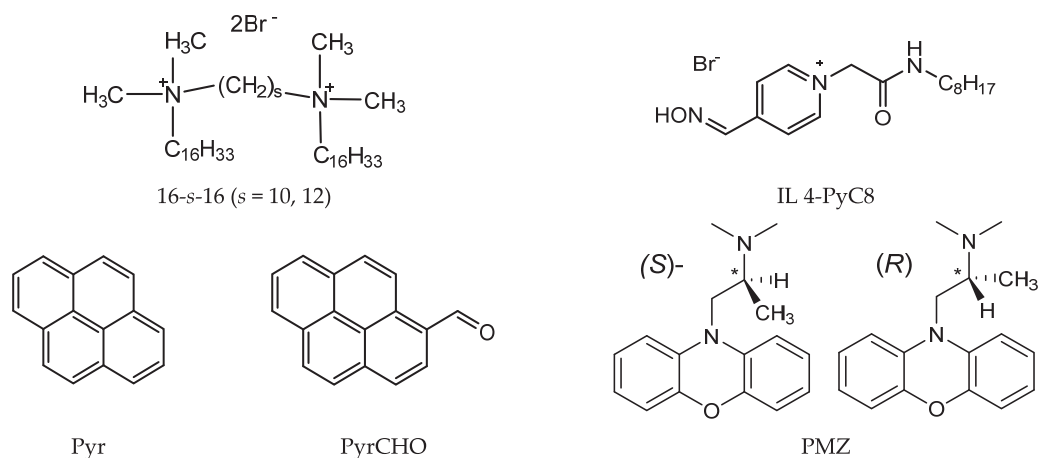
1. Introduction

The increasing concern about chiral pharmaceutical pollutants is connected to environmental contamination causing both chronic and acute harmful effects on living organisms. It is a problem of direct importance to detect chiral compounds [1], including chiral pollutants of different natures [2]. Using surfactants for increasing analytical signals and, consequently, reducing the detection concentration of the pollutants is one of the attractive strategies in chemical analysis [3,4] since it may ensure selective binding of one of the components, providing more reliable detection in the cases when the structurally similar compounds are present in the mixture. For example, dimeric (gemini) surfactants were reported to exhibit selectivity toward the binding of calixarenes modified with different

amino acid (L-Ala and L-Val) moieties [5]. An additional tool to evaluate the presence of a pollutant may be provided based on the sensitivity of self-assembly aggregates to the binding of target compounds, causing structural rearrangement of the aggregate's type, size and shape. Surfactant-based systems can effectively remove pollutant residues from surfaces of various types [6]. The design and application of sustainable surfactants in the remediation of polluted sites require knowledge of the interaction between surfactants and potential pollutants. Recently, environmentally friendly ionic liquids (ILs) have emerged as a novel system for the studies of green chemistry and environmental sciences [7–9]. ILs have been used significantly in organic synthesis [10,11], drug delivery [12], catalysis [13–15], separation processes [16,17] and the preparation of nanostructured materials [18]. The development of biocompatible and biodegradable ILs results in finding sustainable fragments to assist the synthesis of sustainable molecular blocks [19]. Garcia et al. [20] reported the micellization behavior and antimicrobial properties of ester- and amide-functionalized [21] pyridinium and imidazolium ILs with respect to the length of the side chain. Introducing an amide group in lieu of an ester group increases the stability of the functionalized ILs toward abiotic hydrolysis and thus extends the range of conditions of their practical application. A versatile approach included introducing an amino acid moiety to link the head group and side chain in the cation of IL/surface-active IL (SAIL) [19,22], which opened an opportunity to develop SAILS with optimized environmental toxicity [23], self-assembly [24] and biodegradability [25] properties. We recently reported the synthesis and study of a series of inherently biodegradable oxime-functionalized ILs [26] proposed as a base for a green decontamination IL–surfactant system. Although it is a well-established fact that the properties of ILs can be tuned with surfactants [27–29], using nonconventional surfactants (e.g., gemini surfactants) calls for more broad and detailed studies [30,31]. The gemini surfactants consist of two hydrophilic head groups and two hydrophobic chains covalently connected through a spacer group [32–34]. They have generated much interest because of their outstanding properties and their diverse applications compared with single-chain surfactants [25,26]. The aggregation behavior of monomeric conventional surfactants is mainly driven by intermolecular interactions, whereas a gemini surfactant is controlled by both inter-molecular and intra-molecular interactions. The physicochemical and interfacial properties of gemini surfactants in an aqueous solution depends upon the concentration, temperature, nature of hydrophobic tails, spacer properties and additives. Gemini surfactants have been studied to shed light on the effect of structural variation of surfactants on their binding ability with drugs, which, in turn, may also open new approaches for designing tunable drug carrier systems [35]. A mixed system of surfactant and ILs/SAILS with distinct morphology and physicochemical properties improves their performance in terms of cooperative combination [27–31]. The IL–surfactant interaction plays a crucial role for some applications in pharmaceutical and biomedical science, namely, in enhancing the permeability of drugs across biological membranes [36]. Ozan [37] described the effect of the imidazolium ILs EmimCl and BmimCl on the interaction and binding properties of phenothiazine and trifluopromazine hydrochloride with a series of nonionic surfactants (Brij 30, Brij 35 and Brij 56). Mahajan et al. [38] studied the micellization and interfacial behavior of a SAIL (C₁₄mimBr) and TTAB in the presence of drugs (dopamine hydrochloride and acetylcholine chloride) using conductivity and surface tension measurements. The binding constant and the Gibbs free energy change (ΔG) for the drug–surfactant complexes were evaluated via cyclic voltammeter measurements. Another work of this group [39] reported aggregation behavior of a series of novel SAILS, namely, diazabicyclo[5.4.0]undec-7-en-8-ium salts, and their interaction with the amphiphilic drug amitriptyline hydrochloride, indicating attractive interactions for the drug and SAILS. Recently, we reported the binding affinity of an inherently biodegradable oxime-functionalized SAIL with the phenothiazine drug promazine hydrochloride [40].

The present study aimed to shed light on surfactant systems containing gemini surfactants, a functionalized SAIL and an antidepressant drug promethazine hydrochloride (PMZ). The interfacial and thermodynamic properties of binary combinations of gemini

surfactants alkanediyl- α,ω -bis (dimethylhexadecyl ammonium bromide) (16-*s*-16, where *s* = 10, 12) (Scheme 1) with functionalized IL 4-((hydroxyimino) methyl)-1-(2-(octylamino)-2-oxoethyl) pyridin-1-iumbromide (4-PyC8), were studied using surface tension, conductivity, fluorescence, FTIR and ^1H NMR techniques. The effect of 4-PyC8 on the aggregation behavior, i.e., critical micelle concentration (CMC), surface excess concentration (Γ_{max}), surface pressure at CMC (π_{cmc}) and minimum area per molecule (A_{min}), were determined using the surface tension method. The thermodynamic parameters, i.e., the standard Gibbs free energy of aggregation ($\Delta G^\circ_{\text{m}}$), Gibbs energy of adsorption ($\Delta G^\circ_{\text{ads}}$), Gibbs energy of transfer ($\Delta G^\circ_{\text{trans}}$), Gibbs energy of micellization per alkyl tail ($\Delta G^\circ_{\text{tail}}$) and air–water interface ($\Delta G^\circ_{\text{min}}$), were evaluated using a conductrometric technique. The CMC, aggregation number (N_{agg}) and Stern–Volmer constant (K_{sv}) were also determined via a fluorescence method using pyrene (Pyr) and 1-pyrene carboxaldehyde (PyrCHO) as the probes. FTIR and NMR techniques were successfully used to study the IL 4-PyC8:gemini interactions. The sizes of the gemini aggregates in the presence of PMZ and IL 4-PyC8 were studied using dynamic light scattering (DLS).



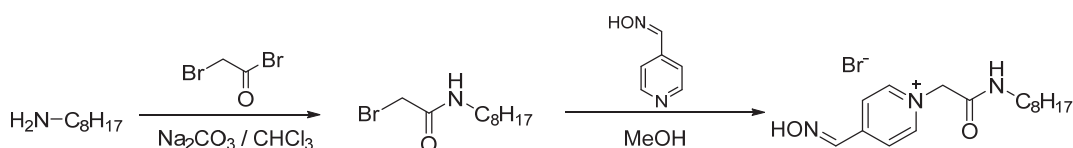
Scheme 1. Structures of the gemini surfactants (16-*s*-16), IL (4-PyC8) and fluorescent probes (Pyr and PyrCHO) studied in the present work, as well as the *S*- (left) and *R*- (right) enantiomers of promethazine (PMZ).

The structures of the gemini surfactants (16-*s*-16), conventional single-chain cationic surfactant cetylpyridinium chloride (CPC), functionalized IL 4-PyC8, antidepressant drug promethazine hydrochloride (PMZ) and fluorescent probes (Pyr and PyrCHO) used in the present study are shown in Scheme 1.

2. Experimental Section

2.1. Materials

1-Pyrene carboxaldehyde (PyrCHO), pyrene (Pyr), potassium chloride, cetylpyridinium chloride (CPC), promethazine hydrochloride (PMZ) and organic solvents were purchased from Sigma Aldrich. The PyrCHO solutions were prepared in pure methanol. All the chemicals were used without further purification. The gemini surfactants alkanediyl-1,4-bis(dimethylhexadecyl ammonium bromide) 16-10-16 and 16-12-16 were synthesized by refluxing the corresponding decanediyl-1,10-*bis*-(cetyldimethylammonium bromide) in dry ethanol for 48 h, followed by recrystallization from hexane/ethyl acetate mixtures [29]. The IL 4-((hydroxyimino)methyl)-1-(2-(octylamino)-2-oxoethyl) (4-PyC8) was synthesized as described in our previous work [26] (see Scheme 2).



Scheme 2. Synthesis of IL 4-((hydroxyimino)methyl)-1-(2-(octylamino)-2-oxoethyl) (4-PyC8).

2.2. Methods

2.2.1. Conductivity

A digital conductivity meter (Systronics, Type 304) equipped with a conductivity cell of cell constant 1.01 cm^{-1} was used to measure the conductance for pure and mixed systems. The conductivity cell was calibrated before the measurements with standard solutions of potassium chloride (KCl) across a 0.01 M to 0.1 M concentration range. A concentrated gemini surfactant stock solution (10–20 times of the CMC) was progressively added using a micropipette to the IL 4-PyC8 solution. After thorough mixing and temperature equilibration at 300 K, the observed conductance was measured at each addition. The breakpoint of the plot of specific conductivity (κ) versus gemini surfactant concentration corresponded to the CMC for the pure gemini surfactant and mixed systems.

2.2.2. Surface Tension Measurements

The surface tension at different concentrations of gemini surfactants in the IL 4-PyC8 media was measured by using a KYOWA automatic surface tensiometer (DY-300) equipped with a platinum ring. The platinum ring was dried using a burner after every measurement to remove the sublimate of the gemini surfactant and the IL 4-PyC8. The surface tensiometer was calibrated by taking the surface tension of Millipore water ($72 \text{ mN} \cdot \text{m}^{-1}$ at 300 K). A 10 mL sample of 4-PyC8 solution was taken in a double-wall jacketed container, and the concentrated gemini surfactant of known concentration (below and above the CMC 10–15 times) was added progressively. The maximum force with which the platinum ring was pulled out from the sample was noted to be the surface tension γ ($\text{mN} \cdot \text{m}^{-1}$) of the particular solution.

2.2.3. Fluorescence Measurements

All fluorescence spectra were measured using a Cary Eclipse Fluorescence (Agilent Technology) spectrophotometer. A strong hydrophobic fluorescent probe 1-pyrene carboxaldehyde (PyCHO) of 0.12 mM concentration was used in an aqueous micellar solution. The excitation wavelength was 334 nm and all fluorescence emission spectra were measured in the range of 340–450 nm. The excitation and emission slit widths were kept at 2.5 nm. Cetylpyridinium chloride (CPC) (0.12 mM) was used as the quencher to calculate the aggregation number.

2.2.4. FTIR Spectroscopy

The FTIR spectra of gemini surfactants and mixed systems were measured on a Bruker-ECO-ATR (attenuated total reflection) Model-i55 FTIR Spectrophotometer. In the mixed systems, the solid films were prepared via the evaporation of a 1:1 ratio water–ethanol solution by stirring the mixture for several minutes and allowing it to dry overnight at room temperature. All the spectra were obtained over the spectral range of $4000\text{--}400 \text{ cm}^{-1}$ at 298 K.

2.2.5. ^1H NMR Measurements

^1H NMR measurements were recorded using a Bruker Avance III NMR spectrometer (400 MHz) in D_2O .

2.2.6. Dynamic Light Scattering Study

The hydrodynamic diameter, size distribution and zeta potential of the aggregates were obtained using a Zetasizer Nano light scattering instrument (Malvern Instruments) with a He-Ne laser (633 nm, 10 mW). The scattering intensity was measured at $\theta = 173^\circ$. The data obtained were processed using the Malvern DTS Software 7.11 package.

3. Results and Discussion

3.1. Determination of the Critical Micelle Concentration

The CMC values were determined for both the gemini surfactants 16-10-16 and 16-12-16 in the presence of 0.2, 0.5, 0.7 and 1 wt% of 4-PyC8 using the conductivity and surface tension.

3.1.1. Conductivity

We investigated the aggregation properties of gemini surfactants in water in the presence and absence of the IL 4-PyC8. The breakpoint of the plot between the specific conductivity (κ) and gemini surfactant concentration gave the CMC of the gemini surfactant and mixed systems, see Figure 1. The aggregation of the surfactant formed at the breakpoint. The counter ion dissociation (α) of gemini surfactants for the pure and mixed system (gemini surfactants/IL 4-PyC8) were also evaluated (Table 1) from the ratio of the post-micellar and pre-micellar concentration range slopes obtained from the plots of specific conductance of the surfactant solution at different concentrations [41]:

$$\alpha = \frac{S_2}{S_1} \quad (1)$$

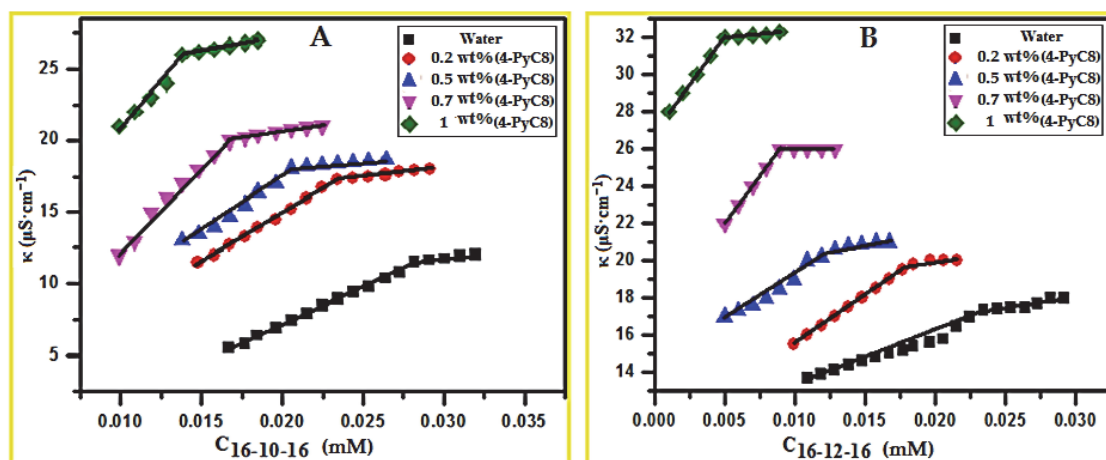


Figure 1. Specific conductivity ($\mu\text{S}\cdot\text{cm}^{-1}$) vs. concentration (mM) of the gemini surfactants 16-10-16 (A) and 16-12-16 (B) in the presence of 0.2, 0.5, 0.7 and 1 wt% of the IL 4-PyC8 at 300 K.

It was observed that on increasing the mass fraction of the IL 4-PyC8, the α values gradually decreased. The CMC and α values are listed in Table 1. It was observed that an increase in the concentration of the IL 4-PyC8 led to a sharp decrease in the CMC value for both gemini surfactants. Increasing the mass fraction of the IL 4-PyC8 lowered the electrostatic repulsion between the charged head groups of the gemini surfactant and reduced the CMC, which favored micellization [42,43].

Table 1. Critical micelle concentration (CMC) and counter ion dissociation (α) of the gemini surfactants 16-s-16 with different contents (wt%) of the IL 4-PyC8 at 300 K.

IL 4-PyC8 (wt%)	CMC (mM)		
	Conductivity	Surface Tension	α
16-10-16			
Water	0.028 ^a	0.029	0.60
0.2	0.023	0.024	0.51
0.5	0.023	0.021	0.31
0.7	0.016	0.016	0.23
1.0	0.013	0.013	0.23
16-12-16			
Water	0.021 ^a	0.022	0.67
0.2	0.017	0.016	0.44
0.5	0.011	0.011	0.39
0.7	0.009	0.009	0.29
1.0	0.005	0.006	0.25

^a Ref [44].

3.1.2. Surface Tension

The surface tension versus the logarithm of the gemini surfactants concentration (M) plots are shown in Figure 2. The decrease in surface tension due to the adsorption of the gemini surfactant in the air/water interface is shown in Figure 2. At a constant gemini surfactant concentration, the surface tension gradually decreased when increasing the IL 4-PyC8 content. The surface tension decreased more rapidly, which may have been due to the longer alkyl chain IL increasing the hydrophobicity in the system [44,45]. Adding the IL 4-PyC8 caused the compression of the diffuse electric double layer, which decreased the electrostatic repulsions between the head groups of the gemini surfactants and reduced the CMC [46]. The CMC values obtained for the two gemini surfactants and mixed systems are listed in Table 1.

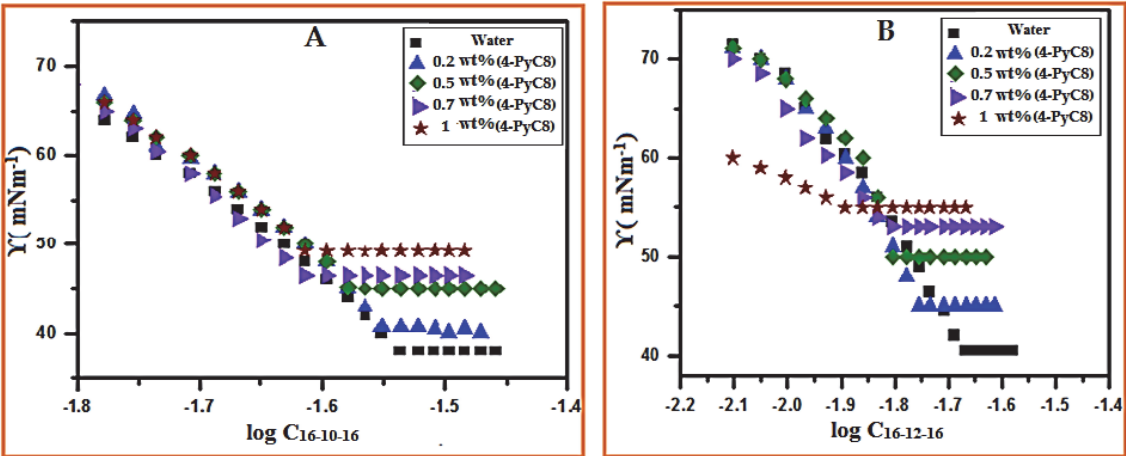


Figure 2. Surface tension vs. logarithm of the concentration of the gemini surfactants 16-10-16 (A) and 16-12-16 (B) in the presence of various mass fractions (0.2, 0.5, 0.7 and 1 wt%) of the IL 4-PyC8 at 300 K.

3.2. Effect of Oxime-Functionalized Ionic Liquid on the Interfacial Properties

The maximum surface excess (Γ_{\max}), minimum surface area per molecule (A_{\min}), surface tension at CMC (γ_{cmc}) and surface pressure at the CMC ($\Pi_{\text{cmc}} = \gamma_0 - \gamma_{\text{cmc}}$) of the

gemini surfactants in the presence of 4-PyC8 were determined using tensiometry. All these data are summarized in Table 2. The values of the maximum surface excess (Γ_{\max}) [33,47] were calculated using the Gibbs adsorption isotherm (Equation (2)):

$$\Gamma_{\max} = -\frac{1}{2.303nRT} \left[\frac{d\gamma}{d \log C} \right]_{T,P} \quad (2)$$

where $\frac{d\gamma}{d \log C}$ denotes the surface activity at a temperature (in Kelvin) and R is the universal gas constant ($8.314 \text{ J}\cdot\text{K}^{-1}\cdot\text{mol}^{-1}$). T is the absolute temperature in Kelvin, C is the concentration of the gemini surfactant and γ is the surface tension at a given concentration of surfactant. Since the gemini surfactant is made up of a divalent surfactant ion and two univalent counter-ions, the constant ‘n’ (pre-factor) value is taken as 3. The values of Γ_{\max} decreased with increasing the mass fraction of 4-PyC8 (Table 2). The values of the minimum area per molecule (A_{\min}) [33,48] of the gemini surfactant at the air–liquid interface were obtained using Equation (3):

$$A_{\min} = \frac{1}{\Gamma_{\max} \cdot N_A} \quad (3)$$

where N_A is the Avogadro’s number ($6.022 \times 10^{23} \text{ mol}^{-1}$) and Γ_{\max} is the maximum surface excess concentration (mol m^{-2}) of adsorbed surfactant molecules at the interface. The A_{\min} values of the mixed systems composed of one of the two gemini surfactants and the IL 4-PyC8 are presented in Table 2. The results indicated that the values of Γ_{\max} and A_{\min} varied with the addition of the ionic liquid, revealing a lower Γ_{\max} (larger A_{\min}) with a higher content of IL. The values of Γ_{\max} decreased and A_{\min} increased due to the reduction in forces between the two head groups of the gemini surfactants in the presence of the IL 4-PyC8 when the molecules were less compactly packed at the air/water interface.

Table 2. Surface excess parameter (Γ_{\max}), surface pressure at CMC (π_{CMC}) and minimum surface area per molecule (A_{\min}) of the studied gemini surfactants for different mass fractions of the IL 4-PyC8 at 300 K.

IL 4-PyC8 (wt%)	γ_{CMC} ($\text{mN}\cdot\text{m}^{-1}$)	Γ_{\max} ($10^6 \text{ mol}\cdot\text{m}^{-2}$)	A_{\min} $10^{20} (\text{m}^2 \text{ mol}^{-1})$	π_{CMC} ($\text{mN}\cdot\text{m}^{-1}$)
16-10-16				
Water	38	2.10	79.18	34.1
0.2	41	1.30	128.36	31.4
0.5	45	1.22	135.75	27.1
0.7	46	1.19	139.04	25.6
1.0	49	0.99	167.09	22.9
16-12-16				
Water	40	1.99	83.88	31.0
0.2	45	1.27	131.45	26.5
0.5	50	1.26	132.04	21.5
0.7	53	1.20	138.21	18.5
1.0	55	0.93	178.72	16.5

Mean errors: $\gamma_{\text{cmc}} = \pm 1 \text{ mN}\cdot\text{m}^{-1}$, $\Gamma_{\max} = \pm 0.02 \text{ mol}\cdot\text{m}^{-2}$, $A_{\min} = \pm 0.02 \text{ m}^2 \text{ mol}^{-1}$, $\pi_{\text{CMC}} = \pm 0.10 \text{ mN}\cdot\text{m}^{-1}$.

The surface pressure at the CMC (π_{cmc}) [49] is a measure of the surface tension reduction at the CMC and is calculated using Equation (4):

$$\pi_{\text{CMC}} = \gamma_0 - \gamma_{\text{CMC}} \quad (4)$$

where γ_0 and γ_{cmc} correspond to pure water and the mixed system at the CMC at 300 K. The π_{cmc} values depend on the interfacial area occupied by the gemini surfactants with their specific position and the structure at the interface. The reduction of the surface tension

of the pure solvent by the gemini surfactants indicated more effective adsorption at the interface in the presence of the IL 4-PyC8 [33].

3.3. Effect of Oxime-Functionalized Ionic Liquid on Thermodynamic Parameters

Oxime-functionalized IL 4-PyC8 modified the physicochemical and thermodynamic properties of both gemini surfactants. The intermolecular forces, such as Van der Waals forces, dipole–dipole interaction and hydrogen bonding, were involved in the interaction of the IL 4-PyC8 with the gemini surfactants. The standard Gibbs free energy of micellization (ΔG°_m) was calculated for the analysis of the IL 4-PyC8 on the micellization process [50] using the following Equation (5):

$$\Delta G^\circ_m = 2(1.5 - \alpha) RT \ln X_{CMC} \quad (5)$$

where α is the degree of counterion dissociation, R is the ideal gas constant, T is the temperature in Kelvin and X_{CMC} is the CMC in the mole fraction unit.

The value of ΔG°_m became more negative as the IL 4-PyC8 concentration increased, which was due to stronger hydrophobic interactions. The calculated value of ΔG°_m is listed in Table 3. The negative value of ΔG°_m led to the spontaneous process. The standard Gibbs free energy of adsorption (ΔG°_{ads}) at the air/water interface [51] was calculated by using Equation (6):

$$\Delta G^\circ_{ads} = \frac{\Delta G^\circ_m - \pi_{CMC}}{\Gamma_{max}} \quad (6)$$

where ΔG°_m is the Gibbs free energy of micellization, Γ_{max} is the maximum surface excess concentration and π_{CMC} is the surface pressure at the CMC. Here, the addition of the IL 4-PyC8 led to an increase in ΔG°_{ads} , which indicated the stronger hydrophobic interaction due to the repulsion forces in the water/hydrophobic interface. The ΔG°_{ads} supported the micellization behavior between the IL 4-PyC8 and the gemini surfactants. The ΔG°_{ads} values also favored the spontaneous micellization process. All these values are listed in Table 3.

Table 3. Gibbs free energy of micellization (ΔG°_m), Gibbs free energy of micellization per alkyl tail ($\Delta G^\circ_{m,tail}$), Gibbs energy of transfer (ΔG°_{trans}), standard free energy of adsorption (ΔG°_{ads}) and Gibbs free energy of the given air/water interface ($\Delta G^{(s)}_{min}$) of the gemini surfactants 16-s-16 with different contents (wt%) of the IL 4-PyC8 at 300 K.

IL 4-PyC8 (wt%)	$\Delta G^{(s)}_{min}$ (kJ/mol)	ΔG°_m (kJ/mol)	$\Delta G^\circ_{m,tail}$ (kJ/mol)	ΔG°_{ads} (kJ/mol)	ΔG°_{trans} (kJ/mol)
16-10-16					
Water	18.12	−14.69	−7.34	−30.95	−
0.2	31.48	−16.55	−8.27	−40.82	−1.86
0.5	36.79	−20.23	−10.11	−42.40	−5.54
0.7	38.93	−22.10	−11.05	−43.55	−7.41
1.0	49.51	−22.68	−11.34	−45.74	−7.99
16-12-16					
Water	20.46	−14.11	−7.57	−29.69	−
0.2	35.62	−18.49	−9.24	−39.4	−4.38
0.5	39.76	−20.39	−10.10	−37.49	−6.28
0.7	44.12	−22.75	−11.30	−38.15	−8.64
1.0	59.19	−25.08	−12.50	−42.83	−10.97

Mean errors: $\Delta G^{(s)}_{min} = \pm 0.04$, $\Delta G^\circ_m = \pm 0.05$, $\Delta G^\circ_{m,tail} = \pm 0.04$, $\Delta G^\circ_{ads} = \pm 0.04$, $\Delta G^\circ_{trans} = \pm 0.04$.

The free energy of the given air/water interface $\Delta G^{(s)}_{min}$ [52] was found using Equation (7):

$$\Delta G^{(s)}_{min} = A_{min} \cdot \gamma_{CMC} \cdot N_A \quad (7)$$

$\Delta G^{(s)}_{\min}$ indicates the free energy change of the solution components from the bulk phase to the surface phase of the solution. Lower $\Delta G^{(s)}_{\min}$ values were reported to indicate [34] a more thermodynamically stable micellar surface. All thermodynamic parameters are given in Table 3. The Gibbs free energy of the micellization per alkyl tail may be expressed as (see Equation (8)) [53]:

$$\Delta G^{\circ}_{m, \text{tail}} = \frac{\Delta G^{\circ}_m}{2} \quad (8)$$

The gemini surfactant tail transfers Gibbs free energy from the solvent mixture to the hydrophobic core of the micelle. The tail of the gemini surfactant detached due to the solvophobic effects. The effect of the IL 4-PyC8 on the micellization process was also evaluated through the Gibbs energy of transfer ($\Delta G^{\circ}_{\text{trans}}$), given by Equation (9) [52]:

$$\Delta G^{\circ}_{\text{trans}} = \Delta G^{\circ}_m (\text{solvent mixed media}) - \Delta G^{\circ}_m (\text{pure water}) \quad (9)$$

As compared with the pure solvent, the addition of the IL 4-PyC8 made the thermodynamics more favorable for the gemini surfactant molecule and the hydrophobic tail part to move from the bulky phase into the micellar phase. As a result, $\Delta G^{\circ}_{\text{trans}}$ decreased with the decrease in the CMC values of the gemini surfactants.

3.4. Fluorescence Measurements

We used 1-pyrene carboxyaldehyde (PyCHO) as a fluorescence probe to obtain the CMC of the gemini surfactants in the presence and absence of the IL 4-PyC8. The fluorescence emission spectra exhibited a characteristic band near 450 nm. PyCHO fluorescence has been used to measure various important micellar parameters [54–56]. Fluorescence spectra were obtained from solutions of varying gemini surfactants in the presence of different mass fractions of the IL 4-PyC8. The CMC was determined by plotting the intensity against the gemini surfactant concentration (Figure 3). It is noteworthy to mention that the CMC of the gemini surfactants decreased with the increasing mass fraction of the IL 4-PyC8 (see Table 1). The CMC values determined using this method were slightly larger than those determined via the conductance and surface tension (see Table 1), which may have been due to the presence of the PyCHO in the micro-organized system [45,46].

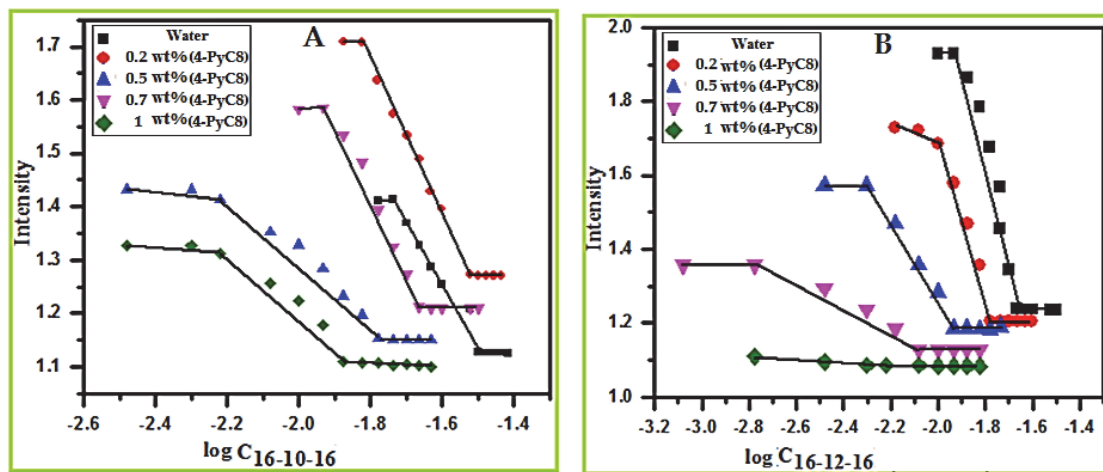


Figure 3. Intensity of the fluorescence vs. the logarithm of the concentration of the gemini surfactants 16-10-16 (A) and 16-12-16 (B) in water and in the presence of the IL 4-PyC8 at 300 K. The excitation wavelength was 334 nm and both excitation and emission slit widths were kept at 2 nm.

3.5. Aggregation Numbers

The aggregation behavior of the gemini surfactants and their interaction with the IL 4-PyC8 have also been studied via static fluorescence quenching measurements, which is a fundamental parameter of micellar properties, by using the following Equation (10):

$$\ln \left[\frac{I_0}{I_Q} \right] = \left[\frac{N_{\text{agg}}[Q]}{[\text{Surfactant}]_T - \text{CMC}} \right] \quad (10)$$

where $[Q]$ is the concentration of quencher (CPC), I_0 is the fluorescence intensities of pyrene with and without the quencher and $[\text{Surfactant}]_T$ is the total surfactant concentration. The plots of $\ln(I_0/I_Q)$ versus $[Q]$ for gemini surfactants 16-10-16 and 16-12-16 for different mass fractions of IL 4-PyC8 are shown in Figure 4. The aggregation numbers (N_{agg} 's) of the pure gemini surfactants and the mixed systems were determined from the slope of the plots of $\ln \left[\frac{I_0}{I_Q} \right]$ versus the quencher concentration. The aggregation number of the gemini surfactants decreased with increasing mass fraction of the IL 4-PyC8, which led to electrostatic repulsion and a hydrophobic effect between the head group of a surfactant and the charged ions (cations and anions) of the IL 4-PyC8 [57]. These factors held the micellization environment of the gemini surfactants in the presence of the IL 4-PyC8 [58]. We may suggest that between the two gemini surfactants, 16-12-16 was slightly more hydrophobic than 16-10-16, which resulted in the IL 4-PyC8 being able to transfer more successfully into the micelles of the gemini surfactant 16-10-16 [34].

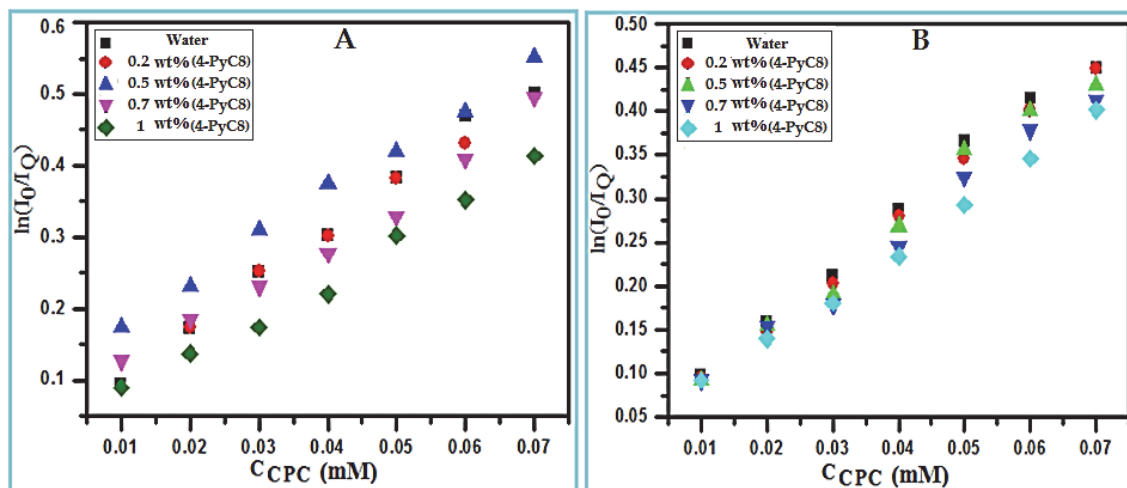


Figure 4. Plots of $\ln(I_0/I_Q)$ vs. concentration of CPC (0.12 mM) in different mass fractions of the IL 4-PyC8 at 300 K: (A) 16-10-16 and (B) 16-12-16. $[16-s-16] = 1 \text{ mM}$.

The nature of the hydrophobicity of the gemini surfactants could be calculated using the Stern–Volmer quenching constant (K_{SV}) (Equation (11)). The K_{SV} values are given in Table 4.

$$\ln \left[\frac{I_0}{I_Q} \right] = 1 + K_{\text{sv}}[Q] \quad (11)$$

Table 4. Critical micelle concentration (CMC), aggregation number (N_{agg}) and Stern–Volmer constants (K_{SV}) of the two gemini surfactants 16-10-16 and 16-12-16 in water and in the presence of 0.2, 0.5, 0.7 and 1.0 wt% of the IL 4-PyC8 at 300 K.

IL 4-PyC8 (wt%)	CMC ^a (mM)	N_{agg}	K_{SV}
16-10-16			
Water	0.030 ^b	57	6.99
0.2	0.025	53	6.50
0.5	0.021	51	6.17
0.7	0.017	49	5.88
1.0	0.013	45	5.45
16-12-16			
Water	0.023 ^b	51	6.25
0.2	0.016	50	6.12
0.5	0.011	48	5.85
0.7	0.009	46	5.55
1.0	0.006	43	5.18

^a Fluorometry method, ^b Refs. [59,60].

The Stern–Volmer quenching constant (K_{SV}) can be assessed using the plots of $\ln(I_0/I_Q)$ versus $[Q]$. A difference in the K_{SV} values was observed, which can be explained using the base hydrophobicity of the micellar environment [55]. The higher the solubility of the probe and a quencher, the higher the K_{SV} value. The aggregation numbers and K_{SV} values are collected in Table 4.

The CMC values obtained using fluorometric techniques and collected in Table 4 were consistent with those obtained from the tensiometry and conductivity data (see Table 1).

3.6. FTIR Spectroscopy

The interaction between the oxime-functionalized IL 4-PyC8 and the gemini surfactants was studied using FTIR spectroscopy. The FTIR spectra of pure 16-s-16 and the IL 4-PyC8 are shown in Figures 5 and 6. In both spectra of 16-10-16 and 16-12-16, as well as for the IL 4-PyC8, there was no sharp peak at $\sim 3450\text{--}3700\text{ cm}^{-1}$, which shows that no water was present in the sample. The FTIR spectrum of 16-10-16 (Figure 5) showed a strong peak at the wavenumber 1467.97 cm^{-1} , which was due to C–N stretching. The different stretching bands observed were the symmetric and asymmetric stretching of the CH_2 vibration of alkyl chains at 2917.27 cm^{-1} and 2850.08 cm^{-1} , the symmetric and asymmetric stretching of the C–H scissoring vibration of the $\text{CH}_3\text{--N}^+$ moiety at 1467.97 cm^{-1} , the C–N⁺ stretching bands' rocking mode of the methylene chain at 889.09 cm^{-1} and the rocking mode of the methylene chain at 721.45 cm^{-1} . After the addition of the IL 4-PyC8, the stretching frequencies were changed to 2917.72 cm^{-1} , 2849.32 cm^{-1} , 1466.07 cm^{-1} , 889.75 cm^{-1} and 720.80 cm^{-1} , respectively. More importantly, the C=O stretching frequency for the IL 4-PyC8 at 1666 cm^{-1} was shifted to 1676 cm^{-1} after mixing with the gemini surfactant 16-10-16.

In the FTIR spectrum of the 16-12-16 gemini surfactant (shown in Figure 6), different frequencies were observed, see Table 5: symmetric and asymmetric stretching of the CH_2 vibration of alkyl chains at 2917.32 cm^{-1} and 2848.35 cm^{-1} , symmetric and asymmetric stretching of the C–H scissoring vibration of the $\text{CH}_3\text{--N}^+$ moiety at 1468.53 cm^{-1} , the C–N⁺ stretching bands' rocking mode of the methylene chain at 889.07 cm^{-1} and the rocking mode of the methylene chain at 721.96 cm^{-1} . For the mixture of the IL 4-PyC8 and gemini surfactants during the process of micellization, the stretching frequency values were changed to 2921.55 cm^{-1} , 2852.26 cm^{-1} , 1464.31 cm^{-1} , 889.60 cm^{-1} and 720.98 cm^{-1} , respectively. The shift of the wavenumber in the mixture of the gemini surfactant 16-12-16 and the IL 4-PyC8 represented some changes that occurred within the system. These variations in these peaks may have been due to +N-(CH₃) or NH₂ stretching. The observed difference in the wavenumber indicated that the additive IL 4-PyC8 interacted with the

gemini surfactants and it may have been due to some of the structural changes that occurred within the IL 4-PyC8:gemini surfactant mixed system. It is noteworthy that the C=O stretching frequency for 4-PyC8 at 1666 cm⁻¹ was shifted to 1681 cm⁻¹ after mixing with the gemini surfactant 16-12-16, indicating an IL:gemini surfactant mixed system. The changes in the IR spectra could be considered as non-specific interactions (ion–ion dipole and induced dipole interactions) between the gemini surfactants and IL that took part in the complexation, similar to what is reported in the literature [56] and in accordance with the ¹H NMR data discussed above.

Table 5. Infrared transmittance band and different modes of vibration of the gemini surfactants, 4-PyC8, and their mixtures.

Assignment	Band Position (cm ⁻¹)			
	16-10-16	16-10-16 + IL 4-PyC8	16-12-16	16-12-16 + IL 4-PyC8
Symmetric and asymmetric stretching of the C-H stretching vibration of the alkyl chains	2917.27, 2850.08	2917.72, 2849.32	2917.32, 2848.35	2921.55, 2852.26
Symmetric and asymmetric stretching of the C-H scissoring vibration of the CH ₃ -N ⁺ moiety	1467.97	1466.07	1468.53	1464.31
C-N ⁺ stretching bands' rocking mode of the methylene chain	889.09	889.75	889.07	889.60
Rocking mode of the methylene chain	721.45	720.80	721.96	720.98

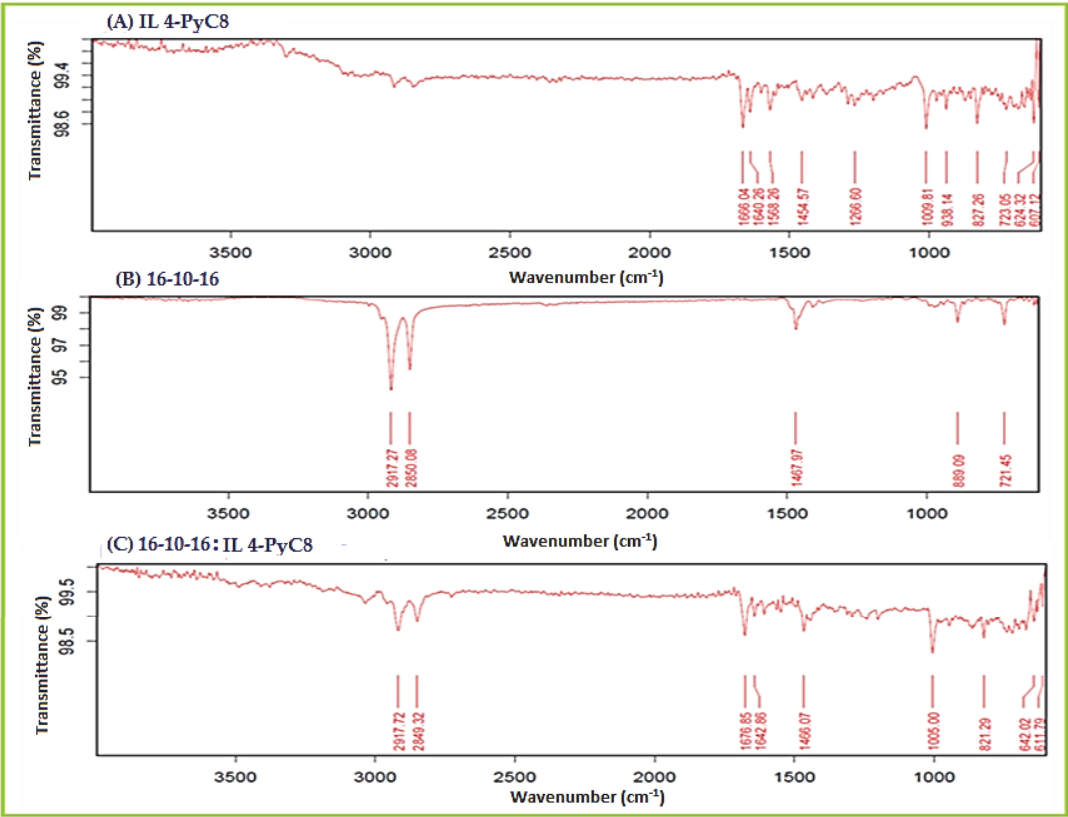


Figure 5. FTIR spectra of the (A) IL 4-PyC8, (B) 16-10-16 and (C) 16-10-16:IL 4-PyC8.

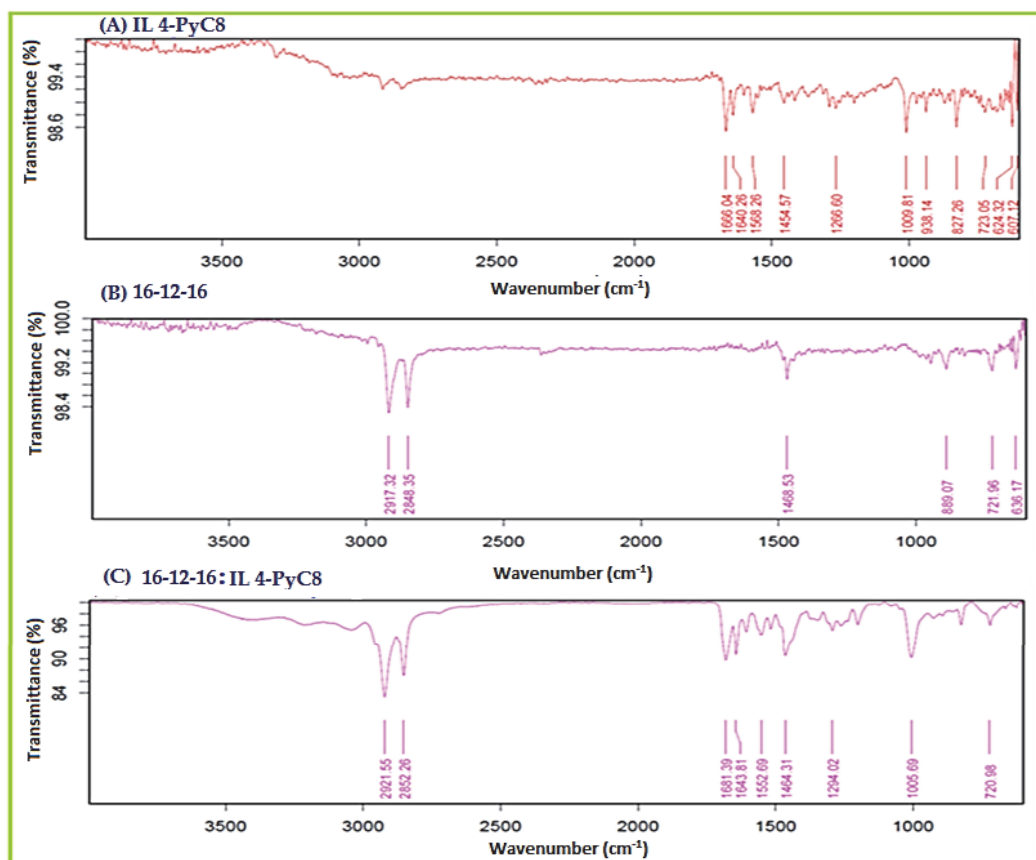


Figure 6. FTIR spectra of the (A) IL 4-PyC8, (B) 16-12-16 and (C) 16-12-16:IL 4-PyC8.

3.7. ^1H NMR Study

^1H NMR techniques are well-known to give information about the aggregate microenvironment and this can be used to probe the surfactant self-assembly of different structures [61]. Although NMR spectroscopy is a very useful technique, it can hardly be expected to recognize the changes in the chemical shifts of the side-chain protons. The hydrophobic tails form the micellar “core”, whereas the detectable changes in the chemical shifts occur mainly in the region close to the interface water/aggregate (e.g., micelle, vesicle). Aromatic protons can be very sensitive to the changes in the microenvironment of the surfactant aggregate [62]. Deprotonation of the oxime moiety due to changes in the micellar micropolarity or tight ion pair formation may also be detected using the changes in chemical shifts of the adjacent groups [61]. The ^1H NMR spectra of the gemini surfactants with the IL 4-PyC8 in D_2O are presented in Figure 7 (for 16-10-16) and Figure 8 (for 16-12-16). We note that no specific interaction confirmed by the changes in the chemical shifts could be reported based on these data; the surfactant aggregates were supposed to form under these concentration conditions, as gemini surfactants aggregates $([\text{D}]_0 \gg \text{CMC})$ with IL molecules were solubilized by the micelles.

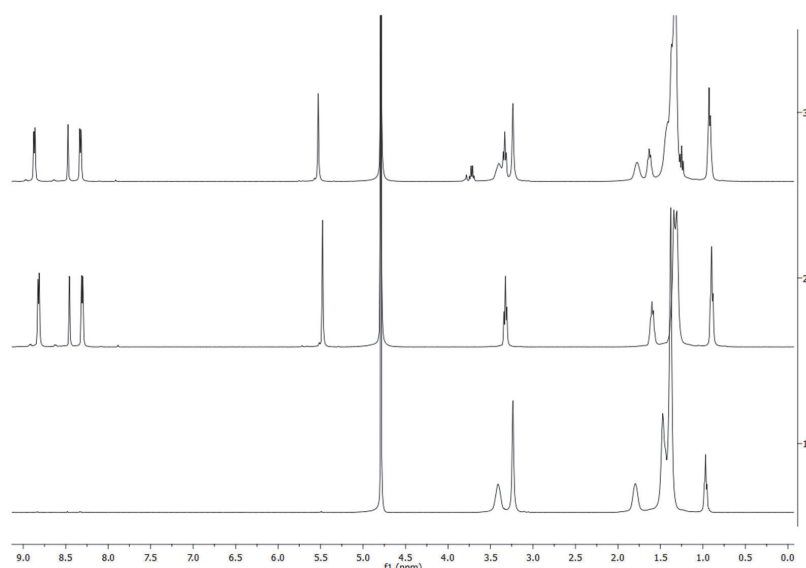


Figure 7. ^1H NMR spectra of the (1) 16-10-16, (2) IL 4-PyC8 and (3) 16-10-16:4-PyC8 in D_2O .

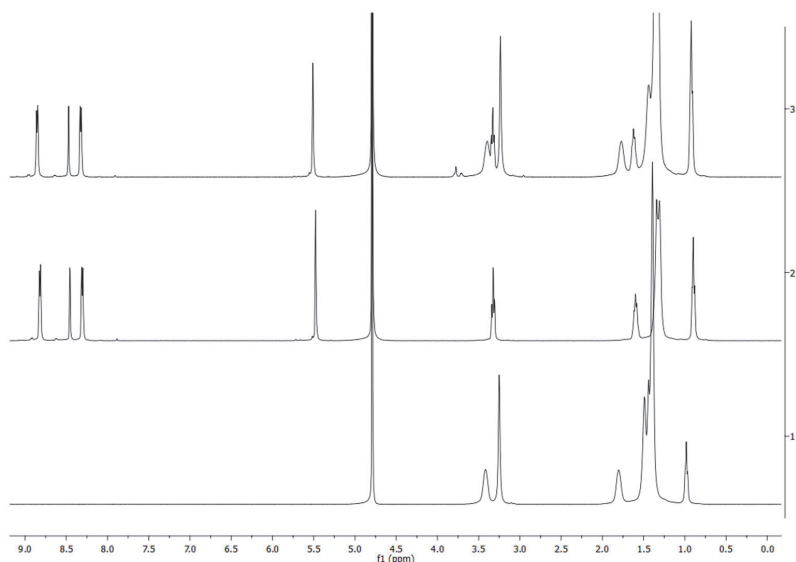


Figure 8. ^1H NMR spectra of the (1) 16-12-16, (2) IL 4-PyC8 and (3) 16-12-16:4-PyC8 in D_2O .

4. Dynamic Light Scattering and Zeta Potential Study of Mixed Gemini:IL System with PMZ

Taking into account the interactions between the oxime-derived IL and another phenothiazine drug called promazine that was reported recently [42], an evaluation of the structural changes of the aggregates of oxime IL/gemini surfactants with the addition of promethazine was carried out. Dynamic light scattering (DLS) studies were performed to shed light on the sizes of the self-assembly aggregates of the various concentrations of the IL 4-PyC8 that were added to the gemini surfactant solution in the presence of the drug PMZ. The aggregate size may be dependent on the solubilize structure, as well as the nature and concentration of the surfactant, and using a low gemini concentration close to the CMC is not suitable since aggregates of different sizes and hardly defined

structures may form [63]. The concentration of the gemini surfactant 16-10-16 was taken significantly above the CMC value (1 mM). The DLS results provided us with information on the size of the gemini surfactant aggregates in the presence and absence of the drug and the IL 4-PyC8. It was observed that the hydrodynamic diameter of 1 mM aqueous gemini surfactant (ca. $35 \times$ CMC in the case of 16-10-16) solution without any other additives was observed to be about 124 nm (see Figure 9a), which was much larger than that of a regular spherical or ellipsoidal micelle [64]. Indeed, gemini surfactants are known to undergo a fast sphere-to-rod transition above the CMC [65], form unexpectedly large aggregates in the presence of polyaromatics [63,66,67] and to assemble into wormlike micelles [67], as well as other complex aggregates [68], at concentrations substantially above the CMC. As it was shown by Pisarcik et al. [69], the extension of the spacer length in the diamide gemini surfactant molecule to $s > 6$ results in a sharp increase in the N_{agg} with a concentration above the value of $2 \times$ CMC. Furthermore, surfactants with the spacer length of $n = 8$ were reported to form aggregates of >100 nm at the concentration of $6 \times$ CMC. Since the aggregation numbers were not large enough to expect vesicle formation, Pisarcik et al. [69] suggested the hydrodynamic size reflected the intermicellar aggregates. We supposed the 16-10-16 surfactants reported in the present work may demonstrate similar behavior at the studied concentration. An addition of PMZ (0.01 mM) to the gemini micellar solution resulted in a significant increase in the aggregate size from 124 nm to 270 nm. It is noteworthy to mention that the addition of 1 wt% of the oxime-functionalized IL 4-PyC8 to the above gemini micellar solutions with the drug added resulted in a drastic structural transition from such larger aggregates of 270 nm to small-sized micelles with sizes of 1 to 2 nm (see Figure 9f). The size distribution at 1–2 nm might correspond to the micelles but is smaller than the real size of the micelles in this technique, which may be ascribed to the high charge density of the gemini surfactant micelles that affects the DLS measurement [70]. Initially, the addition of the drug produced a significant increase in the micellar size due to the partition of the drug within the (inter)micellar aggregate interior region, but the addition of the IL 4-PyC8 to this system caused drastic changes in the micellar size of the gemini:IL:PMZ system. These changes in the self-assembly structural transition may indicate stronger IL:PMZ, gemini:IL and gemini:PMZ interactions.

The values of the zeta potential measurement (ξ , (mV)) in these systems depend on the difference in potential between the dispersion medium and on the stationary liquid layer that is attached to the dispersed aggregates [71]. Initially, the value of ξ insignificantly increased with the addition of drug (24.8 mV) to the gemini micellar solution (22.6 mV), reflecting the positive charges on the overall surface of the carrier. Upon the addition of IL4-PyC8 to the gemini:PMZ system, the value of ξ slightly decreased (Table 6). This may have reflected the strong electrostatic interactions that took place between the oppositely charged ions present within the micellar system [72]. As a result, a different self-assembly shape appeared, which caused the lowering of the values of ξ [63,73]. Further, adding higher concentrations of the IL 4-PyC8 (1.0 wt%) into the mixture of the gemini:PMZ solution resulted in an increase in the surface charge density. The overall strong interactions (16-s-16:IL:PMZ) led to the significant structural changes of gemini aggregates in the presence of 1 wt% of the oxime-functionalized IL 4-PyC8 to the gemini surfactant solutions with the drug added. There was a correlation between the surface potential and the aggregates' sizes and morphologies, as the aggregates were formed with varying morphologies [74] in the presence of the drug and the IL 4-PyC8.

Table 6. Micellar size d (nm) as a size distribution by number and zeta potential in the presence of various concentrations of the IL 4-PyC8 in the drug PMZ and the gemini micellar solution.

System Composition	Aggregate Characteristics	
	d (nm)	Zeta Potential, ξ (mV)
16-10-16 (1 mM)	124 (105–164)	22.6
16-10-16 + PMZ (0.01 mM)	270 (220–395)	24.8
16-10-16 + PMZ + 0.1 wt% IL4-PyC8	210 (165–255), 825 (615–1105)	24.1
16-10-16 + PMZ + 0.5 wt% IL4-PyC8	182 (142–220)	20.6
16-10-16 + PMZ + 1.0 wt% IL4-PyC8	1.4 (1.1–1.8)	23.7

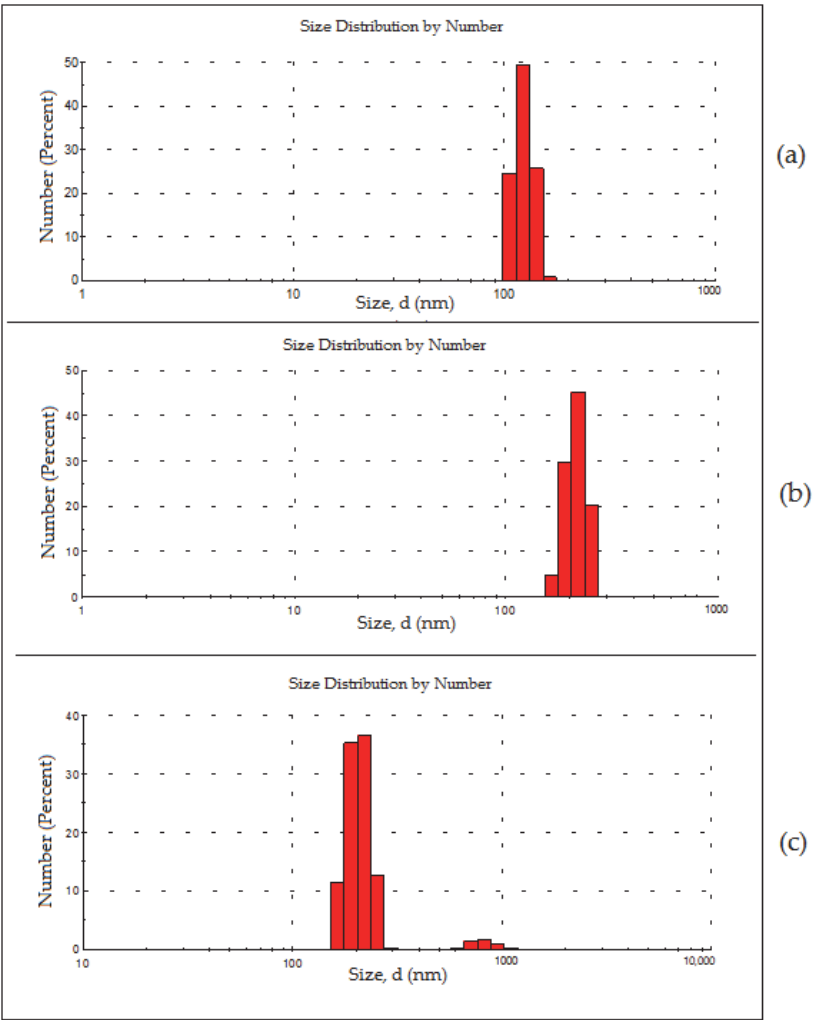


Figure 9. Cont.

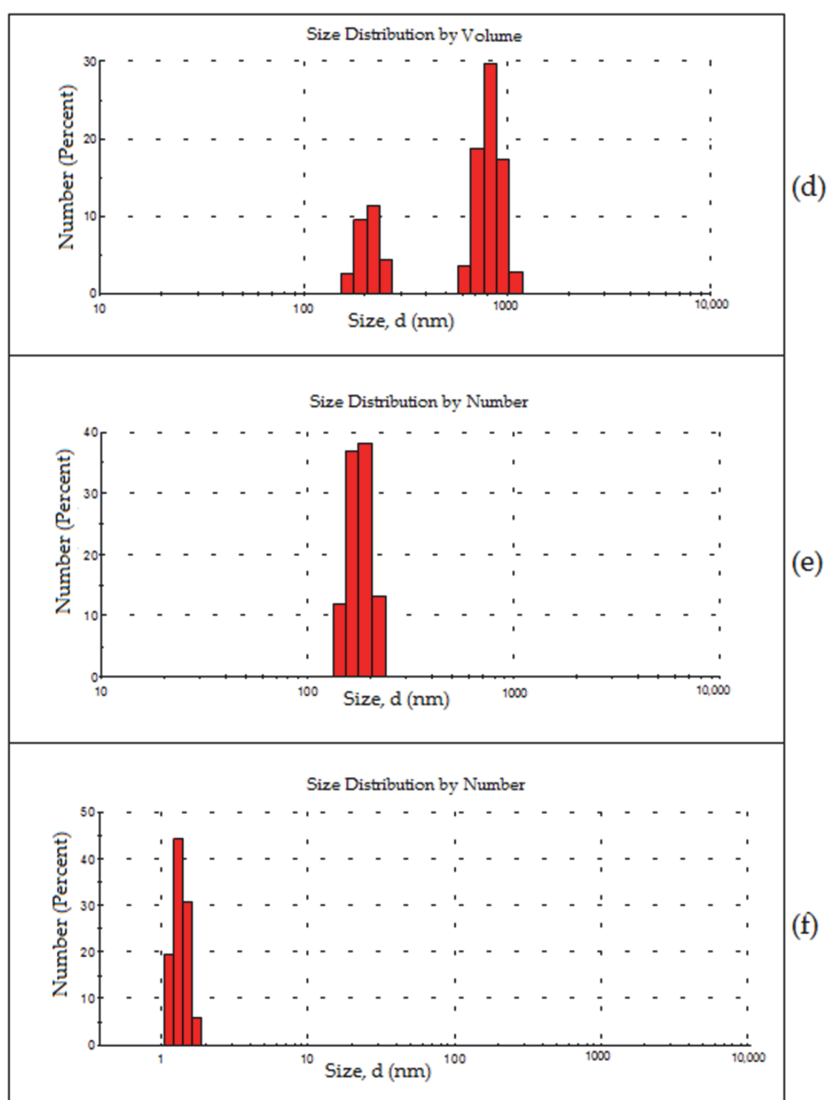


Figure 9. Aggregates size distribution obtained from DLS for various concentrations of the IL 4-PyC8 in drug PMZ and gemini surfactant 16-10-16: (a) 16-10-16 (without additives), (b) 16-10-16:PMZ, (c,d) 16-10-16:PMZ:0.1 wt% IL 4-PyC8, (e) 16-10-16:PMZ:0.5 wt% IL 4-PyC8 and (f) 16-10-16:PMZ:1.0 wt% IL 4-PyC8.

5. Conclusions

The design and application of sustainable surfactants in the remediation of contaminated areas were considered regarding promethazine, a chiral pharmaceutical pollutant. The micellization behavior and physicochemical properties of the gemini surfactants 16-10-16 and 16-12-16 in the presence of the functionalized IL 4-PyC8 were investigated using surface tension, conductivity, fluorescence, FTIR, ^1H NMR and DLS techniques. The surface tension and conductivity results revealed a decrease in the CMC of both the gemini surfactants in the presence of the IL 4-PyC8, thus favoring the micelle formation process. The negative values of ΔG_m^0 and ΔG_{ads}^0 indicated that the micellization process

was spontaneous. The aggregation number (N_{agg}) and Stern–Volmer constant (K_{SV}) of the gemini surfactants decreased with the increasing mass fraction of the IL 4-PyC8. The cmc and N_{agg} results may be ascribed to the presence of counterions near the polar heads of the gemini surfactant molecules that tended to decrease the electrostatic repulsion forces between the gemini surfactant head groups, leading to the compact aggregation of surfactant monomers. The aggregate sizes obtained from the DLS measurements demonstrated that the addition of 1 wt% of the oxime-functionalized IL 4-PyC8 to the gemini surfactant solutions in the presence of promethazine may have resulted in a structural transition from very large aggregates (270 nm) to small compact micelles following strong gemini:IL:PMZ interactions. The structural transitions in the presence of promethazine reported in the present work may be used for designing systems responsive to changes in the size and shape of the aggregates as an analytical signal for the selective binding of biologically important molecules and potential chiral pollutants.

Author Contributions: Conceptualization and idea of the research, Y.K.; K.K.G. and V.B.; synthesis of compounds, methodology, I.V.K.; experimental techniques, data curation analysis of the results, conceptualization, methodology, S.J.P., M.K.B. and K.B.; analysis and interpretation, M.K.B., I.V.K.; formal analysis and interpretation, K.B.; writing—original draft preparation, S.J.P.; writing—review and editing, I.V.K., Y.K., V.B.; funding acquisition, Y.K., K.K.G. and V.B. All authors have read and agreed to the published version of the manuscript.

Funding: This work was supported by a DST-FIST grant (no. SR/FST/CSI-259/2014(C)) and UGC-SAP-DRS-II (for K.K.G. and S.J.P.), European Union’s H2020-FETOPEN grant 828779 (INITIO) (for V.B.), NATO SPS MYP no. G5565 (DEFIR) (for Y.K.), Estonian Research Council grants ETAG20049 (COVSG5) (for Y.K.) and PRG399 (for V.B.).

Institutional Review Board Statement: Not applicable.

Informed Consent Statement: Not applicable.

Data Availability Statement: All the data gathered for this study are available in the article.

Acknowledgments: The authors are grateful to the National Center for Natural Resources (NCNR), Pt. Ravishankar Shukla University, Raipur (C.G.), for providing the FTIR and NMR facilities.

Conflicts of Interest: The authors declare no conflict of interest.

References

- Hembury, G.A.; Borovkov, V.V.; Inoue, Y. Chirality sensing supramolecular systems. *Chem. Rev.* **2008**, *108*, 1–73. [\[CrossRef\]](#) [\[PubMed\]](#)
- Konrad, N.; Horetski, M.; Sihtmae, M.; Truong, K.-N.; Osadchuk, I.; Burankova, T.; Kielmann, M.; Adamson, J.; Kahru, A.; Rissanen, K.; et al. Thiourea organocatalysts as emerging chiral pollutants: En route to porphyrin-based (chir)optical sensing. *Chemosensors* **2021**, *9*, 278. [\[CrossRef\]](#)
- Shtykov, S. (Ed.) *Nanoanalytics: Nanoobjects and Nanotechnologies in Analytical Chemistry*; Walter de Gruyter GmbH: Berlin, Germany, 2018; p. 463.
- Patel, M.; Kumar, R.; Kishor, K.; Mlsna, T.; Pittman, C.U., Jr.; Mohan, D. Pharmaceuticals of Emerging Concern in Aquatic Systems: Chemistry, Occurrence, Effects, and Removal Methods. *Chem. Rev.* **2019**, *119*, 3510–3673. [\[CrossRef\]](#) [\[PubMed\]](#)
- Zakharova, L.Y.; Serdyuk, A.A.; Mirgorodskaya, A.B.; Kapitanov, I.V.; Gainanova, G.A.; Karpichev, Y.; Gavrilova, E.L.; Sinyashin, O.G. Amino acid-functionalized calix [4]resorcinarene solubilization by mono- and dicationic surfactants. *J. Surfactants Deterg.* **2016**, *19*, 493–499. [\[CrossRef\]](#)
- Rasheed, T.; Shafi, S.; Bilal, M.; Hussain, T.; Sherd, F.; Rizwan, K. Surfactants-based remediation as an effective approach for removal of environmental pollutants—A review. *J. Mol. Liq.* **2020**, *318*, 113960. [\[CrossRef\]](#)
- Anastas, P.; Eghbali, N. Green Chemistry: Principles and Practice. *Chem. Soc. Rev.* **2010**, *39*, 301–312. [\[CrossRef\]](#)
- Ranke, J.; Stolte, S.; Stormann, R.; Arning, J.; Jastorff, B. Design of sustainable chemical products—The example of ionic liquids. *Chem. Rev.* **2007**, *107*, 2183–2206. [\[CrossRef\]](#)
- Clarke, C.J.; Tu, W.-C.; Levers, O.; Bröhl, A.; Hallett, J.P. Green and Sustainable Solvents in Chemical Processes. *Chem. Rev.* **2018**, *118*, 747–800. [\[CrossRef\]](#)
- Sheldon, R.A. Green solvents for sustainable organic synthesis: State of the art. *Green Chem.* **2005**, *7*, 267–278. [\[CrossRef\]](#)
- MacFarlane, D.R.; Chong, A.L.; Forsyth, M.; Kar, M.; Vijayaraghavan, R.; Somers, A.; Pringle, J.M. New dimensions in salt-solvent mixtures: A 4th evolution of ionic liquids. *Faraday Discuss.* **2018**, *206*, 9–28. [\[CrossRef\]](#)

12. Egorova, K.S.; Gordeev, E.G.; Ananikov, V.P. Biological Activity of Ionic Liquids and Their Application in Pharmaceuticals and Medicine. *Chem. Rev.* **2017**, *117*, 7132–7189. [\[CrossRef\]](#) [\[PubMed\]](#)
13. Aldous, L.; Khan, A.; Hossain, M.M.; Zhao, C.; C Hardacre, V.P. *Catalysis in Ionic Liquids: From Catalyst Synthesis to Application*; Royal Society of Chemistry: London, UK, 2014; Volume 15, pp. 1–620.
14. Bica, K.; Gartner, P.; Gritsch, P.J.; Ressmann, A.K.; Schroder, C.; Zirbs, R. Micellar catalysis in aqueous-ionic liquid systems. *Chem. Commun.* **2012**, *48*, 5013–5015. [\[CrossRef\]](#) [\[PubMed\]](#)
15. Steinruck, H.P.; Wasserscheid, P. Ionic Liquids in Catalysis. *Catal. Lett.* **2015**, *145*, 380–397. [\[CrossRef\]](#)
16. Han, X.; Armstrong, D.W. Ionic liquids in separations. *Acc. Chem. Res.* **2007**, *40*, 1079–1086. [\[CrossRef\]](#) [\[PubMed\]](#)
17. Smiglak, M.; Metlen, A.; Rogers, R.D. The second evolution of ionic liquids: From solvents and separations to advanced materials—energetic examples from the ionic liquid cookbook. *Acc. Chem. Res.* **2007**, *40*, 1182–1192. [\[CrossRef\]](#)
18. Torimoto, T.; Tsuda, T.; Okazaki, K.; Kuwabata, S. New Frontiers in Materials Science Opened by Ionic Liquids. *Adv. Mater.* **2010**, *22*, 1196–1221. [\[CrossRef\]](#)
19. Jordan, A.; Haib, A.; Spulak, M.; Karpichev, Y.; Kummerer, K.; Gathergood, N. Synthesis of a Series of Amino Acid Derived Ionic Liquids and Tertiary Amines: Green chemistry metrics including microbial toxicity and preliminary biodegradation data analysis. *Green Chem.* **2016**, *18*, 4374–4392. [\[CrossRef\]](#)
20. Garcia, M.T.; Ribosa, I.; Perez, L.; Manresa, A.; Comelles, F. Aggregation Behavior and Antimicrobial Activity of Ester-Functionalized Imidazolium- and Pyridinium-Based Ionic Liquids in Aqueous Solution. *Langmuir* **2013**, *29*, 2536–2545. [\[CrossRef\]](#)
21. Teresa Garcia, M.; Ribosa, I.; Perez, L.; Manresa, A.; Comelles, F. Self-assembly and antimicrobial activity of long-chain amide-functionalized ionic liquids in aqueous solution. *Colloids Surf. B Biointerfaces* **2014**, *123*, 318–325. [\[CrossRef\]](#)
22. Haiss, A.; Jordan, A.; Westphal, J.; Logunova, E.; Gathergood, N.; Kummerer, K. On the way to greener ionic liquids: Identification of a fully mineralizable phenylalanine-based ionic liquid. *Green Chem.* **2016**, *18*, 4361–4373. [\[CrossRef\]](#)
23. Kusumahastuti, D.K.A.; Sihtmae, M.; Kapitanov, I.V.; Karpichev, Y.; Gathergood, N.; Kahru, A. Toxicity profiling of 24 L-phenylalanine derived ionic liquids based on pyridinium, imidazolium and cholinium cations and varying alkyl chains using rapid screening Vibrio fischeri bioassay. *Ecotoxicol. Environ. Saf.* **2019**, *172*, 556–565. [\[CrossRef\]](#) [\[PubMed\]](#)
24. Kapitanov, I.; Jordan, A.; Karpichev, Y.; Spulak, M.; Perez, L.; Kellett, A.; Kummerer, K.; Gathergood, N. Synthesis, self-assembly, antimicrobial activity, and preliminary biodegradation studies of a series of L-phenylalanine-derived surface active ionic liquids. *Green Chem.* **2019**, *21*, 1777–1794. [\[CrossRef\]](#)
25. Suk, M.; Haib, A.; Westphal, J.; Jordan, A.; Kellett, A.; Kapitanov, I.; Karpichev, Y.; Gathergood, N.; Kummerer, K. Design rules for environmental biodegradability of phenylalanine alkyl ester linked ionic liquids for green chemistry. *Green Chem.* **2020**, *22*, 4498–4508. [\[CrossRef\]](#)
26. Pandya, S.J.; Kapitanov, I.V.; Usmani, Z.; Sahu, R.; Sinha, D.; Gathergood, N.; Ghosh, K.K.; Karpichev, Y. An example of green surfactant systems based on inherently biodegradable IL-derived amphiphilic oximes. *J. Mol. Liq.* **2020**, *305*, 112857. [\[CrossRef\]](#)
27. Pal, B.K.; Moulik, S.P. *Ionic Liquid-Based Surfactant Science: Formulation, Characterization, and Applications*; John Wiley & Sons Inc.: Hoboken, NJ, USA, 2015; p. 576.
28. Chen, L.G.; Strassburg, S.H.; Bermudez, H. Micelle co-assembly in surfactant/ionic liquid mixtures. *J. Colloid Interface Sci.* **2016**, *477*, 40–45. [\[CrossRef\]](#)
29. Kumar, A.; Banjare, M.K.; Sinha, S.; Yadav, T.; Sahu, R.; Satnami, M.L.; Ghosh, K.K. Imidazolium-Based Ionic Liquid as Modulator of Physicochemical Properties of Cationic, Anionic, Nonionic, and Gemini Surfactants. *J. Surfactants Deterg.* **2018**, *21*, 355–366. [\[CrossRef\]](#)
30. Shang, Y.Z.; Wang, T.F.; Han, X.; Peng, C.J.; Liu, H.L. Effect of Ionic Liquids C(n)mimBr on Properties of Gemini Surfactant 12-3-12 Aqueous Solution. *Ind. Eng. Chem. Res.* **2010**, *49*, 8852–8857. [\[CrossRef\]](#)
31. El Seoud, O.; Keppeler, N.; Malek, N.I.; Galdano, P.D. Ionic Liquid-Based Surfactants: Recent Advances in Their Syntheses, Solution Properties, and Applications. *Polymers* **2021**, *13*, 1100. [\[CrossRef\]](#)
32. Menger, F.M.; Keiper, J.S. Gemini surfactants. *Angew. Chem. Int. Ed.* **2000**, *39*, 1907–1920. [\[CrossRef\]](#)
33. Zana, R. Dimeric and oligomeric surfactants. Behavior at interfaces and in aqueous solution: A review. *Adv. Colloid Interface Sci.* **2002**, *97*, 205–253. [\[CrossRef\]](#)
34. Zana, R. Gemini (dimeric) surfactants. *Curr. Opin. Colloid Interface Sci.* **1996**, *1*, 566–571. [\[CrossRef\]](#)
35. Akram, M.; Anwar, S. Biophysical investigation of promethazine hydrochloride binding with micelles of biocompatible gemini surfactants: Combination of spectroscopic and electrochemical analysis. *Spectrochim. Acta Part A Mol. Biomol. Spectrosc.* **2019**, *215*, 249–259. [\[CrossRef\]](#) [\[PubMed\]](#)
36. Ferraz, R.; Branco, L.C.; Prudencio, C.; Noronha, J.P.; Petrovski, Z. Ionic Liquids as Active Pharmaceutical Ingredients. *ChemMedChem* **2011**, *6*, 975–985. [\[CrossRef\]](#) [\[PubMed\]](#)
37. Ozan, M.; Gokturk, S. Effect of ionic liquids as active pharmaceutical ingredients on the micellar binding of an amphiphilic drug trifluopromazine hydrochloride. *J. Dispers. Sci. Technol.* **2019**, *14*, 214–222. [\[CrossRef\]](#)
38. Mahajan, S.; Sharma, R.; Mahajan, R.K. An investigation of drug binding ability of a surface active ionic liquid: Micellization, electrochemical, and spectroscopic studies. *Langmuir* **2012**, *28*, 17238–17246. [\[CrossRef\]](#)
39. Mahajan, S.; Sharma, R.; Mahajan, R.K. Interactions of new 1,8-diazabicyclo[5.4.0]undec-7-ene (DBU) based surface active ionic liquids with amitriptyline hydrochloride: Micellization and interfacial studies. *Colloids Surf. A Physicochem. Eng. Asp.* **2013**, *424*, 96–104. [\[CrossRef\]](#)

40. Banjare, M.K.; Behera, K.; Banjare, R.K.; Pandey, S.; Ghosh, K.K.; Karpichev, Y. Molecular interactions between novel synthesized biodegradable ionic liquids with antidepressant drug. *Chem. Thermodyn. Therm. Anal.* **2021**, *3*, 100012. [\[CrossRef\]](#)
41. Pal, M.; Rai, R.; Yadav, A.; Khanna, R.; Baker, G.A.; Pandey, S. Self-aggregation of sodium dodecyl sulfate within (choline chlo-ride+urea) deep eutectic solvent. *Langmuir* **2014**, *30*, 13191–13198. [\[CrossRef\]](#)
42. Sun, T.; Gao, S.; Chen, Q.; Shen, X. Investigation on the interactions between hydrophobic anions of ionic liquids and Triton X-114 micelles in aqueous solutions. *Colloids Surf. A Physicochem. Eng. Asp.* **2014**, *456*, 18–25. [\[CrossRef\]](#)
43. Abdul Rub, M. Aggregation and interfacial phenomenon of amphiphilic drug under the influence of pharmaceutical excipients (green/biocompatible gemini surfactant). *PLoS ONE* **2019**, *14*, e0211077. [\[CrossRef\]](#)
44. Khan, I.A.; Mohammad, R.; Alam, M.S.; Kabir-ud-Din. Effect of alkylamine chain length on the critical micelle concentration of cationic Gemini butanediyl-a,x-bis(dimethylcetylammmonium bromide) surfactant. *J. Dispers. Sci. Technol.* **2009**, *30*, 1486–1493. [\[CrossRef\]](#)
45. Markiewicz, R.; Klimaszcz, A.; Jarek, M.; Taube, M.; Florczak, P.; Kempka, M.; Fojud, Z.; Jurga, S. Influence of Alkyl Chain Length on Thermal Properties, Structure, and Self-Diffusion Coefficients of Alkyltriethylammonium-Based Ionic Liquids. *Int. J. Mol. Sci.* **2021**, *22*, 5935. [\[CrossRef\]](#) [\[PubMed\]](#)
46. Khan, F.; Siddiqui, U.S.; Khan, I.A. Physicochemical study of cationic Gemini surfactant butanediyl-1,4- bis(dimethyldodecylammonium bromide) with various counterions in aqueous solution. *Colloids Surf. A Physicochem. Eng. Asp.* **2012**, *394*, 46–56. [\[CrossRef\]](#)
47. Wattebled, L.; Laschewsky, A. Effects of organic salt additives on the behavior of dimeric (“Gemini”) surfactants in aqueous solution. *Langmuir* **2007**, *23*, 10044–10052. [\[CrossRef\]](#) [\[PubMed\]](#)
48. Huddleston, J.G.; Visser, A.E.; Reichert, W.M.; Willauer, H.D.; Broker, G.A.; Rogers, R.D. Characterization and comparison of hydrophilic and hydrophobic room temperature ionic liquids incorporating the imidazolium cation. *Green Chem.* **2001**, *3*, 156–164. [\[CrossRef\]](#)
49. Tikariha, D.; Singh, N.; Satnami, M.L.; Ghosh, K.K.; Barbero, N.; Quagliotto, P. Physicochemical characterization of cationic Gemini surfactants and their effect on reaction kinetics in ethylene glycol–water medium. *Colloids Surf. A Physicochem. Eng. Asp.* **2012**, *411*, 1–11. [\[CrossRef\]](#)
50. Comelles, F.; Ribosa, I.; Gonzalez, J.J.; Garcia, M.T. Micellization of sodium laurylthoxy sulfate (SLES) and short chain imidazolium ionic liquids in aqueous solution. *J. Colloid Interface Sci.* **2014**, *425*, 44–45. [\[CrossRef\]](#)
51. Wang, X.; Yan, F.; Li, Z.; Zhang, L.; Zhao, S.; An, J.; Jiayong, Y. Synthesis and surface properties of several nonionic–anionic surfactants with straight chain alkyl-benzyl hydrophobic group. *Colloids Surf. A Physicochem. Eng. Asp.* **2007**, *302*, 532–539. [\[CrossRef\]](#)
52. Li, N.; Gao, Y.A.; Zheng, L.; Zhang, J.; Yu, L.; Li, X. Studies on the micro polarities of bmimBF₄/TX-100/toluene ionic liquid microemulsions and their behaviors characterized by UV–visible spectroscopy. *Langmuir* **2007**, *23*, 1091–1097. [\[CrossRef\]](#)
53. Bhaisare, M.L.; Pandey, S.; Khan, M.S.; Talib, A.; Wu, H.F. Fluorophotometric determination of critical micelle concentration (CMC) of ionic and non-ionic surfactants with carbon dots via stokes shift. *Talanta* **2015**, *132*, 572–578. [\[CrossRef\]](#)
54. More, U.; Kumari, P.; Vaid, Z.; Behra, K.; Malek, N.I. Interaction between ionic liquids and Gemini surfactant: A detailed investigation into the role of ionic liquids in modifying properties of aqueous Gemini surfactant. *J. Surfactants Deterg.* **2016**, *19*, 75–89. [\[CrossRef\]](#)
55. Palchowdhury, S.; Bhargava, B.L. Effect of cation asymmetry on the aggregation in aqueous 1-alkyl, 3-decylimidazolium bromide solutions: Molecular dynamics studies. *J. Phys. Chem. B* **2014**, *118*, 6241–6249. [\[CrossRef\]](#) [\[PubMed\]](#)
56. Banjare, M.K.; Kurrey, R.; Yadav, T.; Sinha, S.; Satnami, M.L.; Ghosh, K.K. A comparative study on the effect of imidazoli-um-based ionic liquid on self-aggregation of cationic, anionic and nonionic surfactants studied by surface tension, conductivity, fluorescence and FTIR spectroscopy. *J. Mol. Liq.* **2017**, *241*, 622–632. [\[CrossRef\]](#)
57. Ba-Salem, A.O.; Duhamel, J. Determination of the Aggregation Number of Pyrene-Labeled Gemini Surfactant Micelles by Pyrene Fluorescence Quenching Measurements. *Langmuir* **2021**, *37*, 6069–6079. [\[CrossRef\]](#) [\[PubMed\]](#)
58. Gargi, B.R.; Indranil, C.; Satya, P.M. Pyrene absorption can be a convenient method for probing critical micellar concentration (CMC) and indexing micellar polarity. *J. Colloid Interface Sci.* **2006**, *294*, 248–254.
59. Karpovich, D.S.; Blanchard, G.J. Relating the polarity-dependent fluorescence response of pyrene to vibronic coupling. Achieving a fundamental understanding of the pyrene polarity scale. *J. Phys. Chem.* **1995**, *99*, 3951–3958. [\[CrossRef\]](#)
60. Dong, D.C.; Winnik, M.A. The py scale of solvent polarities. *Can. J. Chem.* **1984**, *62*, 2560–2565. [\[CrossRef\]](#)
61. Derman, O.S.; Stilbs, P.; Price, W.S. NMR Studies of Surfactants. *Concepts Magn. Reson. Part A Educ. J.* **2004**, *23*, 121–135. [\[CrossRef\]](#)
62. Savsunenko, O.; Matondo, H.; Messant, S.F.; Perez, E.; Popov, A.F.; Lattes, I.R.; Lattes, A.; Karpichev, Y. Functionalized vesicles based on amphiphilic boronic acids: A system for recognizing biologically important polyols. *Langmuir* **2013**, *29*, 3207–3213. [\[CrossRef\]](#)
63. Serdyuk, A.A.; Mirgorodskaya, A.B.; Kapitanov, I.V.; Gathergood, N.; Zakharova, L.Y.; Sinyashin, O.G.; Karpichev, Y. Effect of structure of polycyclic aromatic substrates on solubilization capacity and size of cationic monomeric and gemini 14-s-14 surfactant aggregates. *Colloids Surf. A Physicochem. Eng. Asp.* **2016**, *509*, 613–622. [\[CrossRef\]](#)
64. Desnoyers, J.E.; Perron, G. Temperature dependence of the free energy of micellization from calorimetric data. *Langmuir* **1996**, *12*, 4044–4045. [\[CrossRef\]](#)
65. Devinsky, F.; Masarova, L.; Lacko, I. Surface activity and micelle formation of some new bisquaternary ammonium salts. *J. Colloid Interface Sci.* **1985**, *105*, 235–239. [\[CrossRef\]](#)

-
66. Shafi, M.; Bhat, P.A.; Dar, A.A. Solubilization capabilities of mixtures of cationic Gemini surfactant with conventional cationic, nonionic and anionic surfactants towards polycyclic aromatic hydrocarbons. *J. Hazard. Mater.* **2009**, *167*, 575–581.
 67. Li, Q.; Wang, X.; Yue, X.; Chen, X. Wormlike micelles formed using Gemini surfactants with quaternary hydroxyethyl methylammonium headgroups. *Soft Matter* **2013**, *9*, 9667–9674. [[CrossRef](#)]
 68. Mahajan, S.; Mahajan, R.K. Interactions of phenothiazine drugs with bile salts: Micellization and binding studies. *J. Colloid Interface Sci.* **2012**, *387*, 194–204. [[CrossRef](#)]
 69. Pisarcik, M.; Polakovicova, M.; Markuliak, M.; Lukac, M.; Devinsky, F. Self-Assembly Properties of Cationic Gemini Surfactants with Biodegradable Groups in the Spacer. *Molecules* **2019**, *24*, 1481. [[CrossRef](#)]
 70. Yu, D.; Huang, X.; Deng, M.; Lin, Y.; Jiang, L.; Huang, J.; Wang, Y.; Zana, R. Effects of Inorganic and Organic Salts on Aggregation Behavior of Cationic Gemini Surfactants. *J. Phys. Chem. B* **2010**, *114*, 14955–14964. [[CrossRef](#)]
 71. Oliver, R.C.; Lipfert, J.; Fox, D.A.; Lo, R.H.; Doniach, S.; Columbus, L. Dependence of Micelle Size and Shape on Detergent Alkyl Chain Length and Head Group. *PLoS ONE* **2013**, *8*, 62488–62497. [[CrossRef](#)]
 72. Ghosh, S.; Roy, A.; Banik, D.; Kundu, N.; Kuchlyan, J.; Dhir, A.; Sarkar, N. How Does the Surface Charge of Ionic Surfactant and Cholesterol Forming Vesicles Control Rotational and Translational Motion of Rhodamine 6G Perchlorate (R6G ClO₄)? *Langmuir* **2015**, *31*, 2310–2320. [[CrossRef](#)]
 73. Geng, Y.; Romsted, L.S.; Menger, F. Specific ion pairing and interfacial hydration as controlling factors in gemini micelle morphology. Chemical trapping studies. *J. Am. Chem. Soc.* **2006**, *128*, 492–501. [[CrossRef](#)]
 74. Zana, R. Dimeric (gemini) surfactants: Effect of the spacer group on the association behavior in aqueous solution. *J. Colloid Interface Sci.* **2002**, *248*, 203–220. [[CrossRef](#)] [[PubMed](#)]

Appendix 3

Publication III

Kapitanov, I.V.; Raba, G.; Špulák, M.; Vilu, R.; Karpichev, Y.; Gathergood, N. Design of sustainable ionic liquids based on L-phenylalanine and L-alanine dipeptides: Synthesis, toxicity and biodegradation studies. *J. Mol. Liq.* **2023**, 374, 121285

Reproducing is permitted by Elsevier Copyright policy / Authors' rights in the article.



Design of sustainable ionic liquids based on L-phenylalanine and L-alanine dipeptides: Synthesis, toxicity and biodegradation studies

Illia V. Kapitanov^{a,1,2}, Grete Raba^{a,1}, Marcel Špulák^b, Raivo Vilu^c, Yevgen Karpichev^{a,*}, Nicholas Gathergood^{a,d,*}

^a Department of Chemistry and Biotechnology, Faculty of Science, Tallinn University of Technology (TalTech), Akadeemia tee 15, 12618 Tallinn, Estonia

^b Department of Organic and Bioorganic Chemistry, Faculty of Pharmacy, Charles University, Heyrovského 1203, Hradec Kralove 500 03, Czech Republic

^c Center of Food and Fermentation Technologies (TFIAK), Akadeemia tee 15a, 12618 Tallinn, Estonia

^d School of Chemistry, College of Science, University of Lincoln, Brayford Pool, Lincoln, LN6 7TS, United Kingdom

ARTICLE INFO

Article history:

Received 10 November 2022

Revised 6 January 2023

Accepted 17 January 2023

Available online 20 January 2023

Keywords:

Amino acid ionic liquids
Dipeptide ionic liquids
Sustainable chemicals
Biodegradability
Transformation products
Closed bottle test

ABSTRACT

A series of dipeptide ionic liquids (ILs) with L-phenylalanine and L-alanine fragments in structure were synthesized and their possible degradation pathways were analyzed. Based on this analysis, potential transformation products (PTPs) were proposed and synthesized. All of these compounds (25 in total) went through microbial toxicity screening and aerobic biodegradation testing. Obtained results demonstrated that by investigating ILs and PTPs with a dipeptide fragment (in tandem with single amino acid analogues), the design of ILs with high biodegradation values in closed bottle test can be accomplished. One finding was that within the scope of the compounds studied, L-phenylalanine containing compounds were more biodegradable than L-alanine derivatives. In addition to the choice of amino acid residue, its position in the dipeptide IL structure also had a significant effect on biodegradability. $\text{PyCH}_2\text{CO-Phe-Ala-OEt}$ IL, where L-phenylalanine was in close proximity to the positively charged pyridinium sub-unit, gave higher biodegradation percentages compared to $\text{PyCH}_2\text{CO-Ala-Phe-OEt}$ IL, where alanine was closer to pyridinium than the phenylalanine residue. Analysis of PTPs data showed that the presence of an alanine residue resulted in undesirable (less green) PTPs more often compared to PTPs containing phenylalanine, especially when alanine was in close proximity to the pyridinium headgroup. Based on both toxicity and biodegradation testing results preferable and less preferable subunits can be chosen for the design of new sustainable chemicals based on amino acids. Results from this study demonstrate a potential of designing new sustainable chemicals using amino acid moieties as part of their structure.

© 2023 Elsevier B.V. All rights reserved.

1. Introduction

The history of ionic liquids (ILs) is usually considered to have begun in 1914 when Paul Walden reported the synthesis of ethylammonium nitrate $[\text{C}_2\text{H}_5\text{NH}_3]^+[\text{NO}_3]^-$ – a salt which is liquid at room temperature [1]. Over the next hundred years ILs have been utilized in diverse applications as alternatives to traditional volatile organic solvents [2]. More than 115,000 research papers on „ionic liquids“ were published by 2022 (SciFinder[®]) principally

due to their desirable properties, such as thermal and chemical stability, low vapour pressure and modularity [3]. In addition to research, ILs are used in applied industrial processes [4,5]. For example, the BASIL[™] process used for the production of photoinitiator precursor alkoxyphenylphosphines and the Dimersol process for dimerisation of alkenes and butenes to more valuable branched hexenes and octenes [5–10].

However, even though ILs with their low vapor pressure have been proposed as *green* solvents, often a dearth of their toxicity and biodegradability assessment is observed [11,12]. These are key elements in the evaluation of the environmental effect of chemicals [13–17]. Ideally, from an environmental point of view, a *green* solvent should be non-toxic, biodegradable, use biore-sources as starting materials and synthesized using effective environmentally friendly synthesis procedures and be recyclable [18–20]. Most ILs are designed to be robust and stable under the various chemical and physical conditions of their target application

* Corresponding authors at: Department of Chemistry and Biotechnology, Faculty of Science, Tallinn University of Technology (TalTech), Akadeemia tee 15, 12618 Tallinn, Estonia (N. Gathergood).

E-mail addresses: yevgen.karpichev@taltech.ee (Y. Karpichev), ngathergood@lincoln.ac.uk (N. Gathergood).

¹ Contributed equally to the publication.

² Current address: Gemini PharmChem Mannheim GmbH, 68305 Mannheim, Germany.

[21]. Concerns have been raised that the design of inert ILs can lead to examples which tend to show poor degradability in environmental conditions [22–25]. Although progress has been made in IL recyclability, reuse is limited to a certain number of cycles before inevitable contamination and the need for ILs to be discarded at the end of their use [18,26]. For that reason, it is extremely important that ILs used in industrial applications result in a minimal impact to the environment [11,27]. This would be best achieved by using ILs which are mineralizable under wastewater treatment plant conditions and in soil and surface water. If microbial communities could metabolize ILs into inorganic CO₂, O₂, water and other innocuous substances, IL persistency would be avoided, and toxicity concerns mitigated. As there are claimed at least 10¹⁸ accessible combinations of cations and anions to form various ILs, a systematic approach is required in order to find mineralizable building blocks for ILs and to propose fragments for a benign-by-design synthesis [18,28–32].

The idea of finding mineralizable IL cations made from renewable sources was the basis of our previously published work, in collaboration with the Kümmerer's group, of a fully mineralizable IL **1** (see Fig. 1) with pyridinium headgroup and L-phenylalanine moiety [33–35].

We concluded, surprisingly, that amide bond cleavage was taking place before esterolysis, resulting in biodegradable and mineralizable transformation products [33]. This was unexpected and thus further studies to analyze the effect of amide bond nature in such type of structures were essential. In essence, to establish the specific influence of amino acid hydrophobicity on biodegradability, and if the presence of the sterically bulky CH₂Ph (c.f. Me; Ala) hydrophobic unit in IL **1** was critically required for effective binding to the active sites of biodegrading enzymes.

To answer these questions L-alanine ionic liquid **2** and a series of L-phenylalanine and L-alanine based dipeptide ILs **3–6** (see Fig. 1) were synthesized, and biodegradability of compounds (**1–6**) was investigated. The overall strategy of IL structure modifications was consistent with our design of imidazolium salts with high antimicrobial activity, but that time our focus was on identifying biodegradable ILs with low toxicity [36].

These novel dipeptides **3–6** have an additional amide bond (compared to amino acid ILs **1** and **2**) and the structural variations enable us to ascertain how the position of amide bond and amino acid residue affects biodegradation. It is widely reported that pyridinium ILs containing an amide not derived from an amino acid generally have poor biodegradability [22,23,37,38]. By extending the amino acid substructure from one residue (**1** and **2**) to two residues (**3–6**), we can determine the effect of an increase of peptide sequence on biodegradation. To investigate the effect of the sterics, π - π stacking and hydrophobicity of the -CH₂Ph of mineralizable Phe IL **1**, the Ala derivative was studied. This CH₃ analogue was selected due to the reduced steric hindrance, absence of π - π interactions and lower hydrophobicity.

Pyridinium ILs toxicity was reported to increase in antimicrobial activity as the substituting alkyl chain lengthened [39–43]. As the focus of this study was to determine the effect of the amino acid residues, the ethyl ester group (e.g. **1**) was selected to minimize potential toxicity complications due to the alkyl ester tail.

We submit that the amino acid side chains of ILs **1–6** are consistent with the concept of cation surfactants ('Charged head group substituted with hydrophobic tail') and thus the results have broad applicability to the synthesis of biodegradable cationic surfactants.

In addition, for each parent compound **1–6** possible breakdown sites and degradation pathways were proposed and analyzed. Based on this analysis potential transformation products (PTPs) were suggested, then synthesized and studied for their biodegradability. Studying PTPs together with parent compounds is of critical

importance when complete mineralization of chemical compounds (including ILs) is the desired outcome. IL parent compounds **1–6** and their PTPs represent the series of compounds selected to enable biodegradation and toxicity SAR studies underpinning the benign-by-design approach.

2. Materials and methods

Biodegradation of two L-amino acid based ILs, four L-phenylalanine and L-alanine based dipeptide ILs with pyridinium sub-unit and their proposed transformation products were studied. 25 compounds (**1–25**) in total were synthesized and underwent antimicrobial activity screening and biodegradation testing under aerobic conditions.

2.1. Selection of target PTPs

Selection of target PTPs for synthesis and study (Fig. 1) was performed from analysis of possible biodegradation pathways (see Scheme 1; **S1**). The proposed first step of biodegradation for studied molecules is hydrolysis to lower molecular mass fragments which will then be ultimately transformed to CO₂, H₂O and N₂ [33,34].

Amino acid ILs **1** and **2** contain two hydrolysable bonds (one ester and one amide bond), either of which could be hydrolyzed first, and can therefore initiate two different biodegradation pathways (Schemes **S1-1** and **S1-2**). Dipeptide ILs **3–6** contain three hydrolysable bonds (one ester and two amide bonds) and, correspondingly, can initiate three distinct biodegradation pathways with different transformation products being formed in the breakdown process (Schemes **S1-3**, **S1-4**, **S1-5**, and **S1-6**). For all pathways the potential ultimate result is the same (full hydrolysis of all ester/amide bonds), although some metabolites will be different due to a change in the order of the bonds hydrolysis. Analysis of each pathway shows that all PTPs for amino acid ILs **1** and **2** can be found also in PTPs for dipeptide ILs **3–6** (see Scheme 1 and **S1-7**). Significant overlap also occurs when comparing the structures of PTPs for dipeptide ILs **3–6** which can be formed through different pathways, and this considerably decreased the number of target molecules. This reduces the resources and time required for the synthesis and testing for their aerobic biodegradability, resulting in an efficient strategy for this type of study. The structures of these target compounds are presented in Fig. 1.

2.2. Chemicals

Reagents and solvents were purchased from Sigma-Aldrich, Acros Organics, Alfa Aesar, Honeywell and used without further purification. Dipeptides (*N*-L-Phe-L-Phe-OH; *N*-L-Phe-L-Ala-OH; *N*-L-Ala-L-Phe-OH; *N*-L-Ala-L-Ala-OH) were provided by Fluorochem Ltd. All other chemicals (amino acid ILs, dipeptide ILs and their PTPs) were synthesized by methods similar to procedures from [34,36,44,45] and are described in **S2** (Appendix A1). Characterization by NMR, HRMS spectra and melting points of studied compounds is also collected in supporting information (see **S2**).

The general synthetic routes to prepare compounds **1–10**, and **12–21** are shown in Scheme 2: corresponding L-amino acid (**12** and **13**) was transformed into ethyl ester hydrochloride (**27**, **28**) with SOCl₂ in ethanol. The obtained product was then neutralized with sodium carbonate and gave an ester (**9** and **10**) in free base form. Next, the L-amino acid ethyl esters (**9**, **10**) was used for the synthesis of *N*-bromoacetyl derivatives (**29** and **30**) via acylation with bromoacetyl bromide in dichloromethane in the presence of sodium carbonate. The Boc-protected dipeptide ethyl esters (**31–34**) were synthesized by coupling with corresponding Boc-

Amino acid and dipeptide based ILs with L-phenylalanine and L-alanine moiety in structure

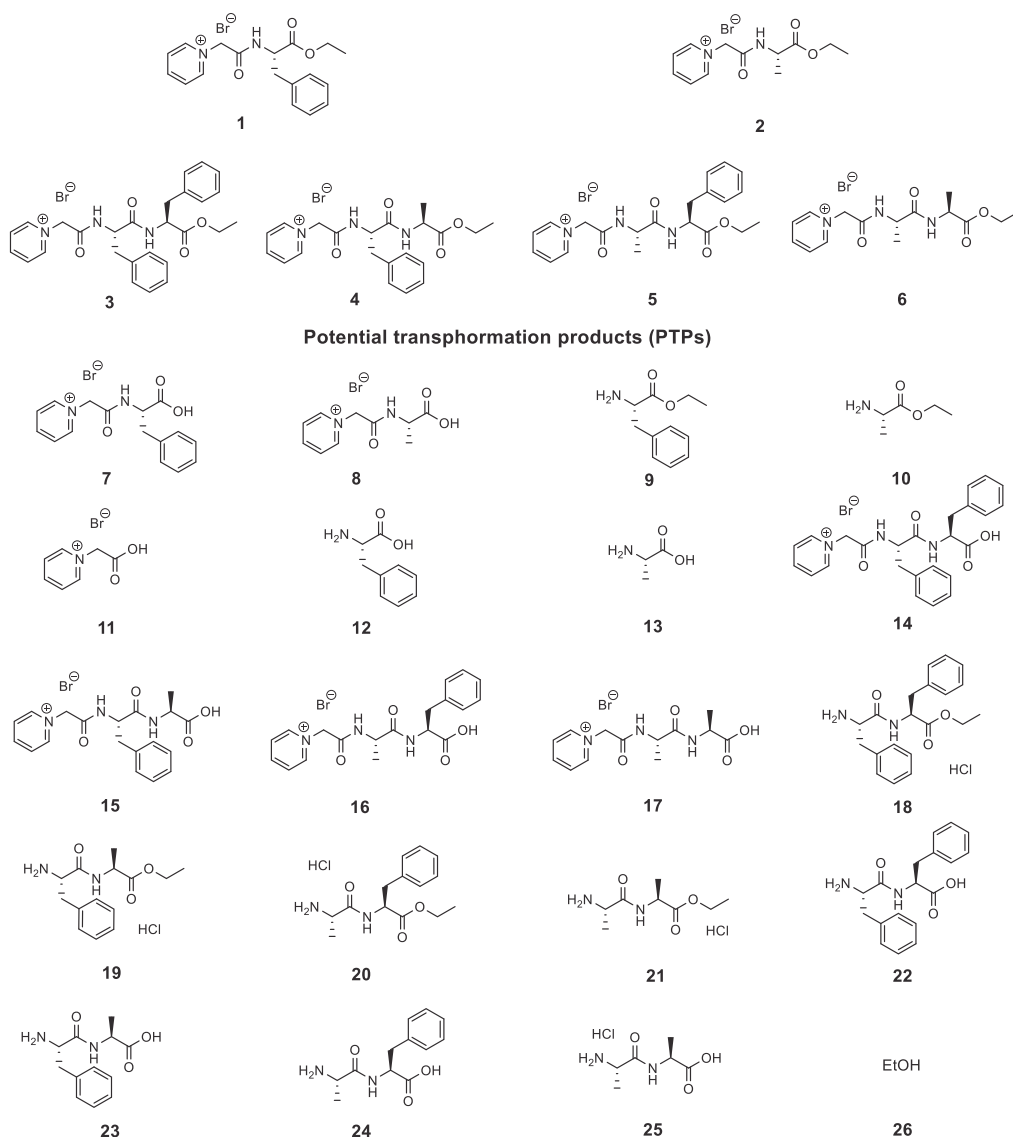
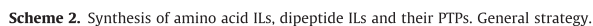
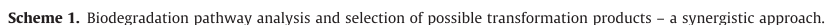


Fig. 1. Amino acid ILs (1, 2) and dipeptide ILs (3–6) with L-phenylalanine and L-alanine moiety in structure and target PTPs (7–26) selected for synthesis and study.

protected L-amino acid). The alkylation of pyridine with *N*-bromoacetyl derivative of L-amino acid ethyl ester (29 and 30) resulted in target amino acid ILs 1 and 2, which could be hydrolyzed to corresponding acids 7 and 8 in mild conditions. The Boc-protected dipeptide ethyl esters (31–34) were deprotected by reflux with PTSA in ethanol and then transformed into free base (35–38) with sodium carbonate. The dipeptide ethyl ester in free base form (35–38) were used for synthesis of hydrochloride salts 18–21 (via neutralization of free base in diethyl ether with solution of hydrochloric acid in diethyl ether). The *N*-bromoacetyl derivatives (39–42) were also prepared from (35–38) by acylation with bromoacetyl bromide in dichloromethane in presence of sodium

carbonate. The products of alkylation of pyridine with *N*-bromoacetyl derivative of dipeptide ethyl ester (39–42) were target dipeptide ILs 3–6, which could also be hydrolyzed to corresponding acids in mild conditions (14–17). Compound 11 was prepared according to our previous paper [34].

Resource efficient synthesis of chemical compounds is an integral part of our strategy to design greener chemicals. Analysis of the synthetic procedures according to Green Chemistry principles were performed with J. Clark's Green Chemistry metrics toolkit [46]. The key parameters of reactions are collected in Table S3. All reactions quantitatively analyzed by yield, conversion and selectivity can be marked with green flag (>90 %), except one case



in the range 40.8–99.4 %, however the majority of reactions have RME > 70 %. Optimum efficiency (OE) was also high with > 80 % determined in 31/35 cases. Analysis of process mass intensity (PMI) parameters shows that PMI workup solvents parameter is

the major contributor to the PMI total and reduced solvent usage in the workup step is recommended in future studies to make the synthesis greener. Several solvents which were used in the synthetic procedures and workup are rated green (water, ethanol, ethyl acetate, acetone), but in some steps problematic solvents (e.g., DMF, DCM, diethyl ether and petroleum ether were used [46]). To reduce the negative impact on the environment all problematic solvents were specifically targeted to be recovered, with recovery yields > 80 % achieved). Evaluation of critical elements used in the synthesis has been marked with green (>500 years supply remaining) or amber flag (50–500 years supply remaining). Based on evaluation of energy parameters (see Table S3) none of the reactions could be marked with red flag (reactions did not run below –20 or above 140 °C). All reaction were done in batch (amber flag), but potentially the hydrolysis step (synthesis of compounds 7, 8, 14, 15, 16, 17) can be performed under flow conditions in the presence of immobilized enzymes (green flag) [46]. The health & safety parameters (by H-code) for used synthetic procedures were also quantitatively assessed (see Green Chemistry Metrics files in Appendix A2).

2.3. Toxicity screening

Toxicity screening was performed with a similar method used in the previous papers [34,36], however the panel of bacterial and fungal strains involved more ATCC species: bacterial strains SA, *Staphylococcus aureus* (ATCC 29213); MRSA, *Staphylococcus aureus* (ATCC 43300); SE, *Staphylococcus epidermidis* (clinical isolate); EF, *Enterococcus faecalis* (ATCC 29212); EC, *Escherichia coli* (ATCC 25922); KP, *Klebsiella pneumoniae* (clinical isolate); SEMA, *Serratia marcescens* (clinical isolate); PA, *Pseudomonas aeruginosa* (ATCC 27853); yeasts CA1, *Candida albicans* (ATCC 24433); CA2, *Candida albicans* (ATCC 90028); CK, *Candida krusei* (ATCC 6258); CG, *Candida glabrata* (ATCC 90030); CP, *Candida parapsilosis* (ATCC 22019); CT, *Candida tropicalis* (ATCC 750); PQ, *Pichia quilliermondii* (ATCC 90877); SC, *Saccharomyces cerevisiae* (ATCC 9763); fungal strains AF, *Aspergillus fumigatus* (ATCC 204305); AFla, *Aspergillus flavus* (CCM 8363); AC, *Absidia corymbifera* (CCM 8077); MC, *Microsporium canis* (CCM8353); TI, *Trichophyton interdigitale* (ATCC 9533). Minimum inhibitory concentration (MIC) values for evaluating antibacterial activity were obtained with microdilution broth method based on EUCAST (The European Committee on Antimicrobial Susceptibility Testing) instructions [47–49]. For experimental method and results see Appendix A1 (S4, Table S4-1, S4-2).

2.4. Inoculum

Effluent from wastewater treatment plant was collected from a municipal wastewater treatment plant in Tallinn, Estonia (Paljassaare wastewater treatment plant, 59°27'55.5"N 24°42'08.8"E). WWTP effluent was filtered through a cellulose filter (membrane Ø 240 mm) before being used as inoculum for aerobic biodegradation testing.

2.5. Aerobic biodegradation according to modified OECD 301D

Aerobic biodegradation testing was performed using modified closed bottle test (CBT) based on OECD 301D guidelines [50,51]. CBT setup with modification where biological oxygen consumption is measured with an optode oxygen sensor system using PTFE-lined Pst3 oxygen sensor spots (Fibox 3 PreSens, Regensburg, Germany) allows measuring BOD without opening the flasks and thereby reducing the number of parallels needed for each compound and increasing test throughput. It has also shown to improve reproducibility compared to the original OECD 301D guideline [50]. Compared to other standard aerobic biodegradation

tests, CBT is better suited for testing compounds with various physico-chemical properties. It is also one of the strictest tests as the amount of inoculum added is very low and thereby compounds passing CBT should show good biodegradation not only under artificial wastewater treatment conditions but also in soil and ground-water systems. Description of experimental setup and detailed results can be found in S5, Appendix A1 (Figures S5-1 _ S5-25).

3. Results and discussion

Six IL parent compounds (1–6) and their PTPs (7–25) were synthesized, screened for antimicrobial activity and their biodegradability under aerobic conditions was determined using modified CBT. Standard aerobic biodegradation tests enable us to have a standardized test where the results can be used to intelligently design chemicals with high biodegradability. However, they only approximate to the conditions found in wastewater treatment plants and/or surface water, soil. They suffer from two drawbacks. Firstly, they do not consider the variability of physico-chemical conditions and microbial communities which can be present in different parts of sewage lines before reaching treatment plants. Secondly, the CBT protocols do not require an evaluation and identification of TPs formed during the test. The common unknown in both these scenarios is the identification of the TPs, the additional chemical compounds present during the timeframe of the test. When considering which are the most labile (or reactive) groups in our ILs in an aqueous environment, the ester and amide functional groups were proposed. It is assumed that the compounds resulting from hydrolysis of the peptide ILs would also be generated in the environment (after accidental release) or during a CBT. For that reason, we included all possible hydrolysis degradation pathways and all resulting PTPs in our study. This strategy gave us more comprehensive information about the possible benign effect on the environment (or harm) of our designed compounds. In addition to the dipeptide ILs, identifying biodegradable PTPs with low toxicity is also a worthwhile endeavor, as they are good candidates to support future green chemical design.

3.1. Microbial toxicity screening

All six IL parent compounds and their PTPs were screened for antimicrobial activity against 4 Gram-positive bacteria strains, four Gram-negative bacteria strains, 8 yeast strains and 4 fungal strains. This was performed to ascertain their possible toxicity and to assist our biodegradation testing strategy. In particular, if any of the compounds showed high antimicrobial activity, it would be taken into consideration that the compound may also inhibit biotransformations in CBT. Results from microbial toxicity screening are summarised in Tables S4-1 and S4-2. Compounds 12 (L-phenylalanine) and 13 (L-alanine) were insoluble in DMSO and could not be screened for antimicrobial activity by the method used but are known to be common metabolites in microbes and other living organisms. Although PTP 26 (ethanol) is a widely used antiseptic it is expected to show no toxic effects at the concentrations used in CBT (<5 mg/L). This screening serves as a starting point for a more thorough investigation of IL toxicity.

The main goal of the microbial toxicity screen was identifying high-toxicity compounds which would be given a low priority in the subsequent time-consuming biodegradability testing. High antimicrobial activity is an undesirable property when designing sustainable ILs with broad applicability and could also negatively affect the microbes used as inoculum in CBT. From the results of this preliminary screening (see Tables S4-1 and S4-2) it was decided that all compounds would be studied in CBT as none

showed high activity (MIC < 10 µM in 24 h) against the strains of bacteria, yeast and fungi they were screened against.

Out of all studied compounds only **6** showed minor antibacterial activity against Gram-positive SA (MIC 125 µM in 24 h), MRSA (MIC 500 µM in 24 h), SE (MIC 1000 µM in 24 h), EF (MIC 2000 µM in 24 h) and Gram-negative EC (MIC 1000 µM in 24 h) and KP (MIC 2000 µM in 24 h), see Table S4-1. The **6** did not show any activity against yeast and fungi at the maximum concentration screened. None of the other ILs and PTPs (compounds **1–5**, **7–25**) exhibited antibacterial properties in the maximum concentrations used against the strains chosen for screening. Screening results with yeast and fungi showed minor antimicrobial activity for **9**, **10** and **18**, but no antibacterial properties were demonstrated. Overall, only minor antimicrobial activity was found with compounds **1–25**. Concentrations used in this screening (up to 2000 µM) exceeded the concentrations which were later used for CBT (5.2–52.1 µM) and resulted in the decision that all 25 compounds were the same priority for aerobic biodegradability testing. The toxicity data was in accordance with previously published results where pyridinium ILs showed low microbial toxicity [34]. Due to the similarity of obtained MIC values no clear SAR comparison can be made.

In addition to antimicrobial activity screening, toxicity was also evaluated during CBT using „toxicity series“ data recorded concurrently. If any of the bottles in this series showed <25 % biodegradation by day 14, this compound would be classified as toxic [50]. None of the studied 25 compounds were toxic to microbes in wastewater treatment plant effluent used as inoculum. This is consistent with our toxicity screening results which showed low antimicrobial activity of studied compounds (Tables S4-1 and S4-2).

Toxicity screening results complement our previously reported findings of a mineralizable pyridinium substituted phenylalanine derived IL (**1**) with low toxicity [33,34]. However, when Hou and co-workers studied cholinium ILs with amino acids as anions, they reported that the phenylalanine analogue had one of the highest antibacterial activities (including SA (MIC 62.5 mM) and EC (MIC 31.3 mM)) among 20 standard amino acids [52]. Similar work with cholinium-amino acid ILs was carried out by Yazdani who reported EC₅₀ values 251 – 1120 mg/L (0.93–5.80 mM) for alanine and phenylalanine anions against two Gram-positive and two Gram-negative bacteria [53]. As the method used in our study was not suitable for screening pure alanine and phenylalanine samples, data cannot be compared directly. However, compounds in our study containing these two amino acid residues did not show high antimicrobial activity. Our aim was not to determine MIC values but to check for high toxicity which could have negatively affected the following biodegradability studies. The MIC values reported previously for phenylalanine and alanine were higher than the concentrations used in CBT (>2 mM) and based on this we concluded that **12** and **13** should not show any inhibition in aerobic biodegradation tests.

These examples demonstrate that the overall structure and charge of a compound can play a big role in toxicity mechanism. Minor changes in the chemical structure of a compound can still have a significant effect when determining its 'greenness'.

3.2. Aerobic biodegradation testing

Microbial toxicity screening results indicated that none of the tested compounds would be expected to show inhibition towards microbes in inoculum during CBT. Thus, based on results from antimicrobial activity testing all six IL parent compounds (**1–6**) and their PTPs (**7–25**) were given equal priorities for further studies and were tested for their aerobic biodegradability. Biodegradation testing was performed using modified CBT method and each

test ran for up to 33–42 days. Most of the tested compounds contained a pyridinium sub-unit which had previously been reported to have a long induction period after which fast biodegradation occurs [33]. To better observe the effects of this phenomenon we prolonged CBT from standard 28 days (suggested by OECD 301 D protocol) to 33–42 days [51]. A general scheme for the proposed breakdown pathways and resulting PTPs are shown in Scheme 1 and Fig. 1, respectively. For specific proposed breakdown pathways for **1–6**, see ESI-1. Biodegradation graphs for amino acid ILs (**1** and **2**) and their PTPs (**7–13**) and dipeptide ILs (**3–6**) and their PTPs (**7–25**) are shown on Figs. 2 and 3. The results are summarized in Table 1. Individual biodegradation curves for each compound together with quality and toxicity controls are presented in S5 (Figures S5-1 _ S5-25). The minor antimicrobial activity demonstrated by IL **6** and PTPs **9**, **10** and **18** did not affect their biodegradability as all of them passed the 60 % threshold in extended CBT with 42 days.

Phenylalanine IL **1** passed the 60 % biodegradation threshold on day 25 and reached 66 % after the extended CBT of 42 days (Fig. 3). These are similar results compared to biodegradation data of **1** previously obtained in our study with the Kümmerer group [33]. All of the evaluated PTPs of **1** (i.e., **7**, **9**, **11** and **12**) also showed high final biodegradation values (61–93 %) (Table 1). Switching amino acid moiety from phenylalanine to alanine, however, significantly decreased biodegradability (Fig. 2) and **2** reached only 30 % in 42 days (25 % in 28 days which is the standard length of CBT) (Table 1). We propose that hydrophobic phenylalanine residue in close proximity to the positively charged pyridinium headgroup makes the cation a more reactive substrate for enzymes responsible for observed biodegradation. A similar trend was shown by PTPs **7** and **8**, esterolysis products of phenylalanine and alanine ILs (**1** and **2**, respectively). **7** passed the 60 % threshold in the CBT standard 28 days (66 % in 42 days) while **8** reached only 43 % in 42 days (40 % in 28 days) (Table 1). Amidolysis products of ILs **1** and **2** are ethyl esters **9** and **10**. Both of these amino esters can be classified as biodegradable (after 28 days, **9** 60 % and **10** 73 %, Table 1), suggesting that amino acid containing TP's resulting from amidolysis of ILs **1** and **2** are more biodegradable compared to amino acid containing TP formed via the alternative initial esterolysis pathway. Amino esters **9** and **10** can also hydrolyse to the corresponding amino acids. These PTPs **12** and **13** were screened, and the results showed a similar trend as seen with the carboxylic acids **7** and **8**, esterolysis products of **1** and **2**, respectively. L-phenylalanine **12** was biodegradable in 28 days (65 %) while L-alanine **13** biodegraded only 48 % in standard 28 days (Table 1). However, while L-alanine pyridinium salt **8** did not further biodegrade on extending the test from 28 to 42 days, L-alanine **13** increased from 48 % to 62 % biodegradation due to the extra 14 days. The pyridinium product of amidolysis of both **1** and **2**, PTP **11**, had a long induction period before starting rapid biodegradation reaching 93 % biodegradation after 42 days. This is in agreement with our previous study of biodegradation of phenylalanine IL **1** [33,34].

In case of monoamino acid ILs, **1** with phenylalanine residue showed significantly improved biodegradability compared to less hydrophobic salt **2**. The Fig. 2 overall shows that high levels of biodegradation for IL **1** and PTPs can be achieved. Although PTP **11** had a long induction period, high biodegradation was observed with 42 days. By plotting the biodegradation data for the IL and PTPs on the same graph, a more thorough analysis of whether the IL has favourable biodegradable properties can be made. The Fig. 2 illustrates a complimentary dataset where again additional analysis of the biodegradation data is possible compared to a study only reporting the CBT results for IL **2**. Although **2** and ester hydrolysis product **8** do not show high biodegradation (and thus applications using **2**, or ILs which degrade to form **8**, are not preferred), ILs

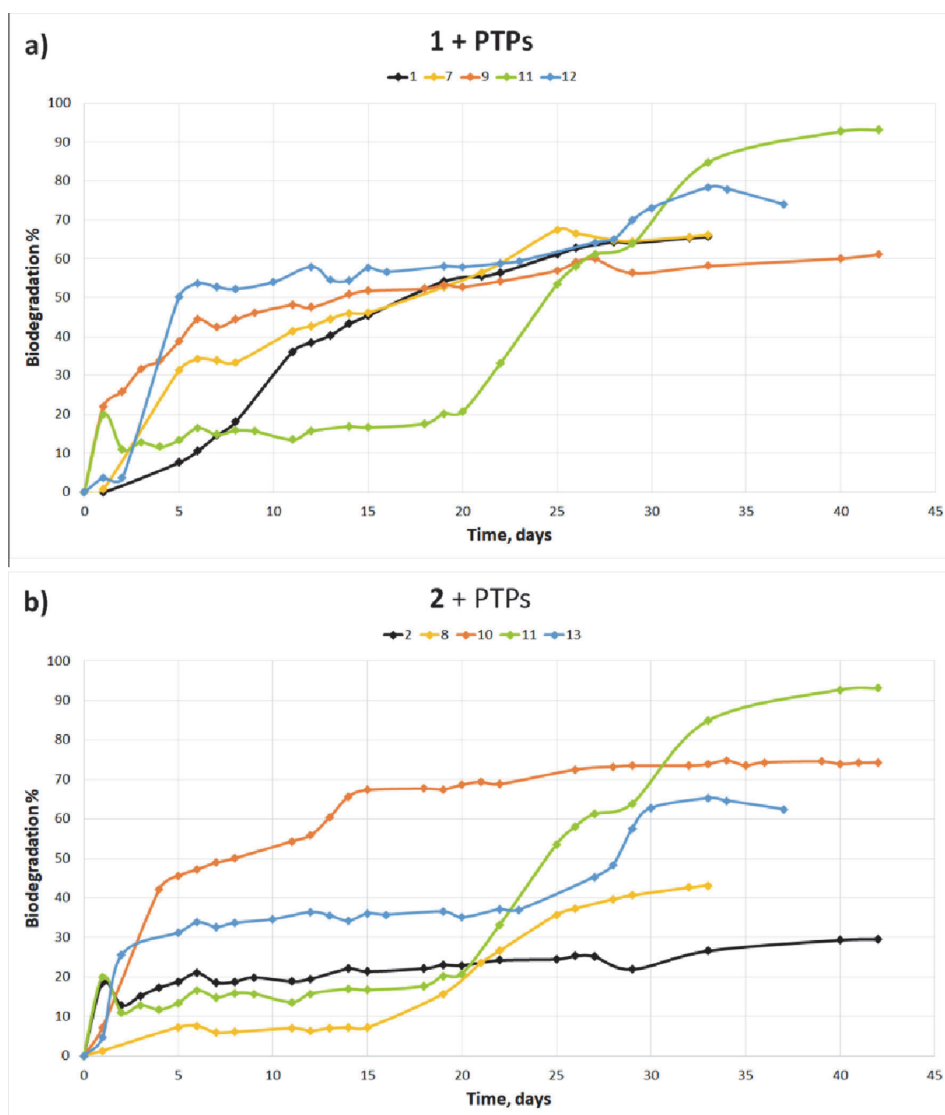


Fig. 2. Aerobic biodegradation curves of a) **1** and PTPs **7**, **9**, **11** and **12**; b) **2** and PTPs **8**, **10**, **11** and **13** using modified CBT. More detailed biodegradation graphs for each compound are presented in **Appendix A1** (Figures **S5-1** (**1**), **S5-2** (**2**), **S5-7** (**7**), **S5-8** (**8**), **S5-9** (**9**), **S5-10** (**10**), **S5-11** (**11**), **S5-12** (**12**) and **S5-13** (**13**)).

which degrade to yield L-alanine ethyl ester **10** and L-alanine **13** are preferred. Results for **2** and its PTPs also indicate that just combining biodegradable „building blocks” does not always guarantee good biodegradability of the product: biodegradation values for all PTPs of **2** showed higher D% compared to **2**. This shows the importance of a systematic study of breakdown pathways of parent compounds and their transformation products if mineralizable ILs are to be developed. While this is undoubtedly the ideal approach, the resources required to complete this for a series of compounds is considerable. We propose that the targeted approach we describe herein, enables researchers to select the preferred compounds for further study.

Biodegradation was evaluated using the monoamino acid ILs (**1** and **2**) as well as dipeptide ILs (**3–6**) and their PTPs (**7–25**). In regular CBT conditions with 28 days, **3** and **4** passed the 60 % threshold and could be classified as biodegradable (see Fig. 3). After extending the test to 42 days dipeptide ILs **5** and **6** also reached biodegradation values > 60 % (see Fig. 3). Out of the four dipeptide IL parent compounds **4** (PyCH₂CO-Phe-Ala-OEt IL) had highest biodegradability: 91 % after 42 days. **3** (PyCH₂CO-Phe-Phe-OEt IL) (84 %) and **5** (PyCH₂CO-Ala-Phe-OEt IL) (73 %) followed and **6** (PyCH₂CO-Ala-Ala-OEt IL) had the lowest biodegradability with 61 % after 42 days, as shown in Table 1. Lower biodegradability of **6** is in accordance with results from toxicity screening where **6** showed some antibacterial activity against tested bacterial

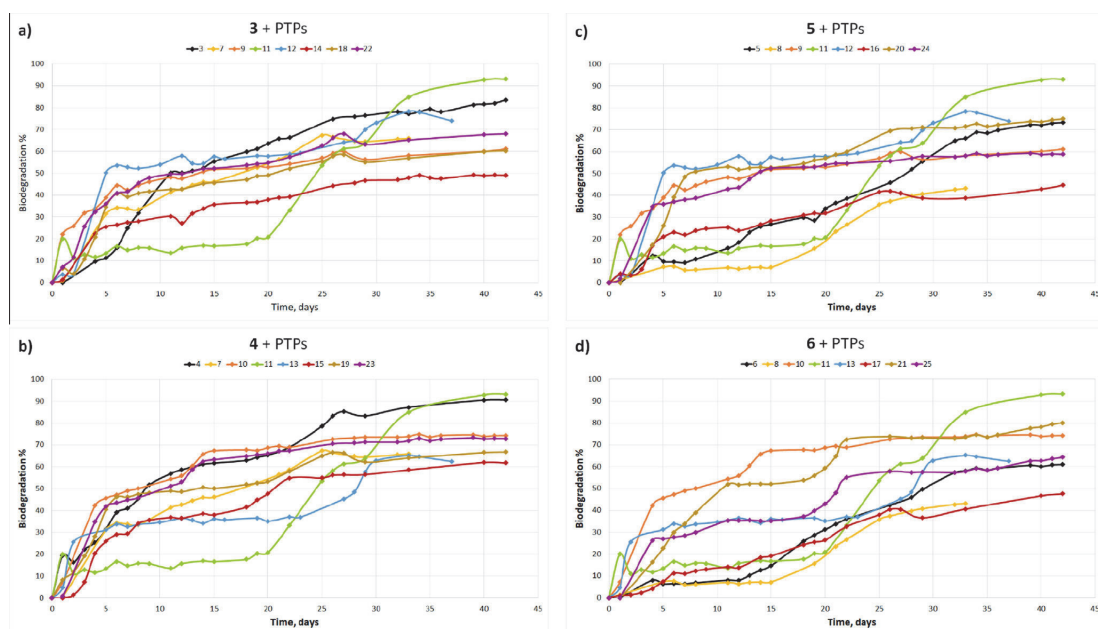


Fig. 3. Aerobic biodegradation curves of a) **3** and PTPs **7, 9, 11, 12, 14, 18** and **22**; b) **4** and PTPs **7, 10, 11, 13, 15, 19** and **23**; c) **5** and PTPs **8, 9, 11, 12, 16, 20** and **24**; d) **6** and PTPs **8, 10, 11, 13, 17, 21** and **25** using modified CBT. More detailed **21**, biodegradation graphs for each compound are found in [Appendix A1 \(Figures S5–3 \(3\), S5–4 \(4\), S5–5 \(5\), S5–6 \(6\), S5–7 \(7\), S5–8 \(8\), S5–9 \(9\), S5–10 \(10\), S5–11 \(11\), S5–12 \(12\), S5–13 \(13\), S5–14 \(14\), S5–15 \(15\), S5–16 \(16\), S5–17 \(17\), S5–18 \(18\), S5–19 \(19\), S5–20 \(20\), S5–21 \(21\), S5–22 \(22\), S5–23 \(23\), S5–24 \(24\), and S5–25 \(25\)\)](#).

strains, most notably SA, and therefore could exhibit similar inhibition to some of the strains in CBT inoculum. These results further prove that inclusion of the phenylalanine moiety into pyridinium ILs leads to dipeptide compounds with high biodegradability under our test conditions. The common structural unit of the three amino acid derived ILs (**1**, **3** and **4**) with the recorded highest values of biodegradation is $\text{PyCH}_2\text{COPhe-}$. Interestingly, it seems that the position of the phenylalanine moiety in the structure of IL cation is important. Significantly lower biodegradation was observed for **5** the $\text{PyCH}_2\text{CO-Ala-Phe-OEt}$ IL compared to $\text{PyCH}_2\text{CO-Phe-Ala-OEt}$ IL **4**. The lowest biodegradation (albeit a good result after 42 days, 61 %) was found when only alanine residues were present in IL **6**. This shows that both the amino acid moiety and its position in IL structure are important factors when biodegradability is considered.

There are three sites susceptible to hydrolysis in ILs **3–6**, two amide bonds and an ethyl ester. A reasonable assumption is that the ethyl ester is more labile and accessible than the two amide bonds and would be cleaved first. After hydrolysis of the ester bond, PTPs **14–17** would be formed. However, all 4 dipeptide ILs **3, 4, 5** and **6** esterolysis products (compounds **14, 15, 16** and **17**, respectively) showed significantly lower biodegradation values – 49 % vs 84 %; 62 % vs 91 %; 45 % vs 73 %; and 48 % vs 61 % (see [Table 1](#)). **15**, PTP of **4**, showed the highest biodegradability out of the four hydrolysis PTPs, reaching 56 % in 28 days and 62 % in 42 days. None of the other hydrolysis PTPs passed the 60 % threshold in 42 days. This indicates that the hydrophilic carboxylic acid residue, which is formed after esterolysis of **3–6**, inhibits biodegradation.

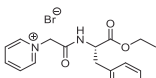
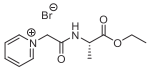
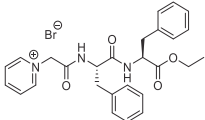
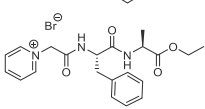
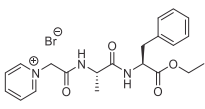
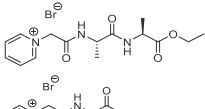
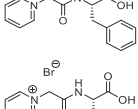
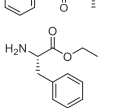
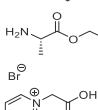
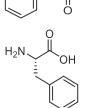
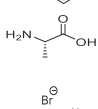
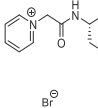
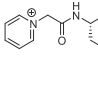


This effect is not apparent with monoamino acid ILs. Ethyl ester **1** and the carboxylic acid derivative **7** CBT results were almost identical, ca. 65 % biodegradation after 28 and 42 days. After 42 days there was no significant difference in biodegradation val-

ues (30 % and 43 %) for the ethyl ester and carboxylic acid alanine ILs, **2** and **8** respectively (see [Table 1](#)).

Considering ILs **3–6**, if the amide bond connecting the two amino acids hydrolyses first, then the PTPs are the carboxylic acids **7** and **8**, and the amino ethyl esters **9** and **10**. Biodegradation values for **7, 9** and **10** are all above 60 % threshold after 28 days. However, **8** is only 43 %, even after 42 days. Therefore, hydrolysis between the two amino acids of $\text{PyCH}_2\text{COPhe-}$ ILs **3** and **4**, would yield PTPs with biodegradation values >60 % (after 28 days). This result is consistent with the high biodegradation values obtained for **3** and **4**. However, comparing the biodegradation data for $\text{PyCH}_2\text{COAla-}$ IL **5** and hydrolysed product **8**, a different trend is observed. Although **5** attained 73 % degradation after 42 days, a significantly lower value was recorded for its PTP **8** (43 %). One possibility is that the degradation of **5** does not have a dominant breakdown pathway via **8**. To further support this claim, we also considered the alternative scenario where the amide bond closest to the pyridinium head group hydrolysed first. IL **5** would be converted into PTPs **11** and **20**. High biodegradation values 93 % and 75 % (after 42 days) were recorded for these PTPs and are consistent with the high biodegradation observed for IL **5** (73 %, 42 days).

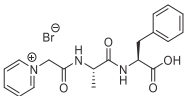
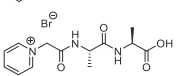
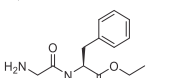
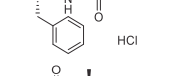
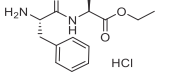
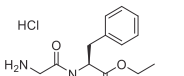
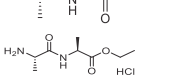
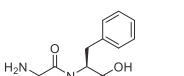
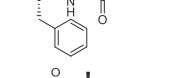
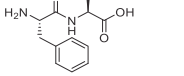
If, instead of esterolysis, breaking of the amide bond near the pyridinium headgroup would be the first transformation during biodegradation, PTPs **18–21** would be formed. These PTPs all showed good biodegradability: **19–21** passed the 60 % threshold in 28 days and **18** reached 59 %. Especially high values were obtained with extended CBT: 60 % for **18**; 67 % for **19**; 75 % for **20** and 80 % for **21**. If amidolysis and loss of pyridinium headgroup is the first step in biodegradation of **3–6** good biodegradation is still achieved. Interestingly, losing pyridinium headgroup would also increase biodegradability of esterolysis products: PTPs **22–25** showed higher biodegradation values compared to PTPs **14–17** which had pyridinium headgroup attached to the molecule. **22**;

Table 1
Biodegradation results for the periods of 14, 28, and 42 days.

#	Structure	Conc. in CBT, μM	10-day-window analysis				D% 14 days	D% 28 days	D% 42 days
			Start day	Start D%	End D%	ΔD%			
1		7.8	6	11 ± 2	45 ± 4	34	43 ± 6	64 ± 3	66 ^a ± 3
2		12.0	2	13 ± 1	20 ± 1	7	22 ± 1	25 ± 2	30 ± 1
3		5.2	5	11 ± 2	55 ± 6	44	52 ± 4	76 ± 1	84 ± 1
4		6.8	2	16 ± 1	59 ± 14	38	61 ± 14	83 ± 8	91 ± 5
5		6.8	4	12 ± 4	26 ± 16	14	26 ± 16	52 ± 4	73 ± 4
6		9.8	13	10 ± 5	36 ± 11	26	13 ± 6	46 ± 7	61 ± 5
7		9.2	5	31 ± 1	46 ± 2	15	46 ± 2	65 ± 6	66 ^a ± 6
8		15.6	19	16 ± 7	41 ± 5	25	7 ± 3	40 ± 6	43 ^a ± 4
9		12.0	2	26 ± 2	48 ± 3	22	51 ± 3	60 ± 5	61 ± 3
10		26.0	4	42 ± 1	66 ± 1	24	66 ± 1	73 ± 1	74 ± 1
11		22.3	2	11 ± 1	16 ± 2	5	17 ± 2	61 ± 16	93 ± 3
12		15.6	5	50 ± 4	58 ± 1	8	54 ± 1	65 ± 2	74 ^b ± 4
13		52.1	2	26 ± 9	36 ± 1	10	34 ± 1	48 ± 1	62 ^b ± 3
14		5.8	4	22 ± 2	34 ± 1	12	34 ± 1	46 ± 2	49 ± 2
15		7.8	4	20 ± 1	39 ± 11	19	39 ± 11	56 ± 2	62 ± 3

(continued on next page)

Table 1 (continued)

#	Structure	Conc. in CBT, μM	10-day-window analysis				D% 14 days	D% 28 days	D% 42 days
			Start day	Start D%	End D%	$\Delta\text{D}\%$			
16		7.8	4	17 \pm 10	27 \pm 11	10	27 \pm 11	41 \pm 9	45 \pm 10
17		12.0	6	11 \pm 1	19 \pm 4	8	18 \pm 4	40 \pm 1	48 \pm 1
18		6.8	3	11 \pm 1	43 \pm 1	32	45 \pm 1	59 \pm 4	60 \pm 3
19		9.8	2	12 \pm 4	49 \pm 1	37	51 \pm 1	66 \pm 4	67 \pm 7
20		9.8	4	17 \pm 1	53 \pm 1	36	53 \pm 2	71 \pm 2	75 \pm 1
21		17.4	4	16 \pm 1	52 \pm 1	36	52 \pm 1	73 \pm 2	80 \pm 1
22		7.8	2	12 \pm 1	50 \pm 1	38	52 \pm 1	68 \pm 1	68 \pm 1
23		12.0	4	35 \pm 1	62 \pm 1	27	62 \pm 1	71 \pm 1	73 \pm 1
24		12.0	4	35 \pm 1	51 \pm 2	16	51 \pm 2	57 \pm 2	59 \pm 2
25		26.0	4	26 \pm 1	35 \pm 1	9	35 \pm 1	57 \pm 1	64 \pm 1

^a 33 days.^b 37 days.

23 and **24** reached biodegradation plateaus in 28 days: 68 %, 71 % and 57 % respectively. **22** and **23** could be classified as biodegradable. **25** reached 57 % in 28 days but after extended CBT passed the 60 % threshold and reached 64 % in 42 days. Overall, analysis of PTPs of **3–6** shows that, in general, hydrophobic phenylalanine moiety improves biodegradability compared to alanine residue. All PTPs of Phe-Ala dipeptide IL **4** passed the 60 % threshold in extended CBT with 42 days.

All four studied dipeptide ILs contained a pyridinium headgroup. Pyridinium cations with short alkyl chains have previously shown poor biodegradability [54,55]. Docherty and Neumann also reported, however, very substantial improvement in biodegradability when pyridinium headgroup was substituted with a long

alkyl chain or if the alkyl chain contained hydrolysable groups. Our results support these and other previously reported findings about substituted pyridinium headgroup's good biodegradability and ability to be mineralizable [33,34,56–58]. However, we also identified a long induction period in pyridinium sub-unit's biodegradation. This induction period, lasting up to ~ 20 days is illustrated well in biodegradation curve of **11** (Figs. 2, 3, and S5–11). Similar pyridinium-induced induction period was reported by Zhang who studied effect of [EtPy][BF₄] on *P. fluorescens* [59]. This long induction period was also the reason why CBT duration was extended from standard 28 days to 33–42 days to allow better observation of biodegradation and to gain more information which could help with future studies of IL biodegradability.

Alanine and phenylalanine biodegradability have been studied using amino acids as anions to cholinium cation [52,53]. In both studies alanine and phenylalanine ILs passed biodegradation test and results are similar to the ones reported in this paper: alanine biodegradation was 80 % (Yazdani. [53]); 64 % (Hou. [52]) and 62 % (current study) in these three studies while phenylalanine biodegradation was 71 % (Yazdani. [53]); 74 % (Hou. [52]) and 74 % (current study). This is a promising result as amino acids, with their possibility of sourcing from renewable materials, are good candidates to prepare environmentally friendly and green chemicals.

Standard biodegradation tests are usually considered passed when a threshold representing degradation of 60 % is achieved. In case of ready biodegradability this threshold has to be reached fast, usually in a 10-day-window after degradation process has begun [51]. This rapid degradation is good as it means less time for the compound to have any effect on the environment, but it also means that a compound passing standard biodegradation test can leave up to 40 % persistent organic pollutants. Furthermore, this type of evaluation gives little indication to what transformations take place with the compound. It is possible that the transformation product itself is recalcitrant or even toxic. For this reason, we argue that it can also be beneficial to study compounds which might go through slower biodegradation but eventually are completely mineralized: transformed into inorganic carbon dioxide, water etc.

OECD 301D guidelines state that for a compound to be classified as „readily biodegradable” it must achieve at least 60 % biodegradation in the following 10 days after reaching 10 % degradation [51]. This is not achieved by phenylalanine IL **1** (Table 1; Figure S5-1) which has been previously studied and is known to be completely mineralizable in 42 days, but was biodegraded 45 % at the end of its 10-day-window. Even lower biodegradation was shown by alanine IL **2** which passed 10 % already at second day of the test but was only degraded by 20 % 10 days later (Table 1; Figure S5-2). Interestingly, PTP **11**, which is also previously known to be completely mineralizable, showed a long induction period for the first 20 days, after which it started to rapidly biodegrade. By OECD guidelines, PTP **11** could not be classified as readily biodegradable, but after 42 days it showed 93 % biodegradation, giving strong indication that PTP **11** is mineralizable in used test conditions. PTP **11** was a key transformation product forming from all our IL parent compounds through various possible degradation pathways and this observed long induction period (and following mineralization) was one of the reasons for prolonging CBT tests to 33–42 days to allow seeing if other compounds behaved similarly. Another compound with long ca 20-day induction period was PTP **8**, the esterolysis product of IL **2**. Unlike **11**, **8** never passed the 60 % threshold during 42 days of CBT.

None of the dipeptide IL parent compounds were shown to be readily biodegradable, however **3** and **4** were very close and reached 55 % and 59 % respectively in the 10-day-window. In addition to giving the highest biodegradability, **3** and **4** were also degraded rapidly, further confirming that changing the amino acid residue to hydrophobic phenylalanine near the positively charged pyridinium sub-unit helped improve the cation's biodegradability. Dipeptide ILs **5** and **6** showed much slower biodegradation and **6** had a long induction period for the first 13 days. Out of all tested 25 compounds only PTPs **10** and **23** can be classified as readily biodegradable having met the criteria of being biodegraded > 60 % in the first 10 days after they had been degraded by 10 %. This shows the importance of studying both the parent compounds and their PTPs, as it gives more information about how the compounds could behave when disposed. Extending the test for another two weeks (42 days in total) is another good practice if mechanisms of biodegradation are studied as even more

information is gathered and biodegradability of test compounds can be evaluated more objectively.

Based on results from toxicity screening and biodegradation studies we propose preferable ILs and PTPs to be used in design of benign and sustainable chemicals: phenylalanine IL **1**, Phe-Phe and Phe-Ala ILs **3** and **4**, esterolysis product **7**, amidolysis products **9**, **10**, **11**, **19**, **20**, **21**, transformation products **22**, **23** and amino acid phenylalanine (**12**) which all can be classified as biodegradable. A little more problematic were Ala-Phe and Ala-Ala ILs **5** and **6**, esterolysis product **15**, amidolysis products **18**, PTP **25** and amino acid alanine (**13**) which showed slower biodegradation but passed the 60 % threshold in prolonged 42 days of CBT. Caution is advised when integrating alanine IL **2**, its esterolysis product **8** or dipeptide esterolysis products **14**, **16**, **17** PTP **24** into the design of new chemicals as these compounds were shown to be poorly biodegradable.

4. Conclusions

To gain an improved understanding of pyridinium ILs biodegradation a series of L-phenylalanine and L-alanine ILs were evaluated. Their possible degradation pathways and resulting TP were proposed and all required ILs and TPs synthesized. These compounds (25 in total) underwent microbial toxicity screening, aerobic biodegradation testing and resulted in a valuable dataset which enabled concurrent analysis of ILs and their PTPs.

One of the key findings was that addition of a second amino acid resulted in dipeptide ILs with improved biodegradability. Specifically, the addition of a second alanine or phenylalanine residue improved biodegradation percentages for all studied ILs. In addition to the amino acid residue present, its position in the dipeptide IL structure also significantly affected the biodegradability of the compound. For example, Phe-Ala IL (**4**), where phenylalanine is in close proximity to the positively charged pyridinium sub-unit, gave higher biodegradation percentages compared to Ala-Phe IL (**5**). Overall, the best biodegradability was observed with Phe-Ala IL (**4**) which was biodegraded 83 % in 28 days and reached up to 91 % in a prolonged CBT of 42 days.

Analysis of PTPs also showed that presence of an alanine residue gave problematic (i.e. more persistent) PTPs compared to most PTPs containing phenylalanine. This was especially the case when alanine was in close proximity to the pyridinium headgroup. Based on both toxicity and biodegradation testing results preferable and less preferable fragments can be chosen for design of new sustainable chemicals based on amino acids.

The modified CBT allows for a measurement of biodegradability with many datapoints (potentially daily) which together with extension of the test period can provide valuable information for future studies of biodegradability and TP investigations. Where biodegradable TPs are found they could be incorporated into the structure of ILs and released via known breakdown pathways.

Results from this study demonstrate a potential of designing new sustainable ILs using amino acid moieties as part of their structure. Combining these functional groups together can create biodegradable ILs with low toxicity which can be used as model compounds when studying biodegradation mechanisms.

CCRediT authorship contribution statement

Illia V. Kapitanov: Methodology, Data curation, Writing – original draft, Conceptualization, Writing – review & editing. **Grete Raba:** Methodology, Data curation, Writing – original draft, Conceptualization. **Marcel Špulák:** Methodology, Data curation, Funding acquisition. **Raivo Vilu:** Conceptualization, Writing – review & editing. **Yevgen Karpichev:** Conceptualization, Methodology, Funding acquisition, Data curation, Writing – original draft, Writ-

ing – review & editing, **Nicholas Gathergood**: Conceptualization, Methodology, Data curation, Writing – original draft, Writing – review & editing, Funding acquisition.

Data availability

Data will be made available on request.

Declaration of Competing Interest

The authors declare that they have no known competing financial interests or personal relationships that could have appeared to influence the work reported in this paper.

Acknowledgements

The authors acknowledge funding from European Union's Seventh Framework Programme for Research, Technological Development, and Demonstration under Grant Agreement no. 621364 (TUTIC-Green), and Estonian Research Council grants PUT1656 (IK, GR, YK, and NG) and COVSG5 (YK). The project was partially funded by the Czech Science Foundation (project No. 22-19209S). The authors thank Jelena Valtin and AS Tallinna Vesi for providing wastewater treatment plant effluent necessary for performing aerobic biodegradation tests in this study.

Appendix A. Supplementary material

Supplementary data to this article can be found online at <https://doi.org/10.1016/j.molliq.2023.121285>.

References

- [1] P. Walden, Molecular weights and electrical conductivity of several fused salts, *Bul. Imp. Acad. Sci.* 1800 (1914) 405–422.
- [2] M. Koel, Ionic liquids in chemical analysis, *Crit. Rev. Anal. Chem.* 35 (3) (2005) 177–192, <https://doi.org/10.1080/10408340500304016>.
- [3] J.S. Wilkes, A short history of ionic liquids - from molten salts to neoteric solvents, *Green Chem.* 4 (2) (2002) 73–80, <https://doi.org/10.1039/b110838g>.
- [4] N.V. Plechkova, K.R. Seddon, Applications of Ionic Liquids in the Chemical Industry, *Chem. Soc. Rev.* 37 (1) (2008) 123–150, <https://doi.org/10.1039/b006677j>.
- [5] A.J. Greer, J. Jacquemin, C. Hardacre, Industrial applications of ionic liquids, *Molecules* 25 (21) (2020) 5207, <https://doi.org/10.3390/molecules25215207>.
- [6] M. Freemantle, BASF's smart ionic liquid, *Chem. Eng. News* (2003) 9, <https://doi.org/10.1021/cen-v081n013.p009>.
- [7] M. Maase, K. Massonne, K. Halbritter, Method for the separation of acids from chemical reaction mixtures by means of ionic fluids, US7351339B, 2008.
- [8] G.W. Phillips, S.N. Falling, S.A. Godleski, J.R. Monnier, Continuous Process for the Manufacture of 2,5-Dihydrofurans from γ , δ -Epoxybutenes. US5315019A, US5315019A, 1994.
- [9] P.J. Piedade, E. Kochańska, R.M. Lukasik, Biodegradable ionic liquids in service of biomass upgrade, *Curr. Opin. Green Sustain. Chem.* 35 (2022), <https://doi.org/10.1016/j.cogsc.2022.100609>.
- [10] P. Pillai, M. Maiti, A. Mandal, Mini-review on recent advances in the application of surface-active ionic liquids: petroleum industry perspective, *Energy Fuel* 36 (15) (2022) 7925–7939, <https://doi.org/10.1021/acs.energyfuels.2c00964>.
- [11] S.S. de Jesus, R. Maciel Filho, Are ionic liquids eco-friendly?, *Renew Sustain. Energy Rev.* 157 (2022), <https://doi.org/10.1016/j.rser.2021.112039>.
- [12] A.R.P. Gonçalves, X. Paredes, A.F. Cristino, F.J.V. Santos, C.S.G.P. Queirós, Ionic Liquids—A review of their toxicity to living organisms, *Int. J. Mol. Sci.* 22 (11) (2021) 5612, <https://doi.org/10.3390/ijms22115612>.
- [13] P. Anastas, N. Eghbali, Green chemistry: principles and practice, *Chem. Soc. Rev.* 39 (1) (2010) 301–312, <https://doi.org/10.1039/b918763b>.
- [14] D. Kowalska, J. Maculewicz, P. Stepnowski, J. Dołżonek, Ionic liquids as environmental hazards – crucial data in view of future PBT and PMT assessment, *J. Hazard. Mater.* 403 (2021), <https://doi.org/10.1016/j.jhazmat.2020.123896>.
- [15] F. Billeci, F. D'anna, M. Feroci, P. Cancemi, S. Feo, A. Forlino, F. Tonnelli, K.R. Seddon, H.Q.N. Gunaratne, N.V. Plechkova, When functionalization becomes useful: ionic liquids with a "Sweet" appended moiety demonstrate drastically reduced toxicological effects, *ACS Sustain. Chem. Eng.* 8 (2) (2020) 926–938, <https://doi.org/10.1021/acssuschemeng.9b05507>.
- [16] A.-K. Amsel, O. Olsson, K. Kümmerer, Inventory of biodegradation data of ionic liquids, *Chemosphere* 299 (2022) 134385, <https://doi.org/10.1016/j.chemosphere.2022.134385>.
- [17] A.A. Quintana, A.M. Sztapka, V. de C. Santos Ebinuma, C. Agatemor, Enabling sustainable chemistry with ionic liquids and deep eutectic solvents: A fad or the future?, *Angew. Chem. Int. Ed.* 61 (37) (2022), <https://doi.org/10.1002/anie.202205609>.
- [18] M. Cvjetko Bubalo, K. Radošević, I. Radojčić Redovniković, J. Halambek, V. Gaurina Srček, A brief overview of the potential environmental hazards of ionic liquids, *Ecotoxicol. Environ. Saf.* 99 (2014) 1–12, <https://doi.org/10.1016/j.jecoen.2013.10.019>.
- [19] A. Brzęczek-Szafran, P. Więcek, M. Guzik, A. Chrobok, Combining amino acids and carbohydrates into readily biodegradable, task specific ionic liquids, *RSC Adv.* 10 (31) (2020) 18355–18359.
- [20] J.B. Zimmerman, P.T. Anastas, H.C. Erythropel, W. Leitner, Designing for a green chemistry future, *Science*, 367 (6476) (2020) 397–400, <https://doi.org/10.1126/science.aay3060>.
- [21] E.M. Siedlecka, M. Czerwica, J. Neumann, P. Stepnowski, J.F. Fernández, J. Thöming, Ionic liquids: methods of degradation and recovery, in: A. Kokorin (Ed.), *Ionic Liquids: Theory, Properties, New Approaches*, InTech, 2011, <https://doi.org/10.1016/j.colsurfa.2011.12.014>.
- [22] A. Jordan, N. Gathergood, Biodegradation of ionic liquids - a critical review, *Chem. Soc. Rev.* 44 (22) (2015) 8200–8237, <https://doi.org/10.1039/C5CS00444F>.
- [23] D. Coleman, N. Gathergood, Biodegradation studies of ionic liquids, *Chem. Soc. Rev.* 39 (2) (2010) 600–637, <https://doi.org/10.1039/B817717C>.
- [24] J. Ranke, S. Stolte, R. Störmann, J. Arning, B. Jastorff, Design of sustainable chemical products - the example of ionic liquids, *Chem. Rev.* 107 (6) (2007) 2183–2206.
- [25] L. Ferrazzano, M. Catani, A. Cavazzini, G. Martelli, D. Corbisiero, P. Cantelmi, T. Fantoni, A. Mattellone, C. de Luca, S. Felletti, W. Cabri, A. Tolomelli, Sustainability in peptide chemistry: current synthesis and purification technologies and future challenges, *Green Chem.* 24 (3) (2022) 975–1020, <https://doi.org/10.1039/D1GC04387K>.
- [26] S.I. Abu-Eishah, Ionic liquids recycling for reuse, in: S. Handy (Ed.), *Ionic Liquids - Classes and Properties*, InTech, 2011, <https://doi.org/10.1016/j.colsurfa.2011.12.014>.
- [27] W. Wilms, M. Woźniak-Karczewska, A. Syguda, M. Niemczak, L. Ławniczak, J. Pernak, R.D. Rogers, L. Chrzanowski, Herbicidal ionic liquids: A promising future for old herbicides? Review on synthesis, toxicity, biodegradation, and efficacy studies, *J. Agric. Food Chem.* 68 (39) (2020) 10456–10488.
- [28] M.J. Earle, K.R. Seddon, Ionic liquids: green solvents for the future, *ACS Symp. Ser.* 819 (7) (2002) 10–25, <https://doi.org/10.1021/bk-2002-0819.ch002>.
- [29] X. Xu, F. He, W. Yang, J. Yao, Effect of homochirality of dipeptide to polymers' degradation, *Polymers (Basel)* 12 (9) (2020) 2164, <https://doi.org/10.1039/polyim12092164>.
- [30] L. Morandeira, A. Martínez-Baltasar, M.Á. Sanromán, A. Rodríguez, F.J. Deive, Designing novel biocompatible oligopeptide-based ionic liquids for greener downstream processes, *J. Clean. Prod.* 279 (2021), <https://doi.org/10.1016/j.jclepro.2020.123356>.
- [31] D. Skarpacez, A. Tzani, E. Avraam, C. Politidis, A. Kyritsis, A. Detsi, Synthesis, structure-properties relationship and biodegradability assessment of novel protic ionic liquids, *J. Mol. Liq.* 344 (2021), <https://doi.org/10.1016/j.molliq.2021.117754>.
- [32] S.J. Pandya, I.V. Kapitanov, Z. Usmani, R. Sahu, D. Sinha, N. Gathergood, K.K. Ghosh, Y. Karpichev, An example of green surfactant systems based on inherently biodegradable IL-derived amphiphilic oximes, *J. Mol. Liq.* 305 (2020) 112857.
- [33] A. Haiß, A. Jordan, J. Westphal, E. Logunova, N. Gathergood, K. Kümmerer, On the way to greener ionic liquids: identification of a fully mineralizable phenylalanine-based ionic liquid, *Green Chem.* 16 (2016) 4361–4373, <https://doi.org/10.1039/C6CG000417B>.
- [34] A. Jordan, A. Haiß, M. Špulák, Y. Karpichev, K. Kümmerer, N. Gathergood, Synthesis of a series of amino acid derived ionic liquids and tertiary amines: green chemistry metrics including microbial toxicity and preliminary biodegradation data analysis, *Green Chem.* 16 (2016) 4374–4392, <https://doi.org/10.1039/C6CG000415F>.
- [35] M. Suk, A. Haiß, J. Westphal, A. Jordan, A. Kellett, I.V. Kapitanov, Y. Karpichev, N. Gathergood, K. Kümmerer, Design rules for environmental biodegradability of phenylalanine alkyl ester linked ionic liquids, *Green Chem.* 22 (14) (2020) 4498–4508.
- [36] D. Coleman, M. Špulák, M.T. Garcia, N. Gathergood, Antimicrobial toxicity studies of ionic liquids leading to a "hit" MRSA selective antibacterial imidazolium salt, *Green Chem.* 14 (5) (2012) 1350–1356, <https://doi.org/10.1039/C2GC16090K>.
- [37] I.F. Mena, E. Diaz, J. Palomar, J.J. Rodriguez, A.F. Mohedano, Cation and anion effect on the biodegradability and toxicity of imidazolium- and choline-based ionic liquids, *Chemosphere* (2020) 240, <https://doi.org/10.1016/j.chemosphere.2019.124947>.
- [38] N. Delgado-Mellado, M. Ayuso, M.M. Villar-Chavero, J. García, F. Rodríguez, Ecotoxicity evaluation towards vibrio fischeri of imidazolium- and pyridinium-based ionic liquids for their use in separation processes, *SN Appl. Sci.* (2019) 896, <https://doi.org/10.1007/s42452-019-0916-3>.
- [39] I.V. Kapitanov, A. Jordan, Y. Karpichev, M. Špulák, L. Perez, A. Kellett, K. Kümmerer, N. Gathergood, Synthesis, self-assembly, bacterial and fungal toxicity, and preliminary biodegradation studies of a series of Toxi-

- phenylalanine-derived surface-active ionic liquids, *Green Chem.* 21 (7) (2019) 1777–1794, <https://doi.org/10.1039/C9GC00030E>.
- [40] D.K.A. Kusumahastuti, M. Sihtmäe, I.V. Kapitanov, Y. Karpichev, N. Gathergood, A. Kahru, Toxicity profiling of 24 L-phenylalanine derived ionic liquids based on pyridinium, imidazolium and cholinium cations and varying alkyl chains using rapid screening vibrio Fischeri assay, *Ecotoxicol. Environ. Saf.* 172 (2019) 556–565, <https://doi.org/10.1016/j.ecoenv.2018.12.076>.
 - [41] M. Trush, L. Metelytsia, I. Semenyuta, L. Kalashnikova, O. Papeykin, I. Venger, O. Tarasyuk, L. Bodachivska, V. Lagodatnyi, S. Rogalsky, Reduced ecotoxicity and improved biodegradability of cationic biocides based on ester-functionalized pyridinium ionic liquids, *Environ. Sci. Pollut. Res.* 26 (2019) 4878–4889, <https://doi.org/10.1007/s11356-018-3924-8>.
 - [42] K.M. Docherty, C.F. Kulpa, Toxicity and antimicrobial activity of imidazolium and pyridinium ionic liquids, *Green Chem.* 7 (4) (2005) 185–189, <https://doi.org/10.1039/b419172b>.
 - [43] D.K.A. Kusumahastuti, M. Sihtmäe, V. Aruoja, N. Gathergood, A. Kahru, Ecotoxicity profiling of a library of 24 L-phenylalanine derived surface-active ionic liquids (SAILs), *Sustain. Chem. Pharm.* 19 (2021), <https://doi.org/10.1016/j.scp.2020.100369>.
 - [44] G. Kaur, L.A. Abramovich, E. Gazit, S. Verma, Ultrastructure of metalloproteinase-based soft spherical morphologies, *RSC Adv.* 4 (110) (2014) 64457–64465, <https://doi.org/10.1039/C4RA10532J>.
 - [45] E. Schröder, K. Lübke, *The Peptides Volume 1: Methods of Peptide Synthesis*, Academic Press, New York and London, 1965.
 - [46] C.R. McElroy, A. Constantinou, L.C. Jones, L. Summerton, J.H. Clark, Towards a holistic approach to metrics for the 21st century pharmaceutical industry, *Green Chem.* 17 (5) (2015) 3111–3121, <https://doi.org/10.1039/C5GC00340G>.
 - [47] ESCMID. (ESCMID) European Committee for Antimicrobial Susceptibility Testing (EUCAST) of the European Society of Clinical Microbiology and Infectious Diseases. Eucast Discussion Document E. Dis 5.1. Determination of Minimum Inhibitory Concentrations (MICs) of An. Clinical Microbiology and Infection, 2003.
 - [48] EUCAST. Method for the Determination of Broth Dilution Minimum Inhibitory Concentrations of Antifungal Agents for Conidia Forming Moulds - EUCAST Definitive Document EDEF 9.3.1.; 2015.
 - [49] EUCAST. Method for the Determination of Broth Dilution Minimum Inhibitory Concentrations of Antifungal Agents for Yeasts - EUCAST Definitive Document EDEF 7.3.1.; 2017.
 - [50] J. Friedrich, A. Längin, K. Kümmerer, Comparison of an electrochemical and luminescence-based oxygen measuring system for use in the biodegradability testing according to closed bottle Test (OECD 301D), *Clean (Weinh)* 41 (3) (2013) 251–257, <https://doi.org/10.1002/cle.201100558>.
 - [51] OECD. OECD Guideline for Testing of Chemicals - Ready Biodegradability. 1992.
 - [52] X.-D. Hou, Q.-P. Liu, T.J. Smith, N. Li, M.-H. Zong, V. Bansal, Evaluation of toxicity and biodegradability of cholinium amino acids ionic liquids, *PLoS One* 8 (3) (2013) e59145.
 - [53] A. Yazdani, M. Sivapragasam, J.M. Leveque, M. Moniruzzaman, Microbial biocompatibility and biodegradability of choline-amino acid based ionic liquids, *J. Microb. Biochem. Technol.* 08 (05) (2016), <https://doi.org/10.4172/1948-5948.1000318>.
 - [54] J. Neumann, S. Steudte, C.-W. Cho, J. Thöming, S. Stolte, Biodegradability of 27 pyrrolidinium, morpholinium, piperidinium, imidazolium and pyridinium ionic liquid cations under aerobic conditions, *Green Chem.* 4 (2014) 2174–2184, <https://doi.org/10.1039/C3GC41997E>.
 - [55] K.M. Docherty, J.K. Dixon, C.F. Kulpa Jr, Biodegradability of imidazolium and pyridinium ionic liquids by an activated sludge microbial community, *Biodegradation* 18 (2007) 481–493, <https://doi.org/10.1007/s10532-006-9081-7>.
 - [56] Y. Deng, I. Beadham, M. Ghavre, M.F. Gomes, N. Gathergood, P. Husson, B. Légeret, B. Quilty, M. Sancelme, P. Besse-Hoggan, When can ionic liquids be considered readily biodegradable? Biodegradation pathways of pyridinium, pyrrolidinium and ammonium-based ionic liquids, *Green Chem.* 3 (2015) 1479–1491, <https://doi.org/10.1039/C4GC01904K>.
 - [57] K.M. Docherty, M.V. Joyce, K.J. Kulacki, C.F. Kulpa, Microbial biodegradation and metabolite toxicity of three pyridinium-based cation ionic liquids, *Green Chem.* 12 (4) (2010) 701.
 - [58] T.P.T. Pham, C.-W. Cho, C.-O. Jeon, Y.-J. Chung, M.-W. Lee, Y.-S. Yun, Identification of metabolites involved in the biodegradation of the ionic liquid 1-butyl-3-methylpyridinium bromide by activated sludge microorganisms, *Environ. Sci. Tech.* (2009) 516–521, <https://doi.org/10.1021/es703004h>.
 - [59] C. Zhang, S.V. Malhotra, A.J. Francis, Toxicity of imidazolium- and pyridinium-based ionic liquids and the co-metabolic degradation of N-ethylpyridinium tetrafluoroborate, *Chemosphere* 82 (11) (2011) 1690–1695.

Appendix 4

Publication IV

Kapitanov, I.V.; Sudheer, S.M.; Yadav, T.; Ghosh, K.K.; Gathergood, N.; Gupta, V.K.; Karpichev, Y. Sustainable phenylalanine-derived SAILs for solubilization of polycyclic aromatic hydrocarbons. *Molecules* **2023**, *28*, 4185

Reproducing is permitted by MDPI Open Access Information and Policy / open access Creative Common CC BY license.

Article

Sustainable Phenylalanine-Derived SAILs for Solubilization of Polycyclic Aromatic Hydrocarbons

Illia V. Kapitanov ^{1,†} , Surya M. Sudheer ¹, Toshikee Yadav ^{1,2}, Kallol K. Ghosh ², Nicholas Gathergood ³ , Vijai K. Gupta ^{1,4}  and Yevgen Karpichev ^{1,*} 

¹ Department of Chemistry and Biotechnology, Tallinn University of Technology (TalTech), 12618 Tallinn, Estonia; vijai.gupta@sruc.ac.uk (V.K.G.)

² School of Studies in Chemistry, Pt. Ravishankar Shukla University, Raipur 92010, India; kallolkghosh@gmail.com

³ School of Chemistry, College of Science, University of Lincoln, Lincoln LN6 7TS, UK; ngathergood@lincoln.ac.uk

⁴ Biorefining and Advanced Materials Research Centre, SRUC, Parkgate, Dumfries DG1 3NE, UK

* Correspondence: yevgen.karpichev@taltech.ee; Tel.: +372-620-4381

† Current address: Gemini PharmChem Mannheim GmbH, 68305 Mannheim, Germany.

Abstract: The solubilization capacity of a series of sustainable phenylalanine-derived surface-active ionic liquids (SAILs) was evaluated towards polycyclic aromatic hydrocarbons—naphthalene, anthracene and pyrene. The key physico-chemical parameters of the studied systems (critical micelle concentration, spectral properties, solubilization parameters) were determined, analyzed and compared with conventional cationic surfactant, CTABr. For all studied PAH solubilization capacity increases with extension of alkyl chain length of PyPheOC_n SAILs reaching the values comparable to CTABr for SAILs with n = 10–12. A remarkable advantage of the phenylalanine-derived SAILs PyPheOC_n and PyPheNHC_n is a possibility to cleave enzymatically ester and/or amide bonds under mild conditions, to separate polycyclic aromatic hydrocarbons in situ. A series of immobilized enzymes was tested to determine the most suitable candidates for tunable decomposition of SAILs. The decomposition pathway could be adjusted depending on the choice of the enzyme system, reaction conditions, and selection of SAILs type. The evaluated systems can provide selective cleavage of the ester and amide bond and help to choose the optimal decomposition method of SAILs for enzymatic recycling of SAILs transformation products or as a pretreatment towards biological mineralization. The concept of a possible practical application of studied systems for PAHs solubilization/separation was also discussed focusing on sustainability and a green chemistry approach.

Keywords: surface-active ionic liquids (SAILs); enzymatic decomposition; biodegradability; sustainability; solubilization; polycyclic aromatic hydrocarbons (PAHs)



Citation: Kapitanov, I.V.; Sudheer, S.M.; Yadav, T.; Ghosh, K.K.; Gathergood, N.; Gupta, V.K.; Karpichev, Y. Sustainable Phenylalanine-Derived SAILs for Solubilization of Polycyclic Aromatic Hydrocarbons. *Molecules* **2023**, *28*, 4185. <https://doi.org/10.3390/molecules28104185>

Academic Editor: Owen Curnow

Received: 30 April 2023

Revised: 16 May 2023

Accepted: 17 May 2023

Published: 19 May 2023



Copyright: © 2023 by the authors. Licensee MDPI, Basel, Switzerland. This article is an open access article distributed under the terms and conditions of the Creative Commons Attribution (CC BY) license (<https://creativecommons.org/licenses/by/4.0/>).

1. Introduction

Ionic liquids (ILs) have been widely used in many industries [1–3] and are one of the core focuses of research over the past two decades [4,5]. ILs are proposed as more desirable than conventional volatile solvents in many physical and chemical processes, often referred as “green” solvents [6]. They can be of natural origin and be prepared by a “benign by design” approach [5,7]. Designing ILs that lead to a reduction in the losses of solvents as well as less damage to the environment is an important aspect in green chemistry [6]. Ionic liquids in general fulfil many of the 12 criteria as a green solvent related to the availability, price, recyclability, synthesis, toxicity, biodegradability, performance, stability, flammability, storage, and renewability [8]. Ionic liquids can offer a better alternative to volatile solvents, which has led to its massive use in industrial applications such as separation and purification, and as chemical catalysts, biorefinery concepts [3], extractions [1] and others [9–12]

Recently, research studies have revealed that some of these ILs demonstrate a significant toxicity level [13,14]. Though the toxicity evaluations of ILs have been extensively reported in the literature, biodegradation data are comparatively limited [15]. Biodegradation is considered as the cleanest ultimate fate for compounds in nature. Although ILs can be easily synthesized, often in only a few steps, it is important to ensure that they are fully mineralizable in case of their introduction into the environment. ILs' persistence in nature, due to their high stability, would result in adverse environmental toxicity [16]. It can lead to problematic wastewater pollution upon release into the environment because ILs, which are highly water soluble and not consistently biodegradable in wastewater aeration tanks, can have varying degrees of biodegradability [17]. The toxicity of ILs is related to the sorption of a surfactant molecule to biological membranes, which is driven by the nonspecific hydrophobic interactions [18]. Such adsorption of surfactants disrupts the cellular membranes and results in acute or chronic effects in microbes. The hydrophobic/hydrophilic balance of the molecule and the cationic charge density ultimately results in antimicrobial activity [19].

The synthesis and investigation of ILs using natural structural elements is a prospective approach in designing new molecules [7,20–24]. The ILs based on the amino acids are considered as one of the green alternatives and have high demand in industrial applications, which lead to the further development of a benign by design approach for the elaboration of an L-phenylalanine ethyl ester platform for designing completely mineralizable ILs [23,25]. After all, biodegradation of a newly synthesized compound can be firstly screened by test methods recommended by OECD guidelines [26,27] and the development in analytical methods such as LC-MS and NMR make it easier to detect the degraded products with a limited sample volume.

In order to describe ILs as a greener solvent, one should show complete and rapid biotic/abiotic degradation in nature. It is worth noting that there is often very little correlation between (i) the rate of chemical and enzymatic hydrolysis and (ii) the rate of biodegradation [28,29]. The biodegradability of ILs depends on their molecular structure [30] and the length of the alkyl chain [7,31,32]. Some ILs are stable to a wide range of chemicals as well as to high temperature, which are not expected to be readily biodegradable [33]. Pyridinium, cholinium, and imidazolium cations are the most studied among IL cations [34–36]. Pyridinium ILs are, in general, biodegradable to a higher extent than imidazolium ILs [23,25]. Thus, in the work [25], it was reported that the combination of ionic head groups with readily biodegradable biomolecules did not necessarily lead to an increase in biodegradability or degradation of the compound. The imidazolium- and pyridinium-derived phenylalanine ethyl ester ILs were shown to be more biodegradable than the proline and choline derivatives [23]. Recent studies provided an insight into the biodegradability of the ethyl ester of cationic phenylalanine-derived ILs [24]. The pyridinium derivatives are found to be the preferred greener IL based on synthesis, toxicity, and biodegradation considerations [7]. Among ILs, special interests are the compounds, which contain significant hydrophobic fragments in their structure and demonstrate remarkable adsorption onto surfaces and change their properties (so-called surface-active ionic liquids, SAILs) [32].

The extraction and separation of polycyclic aromatic hydrocarbons (PAHs) are challenging problems [4] having both technological and environmental impacts [37]. Applying a water/surfactant system instead of organic solvents can particularly solve the aforementioned problems and make systems “greener” [38]. Water solutions of low toxic and biodegradable SAILs are prospective alternatives to conventional surfactants in the creation of sustainable ecologically friendly mixed compositions [39].

In this study, we evaluated the efficacy of pyridinium SAILs in the solubilization of model representative PAHs (naphthalene, anthracene and pyrene) in water/SAIL systems (Figure 1) and proved a strategy for direct degradation/hydrolysis of these SAILs by commercial enzymes. This concept can be applied in the design of recyclable environmentally friendly systems for PAHs solubilization/separation.

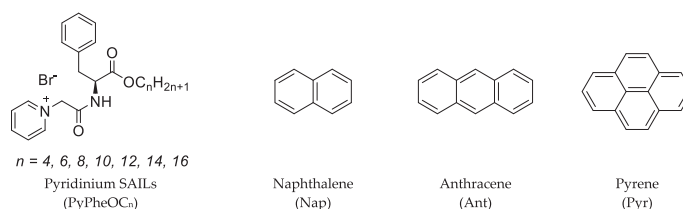


Figure 1. Structures of studied pyridinium SAILs and polycyclic aromatic hydrocarbons.

2. Results and Discussion

2.1. Study of Solubilization Capacity

The solubilization capacity of PyPheOC_n surfactants ($n = 4, 6, 8, 10, 12, 14, 16$) was evaluated, related to model representative PAH (naphthalene, anthracene and pyrene) and compared with the solubilization capacity of the widely used conventional cationic surfactant cetyltrimethylammonium bromide (CTABr) (Table 1).

Table 1. Critical micelle concentration (cmc), β parameter and solubilization capacity (S) for PyPheOC_n surfactants, and cetyltrimethylammonium bromide (CTABr).

PyPheOC _n Chain Length (n)	Surface Tension	cmc , mM				β			Solubilization Capacity (S)		
		Conductivity	Solubilization			Nap	Ant	Pyr	Nap	Ant	Pyr
			Nap	Ant	Pyr						
4	57	89	80	90	80	21.4	5.6	90.4	0.067	0.00037	0.0014
6	11	19.9	25	23	26	32.7	9	251.9	0.102	0.00060	0.0040
8	2.25	4.9	5.2	3.7	4.9	36.9	11.7	366.6	0.115	0.00077	0.0058
10	0.65	1.6	1.6	1	1.4	48.1	27.9	503	0.150	0.00185	0.0080
12	0.19	0.5	0.2	0.1	0.3	67.1	31.3	745.7	0.210	0.00207	0.0119
14	0.056	0.18	0.1	0.07	0.08	84.9	47.4	905.2	0.265	0.00314	0.0144
16	0.0125	0.037	0.05	0.04	0.05	100.5	60.3	996	0.314	0.00399	0.0159
CTABr	0.9	1	1	1	0.8	62.5	43.9	573.6	0.195	0.00291	0.0091

Notes. Values of critical micelle concentration (cmc) for PyPheOC_n surfactants, determined by surface tension and conductivity methods, were taken from Kapitanov et al. [32]. Values of critical micelle concentration (cmc) for CTABr, determined by surface tension and conductivity methods, were taken from Serdyuk et al. [38].

The observed regularities for dependencies “concentration of PyPheOC_n–PAH absorbance” are typical for such types of systems [38,40–42]: below the cmc , no dramatical changes of PAH concentration (absorbance) in the solution appeared, but beyond the cmc , an increasing of PAH concentration (absorbance) in the solution was observed (Figure 2). The brake-point on dependencies “concentration of PyPheOC_n–PAH absorbance” corresponds to the cmc of the studied SAILs. The cmc values for PyPheOC_n SAILs and CTABr, obtained with different PAH, correspond well with each other and with the cmc of these compounds, determined using surface tension and conductivity measurements (Table 1; see also [32]).

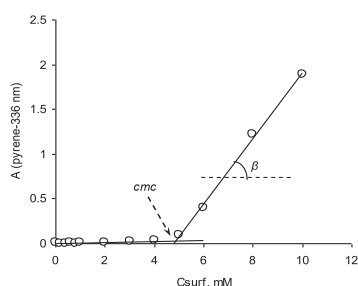


Figure 2. Dependence of the PAH absorbance vs. concentration of SAILs for the system PyPheOC₁₀/pyrene: determination of cmc and β parameters.

For all studied PAH, the solubilization capacity increases with an extension of the alkyl chain length of PyPheOC_n SAILs (Figure 3). The solubilization capacity, comparable with CTABr, demonstrates PyPheOC_n with $n = 10$ –12 (naphthalene, pyrene) and $n = 12$ –14 (anthracene). It corresponds to aggregation properties of the studied compounds: the *cmc* of CTABr are similar to PyPheOC_n with $n = 10$ –12 (Table 1).

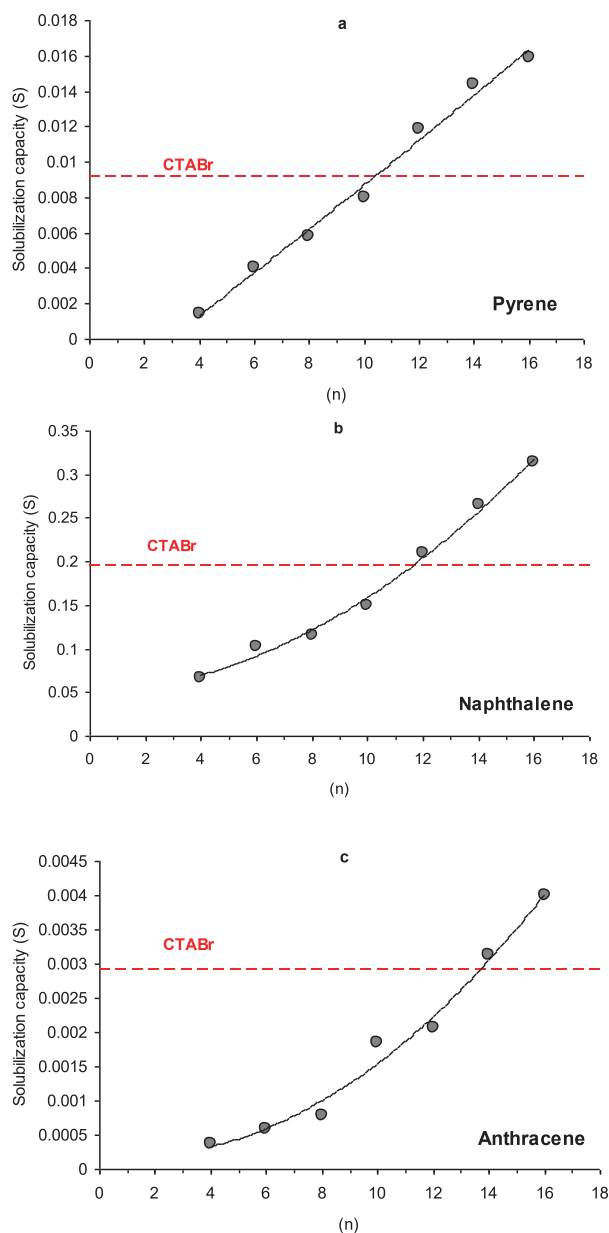


Figure 3. Dependencies of solubilization capacity (S) on alkyl chain length (n) of PyPheOC_n SAILs towards pyrene (a), naphthalene (b), and anthracene (c) compared to solubilization capacity of CTABr.

2.2. Study of Enzymatic Degradation/Hydrolysis of PyPheOC_n SAILs

Selecting a suitable enzyme which has higher degradation potential over the chemical compounds is very important [43,44]. Amidase and protease are the most representative groups of enzymes belonging to the class hydrolases in the remediation of polluted environments. The breakdown of ester, amide and peptide bonds by esterases, amidases and proteases may lead to products with little or no toxicity [45]. A previous report by Neumann et al. [46] shows that primary biodegradation of the test samples cyanomethyl side chain and its transformation product was enabled by a microorganism. This suggests that hydrolysis happened via nitrile degrading enzymes such as nitrilases or nitrile hydratases together with amidase. These studies support the role of the amidase enzyme as a catalyst for the biodegradation. Similar studies also reported that enzymes such as nitrilases and amidase are commonly applied as catalysts in organic synthesis for the hydrolysis of nitrile groups in the pharmaceutical industry and for bioremediation purposes, amongst others [47,48]. Protease is one of the most important groups of industrial enzymes, having a unique catalytic mechanism, broad substrate specificity and high robustness, which has widened their application into bioremediation and waste management [49].

This study again reveals the use of direct enzymes to accelerate the process of degradation in the wastewater treatment plants before the release of ILs to the environment so that we can reduce the chances of adverse toxicity effects in the future. It will be a promising finding and provide insightful information for the chemical industries, where they use a specific class of ILs that do not have any alternative replacements and are more persistent in the environment. Once we have the information on the degradability data as described in the current study, it is more applicable to change the molecular structure of the ILs to synthesize 100% biodegradable compounds. This is because chemical modification of the IL side chains may compromise the ability of the enzymes to recognize the modified structure as a suitable substrate and effect the complete degradation of the compound [50].

The commercial amidase enzymes purchased were obtained from the source *Escherichia coli* and *Achromobacter* with a penicillin hydrolytic activity unit of NLT 850 U/g and NLT 250 U/g, respectively. Protease enzymes were obtained from bacteria, fungi and plant sources with different enzyme activity as given in Table 2. Amidase enzymes are a large group of hydrolytic enzymes that contain a conserved stretch of approximately 130 amino acids. They are widespread, being found in both prokaryotes and eukaryotes. Amidase enzymes catalyze the hydrolysis of amide bonds, although they have a wide range of substrate specificity and function. Nonetheless, these enzymes maintain a core alpha/beta/alpha structure, where the topologies of the N- and C-terminal halves are similar. These enzymes possess a unique, highly conserved Ser-Ser-Lys catalytic triad used for amide hydrolysis, although the catalytic mechanism for acyl-enzyme intermediate formation can differ between enzymes [51], whereas protease enzymes work by hydrolyzing the peptide bonds and have the highest market share among industrial enzymes [52]. Proteases are classified as acidic, alkaline and neutral proteases according to the pH, and they exhibit maximum efficacy within a specific pH range. Proteases (also known as proteinases or peptidases) hydrolyze the peptide bond between amino acid residues in a polypeptide chain. Proteases may be specific and limited to one or more sites within a protein, or they may be nonspecific, digesting proteins into individual amino acids. Proteases are found in all organisms and are involved in all areas of metabolism [53].

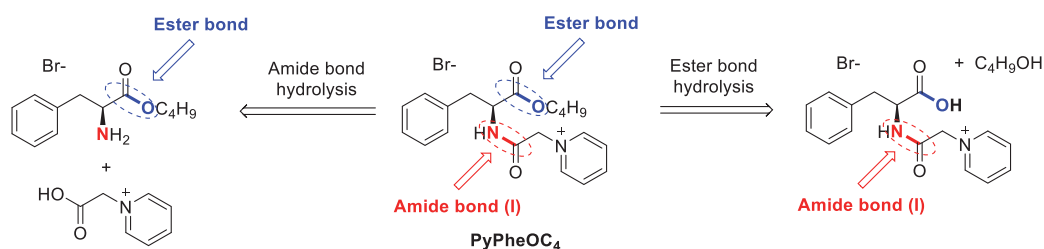
In the present study, we revealed the enzymatic hydrolysis of pyridinium-based ILs of PyPheOC₄ (as a representative example of SAILs of PyPheOC_n series), which have ester and amide bonds with amidase and protease enzymes. During the enzymatic hydrolysis, the enzymes enhanced the bond cleavage in molecules with water.

Table 2. Sources of enzymes used for enzymatic hydrolysis of studied ionic liquids.

Enzyme	Source	Activity
A1	<i>Escherichia coli</i>	NLT 850 U/g
A2	<i>Achromobacter</i>	NLT 250 U/g
E1	<i>Pichia sp.</i>	NLT 10,000 PLU/g
E2	<i>Pichia sp.</i>	NLT 10,000 PLU/g
P1	<i>Bacillus sp.</i>	400 ELU/g
P2	<i>Bacillus sp.</i>	750 ELU/g
P3	<i>Bacillus sp.</i>	100 ELU/g
P4	<i>Bacillus sp.</i>	275 ELU/g
P5	<i>Mucor miehei</i>	8 ELU/g
P6	<i>Bacillus licheniformis</i>	400 ELU/g
P7	<i>Bacillus amyloliquefaciens</i>	15 ELU/g
P8	<i>Geobacillus sp.</i>	5 ELU/g
P9	<i>Trichoderma reesei</i>	5 ELU/g
P10	<i>Bacillus subtilis</i>	225 ELU/g
P11	<i>Bacillus subtilis</i>	400 ELU/g
P12	<i>Aspergillus oryzae var.</i>	5 ELU/g
P13	<i>Aspergillus oryzae</i>	65 ELU/g
P14	<i>Bacillus subtilis</i>	150 ELU/g
P15	<i>Aspergillus niger</i>	5 ELU/g
P16	<i>Bacillus subtilis</i>	10 ELU/g
P17	<i>Bacillus subtilis</i>	175 ELU/g
P18	<i>Carica papaya</i>	5 ELU/g
P19	<i>Pineapple stem</i>	5 ELU/g
P20	<i>Fig tree latex</i>	5 ELU/g

In theory, hydrolysis of an amide breaks the carbon–nitrogen bond and produces an acid and either ammonia or an amine. Though this reaction bears a resemblance to the hydrolysis of esters, there are, however, important differences. The hydrolysis of esters occurs relatively easily, whereas amides are much more resistant to hydrolysis. In the case of ester bonds, carboxylic esters readily hydrolyze to the parent carboxylic acid and an alcohol. Ester bond hydrolysis is the most prevalent type of biodegradation because they are a hydrolytically unstable functional group. Amides can be hydrolyzed only by heating for hours with a strong acid or strong base unless an enzyme is used. If amide hydrolysis occurs in a basic solution, the salt of the carboxylic acid forms, i.e., one mole of the base is required per mole of amide. If hydrolysis proceeds under acidic conditions, the ammonium salt of the amine is formed, and one mole of acid is required per mole of amide [54].

The possible way by which ester bond and amide bond hydrolysis proceeded in the PyPheOC₄ compound is illustrated in Figure 4.

**Figure 4.** Expected pathways of C-O and C-N bonds hydrolysis in PyPheOC₄.

When 2% PyPheOC₄ was treated with 0.2 g amidase enzymes (1 and 2) at the incubation temperature of 40 °C, pH 5.5, shaking speed of 170 rpm, and 3 days incubation time, showed 55 to 80% ester bond hydrolysis. With amidase enzyme 1, 80% of the ester bonds were hydrolyzed whereas, with amidase 2, only 55% ester bond hydrolysis was

observed. In both cases, no significant (less than 5%) amide bond hydrolysis product was recorded. The high stability of amide bonds is subjected to its propensity to form a resonating structure, which brings a double bond character to the amide CO-N bond [54].

When the concentration of PyPheOC₄ was reduced to 1% (*w/v*) while maintaining the same incubation conditions as mentioned before with both amidase (1 and 2), 95% of the ester bond was hydrolyzed in PyPheOC₄ and no significant amounts of amide bond break occurred. These studies revealed that with PyPheOC₄, it was easier to hydrolyze the ester bonds by amidase enzymes compared to amide bonds. Moreover, the reduced concentration further made it feasible for the amidase enzymes to open more active sites for ester bonds. The transformation products formed from the studies are given in Figure 4. Based on the results, more enzymes were applied in this study in order to find complete hydrolysis of the compounds. Experiments were further carried out with 0.1 g of 1–20 types of protease enzymes (Table 2) along with amidase 1 and 2.

Based on the results mentioned above, the concentration of PyPheOC₄ was maintained as 1% followed by an incubation temperature of 50 °C, shaking speed of 100 rpm and incubation for 7 days.

The applied protease enzymes work better at slightly higher temperatures, therefore the temperature 50 °C was selected for these test trials. The shaking speed was reduced to 100 rpm due to the optimum shaking speed recommended for the enzymes with an extended incubation time to 7 days. Among the 20 different types of protease enzymes tested on PyPheOC₄, 100% ester bond hydrolysis was observed for all the samples except enzymes P8, P9 (86%) and P18 (79%); P13 also gives ca. 8% amidolysis; and representative examples of the NMR spectra are given in Figure 5.

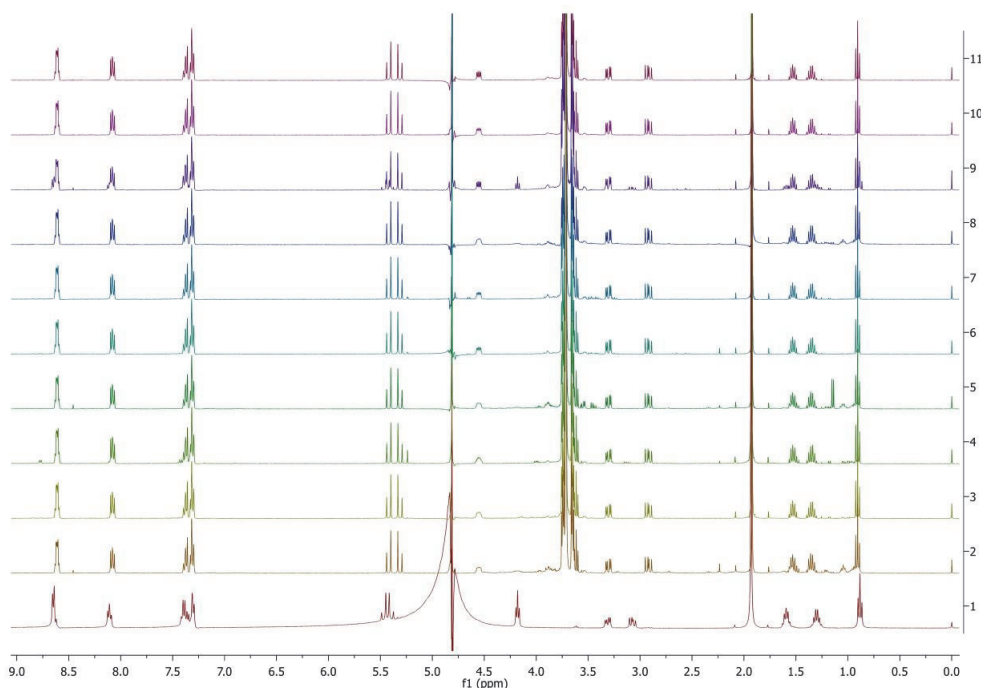


Figure 5. ¹H NMR spectra of PyPheOC₄ solutions after incubations with selected protease enzymes (concentration of PyPheOC₄ 1%). Spectrum 1 (bottom) corresponds to PyPheOC₄ after incubation in buffer without enzymes; the spectra 2→11 represent incubation with enzymes P11→P20.

Based on these results, we further reduced the concentration of the tested IL PyPheOC₄ to 0.5% in order to study the possibility of complete hydrolysis of ester and amide bonds

(100%). The optimum activity of the protease enzyme was reported with a pH of 6–7 [55]. Therefore, the pH of the sodium acetate buffer was further increased to 6.5 to improve the degradation rate. Incubation temperature, shaking speed and time were maintained at 50 °C, 100 rpm and 7 days, respectively.

Only selected protease enzymes from 1–20 that have high enzyme activity (P1, P2, P3, P4, P6, P10, P11, P13, P14, P17) and amidase 1 and amidase 2 were selected based on the previous test results. When the selected protease enzymes were used (based on higher enzyme activity), all the samples showed 100% ester bond hydrolysis with PyPheOC₄. Among those, only P13 enzymes showed about 10–20% amide bond hydrolysis (Figure 6). In the case of amidase 1 and 2, only ester bond hydrolysis (100%) was observed.

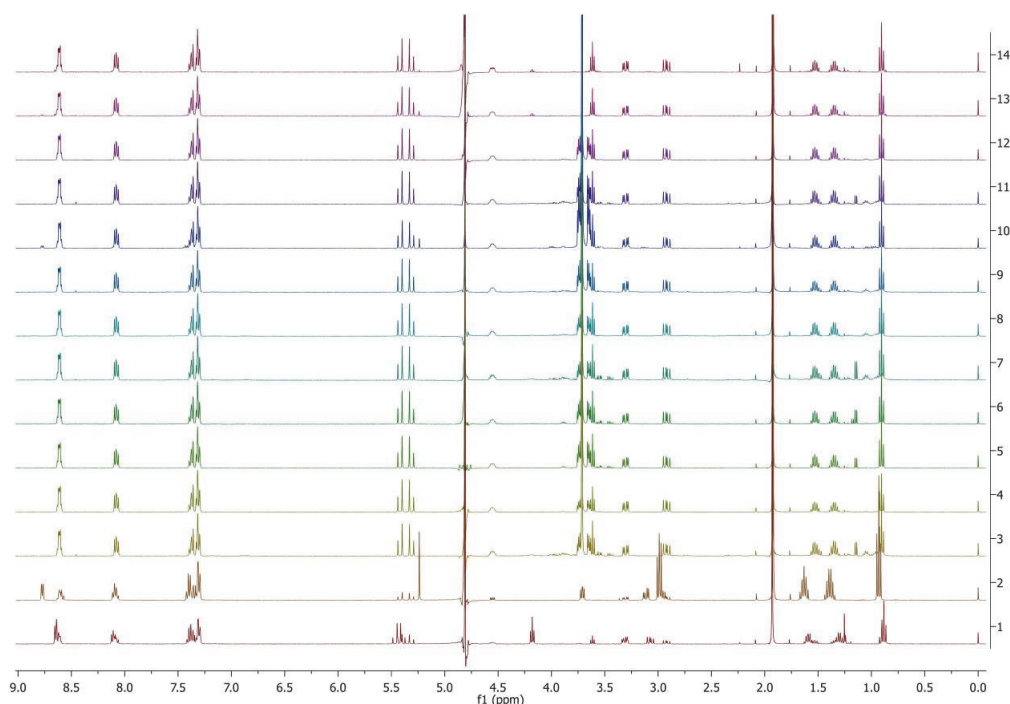


Figure 6. ¹H NMR spectra of PyPheOC₄ solutions after incubations with selected protease enzymes at pH 6.5 (concentration of PyPheOC₄ 0.5%). Spectrum 1 (bottom) corresponds to PyPheOC₄ after incubation in buffer without enzymes; spectrum 2 recorded the model mixture of expected hydrolytic products; spectra 3–12 represent incubation with proteases P1, P2, P3, P4, P6, P10, P11, P13, P14, P17; spectra 13 and 14 represent incubation with amidase 1 and amidase 2, correspondingly.

PyPheOC₄ in presence of the P13 enzyme showed a degradation pathway as presented in pathway A (90% of transformations) and pathway B (10% of transformations) (Figure 7). Transformations by pathway A are faster up to the first step (i.e., ester hydrolysis), whereas further hydrolysis of amide bonds in degradation product Py⁽⁺⁾-CH₂-CO-NH-Phe-COOH is a very slow process. It can be connected to the reason that during the degradation process stabilizers, activators, or inhibitory products can form in the medium, which result from the material degradation or leaching out of enzyme additives, and those could affect the enzyme catalyzed reactions by influencing enzyme adsorption and activity, resulting from material degradation [56].

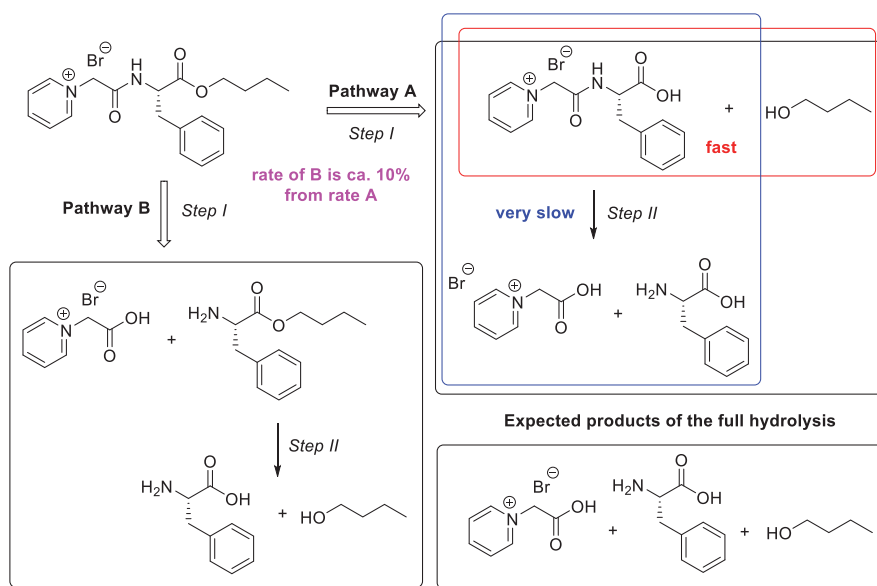


Figure 7. Degradation pathways analysis for PyPheOC₄ based on NMR data.

The intermediates and final products of enzymatic decomposition were not dependent on the degradation pathway (A or B) and were readily biodegradable compounds [24], which is critically important for the design of sustainable ecologically friendly systems.

2.3. Structural Modification of PyPheOC₄ SAIL: Diamide Derivative PyPheNHC₄

The change of ester bond in PyPheOC₄ SAIL structure to amide bond can help to create compounds (Figure 8), which are more stable to alkaline hydrolysis [57,58] and can expand the possible application range of this type of compound, but also requires an evaluation of enzymatic decomposition.

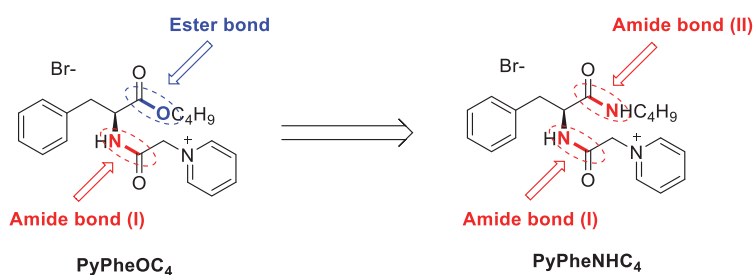


Figure 8. Structural modification of PyPheOC₄ SAIL.

The rate of enzymatic hydrolysis reaction is influenced by the physicochemical properties of the substrate and also by the inherent characteristics of a specific enzyme, which can be enzyme activity and its stability, local concentration, amino acid composition, and 3D conformation. Moreover, it is again very important to consider the medium conditions such as pH and temperature, since they strongly influence the properties of the substrate and the enzyme.

2.4. Study of Enzymatic Degradation/Hydrolysis of PyPhenHC₄ SAIL

It is expected that when compound PyPhenHC₄ has been treated with enzymes, the hydrolysis may happen at either of these bonds, i.e., amide bond I or amide bond II, and ultimately lead to complete hydrolysis of the compound (Figures 9 and 10).

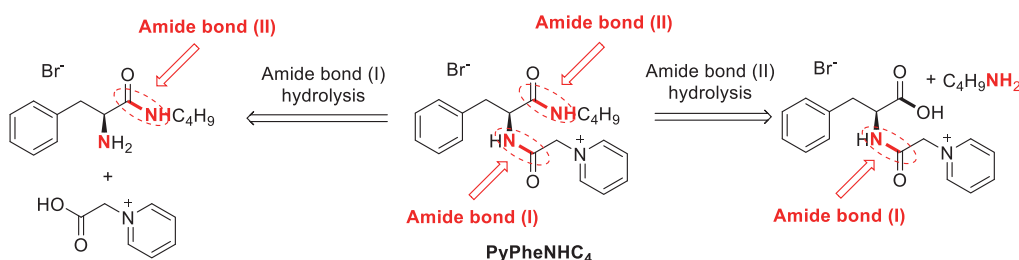


Figure 9. Expected ways of bonds hydrolysis in PyPhenHC₄.

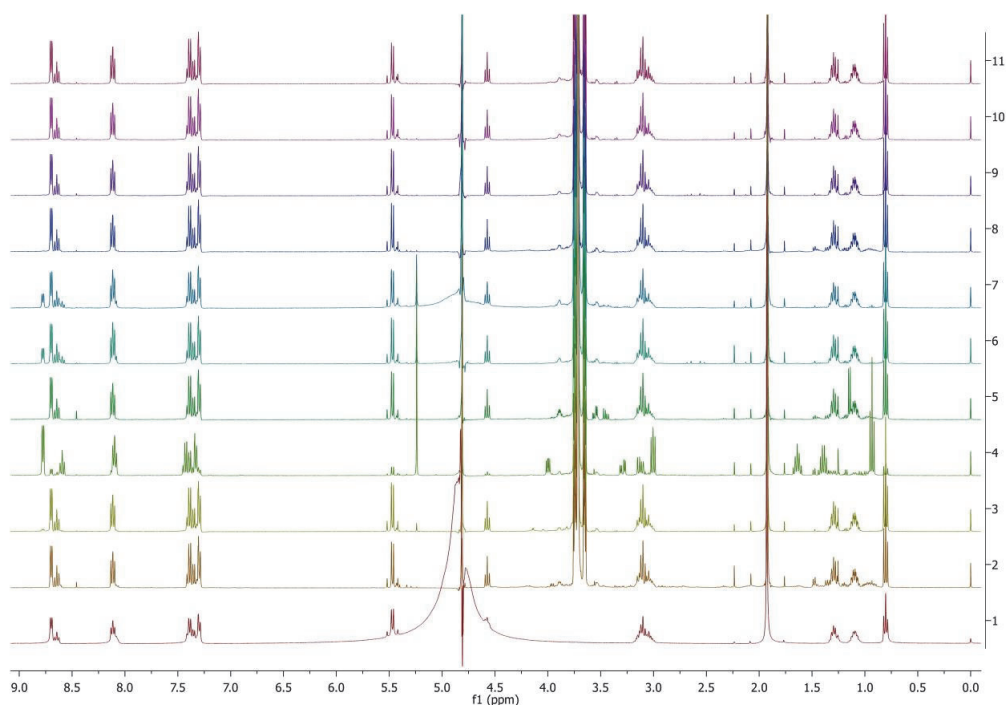


Figure 10. ¹H NMR spectra of PyPhenHC₄ solutions after incubations with selected protease enzymes (concentration of PyPhenHC₄ 1%). Spectrum 1 (bottom) corresponds to PyPhenHC₄ after incubation in buffer without enzymes; the spectra 2→11 represent incubation with enzymes P11→P20.

The experimental trials and conditions explored and discussed before with PyPhenOC₄ have been tried with the new synthesized amide compounds. The first trial, i.e., 2% PyPhenHC₄ with 0.2 g amidase enzymes (1 and 2) with an incubation temperature of 40 °C, pH of 5.5, shaking speed of 170 rpm, and 3 days incubation time, showed no evidence of amide bond hydrolysis with both the enzymes amidase 1 and 2. Thus, it is assumed that the stability of amide bonds is too strong to be cleaved by amidase enzymes or is inaccessible to the active site. The high stability of amide bonds is subjected to its propensity to form a

resonating structure, which brings a double bond character to the amide CO-N bond [54]. When the concentration of ionic liquids was reduced to 1% (*w/v*) by maintaining the same incubation conditions as mentioned before with both amidase enzymes (1 and 2) again, no traces of amide hydrolysis were observed. Experiments were further performed with 0.1 g of the 1–20 types of protease enzymes (Table 2) along with amidase 1 and 2. Among the 20 different types of protease enzymes tested with PyPheNHC₄, the P1–P9 enzymes did not show any significant amide bond hydrolysis. Among the proteases P11–P20, the P13 enzyme showed 87% amide bond hydrolysis. The proteases P12, P15 and P16 demonstrated 10–20% amide bond hydrolysis (Figure 10). As shown in Table 2, all of the proteases were obtained from different sources. Among them, the P13 obtained from the source *Aspergillus oryzae* with an enzyme activity of 65 ELU/g worked well for hydrolysis of amide bonds in PyPheNHC₄. It reveals that each enzyme has its optimum hydrolytic activity with the compounds under optimum conditions.

The pathway by which a protease enzyme breaks the amide bonds is illustrated in Figure 11.

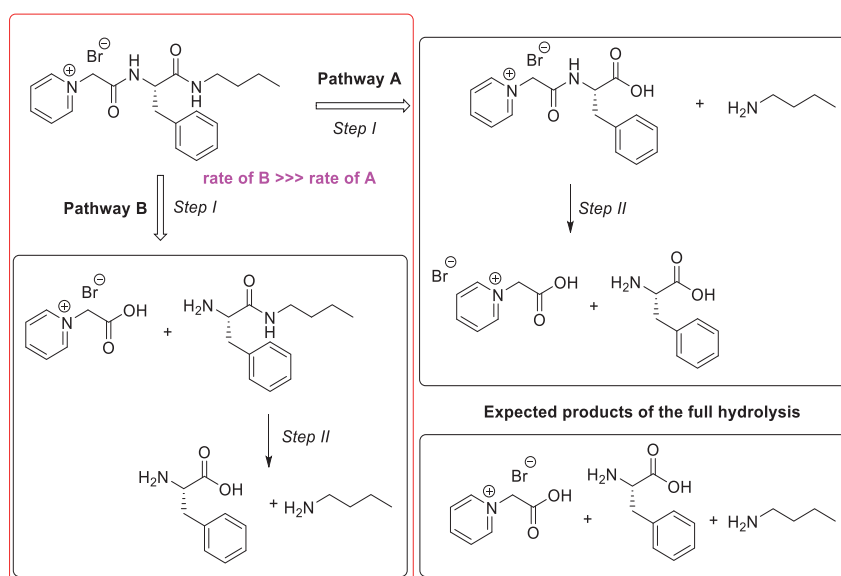


Figure 11. Degradation pathway analysis for PyPheNHC₄ based on NMR data.

To enhance the complete degradation, the concentration of PyPheNHC₄ was further reduced to 0.5% as investigated with PyPheOC₄. The incubation temperature, shaking speed and time were maintained at 50 °C, 100 rpm and 7 days, respectively. Only selected protease enzymes from 1–20 that had high enzyme activity (P1, P2, P3, P4, P6, P10, P11, P13, P14, P17) and amidase 1 and 2 were selected based on the previous test results. With the reduced concentration (0.5%) of PyPheNHC₄, the P13 enzyme showed 100% amide hydrolysis (Figure 12). PyPheNHC₄ in the presence of the P13 enzyme showed 100% transformation by pathway B; i.e., hydrolysis of amide bond I. Transformations by pathway A by the hydrolysis of amide bond II is relatively slow in comparison with the rate of transformation by pathway B. The reaction showed a total cleavage of all amide bonds and observed Py⁽⁺⁾-CH₂-COOH, phenylalanine and Bu-NH₂ in the solution (Figures 11 and 12).

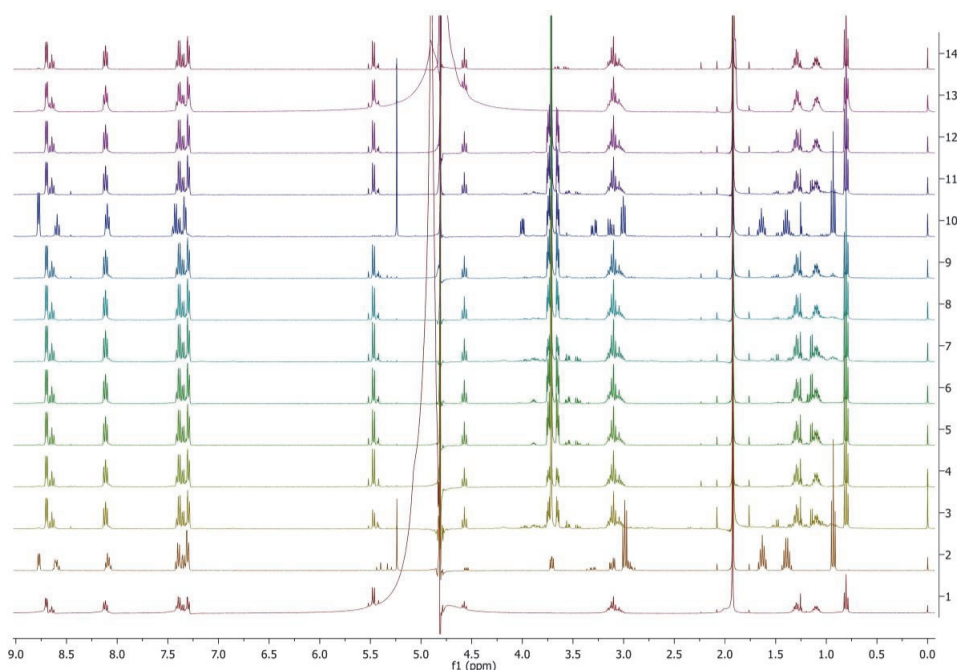


Figure 12. NMR spectra of PyPheNHC₄ solutions after incubations with selected protease enzymes (concentration of PyPheNHC₄ 0.5%). Spectrum 1 (bottom) corresponds to PyPheNHC₄ after incubation in buffer without enzymes; spectrum 2 recorded the model mixture of expected hydrolytic products; spectra 3–12 represent incubation with proteases P1, P2, P3, P4, P6, P10, P11, P13, P14, P17; spectra 13 and 14 represent incubation with amidase 1 and amidase 2, correspondingly.

2.5. Concept of PyPheOC_n and PyPheNHC_n SAILS Application to Solubilization of Polycyclic Aromatic Hydrocarbons

The application of surfactants and SAILS in the design of effective and ecologically friendly sustainable systems for the solubilization of polycyclic aromatic hydrocarbons is very often limited due to the negative influence of surfactants and SAILS on the environment [14] and technological problems connected with the separation of solubilized PAH from surfactant solutions [4]. Among the SAILS PyPheOC_n and PyPheNHC_n, which were the focus of our current study, there are several examples of compounds (with $n = 4–8$) that could be considered as low toxicity and readily biodegradable ILs [7]. An evaluation of the toxicity and biodegradability of potential hydrolytic decomposition products of PyPheOC_n and PyPheNHC_n, performed in our recent studies [10,24,32], also confirm a great potential of these SAILS as a platform for ecologically friendly sustainable systems. The solubilization capacity of PyPheOC_n surfactants, evaluated related to model representative PAH (naphthalene, anthracene and pyrene), is comparable to the solubilization capacity of conventional cationic surfactant CTABr (see Table 1 and Figure 3; compare parameters for CTAB and SAILS with $n = 8–12$), but in the cases of PyPheOC_n and PyPheNHC_n, polycyclic aromatic hydrocarbons could be easily separated from the SAILS water solution using enzymatic decomposition of SAILS under mild conditions. The decomposition of SAILS could be adjusted via the choice of enzyme system, reaction conditions and/or choice of SAILS type. Despite the possibility of solubilized aromatic carbons to have an impact on the enzymatic degradation of phenylalanine-derived SAILS, we suggest that enzymatic cleavage of surfactant monomers occurs [49]. Since the monomer is in the equilibrium with dynamic micellar aggregates [40], the drop in the monomer concentration will affect the micelle concentration in the system and thus reduce the PAH solubilized by the surfactant

aggregates. The PAH initially bound by the micelles will be released in the bulk aqueous solution and precipitate. After SAILs decomposition, PAH, immobilized enzymes, and the water solution of SAILs decomposition products could be separated from each other using filtration techniques. The water solution of SAILs decomposition products could be completely biodegraded by the microorganisms in the environment or used for enzymatic re-synthesis of SAILs from decomposition products with future usage of the obtained solution for the next cycle of PAH extraction/solubilization (Figure 13).

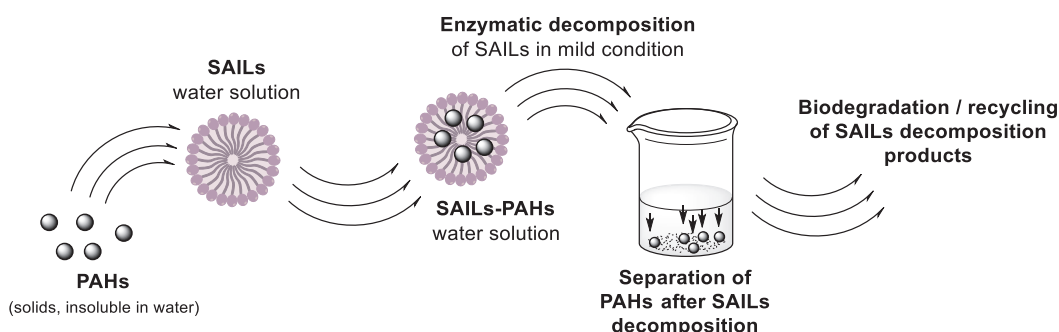


Figure 13. Concept of PyPheOC_n and PyPheNHC_n SAILs application to solubilization of PAHs.

3. Experimental Section

3.1. Materials

Naphthalene (Nap), anthracene (Ant) and pyrene (Pyr), cetyltrimethylammonium bromide (CTABr), inorganic and organic salts for preparation of working buffer solutions, acids and organic solvents were purchased from Sigma-Aldrich/Merck KGaA or Acros Organics/Fisher Scientific. Deuterated solvents for NMR analysis were purchased from Deutero GmbH (Kastellaun, Germany). Deionized water was prepared using the Direct-Q UV 5 water purification system.

Synthesis of SAILs PyPheOC_n is previously described [32]. Synthesis of PyPheNC₄ was performed according to common synthetic procedures [10,24], confirmation of the structure and purity was performed using ¹H, ¹³C, ¹H-¹H, ¹H-¹³C, DETP 135 NMR techniques and by HRMS.

Amidase and protease enzymes (Table 2) were purchased from Fermenta Biotech Ltd. (Mumbai, India) and ChiralVision B.V. (Den Hoorn, The Netherlands), respectively. The enzymes were stored in a cold room until the start of the experiment.

3.2. Methods

3.2.1. Study of Solubilization Capacity

Solubilization capacity of micellar systems was evaluated by determining the maximal solubility of the substrates (naphthalene, anthracene and pyrene) in surfactant solutions [38,40]. To a series of corresponding PyPheOC_n surfactant solutions (10–15 different concentrations in total, which cover concentration range before and after cmc; 3 mL of surfactant solution per each concentration) was added a fixed amount (5 mg per each concentration) of studied substrate, shaken intensively and leaved for equilibration for 48 h at 25 °C [38]. After equilibration, insoluble residue was filtered through Millipore filters (Durapore® PVDF membrane, pore size 0.22 µm), the filtrate was placed in the quartz cell and the UV-vis spectrum was recorded using UV-Vis spectrophotometer JASCO V-730 in the wavelength range from 200 to 400 nm. For studied solutions obtained value of absorbance (A) was recalculated on a pathlength 10 mm at the 311 nm ($\epsilon = 320 \text{ M}^{-1} \cdot \text{cm}^{-1}$) for naphthalene, 378 nm ($\epsilon = 15,100 \text{ M}^{-1} \cdot \text{cm}^{-1}$) for anthracene and 336 nm ($\epsilon = 62,800 \text{ M}^{-1} \cdot \text{cm}^{-1}$) for pyrene. Molar extinction coefficients (ϵ , $\text{M}^{-1} \cdot \text{cm}^{-1}$) for substrates were determined in independent experiments in hexane. Solubilization capacity of the surfactant (S) was

calculated from the ratio $S = \beta / \varepsilon$, where β is the slope of the linear part of the A vs. C_{surf} dependence [38,41].

3.2.2. Enzymatic Degradation/Hydrolysis Studies

In this experiment, two representative examples of pyridinium SAILs have been tested. Firstly, the experiments were started with compound PyPheOC₄. Once the enzymatic degradability of this compound and its transformation products are obtained, the test trials were continued with the compound PyPheNHC₄ (which is a result of structure improvement of PyPheOC_n SAILs series). Degradation tests were performed with different reaction conditions, such as doses of enzymes, pH, temperature, shaking speed and incubation period to optimize the best parameters for the test. We started the test trials with ester-based SAIL, PyPheOC₄, with a concentration of 2% was prepared in 0.1 M sodium acetate buffer (pH 5.5). Then, 0.2 g of enzymes such as amidase 1 and 2 were weighed in separate 15 mL tubes. To this, 1 mL of the samples (i.e., ionic liquid in sodium acetate buffer) was added. The tubes were then placed in an incubator with a shaking speed of 170 rpm and a temperature of 40 °C for 7 days. Respective controls were kept without the addition of enzymes. The supernatants were then collected and stored in fresh tubes and preserved for NMR analysis; before recording the ¹H NMR spectra, up to 20% *v/v* of D₂O was added to a sample for locking.

After obtaining the results, similar tests were performed with a further concentration of PyPheOC₄ (1% and 0.5%), doses of amidase 1 and 2, and protease 1–20 enzymes (0.1 g), pH (5.5, 6.5), temperature (50 °C), and shaking speed (100 rpm) (see Table 3). Once the test results were analyzed, similar trials were performed with the compound PyPheNHC₄.

Table 3. Experiment set up and reaction conditions of ILs enzymatic degradation studies.

Test	ILs Tested	IL Test Conc. (% <i>w/v</i>)	pH	Enzymes Tested	Enzyme Test Conc. (g)	Incubating Temperature (°C)	Incubation Speed (rpm)	Incubation Time (Days)
1	PyPheOC ₄ PyPheNHC ₄	2	5.5	Amidase 1 and 2	0.2	40	170	3 days
2	PyPheOC ₄ PyPheNHC ₄	1	5.5	Amidase 1 and 2	0.2	40	170	3 days
3	PyPheOC ₄ PyPheNHC ₄	1	5.5	Amidase 1 and 2 Protease 1–20	0.1	50	100	7 days
4	PyPheOC ₄ PyPheNHC ₄	0.5	6.5	Amidase 1 and 2 Protease (P1–P4, P6, P10, P11, P13, P14, P17)	0.1	50	100	7 days

3.2.3. NMR Analysis of Enzymatic Degradation/Hydrolysis Products

The NMR spectra were recorded on a Bruker Avance III 400 MHz spectrometer. For analysis, 400 µL of clear supernatant was used, which was transferred to NMR tubes and mixed with 100 µL of deuterium oxide (99.9%). NMR spectra were recorded using the standard water suppression method. Identification of enzymatic hydrolysis products were performed by comparison of ¹H NMR spectra of potential transformation products with ¹H NMR spectra of reaction mixtures of corresponding SAILs after incubation with the immobilized enzymes.

4. Conclusions

The solubilization capacity of a series of sustainable phenylalanine-derived surface-active ionic liquids (SAILs) was evaluated towards polycyclic aromatic hydrocarbons—naphthalene, anthracene and pyrene. The key physico-chemical parameters of the studied systems (critical micelle concentration, spectral properties, solubilization parameters) were determined, analyzed and compared with a conventional cationic surfactant, CTABr. For all studied PAHs, the solubilization capacity increases with an extension of the alkyl chain

length of PyPheOC_n SAILs reaching the values comparable to CTABr for SAILs with $n = 10\text{--}12$. A remarkable advantage of the phenylalanine-derived SAILs PyPheOC_n and PyPheNHC_n consists in a possibility to cleave enzymatically ester and/or amide bonds under mild conditions, to separate polycyclic aromatic hydrocarbons in situ. A series of immobilized enzymes was tested to determine the most suitable candidates for tunable decomposition of SAILs. The decomposition pathway could be adjusted depending on the choice of enzyme system, reaction conditions and SAILs type. The evaluated systems can provide selective cleavage of the ester and/or amide bonds and help to choose optimal decomposition of SAILs for enzymatic recycling of SAILs transformation products or as a pretreatment towards biological mineralization. The concept of a possible practical application of the studied systems for PAHs solubilization/separation was also discussed, focusing on sustainability and green chemistry approaches.

Author Contributions: Conceptualization and idea of the research, Y.K., K.K.G., N.G. and V.K.G.; synthesis of compounds, methodology, I.V.K.; experimental techniques, data curation analysis of the results, conceptualization, methodology, T.Y., S.M.S. and I.V.K.; analysis and interpretation, S.M.S. and I.V.K.; formal analysis and interpretation, S.M.S.; writing—original draft preparation, I.V.K. and S.M.S.; writing—review and editing, Y.K., V.K.G., K.K.G. and N.G.; funding acquisition, Y.K. and N.G. All authors have read and agreed to the published version of the manuscript.

Funding: This work was supported by Estonian Research Council grants PUT1656 (for Y.V.K., N.G., Y.K.) and COVSG5 (Y.K.); ERDF Dora Plus program (for T.Y.).

Institutional Review Board Statement: Not applicable.

Informed Consent Statement: Not applicable.

Data Availability Statement: All the data gathered for this study are available in the article.

Acknowledgments: Not applicable.

Conflicts of Interest: The authors declare no conflict of interest.

Sample Availability: Samples of the compounds could be available from the authors upon request.

References

- Greer, A.J.; Jacquemin, J.; Hardacre, C. Industrial Applications of Ionic Liquids. *Molecules* **2020**, *25*, 5207. [\[CrossRef\]](#) [\[PubMed\]](#)
- Plechkova, N.V.; Seddon, K.R. Ionic Liquids: “Designer” Solvents for Green Chemistry. In *Methods and Reagents for Green Chemistry*; John Wiley & Sons, Inc.: Hoboken, NJ, USA, 2007; pp. 103–130. [\[CrossRef\]](#)
- Usmani, Z.; Sharma, M.; Gupta, P.; Karpichev, Y.; Gathergood, N.; Bhat, R.; Gupta, V.K. Ionic liquid based pretreatment of lignocellulosic biomass for enhanced bioconversion. *Bioresour. Technol.* **2020**, *304*, 123003. [\[CrossRef\]](#) [\[PubMed\]](#)
- Pillai, P.; Maiti, M.; Mandal, A. Mini-review on Recent Advances in the Application of Surface-Active Ionic Liquids: Petroleum Industry Perspective. *Energy Fuels* **2022**, *36*, 7925–7939. [\[CrossRef\]](#)
- Jordan, A.; Gathergood, N. Biodegradation of ionic liquids—a critical review. *Chem. Soc. Rev.* **2015**, *44*, 8200–8237. [\[CrossRef\]](#) [\[PubMed\]](#)
- Zimmerman, J.B.; Anastas, P.T.; Erythropel, H.C.; Leitner, W. Designing for a green chemistry future. *Science* **2020**, *367*, 397–400. [\[CrossRef\]](#)
- Suk, M.; Haiß, A.; Westphal, J.; Jordan, A.; Kellett, A.; Kapitanov, I.V.; Karpichev, Y.; Gathergood, N.; Kümmerer, K. Design rules for environmental biodegradability of phenylalanine alkyl ester linked ionic liquids. *Green Chem.* **2020**, *22*, 4498–4508. [\[CrossRef\]](#)
- Gu, Y.; Jérôme, F. Bio-based solvents: An emerging generation of fluids for the design of eco-efficient processes in catalysis and organic chemistry. *Chem. Soc. Rev.* **2013**, *42*, 9550–9570. [\[CrossRef\]](#)
- Kapitanov, I.V.; Mirgorodskaya, A.B.; Valeeva, F.G.; Gathergood, N.; Kuca, K.; Zakharova, L.Y.; Karpichev, Y. Physicochemical properties and esterolytic reactivity of oxime functionalized surfactants in pH-responsive mixed micellar system. *Colloids Surf. A Physicochem. Eng. Asp.* **2017**, *524*, 143–159. [\[CrossRef\]](#)
- Pandya, S.J.; Kapitanov, I.V.; Usmani, Z.; Sahu, R.; Sinha, D.; Gathergood, N.; Ghosh, K.K.; Karpichev, Y. An example of green surfactant systems based on inherently biodegradable IL-derived amphiphilic oximes. *J. Mol. Liq.* **2020**, *305*, 112857. [\[CrossRef\]](#)
- Banjare, M.K.; Behera, K.; Banjare, R.K.; Pandey, S.; Ghosh, K.K.; Karpichev, Y. Molecular interactions between novel synthesized biodegradable ionic liquids with antidepressant drug. *Chem. Thermodyn. Therm. Anal.* **2021**, *3*, 100012. [\[CrossRef\]](#)
- Pandya, S.J.; Kapitanov, I.V.; Banjare, M.K.; Behera, K.; Borovkov, V.; Ghosh, K.K.; Karpichev, Y. Mixed Oxime-Functionalized IL/16-s-16 Gemini Surfactants System: Physicochemical Study and Structural Transitions in the Presence of Promethazine as a Potential Chiral Pollutant. *Chemosensors* **2022**, *10*, 46. [\[CrossRef\]](#)

13. Gonçalves, A.R.; Paredes, X.; Cristino, A.F.; Santos, F.J.; Queirós, C.S. Ionic Liquids—A Review of Their Toxicity to Living Organisms. *Int. J. Mol. Sci.* **2021**, *22*, 5612. [\[CrossRef\]](#) [\[PubMed\]](#)
14. Kowalska, D.; Maculewicz, J.; Stepnowski, P.; Dołżonek, J. Ionic liquids as environmental hazards—Crucial data in view of future PBT and PMT assessment. *J. Hazard. Mater.* **2021**, *403*, 123896. [\[CrossRef\]](#)
15. Amsel, A.-K.; Olsson, O.; Kümmerer, K. Inventory of biodegradation data of ionic liquids. *Chemosphere* **2022**, *299*, 134385. [\[CrossRef\]](#)
16. Bubalo, M.C.; Radošević, K.; Redovniković, I.R.; Slivac, I.; Srček, V.G. Toxicity mechanisms of ionic liquids. *Arch. Ind. Hyg. Toxicol.* **2017**, *68*, 171–179. [\[CrossRef\]](#) [\[PubMed\]](#)
17. Docherty, K.M.; Aiello, S.W.; Buehler, B.K.; Jones, S.E.; Szymczyna, B.R.; Walker, K.A. Ionic liquid biodegradability depends on specific wastewater microbial consortia. *Chemosphere* **2015**, *136*, 160–166. [\[CrossRef\]](#)
18. Kusumahastuti, D.K.; Sihtmäe, M.; Kapitanov, I.V.; Karpichev, Y.; Gathergood, N.; Kahru, A. Toxicity profiling of 24 l-phenylalanine derived ionic liquids based on pyridinium, imidazolium and cholinium cations and varying alkyl chains using rapid screening *Vibrio fischeri* bioassay. *Ecotoxicol. Environ. Saf.* **2019**, *172*, 556–565. [\[CrossRef\]](#)
19. Pinazo, A.; Manresa, M.; Marques, A.; Bustelo, M.; Espuny, M.; Pérez, L. Amino acid-based surfactants: New antimicrobial agents. *Adv. Colloid Interface Sci.* **2016**, *228*, 17–39. [\[CrossRef\]](#)
20. Mero, A.; Mezzetta, A.; Nowicki, J.; Luczak, J.; Guazzelli, L. Betaine and l-carnitine ester bromides: Synthesis and comparative study of their thermal behaviour and surface activity. *J. Mol. Liq.* **2021**, *334*, 115988. [\[CrossRef\]](#)
21. Mezzetta, A.; Luczak, J.; Woch, J.; Chiappe, C.; Nowicki, J.; Guazzelli, L. Surface active fatty acid ILs: Influence of the hydrophobic tail and/or the imidazolium hydroxyl functionalization on aggregates formation. *J. Mol. Liq.* **2019**, *289*, 111155. [\[CrossRef\]](#)
22. Rantamäki, A.H.; Ruokonen, S.-K.; Sklavounos, E.; Kyllönen, L.; King, A.W.T.; Wiedmer, S.K. Impact of Surface-Active Guanidinium-, Tetramethylguanidinium-, and Cholinium-Based Ionic Liquids on *Vibrio Fischeri* Cells and Dipalmitoylphosphatidylcholine Liposomes. *Sci. Rep.* **2017**, *7*, 46673. [\[CrossRef\]](#)
23. Jordan, A.; Haiß, A.; Spulak, M.; Karpichev, Y.; Kümmerer, K.; Gathergood, N. Synthesis of a series of amino acid derived ionic liquids and tertiary amines: Green chemistry metrics including microbial toxicity and preliminary biodegradation data analysis. *Green Chem.* **2016**, *18*, 4374–4392. [\[CrossRef\]](#)
24. Kapitanov, I.V.; Raba, G.; Špulák, M.; Vilu, R.; Karpichev, Y.; Gathergood, N. Design of sustainable ionic liquids based on l-phenylalanine and l-alanine dipeptides: Synthesis, toxicity and biodegradation studies. *J. Mol. Liq.* **2023**, *374*, 121285. [\[CrossRef\]](#)
25. Haiß, A.; Jordan, A.; Westphal, J.; Logunova, E.; Gathergood, N.; Kümmerer, K. On the way to greener ionic liquids: Identification of a fully mineralizable phenylalanine-based ionic liquid. *Green Chem.* **2016**, *18*, 4361–4373. [\[CrossRef\]](#)
26. OECD. *OECD Test Guidelines for Chemicals*; OECD: Paris, France, 1992.
27. Friedrich, J.; Längin, A.; Kümmerer, K. Comparison of an Electrochemical and Luminescence-Based Oxygen Measuring System for Use in the Biodegradability Testing According to Closed Bottle Test (OECD 301D). *Clean* **2013**, *41*, 251–257. [\[CrossRef\]](#)
28. Zubareva, T.M.; Anikeev, A.V.; Karpichev, E.A.; Red'ko, A.N.; Prokop'eva, T.M.; Popov, A.F. Cleavable dicationic surfactant micellar system for the decomposition of organophosphorus compounds. *Theor. Exp. Chem.* **2012**, *47*, 377–383. [\[CrossRef\]](#)
29. Tehrani-Bagha, A.; Holmberg, K. Cleavable surfactants. *Curr. Opin. Colloid Interface Sci.* **2007**, *12*, 81–91. [\[CrossRef\]](#)
30. Stolte, S.; Steudte, S.; Areitioaurtena, O.; Pagano, F.; Thöming, J.; Stepnowski, P.; Igartua, A. Ionic liquids as lubricants or lubrication additives: An ecotoxicity and biodegradability assessment. *Chemosphere* **2012**, *89*, 1135–1141. [\[CrossRef\]](#)
31. Stolte, S.; Steudte, S.; Igartua, A.; Stepnowski, P. The Biodegradation of Ionic Liquids—the View from a Chemical Structure Perspective. *Curr. Org. Chem.* **2011**, *15*, 1946–1973. [\[CrossRef\]](#)
32. Kapitanov, I.V.; Jordan, A.; Karpichev, Y.; Spulak, M.; Perez, L.; Kellett, A.; Kümmerer, K.; Gathergood, N. Synthesis, self-assembly, bacterial and fungal toxicity, and preliminary biodegradation studies of a series of l-phenylalanine-derived surface-active ionic liquids. *Green Chem.* **2019**, *21*, 1777–1794. [\[CrossRef\]](#)
33. Coleman, D.; Gathergood, N. Biodegradation studies of ionic liquids. *Chem. Soc. Rev.* **2010**, *39*, 600–637. [\[CrossRef\]](#)
34. Gathergood, N.; Garcia, M.T.; Scammells, P.J. Biodegradable ionic liquids: Part I. Concept, preliminary targets and evaluation. *Green Chem.* **2004**, *6*, 166–175. [\[CrossRef\]](#)
35. Garcia, M.T.; Gathergood, N.; Scammells, P.J. Biodegradable ionic liquids: Part II. Effect of the anion and toxicology. *Green Chem.* **2005**, *7*, 9–14. [\[CrossRef\]](#)
36. Gathergood, N.; Scammells, P.J.; Garcia, M.T. Biodegradable ionic liquids: Part III. The first readily biodegradable ionic liquids. *Green Chem.* **2006**, *8*, 156–160. [\[CrossRef\]](#)
37. Sharma, K.; Kumar, P.; Sharma, J.; Thapa, S.D.; Gupta, A.; Rajak, R.; Baruah, B.; Prakash, A.; Ranjan, R.K. Characterization of Polycyclic Aromatic Hydrocarbons (PAHs) associated with fine aerosols in ambient atmosphere of high-altitude urban environment in Sikkim Himalaya. *Sci. Total Environ.* **2023**, *870*, 161987. [\[CrossRef\]](#)
38. Serdyuk, A.A.; Mirgorodskaya, A.B.; Kapitanov, I.V.; Gathergood, N.; Zakharova, L.Y.; Sinyashin, O.G.; Karpichev, Y. Effect of structure of polycyclic aromatic substrates on solubilization capacity and size of cationic monomeric and gemini 14-s-14 surfactant aggregates. *Colloids Surf. A Physicochem. Eng. Asp.* **2016**, *509*, 613–622. [\[CrossRef\]](#)
39. Seitkalieva, M.M.; Kashin, A.S.; Egorova, K.S.; Ananikov, V.P. Ionic Liquids As Tunable Toxicity Storage Media for Sustainable Chemical Waste Management. *ACS Sustain. Chem. Eng.* **2018**, *6*, 719–726. [\[CrossRef\]](#)
40. Holmberg, K. (Ed.) *Handbook of Applied Surface and Colloid Chemistry*; John Wiley & Sons: Chichester, UK, 2002.

41. Zakharova, L.Y.; Serdyuk, A.A.; Mirgorodskaya, A.B.; Kapitanov, I.V.; Gainanova, G.A.; Karpichev, Y.; Gavrilova, E.L.; Sinyashin, O.G. Amino Acid-Functionalized Calix [4] Resorcinarene Solubilization by Mono- and Dicationic Surfactants. *J. Surfactants Deterg.* **2016**, *19*, 493–499. [\[CrossRef\]](#)
42. Mirgorodskaya, A.B.; Karpichev, Y.; Zakharova, L.Y.; Yackevich, E.I.; Kapitanov, I.V.; Lukashenko, S.S.; Popov, A.F.; Konovalov, A.I. Aggregation behavior and interface properties of mixed surfactant systems gemini 14-s-14/CTABr. *Colloids Surf. A Physicochem. Eng. Asp.* **2014**, *457*, 425–432. [\[CrossRef\]](#)
43. Konopka, A.; Zakharova, T.; Oliver, L.; Turco, R. Microbial biodegradation of organic wastes containing surfactants in a continuous-flow reactor. *J. Ind. Microbiol. Biotechnol.* **1997**, *18*, 235–240. [\[CrossRef\]](#)
44. Sudheer, S.; Raba, G.; Kapitanov, I.; Karpichev, Y.; Gupta, V.K.; Vilu, R.; Gathergood, N. A Greener Approach to Hydrolyse Ionic Liquids. *Basic Clin. Pharmacol. Toxicol.* **2018**, *124*, 21.
45. Ray, S.S. Environmentally friendly polymer matrices for composites. In *Environmentally Friendly Polymer Nanocomposites*; Elsevier: Amsterdam, The Netherlands, 2013; pp. 25–40. [\[CrossRef\]](#)
46. Neumann, J.; Steudte, S.; Cho, C.-W.; Thöming, J.; Stolte, S. Biodegradability of 27 pyrrolidinium, morpholinium, piperidinium, imidazolium and pyridinium ionic liquid cations under aerobic conditions. *Green Chem.* **2014**, *16*, 2174–2184. [\[CrossRef\]](#)
47. Kobayashi, M.; Shimizu, S. Metalloenzyme nitrile hydratase: Structure, regulation, and application to biotechnology. *Nat. Biotechnol.* **1998**, *16*, 733–736. [\[CrossRef\]](#) [\[PubMed\]](#)
48. Mascharak, P.K. Structural and functional models of nitrile hydratase. *Coord. Chem. Rev.* **2002**, *225*, 201–214. [\[CrossRef\]](#)
49. Rawlings, N.D.; Salvesen, G. (Eds.) *Handbook of Proteolytic Enzymes*, 3rd ed.; Academic Press: Cambridge, MA, USA, 2013.
50. Tomihata, K.; Ikada, Y. In vitro and in vivo degradation of films of chitin and its deacetylated derivatives. *Biomaterials* **1997**, *18*, 567–575. [\[CrossRef\]](#)
51. Klebe, G. Inhibitors of Hydrolases with an Acyl-Enzyme Intermediate. In *Drug Design*; Springer: Berlin/Heidelberg, Germany, 2013; pp. 493–532. [\[CrossRef\]](#)
52. Korhonen, H.; Pihlanto, A. Bioactive peptides: Production and functionality. *Int. Dairy J.* **2006**, *16*, 945–960. [\[CrossRef\]](#)
53. López-Otín, C.; Bond, J.S. Proteases: Multifunctional Enzymes in Life and Disease. *J. Biol. Chem.* **2008**, *283*, 30433–30437. [\[CrossRef\]](#) [\[PubMed\]](#)
54. Ouellette, R.J.; Rawn, J.D. *Principles of Organic Chemistry*; Elsevier: Amsterdam, The Netherlands, 2015. [\[CrossRef\]](#)
55. Areeksiree, M.; Engkagul, A.; Kovitvadhi, U.; Thongpan, A.; Mingmuang, M.; Pakkong, P.; Rungruangsak-Torrissen, K. Temperature and pH characteristics of amylase and proteinase of adult freshwater pearl mussel, *Hyriopsis (Hyriopsis) bialatus* Simpson 1900. *Aquaculture* **2004**, *234*, 575–587. [\[CrossRef\]](#)
56. Azevedo, H.S.; Reis, R.L. Understanding the Enzymatic Degradation of Biodegradable Polymers and Strategies to Control Their Degradation Rate. In *Biodegradable Systems in Tissue Engineering and Regenerative Medicine*; CRC Press: Boca Raton, FL, USA, 2004. [\[CrossRef\]](#)
57. Bender, M.L.; Ginger, R.D.; Unik, J.P. Activation Energies of the Hydrolysis of Esters and Amides Involving Carbonyl Oxygen Exchange¹. *J. Am. Chem. Soc.* **1958**, *80*, 1044–1048. [\[CrossRef\]](#)
58. Jencks, W.P.; Carriuolo, J. Reactivity of Nucleophilic Reagents toward Esters. *J. Am. Chem. Soc.* **1960**, *82*, 1778–1786. [\[CrossRef\]](#)

Disclaimer/Publisher's Note: The statements, opinions and data contained in all publications are solely those of the individual author(s) and contributor(s) and not of MDPI and/or the editor(s). MDPI and/or the editor(s) disclaim responsibility for any injury to people or property resulting from any ideas, methods, instructions or products referred to in the content.

Appendix 5

Publication V

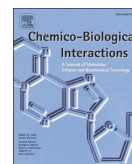
Kapitanov, I.V.; Spulak, M.; Pour, M.; Soukup O.; Marek, J.; Jun, D.; Novak, M.; Diz de Almeida, J.S.F.; Costa França, T.C.; Gathergood, N.; Kuca, K.; Karpichev, Y. Sustainable ionic liquids-based molecular platforms for designing acetylcholinesterase reactivators. *Chem.-Biol. Interact.*, **2023**, 385, 110735

Reproducing is permitted by Elsevier Copyright policy / Authors' rights in the article.



Contents lists available at ScienceDirect

Chemico-Biological Interactions

journal homepage: www.elsevier.com/locate/chembioint

Sustainable ionic liquids-based molecular platforms for designing acetylcholinesterase reactivators

Illia V. Kapitanov^{a,1}, Marcel Špulák^b, Milan Pour^b, Ondřej Soukup^{c,d}, Jan Marek^{c,e},
Daniel Jun^e, Martin Novák^c, Joyce S.F. Diz de Almeida^f, Tanos C.C. França^{f,g},
Nicholas Gathergood^h, Kamil Kuča^{g,**}, Yevgen Karpichev^{a,*}

^a Department of Chemistry and Biotechnology, Tallinn University of Technology, Akadeemia Tee 15, 12618 Tallinn, Estonia^b Department of Organic and Bioorganic Chemistry, Faculty of Pharmacy in Hradec Králové, Charles University, Heyrovského 1203, 500 05 Hradec Kralove, Czech Republic^c Biomedical Research Center, University Hospital Hradec Kralove, Sokolska 581, 500 05 Hradec Kralove, Czech Republic^d Department of Toxicology and Military Pharmacy, Faculty of Military Health Sciences, University of Defense, Trebesska 1575, 500 01 Hradec Kralove, Czech Republic^e Department of Epidemiology, Faculty of Military Health Sciences, University of Defense, Trebesska 1575, 500 01 Hradec Kralove, Czech Republic^f Laboratory of Molecular Modeling Applied to the Chemical and Biological Defense (LMCBD), Military Institute of Engineering, Rio de Janeiro, RJ, Brazil^g Department of Chemistry, Faculty of Science, University of Hradec Kralove, Rokytanského 62, 500 03 Hradec Kralove, Czech Republic^h School of Chemistry, College of Science, University of Lincoln, Lincoln LN6 7TS, UK

ARTICLE INFO

Keywords:

Acetylcholinesterase reactivators

Oximes

Functionalized ionic liquids

Green chemistry

Sustainability

ABSTRACT

We report a green chemistry approach for preparation of oxime-functionalized ILs as AChE reactivators: amide/ester linked IL, L-alanine, and L-phenylalanine derived salts bearing pyridinium aldioxime moiety. The reactivation capacities of the novel oximes were evaluated towards AChE inhibited by typical toxic organophosphates, sarin (GB), VX, and paraoxon (PON). The studied compounds are mostly non-toxic up to the highest concentrations screened (2 mM) towards Gram-negative and Gram-positive bacteria cell lines and both filamentous fungi and yeasts in the *in vitro* screening experiments as well as towards the eukaryotic cell (CHO-K1 cell line). Introduction of the oxime moiety in initially biodegradable structure decreases its ability to biodegradation. The compound **3d** was shown to reveal remarkable activity against the AChE inhibited by VX, exceeding conventional reactivators 2-PAM and obidoxime. The regularities on antidotal activity, cell viability, plasma stability, biodegradability as well as molecular docking study of the newly synthesized oximes will be used for further improvement of their structures.

1. Introduction

Acetylcholinesterase (AChE, EC 3.1.1.7) is a hydrolytic enzyme playing a key role in cholinergic synaptic transmission. AChE is a main target for organophosphorus (OP) neurotoxins, either nerve agents [1,2] or pesticides (Fig. 1). The nerve agents can be classified as G-agents (e.g. sarin, soman, tabun, etc.) and V-agents (e.g., VX), and also more recently so-called A-agents (known as Novichok [3–6]), a group chemical warfare agents developed in the former Soviet Union getting a worldwide attention recently due to Skripals [7] and Navalnyi [8] poisoning cases. The toxic OPs inhibit serine esterases by covalently binding to a Ser

residue in the catalytic site. Inactivation of AChE results in the accumulation of neurotransmitter acetylcholine at synapses, leading to nervous and respiratory failure and causing death if untreated [1].

Chemical warfare agents (CWA) pose a serious concern in the age of terrorist activity and the risk of using them by a terrorist group or rogue regimes since a facility producing OP pesticides can be repurposed to make nerve agents, or the OP pesticides in higher amounts can be used for the same purpose as nerve agents. They are the likeliest weapons of choice for terrorists due to their high lethality and moderately skilled chemists can prepare them [9–11]. Although the major world powers have agreed to abandon the use of these weapons and destroy the

* Corresponding author. Department of Chemistry and Biotechnology, Tallinn University of Technology, Akadeemia Tee 15, 12618 Tallinn, Estonia.

** Corresponding author. Department of Chemistry, Faculty of Science, University of Hradec Kralove, Rokytanského 62, 500 03 Hradec Kralove, Czech Republic.

E-mail addresses: kamil.kuca@uhk.cz (K. Kuča), yevgen.karpichev@taltech.ee (Y. Karpichev).¹ Current address: Gemini PharmChem Mannheim GmbH, 68305 Mannheim, Germany.<https://doi.org/10.1016/j.cbi.2023.110735>

Received 19 July 2023; Received in revised form 9 September 2023; Accepted 25 September 2023

Available online 4 October 2023

0009-2797/© 2023 Elsevier B.V. All rights reserved.

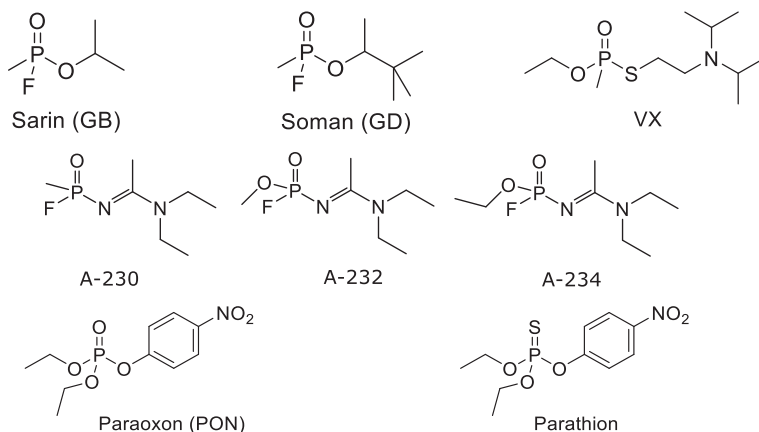


Fig. 1. Structure of typical organophosphorus neurotoxins.

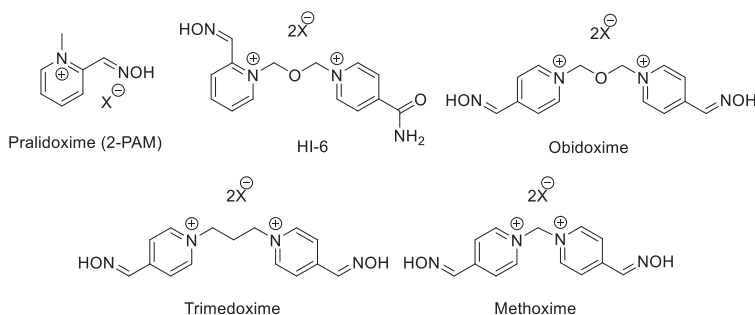


Fig. 2. Structure of quaternary oximes - reactivators of the OP-inhibited AChE.

existing stock and there are internationally regulated controls put in place on the starting materials, the key intermediates are easily accessible, and there are still countries (e.g. North Korea and Syria) that have not ratified the Chemical Weapon Convention.

The quaternary pyridine oximes represent the lead compounds for reactivation of the OP-inhibited AChE. They fit into the choline pocket of the enzyme's active site via a quaternary, positively charged pyridinium scaffold, while the nucleophilic attack by the oxime group at the P atom of the OP conjugate restores the activity of the AChE. The cleavage of the OP conjugate by oxime antidote results in restoring AChE catalytic activity [1].

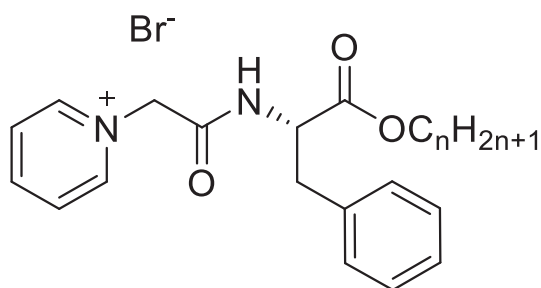
Research on effective antidotes against OP poisoning continues for almost seven decades since pralidoxime was employed, and all lead reactivators developed later bear hydroximinomethyl pyridinium fragment in their structure (Fig. 2) [12]. To overcome the drawbacks of low BBB penetration so called non-quaternary reactivators were also studied. It started with pro-2-PAM (a lipid permeable 2-PAM derivative), monoisonitrosoacetone (MINA) and diacetyl monoxime (DAM) [13] showing protection of the CNS damage [14]. Further research discovered structurally diverse groups of novel uncharged reactivators possessing comparable activity to clinically used quaternary oximes *in vitro*. Despite of the fact that some compounds were highlighted as promising for post-exposure treatment [15,16], uncharged compounds often suffer from unsuitable physicochemical properties mostly associated with a molecular obesity and low solubility hampering the *in vivo*. Nevertheless, the quaternary pyridinium oxime antidotes are currently in use as the most efficient agents for OP poisoning treatment, see Fig. 2 [17]. The

structural modifications of these compounds are usually performed with focus on improvement of activity level [18] or suitable hydrophobic-hydrophilic balance in order to ensure the reactivation activity and, at the same time, to increase the chance for the BBB crossing [2,19,20].

The contemporary concept requires targeting a synergy between principles of green chemistry and the core areas of chemical disarmament and nonproliferation [21]. The CWA and military chemical compounds must be researched further, including designing sustainable remediation technologies, both eco-friendly and low-cost [22].

Design of sustainable chemicals is a fundamental and critical task on a way to realize a sustainable economy [23]. Implementation of green chemistry principles in process development promotes responsible usage of natural sources [24,25]. The strong trend in recent decades is the exchange of non-renewable sources of reagent and materials (e.g., from petroleum, gas, and coal) on a new greener alternative (e.g., biomass derived, waste stream recycling, food waste valorization). Another trend is a switch to sustainable alternative green solvents from widely used conventional organic solvents (especially undesirable volatile organic compounds). Some examples include substitution using "greener" media, biobased solvents (e.g., ethanol, Cyrene™ (dihydrolevoglucosenone), or 2,2,5,5-tetramethyloxolane), ionic liquids, and deep eutectic solvents [26,27].

Ionic liquids (ILs) have undeniable advantages compared with other reaction media. The ILs fulfil the main part of criteria for green solvents [28,29], and their role in modern technological processes is constantly increasing [30–32]. Important points in selection of ILs for future



$$n = 2, 4, 6, 8, 10, 12, 14, 16$$

Fig. 3. Low microbial toxicity biodegradable L-phenylalanine-derived ILs.

application in sustainable technological processes are ecotoxicity of corresponding ILs [33,34], their biodegradability [35] and possibility to synthesize them from renewable sources [36]. Evaluation of ecotoxicity and biodegradability of ILs are necessary to minimize impact of IL-containing wastes on the environment [37,38]. The choice of renewable materials as source of a key structural element for ILs could help to solve problems with availability of these structural elements in long-term perspective [39–42]. Following this strategy, a series of low microbial toxicity, biodegradable L-Phe-derived ILs were developed (Fig. 3) [40,43] and tested for possible applications (e.g., solubilization of polycyclic aromatic hydrocarbons [44]).

The structural improvement (synthesis of dipeptide derived ILs) and investigation of obtained compounds helped to more deeply understand dependency between structure and biodegradability [38,43,45,46], but foremostly create green systems for organophosphates decomposition [47], and pharmaceuticals binding/detection [48,49]. In summary, previous results have demonstrated a very high flexibility of such type of compounds in scope of practical application. A prospective way to

expand the application field of studied ionic liquids-based molecular platforms is their structural modification and testing new sustainable AChE reactivators.

In this study we have proposed, synthesized, and studied series of acetylcholinesterase reactivators using previously selected [50] ionic liquids-based molecular platforms. The changes in structure from compounds type 1 to compounds type 4 (Fig.4) could help to determine an influence of each newly introduced fragment on observed biological effects: compounds type 1 is a simplest basic structure among studied ionic liquids-based acetylcholinesterase reactivators and it will be used as a starting point in evaluation of all changes made; compounds type 2 is a structure with introduced non-bulky amino acid fragment (L-Ala residue); compounds type 3 represents a structural modification with the introduction of bulky hydrophobic element (L-Phe residue) into the molecule; compounds type 4 is an example of functionalization with the oxime group on low-toxic biodegradable L-Phe-derived ILs, presented on Fig. 3. The difference of these compounds compared to compounds type 3 is a replacement of the amide bond in C-carboxylic fragment of phenylalanine with the ester group.

Series 1–4 were evaluated for hydrophobicity and BBB permeability, we determined toxicological properties (antibacterial activity, antifungal activity, the effect of the compounds on the cell viability), stability in human plasma, and biodegradability. Reactivation capacity towards AChE inhibited by sarin (GB), VX and paraoxon (PON) – typical toxic organophosphate agents – were also evaluated and corroborated with the docking studies to explain the reactivation activity observed.

2. Materials and methods

2.1. Materials

All commercial chemicals and solvents were purchased from Sigma Aldrich, Alfa Aesar, or TCI Europe and used without further purification. Deionized water from a Milli-Q system was used in all sample preparation. Silica gel 60 F₂₅₄ plates were used for TLC. Pralidoxime chloride and obidoxime were prepared at Department of Toxicology and Military Pharmacy, Faculty of Military Health Sciences, University of Defence

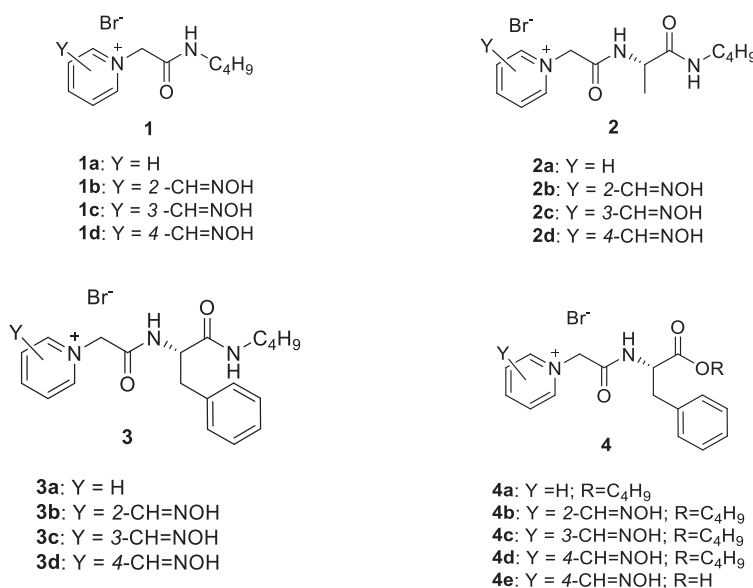
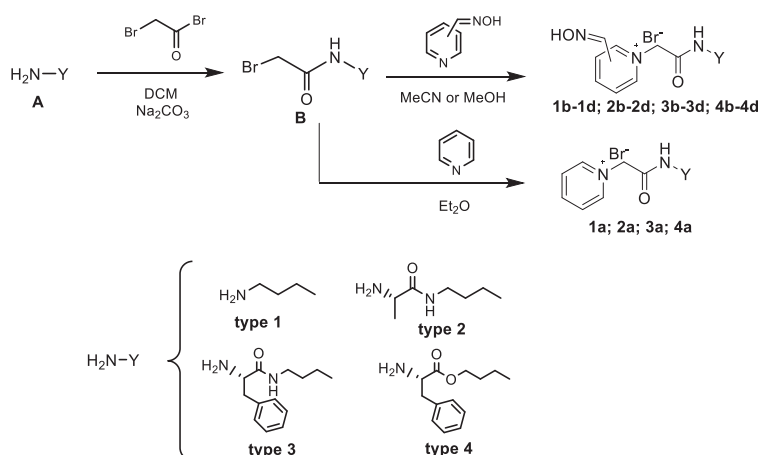


Fig. 4. Structure of studied ionic liquids-based acetylcholinesterase reactivators.



Scheme 1. General method of synthesis of compounds type 1–4.

(Hradec Králové, Czech Republic). Sarin (isopropyl methylphosphonofluoridate, GB) and VX (O-ethyl S-diisopropylaminomethyl methylphosphonothiolate) were obtained from Military Technical Institute in Brno (Brno, Czech Republic) and its purity was higher than 95%. Para-oxon (diethyl 4-nitrophenyl phosphate) of analytical purity was purchased from Sigma-Aldrich.

2.2. Synthesis and characterization of products

For recording of NMR spectra Bruker Avance III 400 MHz spectrometer operating at 400 MHz for ^1H NMR and 101 MHz for ^{13}C NMR was used. Samples were run in deuterated chloroform (CDCl_3) or deuterated dimethyl sulfoxide ($\text{DMSO}-d_6$) where appropriate. The HRMS identification of compounds was performed on an Agilent 6540 UHD Accurate-Mass Q-TOF LC/MS G6540A Mass Spectrometer. ^1H and ^{13}C NMR spectra, HRMS of the obtained compounds are collected in ESI.

The general method of synthesis of compounds type 1–4 is presented on a Scheme 1.

Boc-Protected amines (A) (synthesis of compounds type 2 and 3). The corresponding *N*-(Boc)-L-amino acid (0.05 mol; Boc-*N*-Phe or Boc-*N*-Ala) was dissolved in dry DMF (25 mL) under argon atmosphere and the reaction mixture was cooled to 0 °C. Then to stirred solution was added portionwise carbonyldiimidazole (8.11 g; 0.05 mol). The reaction mixture was stirred 15 min more after stopped of gas formation. After that, solution of 1-butylamine (4.94 mL; 0.05 mol) in alcohol-free amylene-stabilized chloroform (25 mL) was added dropwise to reaction mixture. The reaction mixture was stirred 24 h at room temperature under argon atmosphere. After that, solvents from reaction mixture were evaporated *in vacuo*, residue dissolved in alcohol-free chloroform (100 mL) and washed with 0.1 N HCl (2×50 mL), 0.1 N Na_2CO_3 (2×50 mL) and water (2×50 mL). The organic layer was dried over anhydrous sodium sulfate and concentrated *in vacuo* to afford the title compounds. The yields were 82–88%.

Synthesis of amines (A) (for compounds type 2 and 3). To obtain the Ala derivatives, to a solution of *N*-(Boc)-L-alanine butyl amide (12.22 g; 0.05 mol) in ethanol (150 mL) was added $\text{PTSA} \cdot \text{H}_2\text{O}$ (12.36 g; 0.065 mol) and refluxed with stirring for 12 h. Then solvent was removed *in vacuo*. Residue was dissolved in dichloromethane and stirred with solid sodium carbonate (13.78 g; 0.13 mol) for 48 h. Then reaction mixture was filtrated, residue on a filter was washed with dichloromethane (2×50 mL). Solvent from filtrate was removed *in vacuo* to afford the title compounds (yield 92%).

To obtain L-Phe derivatives, to a solution of *N*-(Boc)-L-phenylalanine

butyl amide (16.02 g; 0.05 mol) in ethanol (150 mL) was added $\text{PTSA} \cdot \text{H}_2\text{O}$ (12.36 g; 0.065 mol) and refluxed with stirring for 12 h. Then solvent was removed *in vacuo*. Residue was dissolved in dichloromethane (150 mL) and washed with solution of Na_2CO_3 (0.1 mol; 10.6 g) in water (150 mL), and then with water (2×100 mL). The organic layer was dried over anhydrous sodium sulfate and concentrated *in vacuo* to afford the title compounds (yield 97%).

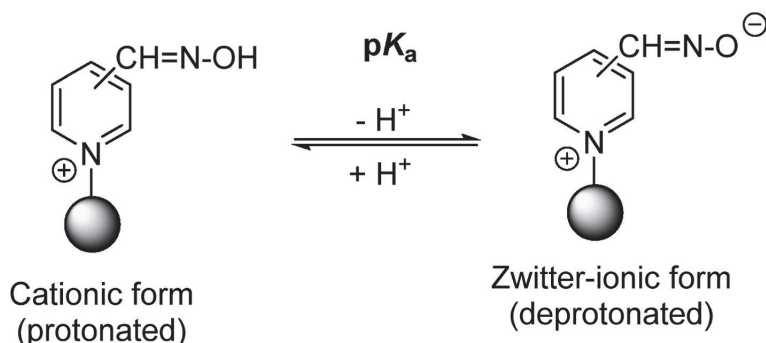
***N*-Bromoacetyl derivatives (B).** To a stirred solution of the corresponding substituted amine type A (0.05 mol) in alcohol-free chloroform (50 mL) was added solid Na_2CO_3 (7.95 g, 0.075 mol). To this mixture was added dropwise bromoacetyl bromide (5.65 mL, 0.065 mol) and stirred for 12 h. Then 50 mL of water was added carefully to reaction mixture and then it was transferred to a separating funnel. The organic layer was separated, washed with 0.1 N Na_2CO_3 (2×50 mL) and water (3×50 mL). The organic phase was dried over sodium sulfate, filtered and volatiles removed *in vacuo* to afford the title compounds. The yields were 91–98%.

Amines (A) and *N*-Bromoacetyl derivatives (B) for compounds type 1 were obtained similarly to the method described in Refs. [47,51] and for compounds type 4 – similarly to the method published for L-phenylalanine ILs [40,43].

Pyridinium aldoximes (1b-1d, 2b-2d, 3b-3d, 4b-4d). The stirring solution of corresponding *N*-bromoacetyl derivative (0.01 mol) and corresponding pyridinealdoxime (1.22 g; 0.01 mol) in 25 mL of acetonitrile (for synthesis of all compounds except 2d and 3d) or 25 mL of methanol (for compounds 2d, and 3d) was refluxed 12 h. After cooling to room temperature the obtained solid product was filtrated, washed with cold acetonitrile (3×10 mL), and then with diethyl ether (2×20 mL), and dried *in vacuo*. The titled compounds was isolated with yields 51–89%.

Pyridinium aldoxime 4e. A sodium hydroxide solution (0.44 g; 0.011 mol) in 2 mL of water was added dropwise with pH control to solution of pyridinium aldoxime 4d (0.01 mol) in water (15 mL) [pH has to be ca. 10.50 by pH-meter], then after 30 min was acidified up to pH 2.0 with concentrated hydrobromic acid. Water from reaction mixture was evaporated in vacuum desiccator, residue was dissolved in cold absolute ethanol (10 mL) and filtrated from solid sodium bromide. Filtrate was evaporated and washed with diethyl ether (3×10 mL). The product was dried *in vacuo*. The yield of the title compound was 95%.

Non-functionalized ILs (1a, 2a, 3a). The stirring solution of corresponding *N*-bromoacetyl derivative (0.01 mol) and pyridine (1.22 g; 0.01 mol) in 25 mL of acetonitrile was refluxed 12 h. After cooling to room temperature, the obtained solid product was filtrated, washed with



Scheme 2. Protolytic equilibria in solutions of quaternary pyridinium oximes.

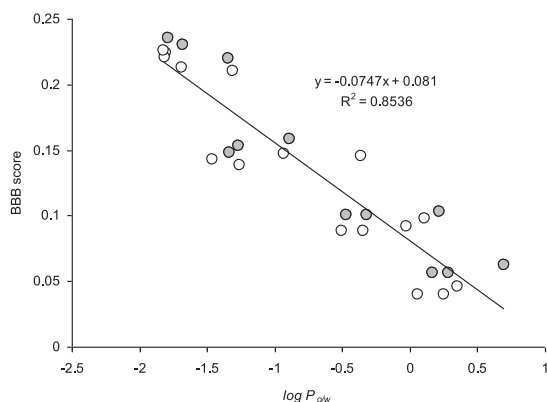
Table 1

Parameters pK_a , $\log P_{o/w}$ and BBB score for ILs types 1 – type 4, calculated using on-line prediction tools.

Compound	pK_a (Chemicalize)	$\log P_{o/w}$ (VCCLAB)		$\log P_{o/w}$ (www.molinspiration.com)		BBB score (www.cbligand.org)	
		Cationic form	Zwitter-ionic form	Cationic form	Zwitter-ionic form	Cationic form	Zwitter-ionic form
1a	–	–1.8	–	–3.93	–	0.224	–
1b	6.72	–1.31	–1.34	–2.3	–5.18	0.21	0.22
1c	7	–1.81	–1.68	–2.59	–5.27	0.221	0.23
1d	7.87	–1.82	–1.79	–3.56	–5.51	0.226	0.235
2a	–	–1.69	–	–4.4	–	0.213	–
2b	6.69	–0.93	–0.89	–2.87	–5.34	0.147	0.158
2c	6.98	–1.26	–1.33	–3.15	–5.41	0.138	0.148
2d	7.87	–1.46	–1.27	–4.12	–5.62	0.143	0.153
3a	–	–0.36	–	–3.03	–	0.145	–
3b	6.66	–0.02	0.22	–1.41	–4.86	0.092	0.103
3c	6.98	–0.34	–0.32	–1.69	–4.97	0.088	0.1
3d	7.87	–0.5	–0.47	–2.66	–5.29	0.088	0.1
4a	–	0.11	–	–2.28	–	0.098	–
4b	6.61	0.35	0.7	–0.65	–4.47	0.046	0.062
4c	6.98	0.25	0.29	–0.94	–4.64	0.04	0.056
4d	7.87	0.06	0.17	–1.91	–5.05	0.04	0.056
4e	7.87 *	–1.09	–0.92	–4.88	–5.3	0.03	0.049

Notes. * pK_a 7.87 corresponds to oxime fragment; calculated pK_a of carboxylic group in **4e** is 3.16.

BBB score was calculated using fingerprint PubChem.

Fig. 5. Dependency of the predicted values of BBB score (www.vcclab.org) on $\log P_{o/w}$ (www.cbligand.org) for cationic (○) and zwitter-ionic (●) species of compounds 1–4.

cold acetonitrile (3×10 mL), and then with diethyl ether (2×20 mL), and dried *in vacuo*. The titled compounds were isolated with yields more than 90%.

L-Phe derived ester **4a** was prepared as described in Ref. [43].

2.3. Evaluation of hydrophobicity and BBB penetration ability

The predicted $P_{o/w}$ values were calculated by means of the online cheminformatics tools: www.chemicalize.com, Molinspiration Cheminformatics free web services, Slovensky Grob, Slovakia (www.molinspiration.com), and VCCLAB (www.vcclab.org) [52]. The BBB score values were calculated by using Blood-Brain Barrier Predictor (www.cbligand.org), version 0.9; this predictor was built by applying the support vector machine (SVM) and LiCABEDS algorithms. These online predicting tools were used previously [19,45] to evaluate properties of compounds with similar structure and functionality and cross-checked using appropriate experimental data.

2.4. Molecular docking study

Construction of Ligands. Before the construction of the tridimensional structures each oxime was submitted to the server Chemicalize (<https://chemicalize.com/>) in order to investigate their protonation states at physiologic pH (7.4). After that, the tridimensional structures of each possible species at pH = 7.4 for each oxime, were built using the software PC Spartan Pro® [53], and their partial atomic charges calculated through RM1 (Recife Model 1) semi-empirical methods [54]. For docking studies the crystallographic water molecules were removed and

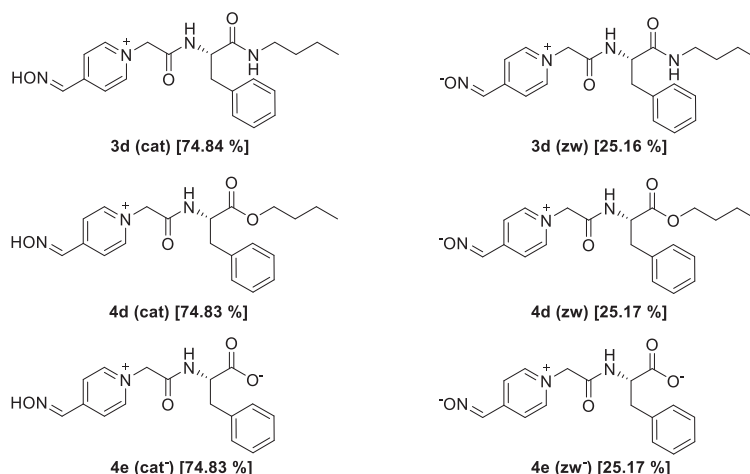


Fig. 6. Possible protonation states for the oximes under study at pH = 7.4 based on <https://chemicalize.com/prediction-tool>.

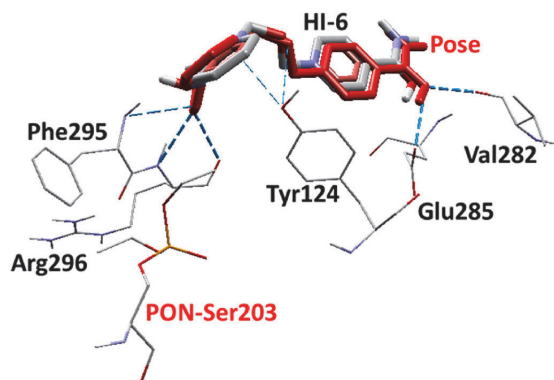


Fig. 7. Best re-docking pose for HI-6 inside the complex *HssAChE-PON*.

protonation states of the protein residues were set to physiological pH.

Construction of the models of AChE inhibited by Sarin (*HssAChE-GB*). The *HssAChE-GB* used in this work was constructed from the crystallographic structure of AChE from *Mus Musculus* (*MmAChE*) inhibited by GB, available in the RSCB PDB Protein Data Bank (<http://www.rcsb.org/pdb/home/home.do>) under the code 2Y2V, chosen based on the availability of a significant amount of data related to the modeling of this type of structures described elsewhere [55,56], including our previously published studies [19]. The primary structures of *MmAChE* and *HssAChE* were aligned using the BLAST tool from the UniProt Data Bank (<https://www.uniprot.org/>). As these enzymes present 93% of overall identity and 100% of identity in the active site, the model of *HssAChE-GB* was constructed just by mutating the mismatching residues. This model was validated using the server PDBSum (<http://www.ebi.ac.uk/pdbsum/>), where the Ramachandran plot and topology analysis for the protein were obtained. The binding sites for the docking studies were restricted into a sphere with a radius of 13 Å, coordinates $x = 29.77$; $y = 20.20$; $z = 11.54$ centered at the oxygen atom of the side chain of Ser203, and the residues 6 Å closest to the OP were considered flexible.

Construction of the models of AChE inhibited by VX (*HssAChE-VX*). The model of *HssAChE-VX* was constructed from the crystallographic structure of *HssAChE* inhibited by VX available in RSCB PDB Protein Data

Bank (<http://www.rcsb.org/pdb/home/home.do>) under the code 6CQZ. The software BIOVIA Discovery Studio® was used to fix the structure of VX and also to make the bond with Ser203 and optimize the receptor with CHARMM force field [57]. This model was validated using the server PDBSum (<http://www.ebi.ac.uk/pdbsum/>), where Ramachandran plot and topology analysis for the protein were obtained. The binding sites for docking studies were restricted into a sphere with a radius of 15 Å, with coordinates: $x = 50.20$; $y = -19.81$; $z = 348.34$ centered at the oxygen atom of the side chain of Ser203, and the residues 6 Å closest to the OP were considered flexible.

***HssAChE* inhibited by Paraoxon (*PON*) (*HssAChE-PON*).** The model of *HssAChE-PON* was constructed from the crystallographic structure of *HssAChE* inhibited by PON and complexed with HI-6 available in RSCB PDB Protein Data Bank (<http://www.rcsb.org/pdb/home/home.do>) under the code 5HF9. The software BIOVIA Discovery Studio® was used to fix the structure of PON and also to make the bond with Ser203 and optimize the receptor with the CHARMM force field [57]. This model was validated using the server PDBSum (<http://www.ebi.ac.uk/pdbsum/>), where Ramachandran plot and topology analysis for the protein were obtained. The binding sites for the dockings were restricted into a sphere with a radius of 13 Å, coordinates $x = -11.31$; $y = -41.29$; $z = 28.99$ centered at the oxygen atom of the side chain of Ser203, and the residues 6 Å closest to the OP were considered flexible.

Re-docking and docking energy calculations. The docking protocol used in this study was validated through re-docking of the experimental structure HI-6 from the crystallographic structure of *HssAChE* inhibited by PON mentioned before. The binding site for the re-docking calculation was restricted into a sphere with a radius of 10 Å, with coordinates: $x = -17.06$; $y = -41.79$; $z = 27.74$ centered at the oxygen atom of the side chain of Ser203.

After charges calculations, the docking energies of the ligands bound to the models *HssAChE-GB*, *HssAChE-VX* and *HssAChE-PON*, were obtained using the software Molegro Virtual Docker (MVD)® [58]. Due to the stochastic nature of the docking evolutionary algorithm, about 10 runs were performed for each compound with 30 poses (conformation and orientation of the ligands) returned to the analysis. Parameters of population size and maximum number of interactions were modified on each run. The best conformation of each compound was selected according to the binding energies, and distance between the O atom (nucleophile) from the $-C=N-OH$ group of the oxime, and the P atom of the organophosphate (OP). The lower this distance, the more favorable is the reactivation reaction. In addition, the hydrogen bonds (H-bond)

Table 2
Best docking results for studied compounds on *HssAChE*-GB, *HssAChE*-VX and *HssAChE*-PON. (*⁺) Hydrophobic Interactions.

IL	HsACHE-GB				HsACHE-VX				HsACHE-PON			
	E_{inter} (kcal•mol ⁻¹)	E_{Hbond} (kcal•mol ⁻¹)	H-bond	Distance O-P (Å)	E_{inter} (kcal•mol ⁻¹)	E_{Hbond} (kcal•mol ⁻¹)	H-bond	Distance O-P (Å)	E_{inter} (kcal•mol ⁻¹)	E_{Hbond} (kcal•mol ⁻¹)	H-bond	Distance O-P (Å)
3d (cat)	-162.37	-1.64	Asp74 Tyr124 Tyr133	5.53	-89.98	-3.12	Tyr124 Tyr341	5.05	-147.55	-1.99	Tyr124 Op	3.82
3d (zw)	-148.87	-0.03	Tyr124	7.08	No pose meeting the selection criteria was obtained				-143.63	-0.70	Tyr124	3.92
4d (cat)	-155.39	-1.93	Gly120 Tyr133	6.22	-73.35	-2.22	Tyr72 Tyr124	5.59	-140.06	-0.58	Tyr124 Op	3.57
4d (zw)	-145.13	-1.66	Asp74 Tyr133	6.00	-87.83	-1.97	Tyr124 Tyr341	5.30	-139.57	-4.06	Tyr124	5.81
4e (cat)	-144.19	-2.01	Ser125 Glu202	4.65	No pose meeting the selection criteria was obtained				-130.97	-1.50	Tyr337 Tyr124	5.82
4e (zw)	-124.49	-2.12	Tyr341* Tyr124 Ser125 Arg296	7.25	-99.19	-1.87	Tyr124 Ser293	5.33	-145.95	-0.56	Tyr124	6.34

and hydrophobic interactions with enzyme residues were also observed.

2.5. Screening for antibacterial and antifungal activity

The antibacterial and antifungal activity (determination of MIC in μM) were evaluated by microdilution broth method according to EUCAST (The European Committee on Antimicrobial Susceptibility Testing) [59–61], following the techniques described in our previous papers [39,40,43].

2.6. In vitro cell viability assessment

Standard MTT assay (Sigma Aldrich) was used according to the manufacturer's protocol on the CHO-K1 cell line (Chinese hamster ovary, ECACC, Salisbury, UK) in order to compare the effect of different compound within the series. The cells were cultured according to ECACC recommended conditions and seeded in a density of 8000 per well as described previously [62–64]. Briefly, tested compounds were dissolved in the growth medium (F-12). Cells were exposed to a tested compound for 24 h. Then the medium was replaced by a medium containing 10 μ M of MTT and cells were allowed to produce formazan for another approximately 3 h under surveillance. Thereafter, medium with MTT was removed and crystals of formazan were dissolved in DMSO (100 μ L). Cell viability was assessed spectrophotometrically by the amount of formazan produced. Absorbance was measured at 570 nm with 650 nm reference wavelength on Synergy HT (BioTek, USA). IC₅₀ calculated from the control - subtracted triplicates using non-linear regression (four parameters) of GraphPad Prism 5 software. Final IC₅₀ and standard error values were obtained as a mean of 2–3 independent measurements.

2.7. In vitro stability testing in human plasma

To produce stock sample solution, the selected compounds **3d** and **4d** were dissolved in DMSO; 10 μL of stock solution was added to 990 μL of human plasma Human Pooled Plasma (Batch S00G71, Biowest, France) to initiate the reaction. The final concentration of DMSO in the incubation mixture did not exceed 1% (v/v) and the concentration of tested compounds was set at 1 μM . Each compound was incubated for 0, 15, 30, 60 and 120 min at 37 $^{\circ}\text{C}$. The reactions were stopped by transferring 100 μL of the sample to 200 μL of acetonitrile containing 2-chloro-6-methoxy-7-(naphthalen-2-ylmethyl)-7H-purine as internal standard (IS) [65] at the appropriate time points and centrifuged at 12,000 rpm for 10 min at 4 $^{\circ}\text{C}$ to precipitate the protein. After that, 150 μL of supernatant was transferred to the vial and analyzed by LC-MS (see below). The areas of the compounds (A_{cmp}) and internal standards (A_{IS}) were detected in extracted ion chromatograms from the mass spectrometer data in positive mode. From the ratio between peak area ratios (compound peak area/internal standard peak area) obtained at incubation times 0 and 120 min, the percentage of remaining compound was calculated. The samples were analyzed by an LC-MS system consisting of UHPLC Dionex Ultimate 3000 RS coupled with a Q Exactive Plus orbitrap mass spectrometer to obtain the areas (Thermo Fisher Scientific, Bremen, Germany). Reverse-phase C18 column Kinetex EVO (Phenomenex, Torrance, CA, USA) was used as a stationary phase, and purified water with 0.1% formic acid (mobile phase A) and LC-MS grade acetonitrile with 0.1% formic acid (mobile phase B) were used as the mobile phases. Gradient elution was used to determine purities and mass spectra. The method started with 5% B for 0.3 min, then the gradient switched to 100% B in the third minute, remained at 100% B for 0.7 min and then went back to 5% B with equilibration for 3.5 min. The total run time of the method was 7.5 min. The column temperature was kept constant at 27 $^{\circ}\text{C}$, the flow of the mobile phase was 0.5 ml/min, and the injection volume was 1 μL . HRMS spectra were collected from the total ion current in the scan range 105–1000 m/z , with the resolution set to 140,000.

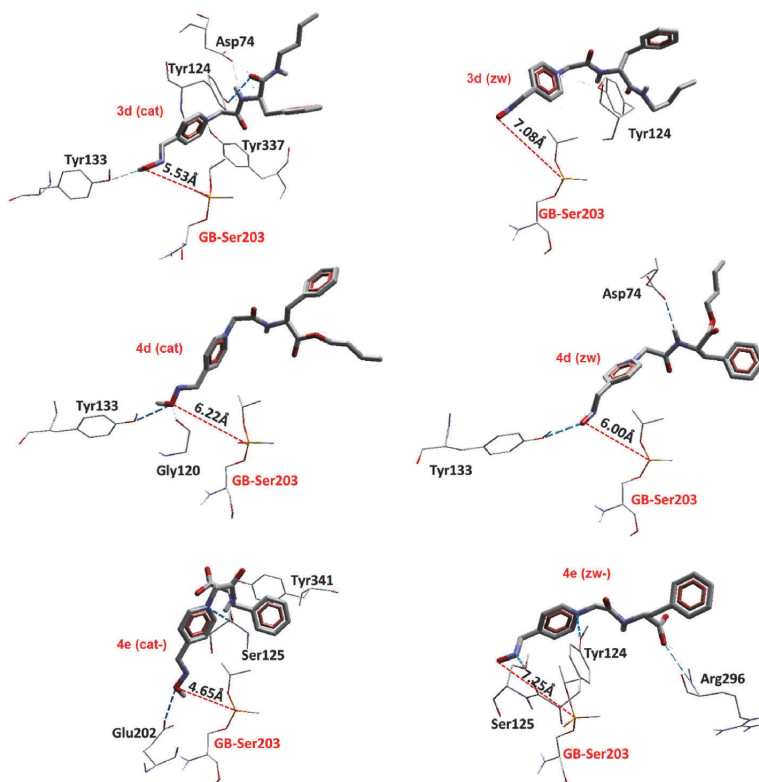


Fig. 8. Best docking poses of all the compounds on HssAChE-GB.

2.8. Aerobic biodegradation testing using CBT

Effluent from wastewater treatment plant was collected from a municipal wastewater treatment plant in Tallinn, Estonia (Paljassaare wastewater treatment plant, 59°27'55.5"N 24°42'08.8"E). WWTP effluent was filtered through a cellulose filter (90 mm diameter, Grade 1, pore size 11 µm) before being used as inoculum. Aerobic biodegradation testing was done using modified OECD 301D Closed Bottle Test (CBT) [66]. CBT setup with modification where biological oxygen consumption is measured with an optode oxygen sensor system using PTFE-lined PSt3 oxygen sensor spots (Fibox 3 PreSens, Regensburg, Germany) allows measuring BOD without opening the flasks and thereby reducing the number of parallels needed for each compound and increasing test throughput. It has also shown to improve reproducibility compared to the original OECD 301D guideline [67].

Each CBT run consisted of four different series each of which have been repeated in duplicates. First was "reference series" in which readily biodegradable sodium acetate in known concentration (6.41 mg L⁻¹) was added to a flask of mineral medium inoculated with effluent from wastewater treatment plant. In "test series" test compound as a sole source of carbon was added to inoculated mineral medium. Test compound was added in concentration corresponding to theoretical oxygen demand (ThOD) of approximately 5 mg/L. ThOD was calculated assuming nitrification would take place as each of the studied compounds included nitrogen atom(s) in their structure. "Toxicity series" containing both sodium acetate and test compound in their respective concentrations were used to evaluate test compounds' toxicity against inoculum – if biodegradation values in these bottles were significantly lower compared to reference series it was concluded that test compound

could be inhibiting or even toxic to microbes in WWTP effluent. To negate the effect of inoculum itself, blank bottles containing only inoculum and mineral medium were added to each CBT run and the value of these bottles was subtracted from all of the other bottles. Each run was performed at least for 28 days (suggested by OECD 301D protocol) [67]. To consider seasonal variations in inoculum composition did not have an effect on biodegradation results, total of 6 CBT runs from June to November were performed.

Results from each run were accepted if following criteria were met: i) difference of extremes of replicate values at the plateau is less than 20%, ii) oxygen concentration in test series bottles must not fall below 0.5 mg/L at any time, iii) sodium acetate in reference series must be degraded ≥60% by day 14. Blank bottles oxygen consumption was also monitored to avoid possibility of system turning from aerobic to anaerobic. In none of the CBT runs oxygen consumption in blank bottles exceeded 34% compared to initial oxygen concentration.

2.9. AChE reactivation assay

Reactivation potency of new oximes and standard reactivators 2-PAM and obidoxime were evaluated on human recombinant AChE. Enzyme was inhibited by the solution of appropriate cholinesterase inhibitor – sarin, VX and paraoxon in propan-2-ol at concentration 0.01 mM for 60 min. Excess of inhibitor was subsequently removed using octadecylsilane-bonded silica gel SPE cartridge. Inhibited enzyme was incubated for 10 min with solution of reactivator in concentrations 0.1 mM and 0.01 mM at 37 °C. The reaction was started by addition of substrate acetylthiocholine. Activity of AChE was then measured spectrophotometrically at 412 nm by the modified method according of

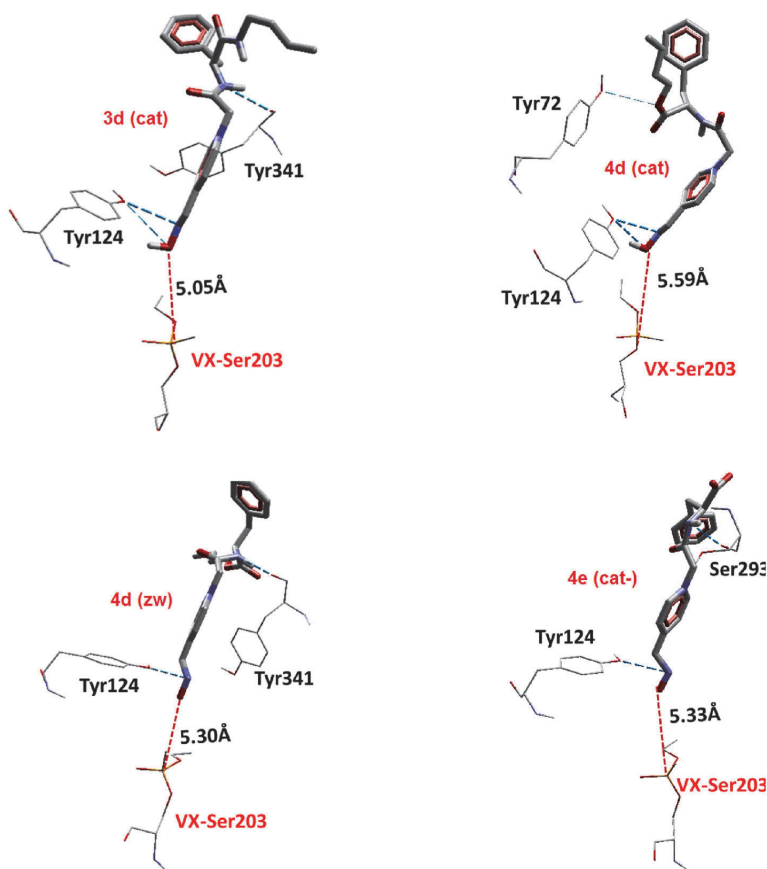


Fig. 9. Best docking poses of all the compounds on HsAChE-VX.

Ellman et al. [68] reported in our previous papers [69,70].

Each concentration of reactivator was assayed in triplicate. The obtained data were used to compute reactivation potency (R ; Equation (1)). Results were corrected for oximolysis and inhibition of AChE by reactivator.

$$R = \left(1 - \frac{\Delta A_0 - \Delta A_r}{\Delta A_0 - \Delta A_i} \right) \times 100 [\%] \quad (1)$$

ΔA_0 indicates absorbance change caused by intact AChE (phosphate buffer was used instead of AChE inhibitor solution), ΔA_i indicates absorbance change provided by cholinesterase exposed inhibitors and ΔA_r indicates absorbance change caused by AChE incubated with solution of reactivator.

3. Results and discussion

3.1. Evaluation of hydrophobicity and BBB permeability

Depending on pH, quaternary pyridinium oximes can be present in solution in two forms: cationic (cat; protonated) and zwitter-ionic (zw; deprotonated), see Scheme 2.

These two forms have different total charge (+1 for cationic form and 0 for zwitter-ionic form) and this difference should influence on hydrophobicity and BBB permeability parameters. Using on-line predictors Chemicalize (www.chemicalize.com), VCCLAB (www.vcclab.org) [52],

Molinspiration (www.molinspiration.com), and www.cbligand.org we have calculated values of pK_a , $\log P_{o/w}$ and BBB score for each compound in two forms (Table 1).

Introduction of oxime moiety into the pyridinium ring has an influence on compounds hydrophobicity (compared to a non-functionalized molecule) only in cases of introduction into positions 2- (high impact) and 3- (low impact). Introduction of oxime group in position 4- does not change it significantly (compare $\log P_{o/w}$ for cationic forms of non-functionalized compounds **a** and functionalized **b-d**; Table 1).

BBB score does not demonstrate sensitivity to a position of oxime moiety in the pyridinium ring, but usually for the cationic forms of non-functionalized compounds **a** it is higher, than for cationic forms of functionalized **b-d** (see Table 1). Based on BBB score evaluation, all studied compounds in cationic and zwitter-ionic forms were considered as species, which could cross blood-brain barrier (BBB+).

Analysis of dependencies “ $\log P_{o/w}$ – BBB score” demonstrates a good correlation ($R^2 = 0.8536$) between $\log P_{o/w}$ (www.vcclab.org) and BBB score (calculated using www.cbligand.org, fingerprint PubChem) (Fig. 5). It should be noted that both cationic and zwitter-ionic species of studied compounds fall on a uniform dependence.

Calculations of $\log P_{o/w}$ performed using Molinspiration (www.molinspiration.com) and using other fingerprints in www.cbligand.org (e.g., MACCS), did not demonstrate satisfactory correlations for dependencies “ $\log P_{o/w}$ – BBB score” ($R^2 < 0.6$). The obtained calculated values were used for preliminary evaluation of expected properties of

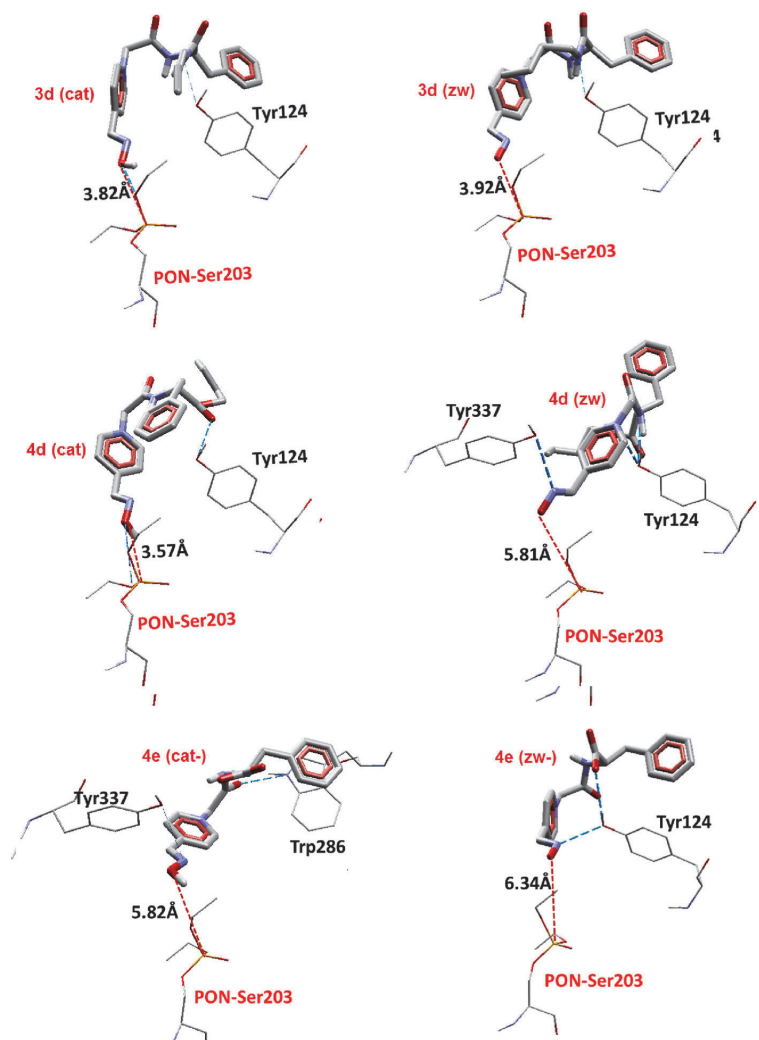


Fig. 10. Best docking poses of all the compounds on HssAChE-PON.

designed compounds.

3.2. Docking study

For docking study compounds 3d, 4d, and 4e were selected as representative examples of compounds with bulky hydrophobic element (L-Phe residue) in the molecule. Compound 4e is a product of hydrolytic decomposition of 4d by ester group in phenylalanine fragment.

3.2.1. Protonation of the ligands. Fig. 6 presents the possible chemical species, at physiologic pH, for the oximes 3d, 4d, 4e under the study, pointed by the Chemicalize server (<https://chemicalize.com/>). The docking studies were performed for all those species inside HssAChE-GB, HssAChE-VX and HssAChE-PON.

3.3. Docking energy calculations

The best re-docking result obtained for HI-6 inside HssAChE-PON was 1.01 Å, with $E_{\text{inter}} = -157.37 \text{ kcal mol}^{-1}$. According to literature, a

RMSD value below 2.5 Å (3.0 Å for ligands with higher degrees of freedom) is considered enough to validate a docking protocol [71]. Fig. 7 shows the best re-docking pose for HI-6 inside HssAChE-PON.

Table 2 shows the docking results of the best pose for each compound inside HssAChE-GB, HssAChE-VX and HssAChE-PON, while Figs. 8–10 illustrate the interactions of each pose inside the enzymes. Table 3 brings the percentages of poses obtained closest to peripheral anionic site (PAS) and closest to the active site of HssAChE-GB, HssAChE-VX and HssAChE-PON for each species studied. It's possible to see in Tables 2 and 3 that all the compounds presented negative values of binding energy for all systems, showing stabilization inside the three complexes.

Regarding the reactivation of HssAChE-GB, the most likely species at pH 7.4 (3d (cat), 4d (cat) and 4e (cat')) also presented the lowest binding energies, being 4e (cat') the one closest to the OP (Table 2). Table 3 shows that most of the poses for all ligands are located on the PAS, pointing to it as the preferential binding site for these compounds. On PAS it is also located the pose with the lowest energy for all compounds, except for ligand 3d (cat). Residues Tyr124, Tyr133 and Tyr341

Table 3
Best docking results for studied compounds on *HssAChE-GB*, *HssAChE-VX* and *HssAChE-PON*.

IL	<i>HssAChE-GB</i>			<i>HssAChE-VX</i>			<i>HssAChE-PON</i>		
	Lowest E_{inter} (kcal.mol ⁻¹)	% Poses OP/active site	% Poses PAS	Lowest E_{inter} (kcal.mol ⁻¹)	% Poses OP/active site	% Poses PAS	Lowest E_{inter} (kcal.mol ⁻¹)	% Poses OP/active site	% Poses PAS
3d (cat)	-184.65 (active site)	37	63	-94.34 (PAS)	10	90	-164.28 (PAS)	13	87
3d (zw)	-163.17 (PAS)	17	83	-101.42	0	100	-155.55 (PAS)	17	83
4d (cat)	-168.77 (PAS)	34	66	-97.65 (PAS)	3	97	-165.44 (PAS)	20	80
4d (zw)	-172.56 (PAS)	47	53	-98.47	17	83	-149.18 (PAS)	20	80
4e (cat)	-165.11 (PAS)	20	80	-101.19 (PAS)	0	100	-141.62 (PAS)	20	80
4e (zw)	-155.05 (PAS)	10	90	-103.20 (PAS)	3	97	-162.63 (PAS)	53	47

Table 4
The effect of studied compounds on the cell viability and their biodegradability in CBT OECD 301D protocol conditions.

Compound	IC ₅₀ ^a (mM ± SEM)	Biodegradability (D%), 28 days
1a	19.2 ± 0.4 ^b	4
1b	10.8 ± 0.3 ^b	4
1c	7.1 ± 0.7 ^b	0
1d	9.9 ± 0.5 ^c	0
2a	63.9 ± 12.3 ^b	3
2b	5.9 ± 1.3 ^b	9
2c	24.7 ± 7.8 ^b	7
2d	>10 ^c	0
3a	4.9 ± 0.9 ^b	0
3b	>10 ^c	8
3c	7.5 ± 0.7 ^c	8
3d	3.2 ± 0.6 ^c	9
4a	4.0 ± 0.2 ^b	49 [43]
4b	3.8 ± 0.2 ^c	11
4c	3.7 ± 0.6 ^c	13
4d	6.2 ± 0.7 ^c	18
4e	>10 ^c	13

Notes. ^a Studied using CHO-K1 cell line; mean ± SEM (mM); ^b n = 2; ^c n = 3.

Table 5
Reactivation capacity for compounds 1–4 and conventional antidotes.

Compound/ concentration	Sarin (10 μM)		VX (10 μM)		Paraoxon (PON) (10 μM)	
	100 μM (% ± SD)	10 μM (% ± SD)	100 μM (% ± SD)	10 μM (% ± SD)	100 μM (% ± SD)	10 μM (% ± SD)
1b	0.22 ± 0.02	0.23 ± 0.01	1.09 ± 0.39	2.26 ± 0.37	1.8 ± 0.34	1.1 ± 0.45
1c	0.94 ± 0.02	0.25 ± 0.01	0.62 ± 0.6	0.22 ± 0.39	1.54 ± 0.04	1.46 ± 0.04
1d	2.99 ± 0.9	0	7.58 ± 1.0	2.12 ± 0.8	4.15 ± 0.9	2.02 ± 0.4
2b	1.61 ± 0.8	1.27 ± 0.34	0.33 ± 0.29	0.17 ± 0.3	0.21 ± 0.48	0.48 ± 0.34
2c	3.15 ± 0.43	0	2.32 ± 0.04	1.65 ± 1.43	1.63 ± 0.4	1.28 ± 0.28
2d	2.11 ± 0.6	0	5.26 ± 0.3	1.52 ± 0.3	2.65 ± 0.1	0
3b	0	0	1.16 ± 0.1	0	0	0
3c	0	0	0	0	0	0
3d	8.66 ± 0.8	0	18.5 ± 1.4	3.17 ± 0.5	2.91 ± 0.2	0
4b	n.d.	n.d.	n.d.	n.d.	n.d.	n.d.
4c	n.d.	n.d.	n.d.	n.d.	n.d.	n.d.
4d	9.91 ± 0.9	1.32 ± 0.8	10.9 ± 0.5	0	1.48 ± 0.9	0
4e	1.22 ± 0.06	1.02 ± 0.41	1.45 ± 0.11	0	0	0
2-PAM	32.9 ± 0.3	10.0 ± 0.7	11.4 ± 0.5	2.81 ± 0.5	19.3 ± 1.1	2.53 ± 0.6
Obidoxime	33.73 ± 1.76	11.57 ± 0.89	17.05 ± 0.62	5.54 ± 2.13	70.26 ± 1.39	34.66 ± 1.22

Notes. n.d.: reactivation cannot be measured due to full inhibition of the enzyme by given compound.

are the most important residues contributing to the stabilization of the ligands inside *HssAChE-GB*. Ligand **4e** (cat) also presented hydrophobic interaction with residue Tyr341, which favors stabilization.

For *HssAChE-VX*, ligands **3d** (cat) and **4d** (zw) were the ones closer to the OP than the other ligands, while ligand **4e** (zw) presented the pose with lowest energy, suggesting higher stabilization. It is important to notice that ligands **3d** (zw) and **4e** (cat) did not present any pose

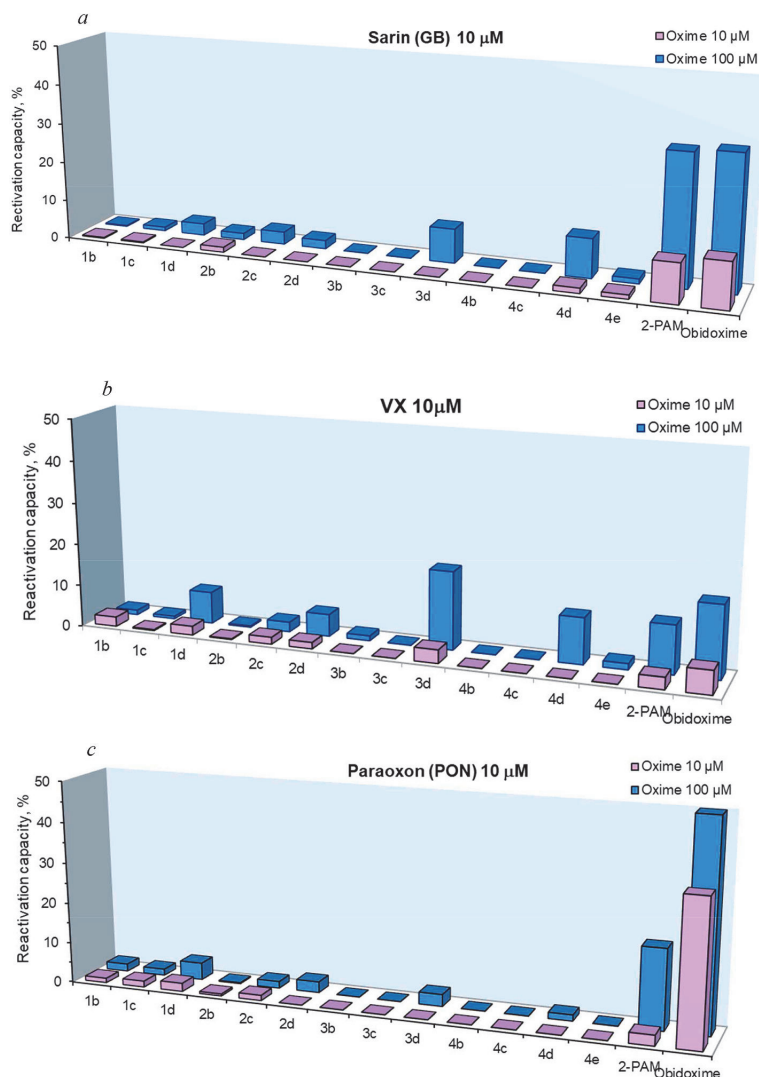
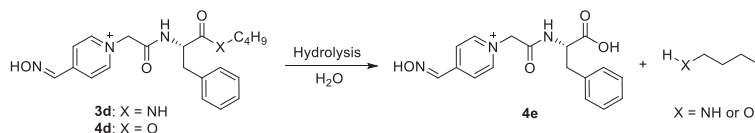


Fig. 11. Potency of studied oximes to reactivate recombinant human AChE inhibited by Sarin (GB) (a), VX (b), and paraoxon (PON) (c), reactivation capacity axis is limited by 50% for more convenient results presentation).



Scheme 3. Hydrolysis (esterolysis or amidolysis) of compounds 3d and 4d.

close to OP. Also, the PAS was the preferential binding site for all compounds. Residues Tyr124 and Tyr341 have the most important contributions for stabilization of the ligands. It's also important to observe that all ligands presented quite higher energies in the complex *HssAChE*-VX when compared to the other two complexes.

For *HssAChE*-PON, ligands 3d (cat) and 4d (cat) came closer to OP

and also presented H-bond with it (see Table 2). PAS was also the preferential binding site for all compounds (Table 3) and Tyr124 was the most important residue for stabilization.

Comparison of the three systems demonstrated that the binding energies for *HssAChE*-PON are similar to *HssAChE*-GB, but the ligands were able to come closer to PON than to GB. This suggests that the ligands

may be better reactivators for *HssAChE*-PON, followed by *HssAChE*-GB, and, in third place, *HssAChE*-VX.

It is important to consider the potential role of the side chain of Trp286 in the orientation of the reactivator since it was already observed in two different conformations in experimental structures 2Y2V, 5FPQ, and 6CQZ (normal to Tyr70) and 5HF9 (parallel to Tyr70), which could influence the outcome of docking calculations. However, in this study Trp286 was not included among the flexible residues since it is farther than 6 Å from the OP. As shown in Table 2, only the best pose of **4e** (**cat**-) showed interactions with Trp286 and none of the best poses demonstrated π -stacking interactions involving these two residues. Further molecular dynamics simulations studies will be envisaged to clarify this possibility.

Although some ligands were able to come closer to OP in *HssAChE*-VX, they presented higher binding energies compared to the other complexes. Meanwhile, two ligands, **3d** (**zw**) and **4e** (**cat**[−]) were not able to come closer to VX.

In summary, our results suggest that the ligands are more effective to reactivate *HssAChE*-PON, followed by *HssAChE*-GB and *HssAChE*-VX. Ligand **3d** (**cat**) and **4e** (**cat**[−]) presented better results for *HssAChE*-GB while ligands **3d** (**cat**) and **4e** (**zw**[−]) were the best for *HssAChE*-VX and ligands **3d** (**cat**) and **4d** (**cat**) were the best for *HssAChE*-PON.

3.4. Toxicological properties (antibacterial activity, antifungal activity, the effect of the compounds on the eukaryotic cell viability), biodegradability, and stability of compounds in plasma

The *in vitro* screen of compounds **1–4** against Gram-positive bacteria, Gram-negative bacteria and fungi demonstrate moderate toxicity only for certain compounds; in general, the studied compounds are non-toxic up to the highest concentrations screened (2 mM) (see Table S1 and Table S2). Compared to non-functionalized compounds (**a**), oximes (**b** and **e**) do not demonstrate any significant change in toxicity. It means, that introduction of oxime group into corresponding ionic liquids-based molecular platform does not change its toxicological properties.

The effect of studied compounds on the eukaryotic cell viability (CHO-K1 cell line) is observed only on mM concentration level (see Table 4), which is much higher, than possible concentration level of such type of compound in blood in case of treatment [72]. Therefore, the compounds **1–4** could be considered as none or low toxic.

Evaluation of biodegradability of compounds **1–4** shows, that ionic liquids with butylamide fragment in the structure (compounds **1–3**) demonstrate biodegradability less than 10% after 28 days not depending on presence or absence of oxime moiety in the structure (Table 4). On the other hand, for the butyl esters **4a** biodegradability is significant (49% after 28 days; Table 4) and can reach a limit in 60% for biodegradable compounds after extension of CBT to 42 days [43]. All oxime derivatives **4b–4e** have biodegradability lower than biodegradability of non-functionalized **4a**. It indicates that introduction of oxime moiety in initially biodegradable structure decreases its ability to biodegradation.

It is worth noting that biodegradability in CBT of butylamine hydrochloride, butylamide of L-alanine hydrochloride, butylamide of L-Phe hydrochloride and butyl ester of L-Phe hydrochloride after 28 days are 66%, 20%, 62% and 99%, respectively. These results confirmed earlier found fact [46] that the products with L-alanine fragment in the structure are less biodegradable (compared to analogs) and give less biodegradable potential transformation products.

The stability of compounds **3d** and **4d** was additionally evaluated in human plasma within 2 h incubation time. Compound **3d** does not show significant degradation, whereas compound **4d** demonstrated low plasma stability and was almost fully decomposed within 60 min, see Fig. S1. This property of **4d**, in contrast to compound **3d**, can be ascribed to the presence of the ester bond in the molecule.

3.5. Reactivation efficacy towards AChE inhibited by sarin (GB), VX and paraoxon (PON)

In silico docking studies performed for cationic and zwitter-ionic form of compounds **3d**, **4d** and **3e** (see section 3.2), provides support to their ability to be AChE reactivators and expediency of these compounds testing *in vitro*.

The reactivation capacity of compounds **1–4** was evaluated towards AChE inhibited by sarin (GB), VX and paraoxon (PON). Oximes, substituted in position (2-), demonstrate minimal reactivation capacity compared to (3-) and (4-) substituted derivatives; the maximal reactivation capacity usually demonstrate (4-) substituted derivatives (Table 5).

Introduction of L-alanine residue (compounds **2**) do not bring any advantages compared to compounds **1** (without this fragment), but introduction of L-phenylalanine residue (compounds **3** and **4**, 4-substituted derivatives) demonstrate higher reactivation capacity than other studied oximes and for **3d** in case of reactivation of AChE inhibited by VX its activity is comparable to conventional reactivator 2-PAM and slightly higher than reactivation capacity of obidoxime (Table 5). Compound **3d** also demonstrate moderate activity in reactivation of AChE inhibited by GB.

Compound **4d** in reactivation of AChE inhibited by sarin demonstrate activity similar to **3d** and they are in 3 times less active than 2-PAM and obidoxime. In reactivation of AChE inhibited by VX, activity of **4d** is comparable to 2-PAM and in ca. 2 times less active than **3d** and obidoxime. In case of AChE inhibited by paraoxon, activity of **4d** is in ca.2 times lower than activity of **3d** and significantly lower (more than 10 times) than of 2-PAM and obidoxime; see Table 5 and Fig. 11.

The reactivation capacity of compound **4e** – product of hydrolytic decomposition of **3d** and **4d** by butylamide or ester bond, correspondently – is significantly lower than activity of initial compounds **3d** and **4d** (see Scheme 3 and Table 5). This fact confirmed, that observed reactivation capacity of compounds **3d** and **4d** is related to these compounds rather than to their possible transformation products.

4. Conclusions

A series of acetylcholinesterase reactivators was synthesized using sustainable ionic liquids-based molecular platforms. Key properties (hydrophobicity, BBB permeability, energy and spatial parameters for complexes with the active site of the human *HssAChE* inhibited by GB, VX, or PON toxicological properties, plasma stability, biodegradability, and reactivation capacity) were determined for these compounds. Out of that, the structure-activity relationship was assessed.

- (i) BBB score of studied compounds linearly depends on their hydrophobicity ($\log P_{o/w}$). Cationic and zwitter-ionic forms of studied compounds fall on a uniform dependence. All studied compounds in cationic and zwitter-ionic forms were considered as species, which can cross blood-brain barrier (BBB+).
- (ii) Results of docking studies suggest that the ligands are more effective to reactivate *HssAChE*-PON, followed by *HssAChE*-GB and *HssAChE*-VX. Ligand **3d** (**cat**) and **4e** (**cat**[−]) presented better results for *HssAChE*-GB while ligands **3d** (**cat**) and **4e** (**zw**[−]) were the best for *HssAChE*-VX and ligands **3d** (**cat**) and **4d** (**cat**) were the best for *HssAChE*-PON. These findings were confirmed also by the *in vitro* reactivation assay for compounds **3d** and **4d**, but not for **4e**.
- (iii) The *in vitro* screening of compounds **1–4** against Gram-positive bacteria, Gram-negative bacteria, and fungi demonstrate moderate toxicity only for certain compounds; in general, tested compounds are non-toxic.
- (iv) The effect of studied compounds on the eukaryotic cell viability (CHO-K1 cell line) is observed only on mM concentration level, also confirming the non-toxicity.

- (v) Introduction of oxime moiety in initially biodegradable structure decreases its ability to biodegradation.
- (vi) The compounds **3d** and **4d** were shown to reveal remarkable activity against the AChE inhibited by VX, compared with, or exceeding those for conventional reactivators, 2-PAM and obidoxime. In addition, compound **3d** was found to be stable against esterases and other enzymes present in human plasma and from this point of view suitable for human treatment.

Application of studied sustainable ionic liquids-based molecular platforms to design of AChE reactivators demonstrated broad prospective of these molecules in solving multipurpose tasks and gives important information about this compound and regularities, which could be used in future for improving molecular platforms.

CRedit authorship contribution statement

Illia V. Kapitanov: Conceptualization; Investigation (synthesis and characterization of studied compounds); Data curation; Visualization; Writing (original draft preparation). Marcel Špulák: Investigation (bacterial and fungal toxicity study), Writing (original draft preparation). Milan Pour: Investigation (bacterial and fungal toxicity study), Resources, Writing (review and editing), Resources. Martin Novak: Investigation (plasma stability study). Ondřej Soukup: Methodology, Investigation (cell viability); Resources; Writing - Reviewing and Editing. Daniel Jun: Investigation (reactivation studies); Resources; Writing (review & editing). Jan Marek: Investigation (antimicrobial and cytotoxicity testing), Resources. Joyce S. F. Diz de Almeida: Investigation (Molecular docking); Writing (review & editing). Tanos C. Costa França: Conceptualization; Formal analysis; Writing (reviewing and editing). Nicholas Gathergood: Conceptualization, Resources, Funding acquisition; Writing (reviewing and editing). Kamil Kuča: Conceptualization, Resources, Funding acquisition; Writing (reviewing and editing). Yevgen Karpichev: Conceptualization, Methodology; Resources; Funding acquisition; Writing (original draft preparation); Writing (reviewing and editing).

Declaration of competing interest

The authors declare the following financial interests/personal relationships which may be considered as potential competing interests: Yevgen Karpichev reports was provided by Tallinn University of Technology.

Data availability

Data will be made available on request.

Acknowledgement

The authors acknowledge funding from acknowledges NATO SPS MYP No. G5565 DEFIR (YK), Estonian Research Council grant PUT1656 (IK, NG, and YK), Ministry of Defense of Czech Republic Long Term Development Plan grant on Medical Aspects of Weapons of Mass Destruction of the Faculty of Military Health Sciences, University of Defense (DJ, JM), Czech Science Foundation grant no 22-12859 S (OS), and Excellence project PrF UHK 2216/2023-2024 and MH CZ - DRO (UHHK, 00179906) (TCCF). The authors express their appreciation to Zeba Usmani and Grete Raba for CBT biodegradation routine and Prof. Teodorico Ramalho (Federal University of Lavras) for licensed use of Molegro Virtual Docker

Appendix A. Supplementary data

Supplementary data to this article can be found online at <https://doi.org/10.1016/j.cbi.2023.110735>.

References

- [1] Handbook of Toxicology of Chemical Warfare Agents, Elsevier, 2020, <https://doi.org/10.1016/C2018-0-04837-9>.
- [2] L. Gorecki, O. Soukup, J. Korabecny, Countermeasures in organophosphorus intoxication: pitfalls and prospects, *Trends Pharmacol. Sci.* 43 (2022) 593–606, <https://doi.org/10.1016/j.tips.2022.04.008>.
- [3] L. Pulkrabkova, L. Muckova, M. Hrabínova, A. Sorf, T. Kobrlova, P. Jost, D. Bezdekova, J. Korabecny, D. Jun, O. Soukup, Differentiated SH-SY5Y neuroblastoma cells as a model for evaluation of nerve agent-associated neurotoxicity, *Arch. Toxicol.* 97 (2023) 2209–2217, <https://doi.org/10.1007/s00204-023-03525-0>.
- [4] H.M. Bolt, J.G. Hengstler, Recent research on Novichok, *Arch. Toxicol.* 96 (2022) 1137–1140, <https://doi.org/10.1007/s00204-022-03273-7>.
- [5] M. Noga, K. Jurowski, What do we currently know about Novichoks? The state of the art, *Arch. Toxicol.* 97 (2023) 651–661, <https://doi.org/10.1007/s00204-022-03437-5>.
- [6] J. Opravil, J. Pejchal, V. Finger, J. Korabecny, T. Rozsypal, M. Hrabínova, L. Muckova, V. Hepnarova, J. Konecny, O. Soukup, D. Jun, A-agents, misleadingly known as “Novichoks”: a narrative review, *Arch. Toxicol.* 97 (2023) 2587–2607, <https://doi.org/10.1007/s00204-023-03571-8>.
- [7] L. Carlsen, After Salisbury nerve agents revisited, *Mol Inform* 38 (2019), <https://doi.org/10.1002/minf.201800106>.
- [8] D. Steindl, W. Boehmerle, R. Körner, D. Praeger, M. Haug, J. Nee, A. Schreiber, F. Scheibe, K. Demin, P. Jacoby, R. Tauber, S. Hartwig, M. Endres, K.U. Eckardt, Novichok nerve agent poisoning, *Lancet* 397 (2021) 249–252, [https://doi.org/10.1016/S0140-6736\(20\)32644-1](https://doi.org/10.1016/S0140-6736(20)32644-1).
- [9] J. Brooks, T.B. Erickson, S. Kayden, R. Ruiz, S. Wilkinson, F.M. Burkle, Responding to chemical weapons violations in Syria: legal, health, and humanitarian recommendations, *Conflict Health* 12 (2018), <https://doi.org/10.1186/s13031-018-0143-3>.
- [10] M. Guidotti, F. Trifirò, Chemical risk and chemical warfare agents: science and technology against humankind, *Toxicol. Environ. Chem.* 98 (2016) 1018–1025, <https://doi.org/10.1080/02722248.2014.996153>.
- [11] T. Okumura, T. Hisaoka, A. Yamada, T. Naito, H. Isonuma, S. Okumura, K. Miura, M. Sakurada, H. Maekawa, S. Ishimatsu, N. Takasu, K. Suzuki, The Tokyo subway sarin attack - lessons learned, in: *Toxicol Appl Pharmacol*, Academic Press Inc., 2005, pp. 471–476, <https://doi.org/10.1016/j.taap.2005.02.032>.
- [12] K. Sakurada, H. Ohta, No promising antidote 25 years after the Tokyo subway sarin attack: a review, *Leg. Med.* 47 (2020), <https://doi.org/10.1016/j.legmed.2020.101761>.
- [13] L. Gorecki, J. Korabecny, K. Musilek, D. Malinak, E. Nepovimova, R. Dolezal, D. Jun, O. Soukup, K. Kuca, SAR study to find optimal cholinesterase reactivator against organophosphorus nerve agents and pesticides, *Arch. Toxicol.* 90 (2016) 2831–2859, <https://doi.org/10.1007/s00204-016-1827-3>.
- [14] J.C. DeMar, E.D. Clarkson, R.H. Ratcliffe, A.J. Campbell, S.G. Thangavelu, C. A. Herdman, H. Leader, S.M. Schulz, E. Marek, M.A. Medynets, T.C. Ku, S.A. Evans, F.A. Khan, R.R. Owens, M.P. Nambiar, R.K. Gordon, Pro-2-PAM therapy for central and peripheral cholinesterases, *Chem. Biol. Interact.* 187 (2010) 191–198, <https://doi.org/10.1016/j.cbi.2010.02.015>.
- [15] T. Zorbaz, P. Mišetić, N. Probst, S. Žunec, A. Zandona, G. Mendes, V. Micek, N. Maček Hrvat, M. Katalinić, A. Braiki, L. Jean, P.-Y. Renard, V. Gabelica Marković, Z. Kovarik, Pharmacokinetic evaluation of brain penetrating morpholine-3-hydroxy-2-pyridine oxime as an antidote for nerve agent poisoning, *ACS Chem. Neurosci.* 11 (2020) 1072–1084, <https://doi.org/10.1021/acschemneuro.0c00032>.
- [16] Y.J. Rosenberg, J. Wang, T. Ooms, N. Rajendran, L. Mao, X. Jiang, J. Lees, L. Urban, J.D. Momper, Y. Sepulveda, Y.-J. Shyong, P. Taylor, Post-exposure treatment with the oxime RS194B rapidly reactivates and reverses advanced symptoms of lethal inhaled paraoxon in macaques, *Toxicol. Lett.* 293 (2018) 229–234, <https://doi.org/10.1016/j.toxlet.2017.10.025>.
- [17] J. Dhguru, E. Zviagin, R. Skouta, FDA-approved oximes and their significance in medicinal chemistry, *Pharmaceuticals* 15 (2022) 66, <https://doi.org/10.3390/ph15010066>.
- [18] T.M. Prokop'eva, YuS. Simanenko, I.P. Suprun, V.A. Savelova, T.M. Zubareva, E. A. Karpichev, Nucleophilic substitution at a four-coordinate sulfur atom: VI. Reactivity of oximate ions, *Russ. J. Org. Chem.* 37 (2001), <https://doi.org/10.1023/A:1012487415041>.
- [19] D. Bondar, I.V. Kapitanov, L. Pulkrabkova, O. Soukup, D. Jun, F.D. Botelho, T.C. C. França, K. Kuča, Y. Karpichev, N-substituted arylhydroxamic acids as acetylcholinesterase reactivators, *Chem. Biol. Interact.* 365 (2022), 110078, <https://doi.org/10.1016/j.cbi.2022.110078>.
- [20] N. Singh, Y. Karpichev, A.K. Tiwari, K. Kuca, K.K. Ghosh, Oxime functionality in surfactant self-assembly: an overview on combating toxicity of organophosphates, *J. Mol. Liq.* 208 (2015), <https://doi.org/10.1016/j.molliq.2015.04.010>.
- [21] J.E. Forman, C.M. Timperley, Is there a role for green and sustainable chemistry in chemical disarmament and nonproliferation? *Curr. Opin. Green Sustainable Chem.* 15 (2019) 103–114, <https://doi.org/10.1016/j.cogsc.2019.01.001>.
- [22] C. Fernandez-Lopez, R. Posada-Baquero, J.-J. Ortega-Calvo, Nature-based approaches to reducing the environmental risk of organic contaminants resulting from military activities, *Sci. Total Environ.* 843 (2022), 157007, <https://doi.org/10.1016/j.scitotenv.2022.157007>.
- [23] H. Mutlu, L. Barner, Getting the terms right: green, sustainable, or circular chemistry? *Macromol. Chem. Phys.* 223 (2022), 2200111 <https://doi.org/10.1002/macp.202200111>.

- [24] J.B. Zimmerman, P.T. Anastas, H.C. Erythropel, W. Leitner, Designing for a green chemistry future, *Science* 367 (2020) 397–400, <https://doi.org/10.1126/science.aay3060>, 1979.
- [25] P.T. Anastas, J. Warner, *Green Chemistry: Theory and Practice*, Oxford University Press, New York, 1998.
- [26] F.P. Byrne, S. Jin, G. Paggiola, T.H.M. Petchey, J.H. Clark, T.J. Farmer, A.J. Hunt, C. Robert McElroy, J. Sherwood, Tools and techniques for solvent selection: green solvent selection guides, *Sustain. Chem. Processes* 4 (2016) 7, <https://doi.org/10.1186/s40508-016-0051-z>.
- [27] N. Winterton, The green solvent: a critical perspective, *Clean Technol. Environ. Policy* 23 (2021) 2499–2522, <https://doi.org/10.1007/s10098-021-02188-8>.
- [28] N. V. Plechkova, K.R. Seddon, *Ionic Liquids: “Designer” Solvents for Green Chemistry*, in: *Methods and Reagents for Green Chemistry*, John Wiley & Sons, Inc., Hoboken, NJ, USA, n.d.: pp. 103–130. <https://doi.org/10.1002/9780470124086.ch5>.
- [29] Y. Gu, F. Jérôme, Bio-based solvents: an emerging generation of fluids for the design of eco-efficient processes in catalysis and organic chemistry, *Chem. Soc. Rev.* 42 (2013) 9550, <https://doi.org/10.1039/c3cs60241a>.
- [30] A.J. Greer, J. Jacquemin, C. Hardacre, Industrial applications of ionic liquids, *Molecules* 25 (2020) 5207, <https://doi.org/10.3390/molecules25215207>.
- [31] Z. Usmani, M. Sharma, P. Gupta, Y. Karpichev, N. Gathergood, R. Bhat, V.K. Gupta, Ionic liquid based pretreatment of lignocellulosic biomass for enhanced bioconversion, *Bioresour. Technol.* 304 (2020), 123003, <https://doi.org/10.1016/j.biortech.2020.123003>.
- [32] P. Pillai, M. Maiti, A. Mandal, Mini-review on recent advances in the application of surface-active ionic liquids: petroleum industry perspective, *Energy Fuels* 36 (2022) 7925, <https://doi.org/10.1021/acs.energyfuels.2c00964>. –7939.
- [33] D. Kowalska, J. Maculewicz, P. Stepnowski, J. Dołżonek, Ionic liquids as environmental hazards – crucial data in view of future PBT and PMT assessment, *J. Hazard Mater.* 403 (2021), 123896, <https://doi.org/10.1016/j.jhazmat.2020.123896>.
- [34] M.C. Bubalo, K. Radošević, I.R. Redovniković, I. Šilvac, V.G. Srček, Toxicity mechanisms of ionic liquids, *Arh. Hig. Rada. Toksikol.* 68 (2017) 171–179, <https://doi.org/10.1515/ahit-2017-68-2979>.
- [35] A.-K. Amsel, O. Olsson, K. Kümmerer, Inventory of biodegradation data of ionic liquids, *Chemosphere* 299 (2022), 134385, <https://doi.org/10.1016/j.chemosphere.2022.134385>.
- [36] S.K. Singh, Production of ionic liquids using renewable sources, in: *Ionic Liquid-Based Technologies for Environmental Sustainability*, Elsevier, 2022, pp. 29–43, <https://doi.org/10.1016/B978-0-12-824545-3.00003-9>.
- [37] K.M. Docherty, S.W. Aiello, B.K. Buehler, S.E. Jones, B.R. Szymczyna, K.A. Walker, Ionic liquid biodegradability depends on specific wastewater microbial consortia, *Chemosphere* 136 (2015) 160–166, <https://doi.org/10.1016/j.chemosphere.2015.05.016>.
- [38] M. Suk, A. Haiß, J. Westphal, A. Jordan, A. Kellett, I.V. Kapitanov, Y. Karpichev, N. Gathergood, K. Kümmerer, Design rules for environmental biodegradability of phenylalanine alkyl ester linked ionic liquids, *Green Chem.* 22 (2020) 4498–4508, <https://doi.org/10.1039/D0GC00918K>.
- [39] A. Haiß, A. Jordan, J. Westphal, E. Logunova, N. Gathergood, K. Kümmerer, On the way to greener ionic liquids: identification of a fully mineralizable phenylalanine-based ionic liquid, *Green Chem.* 18 (2016) 4361–4373, <https://doi.org/10.1039/C6GC00417B>.
- [40] A. Jordan, A. Haiß, M. Spulak, Y. Karpichev, K. Kümmerer, N. Gathergood, Synthesis of a series of amino acid derived ionic liquids and tertiary amines: green chemistry metrics including microbial toxicity and preliminary biodegradation data analysis, *Green Chem.* 18 (2016), <https://doi.org/10.1039/c6gc00415f>.
- [41] A. Jordan, N. Gathergood, Biodegradation of ionic liquids – a critical review, *Chem. Soc. Rev.* 44 (2015) 8200–8237, <https://doi.org/10.1039/C5CS00444F>.
- [42] J. Hulsbosch, D.E. De Vos, K. Binnemans, R. Ameloot, Biobased ionic liquids: solvents for a green processing industry? *ACS Sustain. Chem. Eng.* 4 (2016) 2917–2931, <https://doi.org/10.1021/acssuschemeng.6b00553>.
- [43] I.V. Kapitanov, A. Jordan, Y. Karpichev, M. Spulak, L. Perez, A. Kellett, K. Kümmerer, N. Gathergood, Synthesis, self-assembly, bacterial and fungal toxicity, and preliminary biodegradation studies of a series of l-phenylalanine-derived surface-active ionic liquids, *Green Chem.* 21 (2019), <https://doi.org/10.1039/c9gc00030e>.
- [44] I.V. Kapitanov, S.M. Sudheer, T. Yadav, K.K. Ghosh, N. Gathergood, V.K. Gupta, Y. Karpichev, Sustainable phenylalanine-derived SAILs for solubilization of polycyclic aromatic hydrocarbons, *Molecules* 28 (2023) 4185, <https://doi.org/10.3390/molecules28104185>.
- [45] D.K.A. Kusumahastuti, M. Shtmäe, I.V. Kapitanov, Y. Karpichev, N. Gathergood, A. Kahru, Toxicity profiling of 24 l-phenylalanine derived ionic liquids based on pyridinium, imidazolium and cholinium cations and varying alkyl chains using rapid screening *Vibrio fischeri* bioassay, *Ecotoxicol. Environ. Saf.* 172 (2019), <https://doi.org/10.1016/j.ecoenv.2018.12.076>.
- [46] I.V. Kapitanov, G. Raba, M. Spulak, R. Vilu, Y. Karpichev, N. Gathergood, Design of sustainable ionic liquids based on l-phenylalanine and l-alanine dipeptides: synthesis, toxicity and biodegradation studies, *J. Mol. Liq.* 374 (2023), 121285, <https://doi.org/10.1016/j.molliq.2023.121285>.
- [47] S.J. Pandya, I.V. Kapitanov, Z. Usmani, R. Sahu, D. Sinha, N. Gathergood, K. K. Ghosh, Y. Karpichev, An example of green surfactant systems based on inherently biodegradable IL-derived amphiphilic oximes, *J. Mol. Liq.* 305 (2020), 112857, <https://doi.org/10.1016/j.molliq.2020.112857>.
- [48] S.J. Pandya, I.V. Kapitanov, M.K. Banjare, K. Behera, V. Borovkov, K.K. Ghosh, Y. Karpichev, Mixed oxime-functionalized IL/16-s-16 Gemini surfactants system: physicochemical study and structural transitions in the presence of promethazine as a potential chiral pollutant, *Chemosensors* 10 (2022) 46, <https://doi.org/10.3390/chemosensors10020046>.
- [49] M.K. Banjare, K. Behera, R.K. Banjare, S. Pandey, K.K. Ghosh, Y. Karpichev, Molecular interactions between novel synthesized biodegradable ionic liquids with antidepressant drug, *Chem. Thermodyn. Thermal Anal.* 3–4 (2021), 100012, <https://doi.org/10.1016/j.ctta.2021.100012>.
- [50] Y. Karpichev, I.V. Kapitanov, N. Gathergood, O. Soukup, V. Hepnarova, D. Jun, K. Kuca, Acetylcholinesterase reactivators based on oxime-functionalized biodegradable ionic liquids, *Mil Med Res* 87 (88) (2018) 87, <https://doi.org/10.1016/j.milmedres.2018.09.033>.
- [51] M.T. García, I. Ribosa, L. Perez, A. Manresa, F. Comelles, Self-assembly and antimicrobial activity of long-chain amide-functionalized ionic liquids in aqueous solution, *Colloids Surf. B Biointerfaces* 123 (2014) 318–325, <https://doi.org/10.1016/j.colsurfb.2014.09.033>.
- [52] I.V. Tetko, J. Gasteiger, R. Todeschini, A. Mauri, D. Livingstone, P. Ertl, V. A. Palyulin, E.V. Radchenko, N.S. Zefirov, A.S. Makarenko, V.Yu Tanchuk, V. V. Prokopenko, Virtual computational chemistry laboratory – design and description, *J. Comput. Aided Mol. Des.* 19 (2005) 453–463, <https://doi.org/10.1007/s10822-005-8694-y>.
- [53] PC SPARTAN Pro Molecular Modeling for the Desktop, *Chemical & Engineering News Archive*. vol. 77 (1999) 2. <https://doi.org/10.1021/cen-v077n017.p002>.
- [54] G.B. Rocha, R.O. Freire, A.M. Simas, J.J.P. Stewart, RM1: a reparameterization of AM1 for H, C, N, O, P, S, F, Cl, Br, and I, *J. Comput. Chem.* 27 (2006) 1101–1111, <https://doi.org/10.1002/jcc.20425>.
- [55] C. Lindgren, N. Forsgren, N. Hoster, C. Akfur, E. Artursson, L. Edvinsson, R. Svensson, F. Worek, P. Ekström, A. Linusson, Broad-spectrum antidote Discovery by untangling the reactivation mechanism of nerve-agent-inhibited acetylcholinesterase, *Chem. Eur J.* 28 (2022), <https://doi.org/10.1002/chem.202200678>.
- [56] H.M. Lee, R. Andrys, J. Jarczyk, K. Kim, A.G. Vishakantegowda, D. Malinak, A. Skarka, M. Schmidt, M. Vaskova, K. Latka, M. Bajda, Y.-S. Jung, B. Malawska, K. Musilek, Pyridinium-2-carbaldoximes with quinuclidine carboxamide moiety are simultaneous reactivators of acetylcholinesterase and butyrylcholinesterase inhibited by nerve agent surrogates, *J. Enzym. Inhib. Med. Chem.* 36 (2021) 437–449, <https://doi.org/10.1080/14756366.2020.1869954>.
- [57] K. Vanommeslaeghe, E. Hatcher, C. Acharya, S. Kundu, S. Zhong, J. Shim, E. Darian, O. Guvench, P. Lopes, I. Vorobyov, A.D. Mackerell, CHARMM general force field: a force field for drug-like molecules compatible with the CHARMM all-atom additive biological force fields, *J. Comput. Chem.* (2009), <https://doi.org/10.1002/jcc.21367>. NA-NA.
- [58] R. Thomsen, M.H. Christensen, MolDock, A new technique for high-accuracy molecular docking, *J. Med. Chem.* 49 (2006) 3315–3321, <https://doi.org/10.1021/jm051197e>.
- [59] Determination of minimum inhibitory concentrations (MICs) of antibacterial agents by broth dilution, *Clin. Microbiol. Infect.* 9 (2003), <https://doi.org/10.1046/j.1469-0691.2003.00790.x> ix–xv.
- [60] EUCAST DEFINITIVE DOCUMENT EDEF 7.3.1, Method for the Determination of Broth Dilution Minimum Inhibitory Concentrations of Antifungal Agents for Yeasts, 2107..
- [61] EUCAST DEFINITIVE DOCUMENT EDEF 9.3.1, Method for the Determination of Broth Dilution Minimum Inhibitory Concentrations of Antifungal Agents for *Conidia* Forming Moulds, 2017..
- [62] D. Malinak, R. Dolezal, J. Marek, S. Salajkova, O. Soukup, M. Vejsova, J. Korabecny, J. Honeg, M. Penhaker, K. Musilek, K. Kuca, 6-Hydroxyquinolinium salts differing in the length of alkyl side-chain: synthesis and antimicrobial activity, *Bioorg. Med. Chem. Lett* 24 (2014) 5238–5241, <https://doi.org/10.1016/j.bmcl.2014.09.060>.
- [63] G. Karabanovich, J. Roh, O. Soukup, I. Pávková, M. Pasdiorová, V. Tambor, J. Stolaríková, M. Vejsova, K. Vávřová, V. Klimešová, A. Hrabálek, Tetrazole regioisomers in the development of nitro group-containing antitubercular agents, *MedChemComm* 6 (2015) 174–181, <https://doi.org/10.1039/C4MD00301B>.
- [64] O. Soukup, J. Korabecny, D. Malinak, E. Nepovimova, N.L. Pham, K. Musilek, M. Hrabínova, V. Hepnarova, R. Dolezal, P. Pavek, P. Jost, T. Kobrlava, J. Jankockova, L. Goreck, M. Psotka, T.D. Nguyen, K. Box, B. Outhwaite, M. Ceckova, A. Sorf, D. Jun, K. Kuca, In vitro and in silico evaluation of non-quaternary reactivators of AChE as antidotes of organophosphorus poisoning - a new hope or a blind alley? *Med. Chem.* 14 (2018) 281–292, <https://doi.org/10.2174/1573406414666180112105657>.
- [65] V. Finger, T. Kucera, R. Kafkova, L. Muckova, R. Dolezal, J. Kubes, M. Novak, L. Prchal, L. Lakatos, M. Andrs, M. Hymanpan, J. Marek, M. Kufa, V. Spiwok, O. Soukup, E. Mezeiova, J. Janousek, L. Nevosadova, M. Benkova, R.R.A. Kitson, M. Kratky, S. Bösze, K. Mikusova, R. Hartkoorn, J. Roh, J. Korabecny, 2,6-Disubstituted 7-(naphthalen-2-ylmethyl)-7H-purines as a new class of potent antitubercular agents inhibiting DPrE1, *Eur. J. Med. Chem.* 258 (2023), 115611, <https://doi.org/10.1016/j.ejmech.2023.115611>.
- [66] J. Friedrich, A. Längin, K. Kümmerer, Comparison of an electrochemical and luminescence-based oxygen measuring system for use in the biodegradability testing according to closed bottle test (OECD 301D), *Clean* 41 (2013) 251–257, <https://doi.org/10.1002/clean.201100558>.
- [67] OECD, OECD Test Guidelines for Chemicals, 1992.
- [68] G.L. Ellman, K.D. Courtney, V. Andres, R.M. Featherstone, A new and rapid colorimetric determination of acetylcholinesterase activity, *Biochem. Pharmacol.* 7 (1961) 88–95, [https://doi.org/10.1016/0006-2952\(61\)90145-9](https://doi.org/10.1016/0006-2952(61)90145-9).
- [69] D. Jun, L. Musilova, K. Musilek, K. Kuca, In Vitro ability of currently available oximes to reactivate organophosphate pesticide-inhibited human acetylcholinesterase and butyrylcholinesterase, *Int. J. Mol. Sci.* 12 (2011) 2077–2087, <https://doi.org/10.3390/ijms12032077>.

- [70] D. Jun, L. Musilova, M. Pohanka, Y.-S. Jung, P. Bostik, K. Kuca, Reactivation of human acetylcholinesterase and butyrylcholinesterase inhibited by leptophos-oxon with different oxime reactivators in vitro, *Int. J. Mol. Sci.* 11 (2010) 2856–2863, <https://doi.org/10.3390/ijms11082856>.
- [71] M. Kontoyianni, L.M. McClellan, G.S. Sokol, Evaluation of docking performance: comparative data on docking algorithms, *J. Med. Chem.* 47 (2004) 558–565, <https://doi.org/10.1021/jm0302997>.
- [72] M. Eddleston, F.R. Chowdhury, Pharmacological treatment of organophosphorus insecticide poisoning: the old and the (possible) new, *Br. J. Clin. Pharmacol.* 81 (2016) 462–470, <https://doi.org/10.1111/bcp.12784>.

Author's publications and conference presentations

Other publications (articles)

1. D.Bondar, I.V.Kapitanov, L.Pulkrabkova, O.Soukup, D.Jun, F.D.Botelho, T.C.C.França, K.Kuča, Ye.Karpichev. N-substituted arylhydroxamic acids as acetylcholinesterase reactivators // *Chemico-Biological Interactions* – **2022** – Vol. 365 – Article 110078.
2. M.Suk, A.Haiß, J.Westphal, A.Jordan, A.Kellett, I.V.Kapitanov, Ye.Karpichev, N.Gathergood, K.Kümmerer. Design rules for environmental biodegradability of phenylalanine alkyl ester linked ionic liquids // *Green Chemistry* – **2020** – Vol. 22 – P. 4498–4508.
3. I.V.Kapitanov, A.Jordan, Ye.Karpichev, M.Spulak, L.Perez, A.Kellett, K.Kümmerer, N.Gathergood. Synthesis, self-assembly, bacterial and fungal toxicity, and preliminary biodegradation studies of a series of L-phenylalanine-derived surface-active ionic liquids // *Green Chemistry* – **2019** – Vol. 21 – P. 1777–1794.
4. D.R.Gabdrakhmanov, D.A.Samarkina, E.S.Krylova, I.V.Kapitanov, Y.Karpichev, S.K.Latypov, V.E.Semenov, I.R.Nizameev, M.K.Kadirov, L.Ya.Zakharova. Supramolecular Systems Based on Novel Amphiphiles and a Polymer: Aggregation and Selective Solubilization // *Journal of Surfactants and Detergents* – **2019** – Vol. 22, N 4. – P. 865–874.
5. D.K.A.Kusumahastuti, M.Sihtmäe, I.Kapitanov, Y.Karpichev, N.Gathergood, A.Kahru. Toxicity profiling of 24 L-Phenylalanine Derived Ionic Liquids based on pyridinium, imidazolium and cholinium cations and varying alkyl chains using rapid screening *Vibrio fischeri* bioassay // *Ecotoxicology and Environmental Safety* – **2019** – Vol. 172. – P. 556–565.
6. I.V.Kapitanov, A.B.Mirgorodskaya, F.G.Valeeva, N.Gathergood, K.Kuča, L.Ya.Zakharova, Ye.Karpichev. Physicochemical properties and esterolytic reactivity of oxime functionalized surfactants in pH-responsive mixed micellar system // *Colloids and Surfaces A: Physicochemical and Engineering Aspects* – **2017** – Vol. 524. – P. 143–159.
7. T.M.Prokop'eva, I.V.Kapitanov, I.A.Belousova, A.E.Shumeiko, M.L.Kostrikin, A.A.Serdyuk, M.K.Turovskaya, N.G.Razumova. Reactivity of co-micellar systems based on dimeric functionalized tetraalkylammonium surfactant in phosphoryl and sulfonyl group transfer processes // *Russian Journal of Organic Chemistry* – **2017** – Vol. 53, N 4. – P. 510–513.
8. M.K.Turovskaya, V.A.Mikhailov, N.I.Burakov, I.V.Kapitanov, T.M.Zubareva, V.L.Lobachev, B.V.Panchenko, T.M.Prokop'eva. Reactivity of inorganic α -nucleophiles in acyl group transfer processes in water and surfactant micelles: I. Systems based on organic complexes of tribromide anion // *Russian Journal of Organic Chemistry* – **2017** – Vol. 53, N 3. – P. 351–358.
9. A.A.Serdyuk, A.B.Mirgorodskaya, I.V.Kapitanov, N.Gathergood, L.Ya.Zakharova, O.G.Sinyashin, Ye.Karpichev. Effect of structure of polycyclic aromatic substrates on solubilization capacity and size of cationic monomeric and gemini 14-s-14 surfactant aggregates // *Colloids and Surfaces A: Physicochemical and Engineering Aspects* – **2016** – Vol. 509. – P. 613–622.

10. L.Ya.Zakharova, A.A.Serdyuk, A.B.Mirgorodskaya, I.V.Kapitanov, G.A.Gainanova, Ye.A.Karpichev, E.L.Gavrilova, O.G.Sinyashin. Amino acid-functionalized calix[4]resorcinarene solubilization by mono- and dicationic surfactants // *Journal of Surfactants and Detergents* – **2016** – Vol. 19, N 3. – P. 493–499.
11. I.V.Kapitanov, A.A.Abakumov, A.A.Serdyuk. Identification of products in the reaction of 2-[(hydroxyimino)methyl]-1,3-dimethylimidazolium iodide with diethyl 4-nitrophenyl phosphate in alkaline medium // *Russian Journal of Organic Chemistry* – **2015** – Vol. 51, N 10. – P. 1368–1375.
12. T.M.Prokop'eva, I.V.Kapitanov, I.A.Belousova, A.E.Shumeiko, M.L.Kostrikin, M.K.Turovskaya, N.G.Razumova, A.F.Popov. Supernucleophilic systems based on functionalized surfactants in the decomposition of 4-nitrophenyl esters derived from phosphorus and sulfur acids: III. Reactivity of mixed micellar systems based on tetraalkylammonium and imidazolium surfactants // *Russian Journal of Organic Chemistry* – **2015** – Vol. 51, N 8. – P. 1083–1090.
13. A.B.Mirgorodskaya, Ye.Karpichev, L.Ya.Zakharova, E.I.Yackevitch, I.V.Kapitanov, S.S.Lukashenko, A.F.Popov, A.I.Konovalov. Aggregation behavior and interface properties of mixed surfactant system gemini 14-s-14 / CTABr // *Colloids and Surfaces A: Physicochemical and Engineering Aspects* – **2014** – Vol. 457. – P. 425–432.
14. I.V.Kapitanov, I.A.Belousova, A.E.Shumeiko, M.L.Kostrikin, T.M.Prokop'eva, A.F.Popov. Supernucleophilic systems based on functionalized surfactants in the decomposition of 4-nitrophenyl esters derived from phosphorus and sulfur acids: II. Influence of the length of hydrophobic alkyl substituents on micellar effects of functionalized monomeric and dimeric imidazolium surfactants // *Russian Journal of Organic Chemistry* – **2014** – Vol. 50, N 5. – P. 693–703.
15. M.A.Orlov, I.V.Kapitanov, N.I.Korotkikh, O.P.Shvaika. Synthesis and recyclisation of 2,3,9,10-tetrahydro-8H-[1,4]dioxino[2,3-f]-[1,3]thiazino[3,2-a]benzimidazolium salts // *Chemistry of Heterocyclic Compounds* – **2014** – Vol. 50, N 1. – P. 111–116.
16. I.V.Kapitanov, I.A.Belousova, A.E.Shumeiko, M.L.Kostrikin, T.M.Prokop'eva, A.F.Popov. Supernucleophilic systems based on functionalized surfactants in the decomposition of 4-nitrophenyl esters derived from phosphorus and sulfur acids: I. Reactivity of a hydroxyimino derivative of gemini imidazolium surfactant // *Russian Journal of Organic Chemistry* – **2013** – Vol. 49, N 9 – P. 1291–1299.
17. A.A.Serdyuk, A.A.Abakumov, I.V.Kapitanov, M.G.Kasianczuk, I.A.Opeida. Anthrone complexation with aliphatic amines in an aprotic medium // *Russian Journal of Physical Chemistry A* – **2013** – Vol. 87, N 9 – P. 1470–1473.
18. I.V.Kapitanov, I.A.Belousova, M.K.Turovskaya, E.A.Karpichev, T.M.Prokopeva, A.F.Popov. Reactivity of micellar systems based on supernucleophilic functional surfactants in processes of acyl group transfer // *Russian Journal of Organic Chemistry* – **2012** – Vol. 48, N 5 – P. 651–662.
19. Ye.Karpichev, H.Matondo, I.Kapitanov, O.Savsunenkenko, M.Vedrenne, V.Poinsot, I.Rico-Lattes, A.Lattes. Preparation of a series of N-alkyl-3-boronopyridinium halides and study of their stability in the presence of hydrogen peroxide // *Central European Journal of Chemistry* – **2012** – Vol. 10, N 4 – P. 1059–1065.
20. Yu.S.Sadovskii, T.N.Solomoichenko, M.K.Turovskaya, I.V.Kapitanov, Zh.P.Piskunova, M.L.Kostrikin, T.M.Prokop'eva, A.F.Popov. Peroxyhydrolysis of 4-nitrophenyl diethyl phosphate in micellar systems based on imidazolium gemini surfactants. // *Theoretical and Experimental Chemistry* – **2012** – Vol. 48, N 2 – P. 122–128.

21. I.V.Kapitanov. Nucleophilicity of micellar systems based on amphiphilic derivatives of 2-(oximinomethyl)imidazole in the decomposition of 4-nitrophenyl diethyl phosphate // *Theoretical and Experimental Chemistry* – **2011** – Vol. 47, N. 5 – P. 317–323.
22. A.A.Serdyuk, M.G.Kasyanchuk, I.V.Kapitanov, I.A.Opeida. Mechanism of the catalysis by aliphatic amines of the oxidation of anthrone with molecular oxygen // *Theoretical and Experimental Chemistry* – **2011** – Vol. 47, N. 2 – P. 129–134.
23. T.M.Zubareva, A.V.Anikeev, E.A.Karpichev, I.V.Kapitanov, T.M.Prokop'eva, A.F.Popov. Catalysis of the alkaline hydrolysis of 4-nitrophenyl diethyl phosphonate by cationic dimeric surfactant micelles // *Theoretical and Experimental Chemistry* – **2011** – Vol. 47, N. 2 – P. 108–114.
24. M.K.Turovskaya, I.V.Kapitanov, I.A.Belousova, K.K.Tuchinskaya, A.E.Shumeiko, M.L.Kostrikin, N.G.Razumova, T.M.Prokop'eva, A.F.Popov. Reactivity of micelle-forming 1-alkyl-3-(1-oximinoethyl)pyridinium halides in acyl group transfers // *Theoretical and Experimental Chemistry* – **2011** – Vol. 47, N. 1 – P. 21–29.
25. A.F.Popov, I.V.Kapitanov, M.A.Orlov, I.A.Belousova, K.K.Tuchinskaya, T.M.Prokop'eva. 1-Methyl-3-hexadecyl-2-(oximinomethyl)imidazolium bromide as a new highly efficient, low-basicity reagent for the decomposition of acyl-containing ecotoxins // *Theoretical and Experimental Chemistry* – **2010** – Vol. 46, N. 5 – P. 309–316.
26. I.A.Belousova, I.V.Kapitanov, A.E.Shumeiko, A.V.Anikeev, M.K.Turovskaya, T.M.Zubareva, B.V.Panchenko, T.M.Prokop'eva, A.F.Popov. Role of the hydrophobic properties of functional detergents on micellar effects in the decomposition of ecotoxins // *Theoretical and Experimental Chemistry* – **2010** – Vol. 46, N. 4 – P. 225–232.
27. T.M.Prokop'eva, E.A.Karpichev, I.A.Belousova, M.K.Turovskaya, A.E.Shumeiko, M.L.Kostrikin, N.G.Razumova, I.V.Kapitanov, A.F.Popov. Characteristic features of the change in reactivity of supernucleophilic functional surfactants in acyl group transfer processes // *Theoretical and Experimental Chemistry* – **2010** – Vol. 46, N. 2 – P. 94–101.
28. T.M.Prokop'eva, V.A.Mikhailov, M.K.Turovskaya, E.A.Karpichev, N.I.Burakov, V.A.Savelova, I.V.Kapitanov, A.F.Popov. New sources of “active” halogen bis(dialkylamide)hydrogen dibromobromates, efficient reagents for destruction of ecotoxins // *Russian Journal of Organic Chemistry* – **2008** – Vol. 44, N. 5 – P. 637–646.
29. I.A.Belousova, I.V.Kapitanov, A.E.Shumeiko, V.A.Mikhailov, N.G.Razumova, T.M.Prokop'eva, A.F.Popov. Reactivity of functional detergents with a pyridine ring and an α -nucleophile fragment in the head group // *Theoretical and Experimental Chemistry* – **2008** – Vol. 44, N. 5 – P. 292–299.
30. I.A.Belousova, I.V.Kapitanov, A.E.Shumeiko, M.K.Turovskaya, T.M.Prokop'eva, A.F.Popov. Structure of the head group, nucleophilicity, and micellar effects of functional detergents in acyl transfer reactions // *Theoretical and Experimental Chemistry* – **2008** – Vol. 44, N. 2 – P. 93–100.
31. T.M.Zubareva, T.M.Prokop'eva, I.V.Kapitanov, I.A.Belousova, N.G.Razumova, A.F.Popov. Reactivity of N-alkyl derivatives of hydroxylamine in decomposition of 4-nitrophenyl diethylphosphonate in water and in cetyltrimethylammonium bromide micelles // *Theoretical and Experimental Chemistry* – **2007** – Vol. 43, N. 4 – P. 247–254.
32. E.A.Karpichev, T.M.Prokop'eva, M.K.Turovskaya, V.A.Mikhailov, I.V.Kapitanov, V.A.Savelova, A.F.Popov. Micellar effects of cetyltrimethylammonium dibromobromate in phosphoryl group transfer reactions // *Theoretical and Experimental Chemistry* – **2007** – Vol. 43, N. 4. – P. 241–246.

33. T.N.Solomoichenko, Yu.S.Sadovskii, T.M.Prokop'eva, E.A.Karpichev, I.V.Kapitanov, Zh.P.Piskunova, V.A.Savelova, A.F.Popov. Micellar effects of surfactants in cleavage of 4-nitrophenyl diethylphosphonate by hydroperoxide anion // *Theoretical and Experimental Chemistry* – **2006** – Vol. 42, N. 6. – P. 364–370.

34. M.K.Turovskaya, T.M.Prokop'eva, E.A.Karpichev, A.E.Shumeiko, M.L.Kostrikin, V.A.Savelova, I.V.Kapitanov, A.F.Popov. Nucleophilicity of functional surface-active substances in the transfer of phosphoryl groups // *Theoretical and Experimental Chemistry* – **2006** – Vol. 42, N. 5. – P. 295–302.

Conference presentations (selected, related to the topic of this PhD Thesis)

1. Ye.Karpichev, I.Kapitanov, D. Bondar, V. Mochalin. Design of AChE reactivators using versatile molecular platforms and nanodiamonds // *15th International Meeting on Cholinesterases / 9th International Conference on Paraoxonases*. 15-18 September **2024**, Kranj, Slovenia [Poster].

2. I.Kapitanov, Ye.Karpichev. Sustainable molecular platforms based on L-phenylalanine derivatives: from ionic liquids to systems for biomedical applications // *VII International (XVII Ukrainian) scientific conference for students and young scientists "Current Chemical Problems"*. 19–21 March **2024**, Vinnytsia, Ukraine [Invited lecture].

3. I.Kapitanov, Ye.Karpichev. Design, Structure Improvement, and Applications of Sustainable Ionic Liquids // *Autumn 2023 Chemistry PhD Student's Conference (TaTech)*. 9-10 November **2023**, Tallinn, Estonia [Oral presentation].

4. S.Sudheer, G.Raba, I.Kapitanov, Y.Karpichev, R.Vilu, V.K.Gupta, N.Gathergood. A greener approach to hydrolyse ionic liquids // *2018 International Conference on Biotechnology and Bioengineering (ICBB2018)*. 24–26 October **2018**, Budapest, Hungary [Poster].

5. Ye.Karpichev, I.Kapitanov, N.Gathergood, O.Soukup, V.Hepnarova, D.Jun, K.Kuca. Acetylcholinesterase Reactivators Based on Oxime-Functionalized Biodegradable Ionic Liquids // *13th International Meeting on Cholinesterases / 7th International Conference on Paraoxonases*. 9-14 September **2018**, Hradec Kralove, Czech Republic [Poster].

6. I.Kapitanov, Ye.Karpichev, N.Gathergood. Synthesis of Dipeptide Ionic Liquids and Their Biotransformation Products // *International Conference on Organic Synthesis Balticum Organicum Synthetium (BOS-2018)*. 1–4 July **2018**, Tallinn, Estonia [Poster].

Total number of invited lectures, oral and poster presentations – more than 120.

Curriculum vitae

Personal data

Name: Illia Kapitanov
Date of birth: 23.09.1984
Place of birth: Kramatorsk, Ukraine
Citizenship: Ukraine

Contact data

E-mail: ivkapitanov@gmail.com

Education

2023–2024 Tallinn University of Technology (Estonia), external PhD candidate
2006–2010 Donetsk National University (Ukraine), PhD (Organic Chemistry)
2005–2006 Donetsk National University (Ukraine), M.Sc. (Biochemistry)
2001–2005 Donetsk National University (Ukraine), B.Sc. (Chemistry)
1991–2001 School # 22 (Kramatorsk, Ukraine), Secondary education

Language competence

English Fluent
German Upper Intermediate
Estonian Beginner
Ukrainian Native
Russian Native

Professional employment

2019–... Gemini PharmChem Mannheim GmbH (Germany); Researcher / Head QC
2016–2019 Tallinn University of Technology; Researcher / Senior Researcher
2006–2016 National Academy of Science of Ukraine; Researcher / Senior Researcher

International research experience

2013 Visiting Researcher, Institut Européen de Chimie et Biologie – Chimie et biologie membranes et nanoobjects (France)
2009 Visiting Researcher, CNRS Laboratory of Molecular Interaction and Chemical and Photochemical Reactivity (France)

Teaching experience

2010–2015 Donetsk National University (Ukraine), Associate Professor (part-time)

Supervisions

2015 A.I.Kukareka, M.Sc thesis; Donetsk National University (Ukraine)
2014 K.K.Tuchinskaya, M.Sc thesis; Donetsk National University (Ukraine)

Elulookirjeldus

Isikuandmed

Nimi: Illia Kapitanov
Sünniaeg: 23.09.1984
Sünnikoht: Kramatorsk, Ukraine
Kodakondsus: Ukraine

Kontaktandmed

E-post: ivkapitanov@gmail.com

Hariduskäik

2023–2024 Tallinna Tehnikaülikool (Eesti), ekstern doktorant
2006–2010 Donetski Riiklik Ülikool (Ukraina), PhD (orgaaniline keemia)
2005–2006 Donetski Riiklik Ülikool (Ukraina), M.Sc. (Biokeemia)
2001–2005 Donetski Riiklik Ülikool (Ukraina), B.Sc. (keemia)
1991–2001 Kool nr 22 (Kramatorsk, Ukraina), keskharidus

Keelteoskus

Inglise keel kõrgtase
Saksa keel ülemine kesktase
Eesti keel algtase
Ukraina keel emakeel
Vene keel emakeel

Teenistuskäik

2019–... Gemini PharmChem Mannheim GmbH (Saksamaa); Teadur / QC juht
2016–2019 Tallinna Tehnikaülikool; Teadur / vanemteadur
2006–2016 Ukraina Riiklik Teaduste Akadeemia; Teadur / vanemteadur

Rahvusvaheline uurimistöö kogemus

2013 Institut Européen de Chimie et Biologie – Chimie et biologie membraanide ja nanoobjektide instituut (Prantsusmaa); Külalisuurija
2009 CNRS-i molekulaarse interaktsiooni ning keemilise ja fotokeemilise reaktsioonivõime labor (Prantsusmaa); Külalisuurija

Õpetamiskogemus

2010–2015 Donetski Riiklik Ülikool (Ukraina), dotsent (osalise tööajaga)

Juhendatud väitekirjad

2015 A.I.Kukareka, M.Sc; Donetski Riiklik Ülikool (Ukraina)
2014 K.K.Tuchinskaya, M.Sc; Donetski Riiklik Ülikool (Ukraina)

ISSN 2585-6901 (PDF)
ISBN 978-9916-80-234-2 (PDF)